Regulation of Mesenchymal Differentiation Potentials in the avian Neural Crest

Bárbara de Faria da Fonseca

UPMC SORBONNE UNIVERSITÉS

UNIVERSITE PIERRE ET MARIE CURIE

ÉCOLE DOCTORALE : CERVEAU-COGNITION-COMPORTEMENT

REGULATION OF MESENCHYMAL DIFFERENTIATION POTENTIALS IN THE AVIAN NEURAL CREST

Bárbara de Faria da Fonseca

Thèse de Doctorat de Neurosciences

Sous la Direction d'Elisabeth Dupin

Présentée et soutenue publiquement le 3 juillet 2017

Devant le jury composé de :

Président :	**Professeur** Claire FOURNIER-THIBAULT
Rapporteurs :	**Professeur** Anne-Hélène MONSORO-BURQ
	Docteur Claire BAKER
Examinateurs :	**Professeur** Nicole LE DOUARIN
	Docteur Marie-Claire DELFINI-FARCOT
Directeur de thèse :	**Docteur** Elisabeth DUPIN

TABLE OF CONTENTS

LIST OF FIGURES

ABBREVIATIONS

AP: anteroposterior
BA: branchial arch
BAT: brown adipose tissue
BMP: bone morphogenetic protein
BSP: bone sialoprotein
CIL: contact inhibition of locomotion
CNS: central nervous system
DNA: deoxyribonucleic acid
ECM: extracellular matrix
EMT: epithelial to mesenchymal transition
ENS: enteric nervous system
ESC: embryonic stem cell
FACS: fluorescence activated cell sorting
FGF: fibroblast growth factor
GRN: gene regulatory network
HDAC: histone deacetylase
iPSC: induced pluripotent stem cells
MMP: matrix metalloproteinase
NC: neural crest
NCC: neural crest cells
NCSC: neural crest stem cells
NPB: neural plate border
PNS: peripheral nervous system
PPARγ: peroxisome proliferator-activated receptor γ
QCPN: quail non-chicken perinuclear antigen
r: rhombomere
RNA: ribonucleic acid
Runx2: runt-related transcription factor 2
αSMA: α-smooth muscle actin
SDF-1: stromal-derived factor-1
Shh: sonic hedgehog
TGF: transforming growth factor
VEGF: vascular endothelial growth factor
UCP1: uncoupling protein 1
WAT: white adipose tissue

INTRODUCTION

I. The Neural Crest

I.1. Overview of the NC development

The Neural Crest (NC) is an embryonic transitory structure derived from the ectoderm layer of the vertebrate embryo. The main steps and characteristics of NC development can be summarized as follows.

During neurulation, the presumptive NC domain is specified at the ectodermal layer, in a boundary between the neural plate and the presumptive epidermis (**Figure 1A**). As the neural plate bends to form the neural tube (i.e. future central nervous system (CNS)), the NC domain is displaced at the leading edges of the closing neural tube, named the neural folds (**Figure 1B**). By undergoing an epithelial to mesenchymal transition (EMT), the NC cells (NCC) delaminate from the neuroectoderm and then migrate along defined routes until reaching their final locations and sites of differentiation in the embryo (**Figure 1C**). There, they will form very diverse structures, often by intermingling with surrounding tissues. As detailed in a next *section* (*I.2*), the NCC will produce nearly all the peripheral nervous system (PNS) and the melanocytes of the skin, inner ear and choroid, and several hormone-producing cell types.

An important feature of NC function in vertebrates is that the anterior most cranial NC differentiates into mesenchymal cell types, contributing to the formation of most craniofacial cartilages and bones, dermis, fat cells and smooth muscle vascular cells. Interestingly, in amniotes, the ability of NCC to differentiate into mesenchymal cell types is restricted to the cephalic NCC, since in the trunk, mesenchymal structures (e.g. vertebral column, limb bones, muscles, blood vessels, adipocytes) are produced by the mesodermal germ layer (Le Douarin and Kalcheim, 1999).

Another feature of the NC is that the NC “per se” is only transitory as this structure, soon after its individualization in the dorsal neural folds, is destined to disappear, through the dissemination of its component cells in the whole embryonic body. This unique property has long kept up the mystery regarding NC identity and fate and it explains the difficulty of studying this structure.

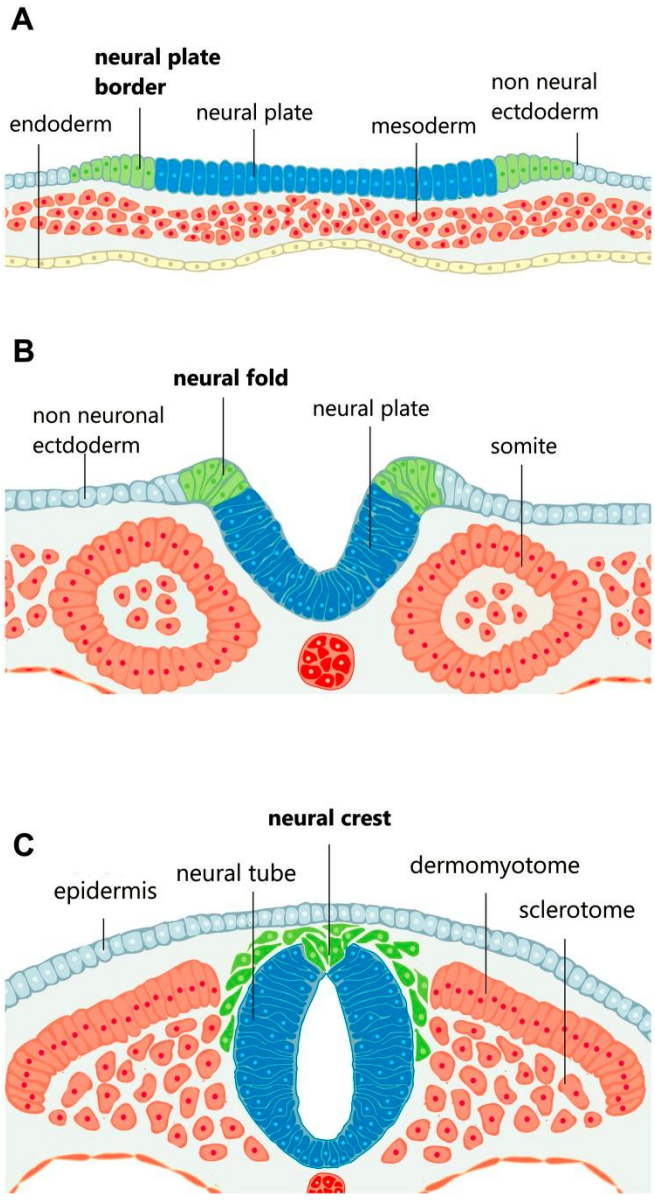

Figure 1: NC formation and migration. Schematic diagram of transverse sections through chick embryo during neurulation**.** (A) NC domain is specified in the neural plate border. (B) During invagination of the neural tube, the future NC is at the elevating edges of the neural tube (i.e. neural folds). (C) The NC delaminates from the neuroectoderm and extensively migrates to occupy distint territories in the embryo (Simões-Costa and Bronner, 2013).

The NC was first visualized in the chick embryo by Wilhelm His in 1868 (His, 1868). In this work, the NC is described as a group of cells localized between the neural tube and the presumptive epidermis, which later migrate to form, laterally to neural tube, the dorsal root ganglia, the first NC structure described (His, 1868). Much of the initial NC studies were concentrated in anamniotes until late 60s (Raven, 1937; Horstadius, 1950), when Weston developed a technique to trace migratory NCC, by labeling dividing cells in the chick neural tube (and premigratory NCC) with tritiated-thymidine incorporation, before transplantation of

the labeled neural tube into a host embryo (Weston, 1963). In these experiments, the progeny of the labeled NCC could be traced until dilution of the radioisotopic marker along cell divisions. One outcome in this technical improvement was the discovery of NC contribution to the mandibular bones of the chick, confirming previous statements made by Platt in salamanders (Platt, 1893, 1897; Johnson, 1966). However, a strong limitation to this technique was the inability to identify NC derivatives at late stages of development, since the radioisotope incorporated into DNA become diluted after several cell divisions. As a consequence, a permanent and reliable labeling technique was needed in order to obtain a detailed and long-term fate map of NC derivatives. This goal was greatly achieved thanks to the use of quail-chick chimeras, developed by Le Douarin and colleagues (Le Douarin and Kalcheim, 1999).

The use of quail-chick chimeras to address developmental issues such as cell migration and fate started from the observation made by Nicole Le Douarin that the cells of these two close-related avian species could be easily distinguished by their nuclear morphology (Le Douarin, 1969). After histological staining of nucleic acids and electron microscopy, it was evidenced that the nucleolus of quail (*Coturnix coturnix japonica*) cells was disproportionately large compared to the chicken one. In quail nuclei, part of deoxyribonucleic acid (DNA) is highly compacted in a huge heterochromatin state associated to the nucleolar ribonucleic acid (RNA), whereas chicken cellular heterochromatin is more dispersed in the cytoplasm. This nuclear characteristic is present in all quail cells and retained during the entire quail development until adulthood. Taking advantage of this new permanent marker, Le Douarin and her collaborators performed a series of “quail to chick” transplantation experiments and further identified quail cells within the host chick embryo, by using Feulgen-Rossenbeck staining and later on, QCPN (quail non-chicken perinuclear antigen) antibody. The position and phenotype of the quail cells recorded at different times after the graft provided a large body of novel and precise information about cell migration pathways and fate acquisition in the developing avian embryo (Le Douarin, 1982; Le Douarin and Kalcheim, 1999). Regarding the fate mapping of NC derivatives, a defined portion of the quail neural tube (or neural fold) was isotopically grafted into a chick embryo of the same developmental stage (**Figure 2**). Such graft experiments were performed in distinct restricted rostrocaudal domains of the NC as small as a single rhombomere (Le Douarin and Kalcheim, 1999), which led to virtually establish a full map of NC derivatives along the neural axis (*see next section*).

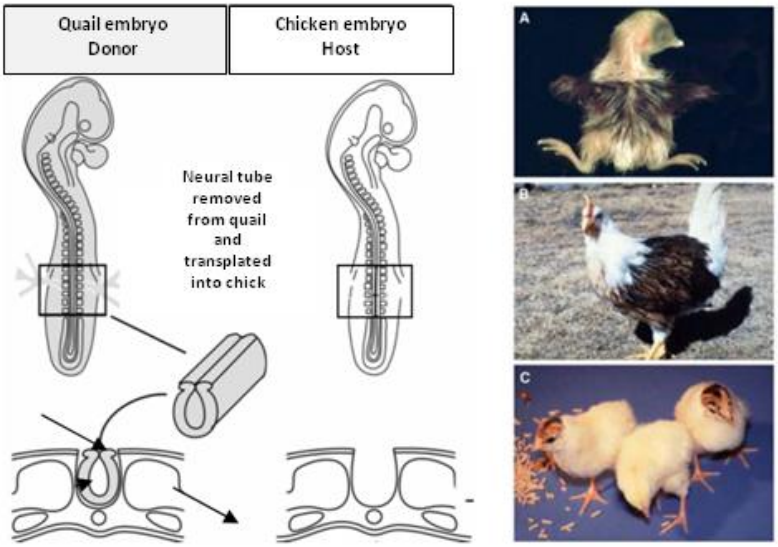

Figure 2: Scheme of isotopic and isochronic NC transplantations in quail-chick chimeras. The neural tube, containing premigratory NC, is removed from the donor quail embryo and transplanted, at the same level and developmental stage, into a host chicken embryo. Left: example of trunk neural tube graft. Right: (A) A chimeric chick after hatching. This embryo received a transplant of a quail neural tube at the presumptive level of the wings. (B) A two-month-old chimera. Note the pigmented feathers, due to the presence of quail melanocytes derived from NCC. (C) The outcome of a cephalic neural tube/NC graft. The resulting chimeric chicks have pigmented feathers at the head level. Note two chimeric chicks and a non-grafted control one in the center (adapted from Le Douarin and Kalcheim, 1999).

NCC fate and migratory pathways have been also investigated with other techniques in chick, zebrafish and amphibian embryos, such as vital dye injection in small populations of premigratory NCC and electroporation or viral transduction of fluorescent reporter-encoding constructs in ovo into the neural tube (Bronner-Fraser and Fraser, 1988; Collazo et al., 1993; Serbedzija et al., 1989; Schilling and Kimmel, 1994; Eisen and Weston, 1993; Kulesa et al., 2013). In addition, genetic and mutational analyses in zebrafish complemented these studies and helped to identify new cell types originated from the NC (Kague et al., 2012; Carney et al., 2006; Mongera et al., 2013; Hockman et al., 2017).

NC fate mapping studies were recently developed in mice, by using Cre/loxP-mediated recombination, which allowed NCC to be investigated in a mammalian model, and also permitted the long-term tracing of NC derivatives in adult animals. Permanent labeling of the NCC in P0-Cre, Sox10-Cre and Wnt-1-Cre mice crossed with reporter lines, for example in the widely employed Wnt1-Cre:R26LacZ mouse line, confirmed most of the conclusions regarding NC derivatives discovered in the avian model (Chai et al., 2000; Danielian et al., 1998; Matsuoka et al., 2005; Yamauchi et al., 1999) and also helped to uncover novel NC derivatives, such as olfactory ensheating cells (Barraud et al., 2010; Forni et al., 2011). However, species-

specific differences in NC fate were also described as, for instance, the mesodermal origin of parietal bones in mice (Jiang et al., 2002), compared to NC-derived parietal bones found in quail-chick chimeras (Couly et al., 1993). Finally, recent genetic studies using stochastic multicolor fluorescent reporters (Livet et al., 2007; Snippert et al., 2010) allows color-coding tracking of NCC, greatly contributing to the lineage tracing of clonal NC populations in vivo (Kaukua et al., 2014; Baggiolini et al., 2015; Kaucka et al., 2016) (*see sections II.1, II.4 and II.5*). Taken together, all these studies applied in birds, amphibians, fish and mice contributed to portray the diversity of NC derivatives.

As a consequence of their contribution to a wide variety of vertebrate tissues and structures, any step of NCC development is susceptible to defects that can result in many syndromes and congenital anomalies, collectively known as neurocristopathies (Bolande, 1974, 1997; Watt and Trainor, 2014; Etchevers et al., 2006). As neurocristopathies, we can include: cleft lip and palate defects (van Limborgh et al., 1983; Passos-Bueno et al., 2009); CHARGE and DiGeorge's syndromes that are associated with deficiencies in the outflow tract septation and craniofacial development (Keyte and Hutson, 2012), Hirschprung's disease caused by partial absence of enteric ganglia (Mundt and Bates, 2010), giant melanocytic nevi disease generated by an excessive proliferation of melanocytes precursors (Etchevers, 2014), among other diseases.

I.2. The NC migratory routes and derivatives

In avian embryos, quail-chick chimera experiments allowed the fate map construction of NC derivatives (**Figure 3**) and revealed the migratory routes of NCC (**Figure 4**). In sum, the NC can be divided in two main domains along the anterior-posterior neural axis: firstly, the cephalic NC, which comprises cells migrating from the level between the posterior diencephalon and the fourth somite included (Couly et al., 1996); and secondly, the trunk NC, which comprises NCC from the level of the fifth somite until the posterior end of the neural tube. These two NC domains can be distinguished by the migration pathways and the fate of their component cells.

Notably, both avian cephalic and trunk NCC yield neurons and glia of the PNS and melanocytes of the skin; in contrast, mesenchymal cell types, such as chondrocytes, adipocytes and osteoblasts, are only derived from cephalic NCC. Of note, other NC subdivisions can be defined according to the NCC final location and function in the embryo. For example, the "cardiac" NC, corresponding to post-otic NCC, migrating from the first three somites, gives rise

to the smooth muscle cells of the cardiac septum separating aorta and pulmonary artery during heart development (Le Lièvre and Le Douarin, 1975; Kirby and Stewart, 1983; Kirby et al., 1983). The "vagal" and "sacral" NC (from somites 1-7 level and posterior to somite 28, respectively) generate the enteric nervous system (ENS) (Le Douarin and Teillet, 1973). In addition to this early regionalization depicted at about E2, the "caudal NC", which develops at later stages (E4) during the secondary neurulation that occurs at the level of the last formed somites (somites 28-43), will yield pigment cells and glial cells of the caudal most part of the trunk (Osório et al., 2009).

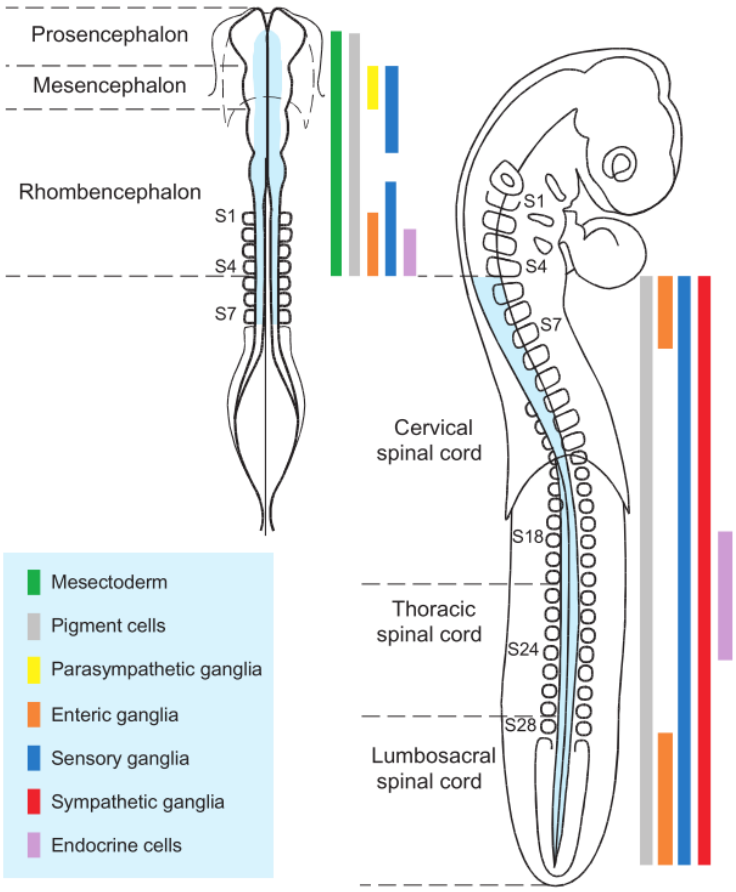

Figure 3: Fate map of NC derivatives in the avian embryo. The different cell types generated by NCC are color-coded as indicated in the box. Left, schematic of the cephalic NC domain (light blue) in a 7 somite-stage embryo. Right, trunk NC region (light blue) shown in a 28 somite-stage embryo; S: somites. (Le Douarin et al., 2004).

Cephalic NCC migration mainly occurs sub-ectodermally towards the frontonasal process and branchial arches. The nasal bud, the periocular mesenchyme and part of the first branchial arch (BA1) are populated by NCC migratory streams derived from the posterior diencephalic and mesencephalic neural folds, while the rest of BA1 is colonized by NCC from rhombomeres 1-2 (r1-r2) and a small subset of NCC originating from r3 (**Figure 4A**). The NCC

occupying the head down to BA1 differentiate mainly into mesenchymal structures, including the craniofacial and maxillary/mandibular skeleton, diverse ocular and periocular structures and connective tissue cells (Couly et al., 1993, 1996, 1998; Creuzet et al., 2005b); these mesenchymal NC derivatives will be detailed in *section IV*. In addition, meninges surrounding the future prosencephalon are derived from posterior diencephalic and mesencephalic NCC (Johnston, 1966; Le Lièvre and Le Douarin, 1975). More caudal branchial arches (BA2 to BA4) are invaded by a mixture of NCC coming from r3 to r8, which yields part of the hypobranchial skeleton (Couly et al., 1996; Köntges and Lumsden, 1996). Finally, the NCC invading the head will contribute to pigmentation of the skin and in the periocular choroid; they will also form the PNS cranial ganglia (sensory and parasympathetic) and will differente into pericytes lining cranial blood vessels (Ayer-Le Lievre and Le Douarin, 1982; Etchevers, 2011).

In the trunk, two main migratory pathways are adopted by NCC: the ventral and the dorsolateral pathways (**Figure 4B**).

In the ventral pathway, NCC migrate either along blood vessels in the intersomitic space, between the neural tube and the anterior half of developing somites, or through invasion of the anterior region of sclerotomes. The cells migrating ventrally will form the sympathetic ganglia, Schwann cells along the nerve fibers and the dorsal root ganglia, according to a ventral-to-dorsal order of colonization Bronner-Fraser, 1986; Teillet et al., 1987; Serbedzija et al., 1994). Notably, molecules secreted by the posterior part of sclerotomes block the invasion of NCC to this portion, helping the establishment of the typical metameric pattern of sympathetic and dorsal root ganglia (Rickmann et al., 1985; Guillory and Bronner-Fraser, 1986; Loring and Erickson, 1987; Teillet et al., 1987; Krull et al., 1997; Gammill, 2006).

Other NCC follow the dorsolateral pathway migrating superficially between the ectoderm and the dermomyotome. In chicken and mice, this route is used mainly by the NCC that will enter the epidermis and later on differentiate into melanocytes (Teillet and Le Douarin, 1970; Weston, 1970; Erickson et al., 1992; Serbedzija et al., 1990). However, both ventral and dorsolateral routes are undertaken simultaneously by murine trunk NCC while in chicken NCC will follow the dorsolateral pathway approximately 24 h after the beginning of NCC ventral migration (Kuo and Erickson, 2010). In zebrafish and *Xenopus*, pigment cell precursors were described as originating from NCC following both migratory pathways (Collazo et al., 1993; Kelsh et al., 2009). Nevertheless, it was recently shown that part of melanocytes is not specified from migratory NCC following a superficial route to the skin but arises later on from NC-derived Schwann cell precursors aligned along peripheral nerve fibers, subsequently

to their initial ventral migration from the neural primordium (Adameyko et al., 2009; Petersen and Adameyko, 2017).

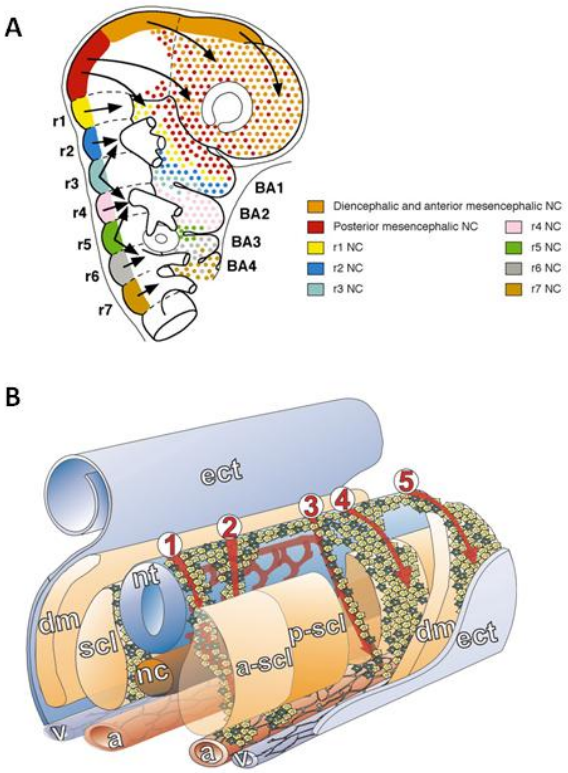

Figure 4: Migratory pathways of the cephalic and trunk NCC in avian embryo. (A) Cephalic NCC migration. The origin of the NCC homing to the frontonasal, periocular regions and in the BA are indicated by colors. The anterior midbrain contributes to the frontonasal and periocular regions. The NCC of the posterior midbrain also migrate to these structures and fill the anterodistal part of the BA1. The complementary part of BA1 is filled with NCC migrating from the level of r1/r), with a small contribution of r3. The largest contribution to BA2 comes from r4. NCC from r3 migrate to BA1/2 and r5-NCC migrate to BA2/3. (B) Ventral migration of trunk NCC (red lines 1, 2 and 3). Trunk NCC also undertake the dorsolateral pathway (red lines 4 and 5). a, dorsal aorta; a-scl, anterior sclerotome; dm, dermomyotome; ect, ectoderm; nc, notochord; nt, neural tube; p-scl, posterior sclerotome; v, vein. (Vega-Lopez et al., 2017; Couly et al., 2002).

I.3. Early steps in NC development: the gene regulatory network of NC induction and specification

NC formation results from a complex interplay between intrinsic gene regulations and extrinsic influences from nearby cells. The molecular players at work during this dynamic process have begun to be understood recently. In the chick embryo, the gene regulatory network (GRN) of NC induction and specification was extensively studied by Marianne Bronner

and colleagues, who defined the genes and their interactions controlling distinct steps in NCC development (Meulemans and Bronner-Fraser, 2004; Sauka-Spengler and Bronner-Fraser, 2008; Simões-Costa et al., 2014; Simoes-Costa and Bronner, 2015). Although the specific transcription factors involved in NC formation can slightly diverge in different vertebrate species, a simplified common mechanism will be summarized here (Prasad et al., 2012; Simoes-Costa and Bronner, 2015; for detailed references comparing vertebrate species, see Milet and Monsoro-Burq, 2012) (**Figure 5**).

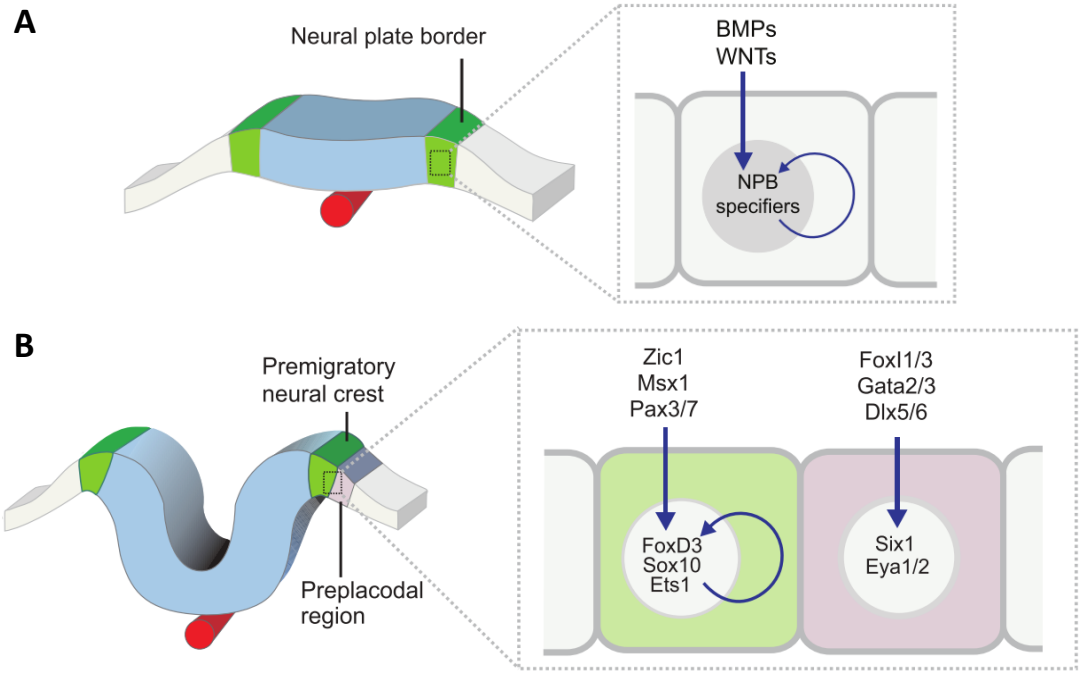

Figure 5: Induction and specification of NCC.(A) Induction of the NPB is mediated by the action of Wnts and BMPs secreted by adjacent tissues. The balance of these signals induces the expression of NPB specifier genes. (B). In the NC specification step, the NPB genes control the activation of NC specifier genes, such as *Foxd3*, *Sox10* and *Ets1*; the lateral portion of the NPB is specified in the preplacodal domain and express genes such as *Six1* and *Eya1/2*. NPB: neural plate border (Simoes-Costa and Bronner, 2015).

The first notable step is the specification of the neural plate border (NPB), a territory at the lateral edges of the future neural plate and which is responsible for the onset of NCC, ectodermal placodes, epidermal cells, roof plate cells and sensory neurons of the CNS (Basch et al., 2006; Fernández-Garre et al., 2002; Streit, 2002; Groves and LaBonne, 2014, for a review). NPB induction occurs during gastrulation concomitantly with neural induction. Briefly, Wnt and bone morphogenetic protein (BMP) factors are secreted by the presumptive epidermis while the future neural plate produces Chordin and Noggin among other Wnt and BMP antagonists. As a result, a BMP/Wnt signaling gradient is generated and intermediate levels of these morphogens achieve an ectodermal territory between the presumptive

epidermis and the future neural plate where the NPB will be specified (Faure et al., 2000, 2002; Nguyen et al., 1998; Garcia-Castro et al., 2002). In addition to ectodermal influences, fibroblast growth factors (FGF) secreted by the early mesoderm, such as FGF2 and FGF8 in *Xenopus*, are involved in NPB induction (Mayor et al., 1997; Monsoro-Burq, 2003). Notch signaling is also involved in this process as it activates and maintains BMP4 expression in the lateral non-neural ectoderm, therefore, avoiding NPB induction in this region (Endo et al., 2002). Thus, an intricate regulatory network, generated by a combination of these signaling pathways, leads to the expression of specific transcription factors in the NPB domain, for instance Dlx5/6, Msx1/2, Pax3/7, Tfap2, Gbx2, Foxi1/3, Gata2/3 and Zic (for references Milet and Monsoro-Burq, 2012; Simoes-Costa and Bronner, 2015) (**Figure 5A**).

Following NPB specification, the next step consists in NC specification. During this process, a subset of cells in the dorsal neural folds is specified into NCC. This specification mainly results from the combined action of NPB specifier genes (described above), which then trigger the expression of NC specifier genes such as *Sox8/9/10*, *Snail1/2*, *c-Myc*, *Foxd3*, *AP2*, *Twist* and *Ets1* (this last one, only at the head NC level) (Monsoro-Burq, 2005; Sato, 2005; Werner et al., 2007; Sauka-Spengler and Barembaum, 2008; Bellmeyer et al., 2003) (**Figure 5B**). Simultaneously, the pre-placodal domain is specified essentially by *Foxi1/3*, *Gata2/3* and *Dlx5/6*, present in a lateral domain of the NPB territory (Kwon et al., 2010; Sato et al., 2010; Pieper et al., 2012). As a result, Six1 and Eya1/2 transcription factors start to be expressed in the pre-placodal domain at this developmental stage (Schlosser and Ahrens, 2004; Brugmann, 2004). Interestingly, the fate of premigratory NCC and pre-placodal cells after NPB specification does not seem to be completely restricted at this stage. For instance, labeling of single cells of the NPB showed that a subset of them can still differentiate into both NC and placodal lineages (Selleck and Bronner-Fraser, 1995). More recently, it was shown that expression of specifier genes for the NC, placodes and neural tube, such as *Msx1/2*, *Six1* and *Sox2*, respectively, overlap in a large set of cells in the NPB, neural plate and even migratory NC, suggesting that restriction to one of these ectodermal lineages is not completed at these early stages of development (Roellig et al., 2017). Nevertheless, although the segregation of cell fate at the NPB is apparently not as early as previously stated, the expression of NC specifier genes, e.g. *Sox8/9/10*, is required to switch on a molecular program that triggers NCC delamination from the ectodermal layer, by an EMT (Haldin and LaBonne, 2010).

I.4. Molecular regulation of the EMT and NCC migration

The EMT is a complex phenomenon in which an epithelial cell loses the characteristic epithelial cell-cell adhesion and junction properties and acquires several features of a mesenchymal cell, such as high mobility and invasion behavior. Interestingly, similar EMT molecular mechanism events occur during development and tumor progression, which stimulated research on NC EMT as a model for understanding tumor cell dissemination and metastasis (Lim and Thiery, 2012; Kerosuo and Bronner-Fraser, 2012; Powell et al., 2013). After NC specification, the NCC of the dorsal neural folds go through EMT modifying their cell shape and polarity, intercellular adhesion and interactions with neighboring tissues. A remarkable feature of EMT is a global switch of cadherin expression: type 1-cadherins (E-cadherin and N-cadherin) are replaced by type 2-cadherins (cadherins 7 and 11), which mediates weaker cell-cell interactions. Moreover, delaminating NCC express diverse proteases to cleave these cadherins and other proteins from the basal lamina and extracellular matrix (Cheung et al., 2005; Chalpe et al., 2010). Consequently, NCC exit from the dorsal neural tube and start their migration process (**Figure 6**). All these molecular changes are partially triggered by the previously mentioned NC specifier genes, with critical actions of Snail1/2 to promote EMT and cell delamination in the avian and *Xenopus* NCC (Nieto et al., 1994; Blanco et al., 2007): Snail1/2, which can be induced by Sox5, represses *N-cadherin* expression (Ferronha et al., 2013), directly interacts with Sox9 (Liu et al., 2013), and it downregulates tight junction molecules such as claudins and occludins, and cell polarity proteins (Ikenouchi et al., 2003; Moreno-Bueno et al., 2008). Sox10 and Foxd3 upregulate *Cadherin11* and *Cadherin 7*, acting together with Snail1/2 to drive EMT (Dottori et al., 2001; Cheung et al., 2005). In addition to Snail1/2, transcription factors of Twist and Zeb families are involved in regulating EMT in both development and cancer. In mouse NCC, Zeb2 and Twist1 (rather than Snail) have been shown to regulate *cadherin* expression and cell polarity in order to control NCC delamination.

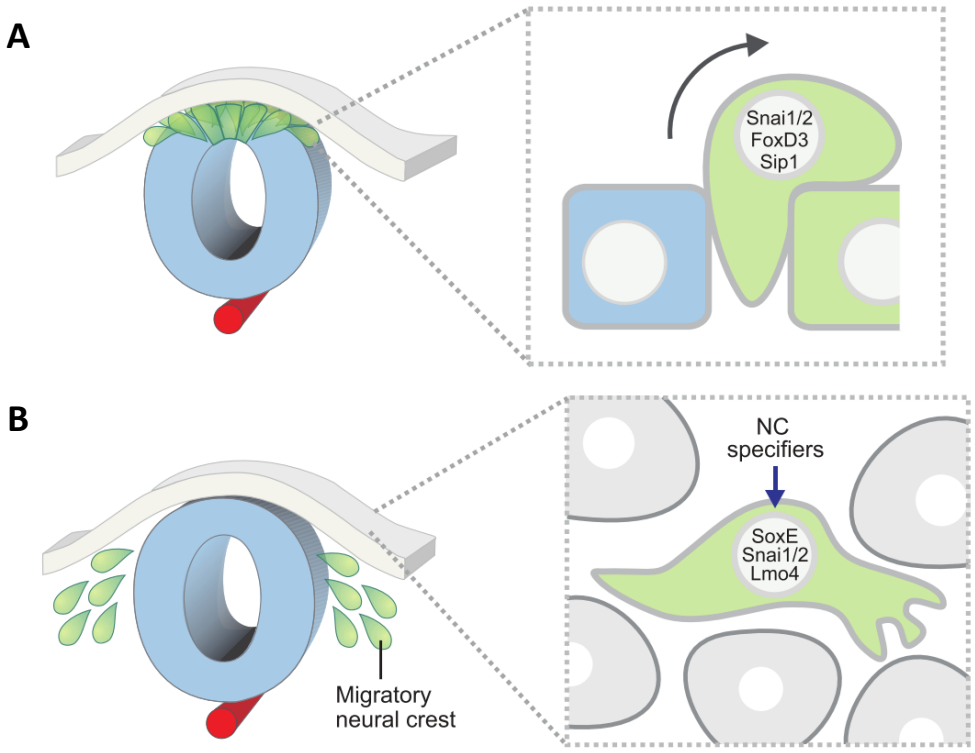

Figure 6: The EMT and migration of NCC. (A). Several combined signals, including extracellular pathways and NC specifier transcription factors, induce the expression of *Snail 1/2* (*Snal1/2*), *Foxd3* and *Sip1* and promote EMT. (B). Migratory NCC population, expressing typical NC markers, such as Lmo4, Snai1/2 and SoxE family of transcription factors (Simoes-Costa and Bronner, 2015).

Besides NC specifier genes, several extracellular signaling pathways are involved in NCC EMT. On one hand, activated BMP and Wnt signalings were reported to control trunk NC delamination by promoting G1/S cell cycle phase transition, which has a permissive role for EMT (Burstyn-Cohen et al., 2004). Moreover, the paraxial mesoderm controls the levels of BMP ligands and antagonists in the dorsal neural tube to further provoke NC delamination, in a mechanism that is coordinated with somite formation (Sela-Donenfeld and Kalcheim, 1999, 2000). On the other hand, EMT of the cranial NCC apparently does not rely upon BMP signaling and does not involve a G1/S cell cycle phase transition (Kalcheim and Burstyn-Cohen, 2005; Osório et al., 2009). These data suggest that distinct molecular mechanisms control cranial and trunk NCC EMT (reviewed by Duband, 2010). In this regard, *Ets1*, a NC specifier gene expressed only by the cephalic NCC, could have a secondary role in EMT, helping Snail1/2 action specifically in these cells. Interestingly, when *Ets1* was ectopically expressed in the trunk premigratory NC, it triggered a massive NCC exit from the dorsal neural tube, resembling stereotyped collective cell migration typical of the cephalic NCC as described below (Theveneau et al., 2007).

After delamination, NCC extensively migrate to occupy diverse sites and reach distant regions in the embryo. The process of NCC migration involves a series of intercellular communications between themselves and with neighboring tissues. It has been described that they secrete chemoattractant molecules such as the complement system component C3a, which induces a brief cell-cell contact mediated by N-cadherin, helping to maintain cohesion inside the migrating NCC population (Carmona-Fontaine et al., 2011; Theveneau et al., 2010). This phenomenon is followed by contact inhibition of locomotion (CIL), where contacting cells rearrange their protrusions, repolarize and separate from each other (Carmona-Fontaine et al., 2008; Teddy and Kulesa, 2004). The balance between co-attraction molecules and CIL favors NCC migration as a loose cell cluster. CIL has been mostly studied in cranial NCC, however it is argued that it could favor cell dispersion also in trunk NCC, since some molecular players controlling CIL are also found in migrating NCC (Moore et al., 2013).

Regarding cephalic and trunk NCC, differential requirement of extrinsic and intrinsic signals can influence the trajectory and shape of the migratory streams specifically in each region. For instance, experiments in chick, mice and *Xenopus* demonstrated that mesencephalic NCC migrate in wider and larger streams, while postotic cranial NCC and trunk NCC move as single-cell wide chains (Kulesa and Fraser, 1998; Teddy and Kulesa, 2004; Wynn et al., 2013; Szabo and Mayor, 2016; Young et al., 2004). A recent work in chick and zebrafish embryos has shown that individual trunk NCC assume, at the onset of migration, a defined position in the cell chain, in which a specific cell will lead the migratory process permanently until NCC are settled in their final destination. This phenomenon is not observed in migrating cephalic NCC, where the relative position of a given cell changes constantly inside the stream (Richardson et al., 2016).

Signaling molecules coming from surrounding tissues especially act in defining the direction of NC migratory streams. Accordingly, at the head level, the developing placodes secrete stromal-derived factor-1 (SDF-1/CXCL12), which will interact with CXCR4-expressing NCC. SDF-1 secretion then creates a chemotactic gradient, which helps NCC guiding toward the placodes (David et al., 2002; Theveneau et al., 2013, 2010). Furthermore, SDF-1/CXCR4 signaling is also important for cardiac NC migration: CXCR4 is expressed by NCC migrating towards the BA3-BA4 whereas SDF-1 is expressed by the ectoderm (Escot et al., 2013). More recently, Tbx1, expressed in the pharyngeal endoderm and lateral ectoderm, was described as an upstream factor to SDF-1/CXCR4 signaling in NCC homing to pharyngeal arches (Escot et al., 2016). Besides, at the trunk level, CXCR4-expressing migratory NCC are attracted by SDF-1

factors expressed along their ventral pathway in order to form dorsal root and sympathetic ganglia (Belmadani, 2005; Kasemeier-Kulesa et al., 2010).

Repulsive signals promoted by ephrins/Eph, plexins/neuropilins and Slit/Robo interactions between NCC and the microenvironment are also important to avoid NCC invasion into non targeted tissues, helping to define the shape of migratory streams. For instance, in *Xenopus*, cranial NCC migrating into the BA3 and BA4 express EphA4/EphB1 receptors whereas adjacent NCC migrating to BA2, and mesodermal cells, express ephrinB2. This repulsive interaction avoids intermingle of NCC migratory streams (Smith et al., 1997). Moreover, during trunk NCC ventral migration, the caudal-half of sclerotomes expresses ephrinB1, which impairs NCC migration to this portion, since NCC express EphB3 (Krull et al., 1997). Similarly, plexin/neuropilin repulsive signals contribute to both cephalic and trunk NCC segregation and impairment in this signaling leads to the crossing of NCC intended to follow distinct migratory streams (Gammill et al., 2007; Gammill, 2006; Osborne et al., 2005). Finally, Slit/Robo repulsive signaling is important, for instance, to assure the homing of the vagal NCC to the developing gut, since Slit1/2/3 ligands in the mesentery repulse trunk NCC expressing Robo1/2 receptors to impair their entry in the gut (De Bellard et al., 2003; Zuhdi et al., 2015). Slit/Robo signaling is also involved in delimiting the ventral migration of early trunk NCC (Jia et al., 2005).

Diverse ECM proteins possess important permissive roles in the NCC migration such as fibronectin, laminin and collagen IV, which are largely present along the pathways taken by migratory NCC, and generally improve, in vivo and in vitro, cell adhesion and dispersion (Newgreen and Thiery, 1980; Rovasio et al., 1983; Dubaud and Thiery, 1987; Perris and Perissinotto, 2000). Another example of ECM protein-related to permissive NC migration is tenascin-C, secreted by vagal NCC and important for NCC colonization of the gut (Akbareian et al., 2013). In contrast, other ECM molecules, such as chondroitin-6-sulfate, collagen IX and aggrecan are generally related to inhibitory or non-permissive effects on NCC migration (Perris and Perissinotto, 2000). In this regard, the proteoglycan versican was recently described as an inhibitory signal for cranial NC migration in *Xenopus* embryos. Versican is present in tissues adjacent to cranial NCC migratory streams and helps to create physical boundaries to limit the dispersion of migratory cells. Surprisingly, by associating computational modeling with experimental approaches, it has been shown that the apparent migration inhibition promoted by versican helped, in the end, to create a spatial confinement of migratory NCC, which later improves the directionally and collective migration of NCC (Szabo and Mayor, 2016).

II. The differentiation potentials of NCC

II.1. Evidence for NCC multipotency in vivo

The remarkable ability of NCC to give rise to a wide variety of cell types stands out from any other structure in the vertebrate embryo. Major questions in the understanding of NCC diversification are whether single NCC are endowed with multiple differentiation potentials in early stages and also to what extent this potentiality is maintained during and after NCC migration (Le Douarin and Kalcheim, 1999). Conversely, another scenario would argue for a heterogeneous NCC population composed of a mosaic of restricted progenitors, already determined towards specific cell types (Krispin et al., 2010). Nonetheless, a significant number of in vivo and in vitro studies tend to favor the NCC multipotency model (**Figure 7**).

In heterotopic transplantation experiments in avian embryos, the replacement of the chick trunk NC, at the adrenomedullary level, by a quail vagal NC, promoted the differentiation of vagal NCC into the appropriate NC-derived cell types of the trunk, including the chromaffin cells of the host adrenal glands (Le Douarin and Teillet, 1974). On the other hand, when thoracic quail NCC were transplanted to the vagal level of the NC, thoracic NCC colonized the gut and differentiated there into enteric ganglia (Le Douarin and Teillet, 1974; Fontaine-Perus et al., 1982; Le Douarin et al., 1975). These experiments represented a strong evidence that some degree of plasticity exists in premigratory NCC, the fate of which could be reprogrammed by changing their embryonic environment. However, in some cases, the donor NCC were unable to produce all the cell types normally derived from the host NC. One remarkable example is the NC differential ability to yield mesenchymal derivatives observed along the rostrocaudal axis: the trunk NC transplanted into the cephalic NC domain failed to yield skeletal derivatives (Chibon, 1967; Nakamura and Ayer-le Lièvre, 1982).

Fate plasticity in the avian NC was also identified by heterochronic, or back-transplantation, experiments where postmigratory NCC, or fragments of tissues containing postmigratory NCC, were grafted into the NC migration pathway of younger host embryos. In these conditions, the non-neuronal NCC present in grafted PNS ganglia from E4-15 quail embryos were still able to generate PNS neurons and glia in a younger chick host embryo (Ayer-Le Lievre and Le Douarin, 1982; Dupin, 1984). Furthermore, the back-transplantation of E4 quail gut pieces, containing NCC, into the NCC migratory route at the trunk level, led to the differentiation of all thoracic NC cell types, except melanocytes, from the donor NC tissue (Rothman et al., 1990). These studies revealed that, at migratory and postmigratory stages, the

NCC population has broader differentiation potentials than those expressed in normal development; however, these studies also point out some gradual restrictions of NCC potentialities as, in many cases, the replacement of all NC derivatives by the donor tissue was not completely achieved (Le Douarin and Kalcheim, 1999). For a better understanding of the timing and mechanisms of segregation of different NC lineages, it is important to analyze the progeny of an individual NCC. Single-cell analyses, in vivo and in vitro, are ideal to solve issues regarding multipotentiality and heterogeneity of the NC population.

The first experiments of NC lineage tracing in vivo were performed by intracellular injection of a fluorescent dextran into individual premigratory NCC in chicken embryos (Bronner-Fraser and Fraser, 1988). Two days after NCC injection, the progeny of individual labeled cells could be detected in different trunk NC-derived structures, such as the dorsal root and sympathetic ganglia, the adrenal medulla, and in Schwann cells lining spinal nerves, and migrating melanocytic cells (Bronner-Fraser and Fraser, 1988, 1989).

Similar experiments were also performed in other species, such as *Xenopus* (Collazo et al., 1993) and mouse (Serbedzija et al., 1994), which confirmed that at least a fraction of the premigratory NCC are multipotent. Nevertheless, in zebrafish embryos, the descendants of individually labeled NCC were detected in only one NC-derived structure, suggesting NC early fate restrictions in this particular model (Raible and Eisen, 1994; Schilling and Kimmel, 1994). Recently, the issue of NCC fate restriction was revisited in amniotes. By single-cell labeling in semi-open trunk neural tube preparations, Krispin and colleagues have shown that the initial ventrodorsal position of a premigratory NCC in the dorsal neural tube could predict its fate (Krispin et al., 2010). Moreover, they found that NCC progeny was restricted to a single rather than multiple NC derivatives, suggesting that the fate of NCC would be determined before cell delamination. These results contradict previous findings in cranial NCC: when grafted at the head level, late-migrating mesencephalic NCC generated the same cranial NC derivatives as early-migrating ones, and *vice versa* (Baker et al., 1997). In other words, cranial NCC in different migratory stages are not fate restricted. Recently, McKinney and colleagues challenged the results from Krispin and co-workers, by using time-lapse imaging of photo-converted cells labeled in the intact chick trunk neural tube (McKinney et al., 2013). They observed that dynamic rearrangements occurred in the premigratory NC, and thus, their position within the dorsal neuroepithelium was not strictly related to their exit time from the neural tube. Furthermore, except for the first migrating NCC that form the sympathetic ganglia, most of the premigratory NCC, issued from different dorsoventral levels in the neural tube, yielded multiple NC derivatives (McKinney et al., 2013). In sum, albeit Krispin and

colleagues obtained discordant results, the latest findings greatly favor the hypothesis of NCC multipotency (**Figure 7**).

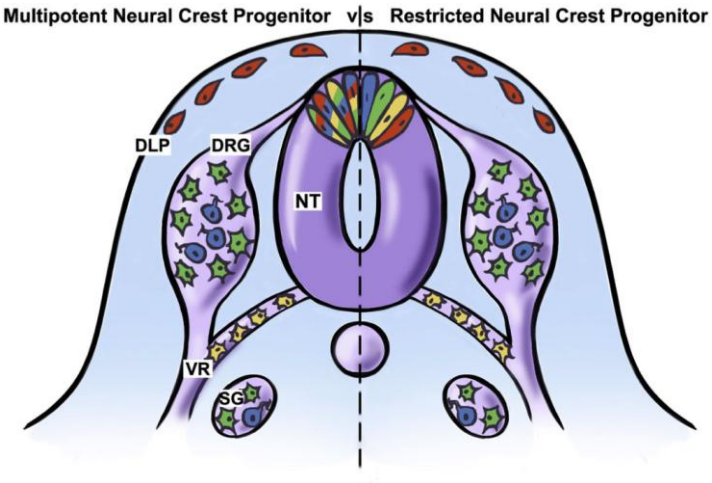

Figure 7: Two hypotheses for the diversity of phenotypes in premigratory trunk NCC. Left: Individual premigratory NCC within the dorsal neural tube (NT) are multipotent, regardless its dorsoventral position in the NT. Right: Alternatively, the premigratory NCC is composed of a mix of restricted progenitors, destined to form a single cell type. Trunk NCC types depicted are neurons (blue) and glia (green) of the dorsal root ganglia (DRG) and sympathetic ganglia (SG); Schwann cells (yellow) of the ventral root nerves (VR); and melanocytes (red) along the dorsolateral pathway (DLP) (adapted from Bronner, 2015).

The hypothesis that NCC are multipotent gained even stronger evidence from the recent single-cell tracing studies that used color-coding with "R26R-Confetti" mice technology. Crossing the R26R-Confetti reporter mice with NC conditional transgenic lines, such as Wnt1-CreER^{T} or Sox10-CreER^{T}, allowed to track color-coded trunk NC-derived clones after permanent genetic labeling at premigratory or early migratory stages, respectively. As a result, Baggiolini and colleagues nicely showed that the descendants of single NCC localized in several NC derivatives, generating dorsal root and sympathetic ganglionic neurons and supportive cells, Schwann cell precursors and melanocytic precursors going along the dorsolateral pathway (Baggiolini et al., 2015). Furthermore, by a series of detailed quantifications, they showed that the vast majority of individual labeled NCC are multipotent, both at premigratory and migratory stages. In the cephalic NC, the R26R-Confetti strategy was also recently used, coupled to Sox10-CreERT2 and PLP-CreERT2 drivers, to investigate the growth, dispersion, and spatial overlapping of clonally-related migratory NCC (Kaucka et al., 2016). Regarding NCC fates, the authors found that different facial subregions at E17.5 contain clones with multiple mesenchymal cell phenotypes, such as bone, dental and peridental mesenchyme in the teeth,

and bone and cartilage cells in the lower jaw. Some other colonies, containing pericytes or glial cells were also described. However, there was no evidence of colonies with both neural and mesenchymal derivatives after analysis of more than one hundred PLP-CreER^{T2} labeled NCC (Kaucka et al., 2016). Therefore, these data do not confirm previous in vivo and in vitro lineage studies of the cranial NCC, which provided clear evidence of multipotent progenitors endowed with both neural and mesenchymal fates (Bronner-Fraser and Fraser, 1988; Baroffio et al., 1991; Ito and Sieber-Blum, 1991; Calloni et al., 2007, 2009) (*see also section II.2*). This apparent discrepancy may arise from technical limitations and widespread dispersion of the NC progeny in the growing head, which restrict the in vivo analysis to clonal microdomains. Further in vivo studies using different NC-specific Cre-drivers would be needed to clarify these issues, for example a Wnt1-Cre driver, in order to target NCC at the premigratory stage, earlier than the time of recombination mediated by the PLP-Cre line.

In summary, the analyses of NCC fate in vivo, in different vertebrate species and with a variety of experimental approaches, propose that the NC is a heterogeneous cell population containing multipotent cells. To understand the full potentiality of the NCC, and to uncover the whole repertoire of cell types generated by a given progenitor, in vitro analyses can be highly advantageous, as they offer the possibility to submit single cells to controlled and distinct environments, which can be more permissive compared with those encountered in the developing embryo. In this regard, the in vitro clonal analyses are of main importance to give further insights concerning the NCC multipotency and the role of environmental factors in NC lineage choices.

II.2. The differentiation potentials of the NCC in vitro

Cohen and Konigsberg were the pioneers to perform clonal assays in avian trunk NCC (Cohen and Konigsberg, 1975), inspired by previous in vitro single cell analysis developed to unveil the diversity of murine bone marrow progenitors (Bradley et al., 1967; for references, Metcalf et al., 2007). Firstly, they devised a technique to obtain isolated trunk NCC, which migrated in vitro from the neural primordium explanted at developmental time preceding NCC exit. With this methodology, they cultured NCC at low-density conditions (limit dilution method) and observed that single NCC expanded in vitro gave rise to clonal populations containing non-pigmented and pigmented cells, indicating a mixed fate adopted by a single NC progenitor (Cohen and Konigsberg, 1975; Sieber-Blum and Cohen, 1980). Afterward, part of the non-pigmented cells present in the NC colonies was defined as sensory and adrenergic

neuroblasts, showing that the clonogenic NCC were indeed multipotent in vitro (Sieber-Blum, 1989).

In vitro clonal assays were further improved with the identification of various phenotypic markers and the optimization of culture conditions. For instance, culturing avian NCC on 3T3 feeder-layers, according to a method adapted from single-cell cultures of human keratinocytes (Barrandon and Green, 1985), greatly improved NCC cloning efficiency, i.e. the percentage of single seeded cells that actually yields a clone. Moreover, the direct and microscopically controlled plating of single cells taken from NCC suspensions helped to ensure clonality of the NC cultures (Baroffio et al., 1988). As a consequence, clonal assays carried out by Dupin and colleagues using quail NCC isolated from the entire neural axis and at different developmental stages, confirmed the heterogeneity of NC progenitors in terms of proliferation, survival and differentiation capacities and further demonstrated the existence of highly multipotent NCC (Baroffio et al., 1988, 1991; Trentin et al., 2004; Calloni et al., 2009; Coelho-Aguiar et al., 2013; Lahav et al., 1998; Dupin et al., 1990).

Among all the advances obtained by avian NC clonal assays, one of the most interesting discoveries was that some cephalic NC progenitors are endowed with both neural and mesenchymal potentialities (Baroffio et al., 1988, 1991; Ito and Sieber-Blum, 1991). For instance, Baroffio and collaborators have shown that neural (neuronal and glial) cells, melanocytes and cartilage nodules could originate from the same NC progenitor, therefore suggesting that neural and mesenchymal progenitors may not be segregated at early stages of NC development (Baroffio et al., 1988, 1991). Nevertheless, in these initial experiments, the neural-mesenchymal clones represented only a small fraction of the resulting clones. However, optimization of the cell culture conditions and isolation of mesencephalic NCC at earlier time points of in vitro migration (15 hours instead of 24 hours), later on led Calloni and colleagues to obtain a larger proportion of cephalic NC-derived clones containing both cartilage and neural/melanocytic cells (Calloni et al., 2007). Moreover, osteoblasts were also observed in these clonal cultures, in approximately 94% of the colonies (Calloni et al., 2009). Interestingly, the authors also showed that a highly multipotent progenitor was able to give rise to six different cell types, that is, glial, neuronal, melanocytic, myofibroblastic, chondrocytic and osteoblastic cells. In summary, these in vitro results revealed the high ability of single cephalic NCC to produce diverse cell types, as previously shown in vivo at the whole cell population level. Also, they evidenced that the cranial NC is composed of highly multipotent NC stem cells in early stages of development.

The trunk NCC of amniotes are devoid of mesenchymal fate (Le Douarin and Kalcheim, 1999; Hall, 2009) with the exception of endoneurial fibroblasts identified in transgenic mice (Joseph et al., 2004). Nevertheless, compelling in vitro clonal assays in avian and mammalian species have shown that a considerable amount of trunk NC colonies contained myofibroblasts, as defined by expression of the alpha smooth muscle actin (αSMA) (Trentin et al., 2004; Calloni et al., 2007; Stemple and Anderson, 1992; Morrison et al., 1999; Shah et al., 1996). Interestingly, after heterotopic transplantation to the cephalic NC domain, the trunk NCC did not produce head skeleton elements but could still differentiate into myofibroblasts and connective tissue cells in vivo (Nakamura and Ayer-le Lièvre, 1982). Taken together, these in vitro results raised the hypothesis that the trunk NC of amniotes may have broader mesenchymal cell potentials than previously thought. Indeed, it was later demonstrated that trunk NCC could differentiate into chondrocytes in long-term cultures (McGonnell and Graham, 2002; Abzhanov et al., 2003) and also into adipocytes when trunk quail NCC are cultured in pro-adipogenic medium conditions (Billon et al., 2007). In addition, Calloni and colleagues described a high rate of chondrocyte differentiation by quail trunk NCC grown in the presence of the morphogen Sonic hedgehog (Shh); moreover, in clonal cultures, they found a rare progenitor (1 out of 200) able to differentiate into chondrocytes, glial cells and myofibroblasts (Calloni et al., 2007).

Taken together, these results reveal that trunk NCC are endowed with the ability of producing several mesenchymal cell types. Recent investigations further corroborated this finding. In culture, trunk NCC expressed early markers of osteogenesis, chondrogenesis and adipogenesis and, when grown in a permissive medium, they fully differentiated into all these mesenchymal phenotypes (Coelho-Aguiar et al., 2013). Additionally, when seeded as single cells, a high proportion of trunk NCC (78%) yielded colonies containing osteoblasts progenitors (*runt-related transcription factor 2; Runx2+*), as previously observed in cephalic NC colonies (Calloni et al., 2009). The vast majority of osteoblast-containing clones formed by trunk as well as cephalic NCC also comprised neural cells, indicating that progenitors endowed with neuro-mesenchymal potentials are present in the early NC along the entire neural axis.

In summary, all of these in vitro studies, mainly performed in quail cells, led to propose a hierarchical model of NC lineage diversification, in cephalic and trunk NCC, in which distinct restricted precursors are derived from a heterogeneous multipotent cell population (**Figure 8**). Furthermore, in vitro clonal investigations have also been undertaken in rat and mouse NCC, and in human NCC derived from embryonic stem cells (ESC), which showed similar results

regarding early NCC multipotency (Stemple and Anderson, 1992; Shah et al., 1994; Ito and Sieber-Blum, 1993; Lee et al., 2007; see Dupin and Coelho-Aguiar, 2013, for a review).

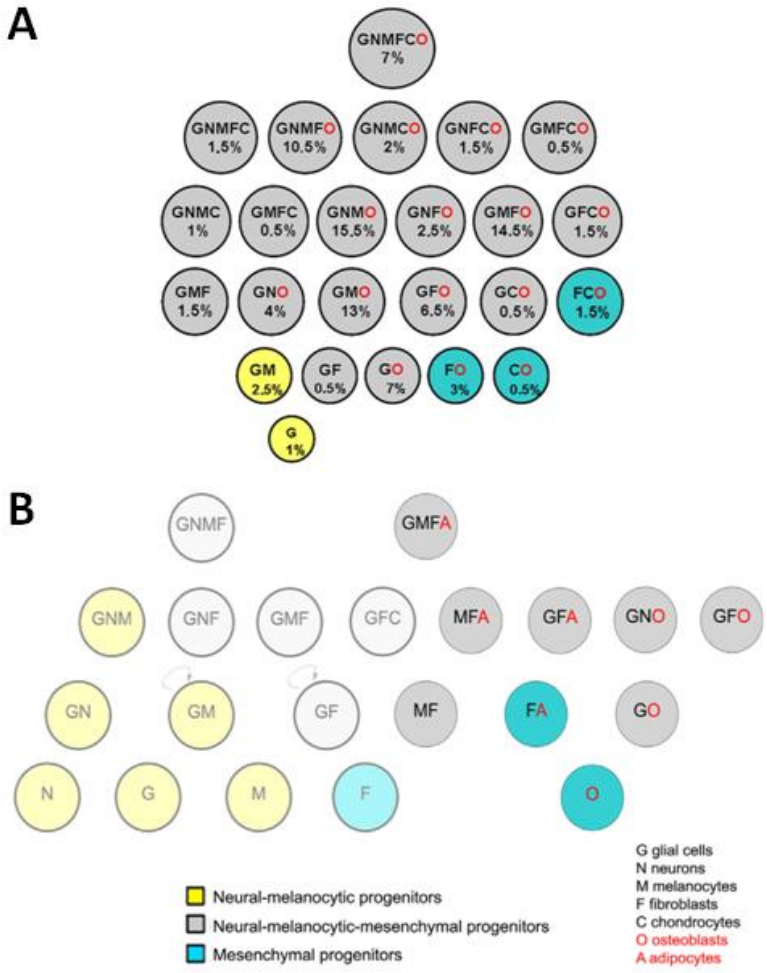

Figure 8: NC progenitor hierarchy identified in clonal assays of quail cephalic and trunk NCC. Progenitors are organized according to the number of cell types in their progeny. (A) In cephalic NCC, a highly multipotent cell (GNMFCO) is upstream of a variety of more restricted progenitors, i.e. intermediate and unipotent progenitors. Most intermediate progenitors are endowed with neural-mesenchymal capacities (gray circles) (B) In the trunk NC, neural-mesenchymal progenitors could also be identified, including GNMF and GMFA multipotent progenitors. Self-renewal (arrows) had been shown for GM and GF progenitors in trunk and cephalic NCC (Trentin et al., 2004; Calloni et al., 2009; Coelho-Aguiar et al., 2013).

II.3. Stem cell properties of NCC

Given the plasticity of NCC, associated with their multipotential feature, it is of great importance to assess whether NCC can be considered as true stem cells with self-renewal capacity, that is the capacity of a cell to generate, in addition to a differentiated progeny, daughter cells that remain undifferentiated and preserve its differentiation potentials (i.e.

stemness). The self-renewing ability of quail trunk and cephalic NCC was tested by successive subcloning experiments in vitro, which revealed that glial-melanocytic and glial-myofibroblastic bipotent progenitors act as stem cells, and can be propagated in vitro upon the influence of endothelin-3 and FGF2, respectively (Trentin et al., 2004; Bittencourt et al., 2013). In mammals, self-renewing trunk NCC, that yield autonomic neurons, glial cells and myofibroblasts, were first isolated by sorting a rat NC subpopulation expressing p75 receptor (Stemple and Anderson, 1992). The latter receptor, together with the HNK1 marker, also led to the isolation of multipotent human cranial NC-like stem cells from ESC cultures (Lee et al., 2007). Recently, it was reported a new procedure to maintain NCC self-renewal for long periods in culture, inspired by sphere-forming assays classically used to identify stem cells in many tissues, such as brain-derived neurospheres (Reynolds and Weiss, 1992). Individual early NCC, derived from chick embryos or human ESC, were grown in low-attachment conditions, which favor the formation of free-floating spheres, herein named crestospheres (Kerosuo et al., 2015). With this methodology, cells inside the crestospheres could be maintained for several weeks in culture in a premigratory NC state expressing early NC markers such as *Sox10*, *Foxd3*, *Snail*, and *AP2a*. In pro-differentiation conditions, cells in the crestospheres gave rise to neural cells, melanocytes and mesenchymal cells (myofibroblasts and osteoblasts). Additionally, individual crestosphere clones could generate new crestospheres, showing that a subpopulation of NCC could maintain its stemness. The development of this technique will contribute to further investigations regarding NCC potency and self-renewal. For instance, by using this technique, it was recently described that *c-myc*, a “pluripotency gene” with an established role in embryonic and adult stem cell maintenance (Chappell and Dalton, 2013, for a review), regulates the size of the premigratory NCC pool in vivo and in vitro (Kerosuo and Bronner, 2016).

In summary, these experiments show that NCC possess many features of true stem cells.

II.4. Maintenance of NC stem cells in adult tissues

Accumulating evidence shows that multipotent and self-renewing NCC, the so-called NC-derived stem cells (NCSC), are present even in postmigratory embryonic and adult stages. Hence, many tissues containing NCSC have been described in rodents and human, by either culturing the adult tissue and further identification of NCSC, via NC-specific markers (e.g. p75, *Sox10*, *Sox9*, Nestin, among others) or by in vivo lineage tracing of NCC in adult murine tissues,

through the use of NC-specific conditional mice. In this way, NCSC were identified in the sciatic nerve (Morrison et al., 1999), intestine (Bixby et al., 2002), dorsal root ganglia (Li et al., 2007), skin (Fernandes et al., 2004; Sieber-Blum et al., 2004; Wong et al., 2006), heart (El-Helou et al., 2008), bone marrow (Nagoshi et al., 2008), cornea (Yoshida et al., 2006; Brandl et al., 2009), teeth (Janebodin et al., 2011; Kaukua et al., 2014) and craniofacial tissues (Kaltschmidt et al., 2012), among others (for further references, Dupin and Coelho-Aguiar, 2013; Dupin and Sommer, 2012). However, in most of these tissues and organs, the localization and marker identity of the NCSC remained rather obscure. Yet, in the carotid body, a small neuroendocrine organ involved in blood oxygen pressure regulation, genetic fate mapping of mouse NCC led to characterize multipotent NCSC in the adult organ as supportive cells expressing the glial marker GFAP, which can reversibly produce new neuron-like glomus cells in vivo for adaptation to hypoxia (Pardal et al., 2007).

II.5. Glia-related postmigratory neural crest stem cells

Recent studies have since put forwards the notion that NC-derived glial cells, particularly Schwann cell precursors, behave as NC-like stem cells in diverse tissues, largely contributing to development and regeneration of different cell types in the many niches they reside (Petersen and Adameyko, 2017, for a review). A striking discovery was that immature Schwann cell precursors in mammalian and avian PNS nerves give rise to a significant part of melanocytes in the body (Adameyko et al., 2009, 2012). Of note, the generation of pigment cells from Schwann cells was previously evidenced in vitro (Dupin et al., 2003; Real et al., 2005; Widera et al., 2011). Besides, the reverse in vitro phenotype conversion, from pigmented melanocytes to Schwann cells, has also been reported in the quail and occurred through a multipotent NC-like intermediate (Dupin et al., 2000; Real et al., 2006). Recently, interesting findings were obtained in zebrafish regarding establishment of the colored stripes of the adult fish: during metamorphosis, the adult pigment cells were generated from post-migratory NCC located along spinal nerve fibers and within the dorsal root ganglia, which also gave rise to PNS neurons and Schwann cells (Dooley et al., 2014; Singh et al., 2016). Other recent findings support a role for nerve-associated glial progenitors in the development of significant subpopulations of PNS neurons in the cranial parasympathetic ganglia (Espinosa-Medina et al., 2014; Dyachuk et al., 2014) and the ENS of mammals (Uesaka et al., 2015). Furthermore, NCSC belonging to the NC glial lineage can adopt phenotypes that exceed neuroglial and melanocytic fates. As already mentioned, Schwann cell precursors in vivo are at the origin of endoneurial

fibroblasts along the sciatic nerve (Joseph et al., 2004). In addition, transdifferentiation of Schwann cells into myofibroblasts has been previously described in in vitro culture (Dupin et al., 2003; Real et al., 2005) and in response to infection of the adult nerve by leprosy bacilli (Masaki et al., 2013). Recent findings from long-term genetic tracing and clonal color-coding in mice have shown that, in the model of continuously renewing incisor tooth, PNS nerve-associated glial cells are at the origin of mesenchymal stem cells involved in the renewal and repair of pulp cells, odontoblasts and osteoblasts during development and adult life (Kaukua et al., 2014).

In conclusions, the above findings demonstrate the cell type diversity arising from early NCC and how a subset of these cells (NCSC) is maintained multipotent and capable to renew adult tissues throughout vertebrate life.

III. Mesenchymal cell types

The term mesenchyme is used to describe tissues where the cells are loosely organized, surrounded by a vast quantity of ECM. In this context, cells are free to migrate as few cell-cell adhesion contacts and no basal membrane impair their movement. Therefore, mesenchymal cells are not polarized in an apical-basal orientation, as are epithelial cells. Among the mesenchymal tissues, we can cite dermis, tendon, muscle, skeletal elements with bones and cartilages, adipose and several others tissues (Le Douarin et al., 2004; Grenier et al., 2009; Dupin et al., 2006).

In amniote vertebrates, the mesenchymal cell types are derived from two main embryonic sources: the mesoderm and the cephalic NC. During development, the mesoderm germ layer is divided into four main regions: the axial (notochord and prechordal mesoderm), paraxial, intermediary and lateral mesoderm. The paraxial mesoderm can be subdivided into cephalic mesoderm and somitic mesoderm (Sambasivan et al., 2011; Gilbert, 2000; Couly et al., 1992). The mesoderm germ layer forms almost all mesenchymal tissues in the vertebrate body. Nevertheless, the cephalic NC is also a significant source of mesenchymal cell types. As the NC comes from the ectoderm germ layer, NC-derived mesenchymal cells are collectively named “ectomesenchyme” or “mesectoderm,” a term designated by Platt (Platt, 1893).

In this Chapter, we present an overview of skeletogenesis in vertebrates and the molecular aspects involved in the differentiation of osteoblasts, chondrocytes, and adipocytes, the main mesenchymal cell types derived from the NC, which we address in this Thesis.

III.1. Endochondral and intramembranous ossification

The process of bone formation occurs by two main mechanisms: the endochondral or the intramembranous ossifications. Endochondral ossification takes place in the majority of bones, particularly long bones in the vertebrate body, while the intramembranous ossification is restricted to dermal bones, such as the clavicle and the skull vault (Karsenty et al., 2009; Kozhemyakina et al., 2015).

In the endochondral ossification, the process of bone formation starts with condensation of mesenchymal cells in a presumptive cartilage template. These mesenchymal progenitors come from either the cranial NC and mesoderm, the somites or the lateral plate mesoderm. They contribute to craniofacial, axial and limb skeletons, respectively. A balance of

extrinsic and intrinsic signals triggers the expression by mesenchymal progenitors of *Sox9*, a key regulator of chondrogenesis (Bi et al., 1999; Akiyama et al., 2002). As a result, mesenchymal progenitors differentiate into proliferating chondrocytes, which then express and secrete specific ECM proteins and glycoproteins such as type 2 collagen and aggrecan (Horton, 1993; Lefebvre et al., 1997). This cartilage structure will serve as a mold for the future bone. Additionally, cells in the periphery of the cartilage template do not differentiate into chondrocytes and form the perichondrium (Caplan and Pechak, 1987). As the cartilage develops, the proliferative chondrocytes, from the central region of the cartilage primordia, exit the cell cycle, increase greatly in volume and become hypertrophic. These hypertrophic chondrocytes start to produce osteopontin, bone sialoprotein II, matrix metalloproteinase (MMP) 13 and collagen 10, which trigger the mineralization of the ECM cartilage (Linsenmayer et al., 1991; Poole, 1991; Inada et al., 1999). As the cartilage primordium develops, proliferating chondrocytes continuously differentiate into hypertrophic chondrocytes along the template. The area in the forming bone containing chondrocytes in these progressive steps (i.e. proliferating and hypertrophic) is known as the growth plate (Karsenty et al., 2009; Kozhemyakina et al., 2015). Simultaneously, cells from a thin mesenchymal layer in the periphery (perichondrium/future periosteum) start to invade the hypertrophic cartilage zone, together with blood vessels and pre-osteoblasts (Nguyen et al., 1998; Kronenberg, 2003; Maes et al., 2010). These osteoprogenitors express *Runx2,* also known as core-binding factor subunit α-1 (Cbfα-1), a key gene for osteoblast commitment and differentiation (*further discussed in sections III.3 and IV.3*). While the hypertrophic chondrocytes die by apoptosis, they are replaced by mesenchymal cells of the osteoblast lineage. The partially degraded cartilage matrix then forms a template for bone matrix deposition, which begins with accumulation of type 1 collagen, produced by the entering osteoblasts, on top of previous ECM-containing collagen 10. The region wherein this process starts is known as the primary ossification area. Soon after, a second ossification area arises within the epiphysis. The growth plate will eventually be restricted to a thin area between the primary and secondary ossification regions. Proliferating chondrocytes remaining in this area allow the longitudinal growth of the skeleton until early adult life (Karsenty and Wagner, 2002; Kronenberg, 2003) (**Figure 9, right**).

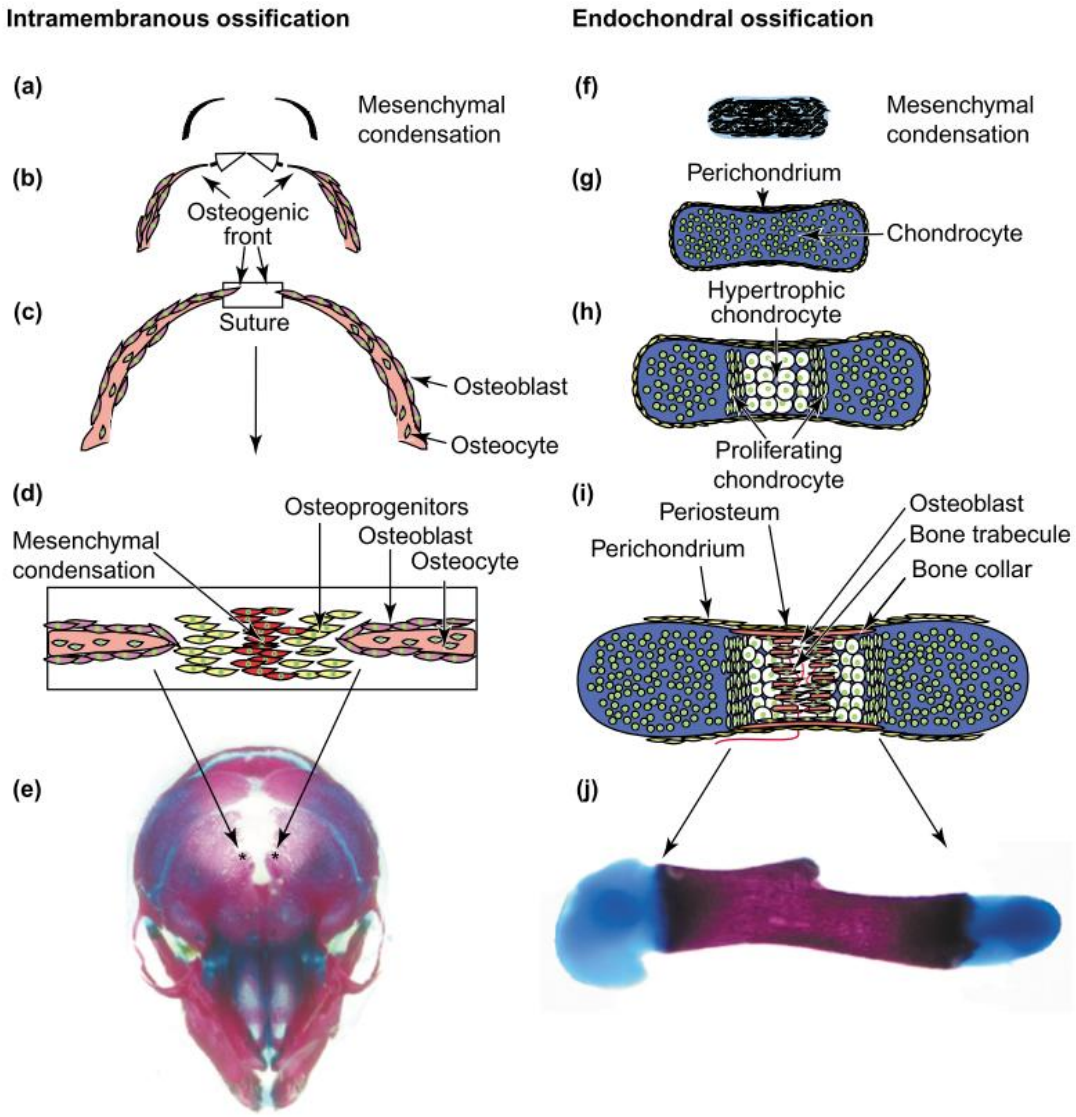

Figure 9: Intramembranous and endochondral ossification. (a-e) Intramembranous ossification. (a) Formation of frontal bones starts directly from mesenchymal condensations on the lateral side of the head. (b) This mesenchymal condensation spreads upward toward the top of the skull (arrows; osteogenic front). Osteoblasts differentiate and produce bone matrix. (c) The osteogenic fronts that originate on each side convene at the midline, where a suture is formed. (d) In the suture, cells differentiate into osteoprogenitors. Osteoprogenitors then differentiate into osteoblasts that produce bone ECM. Next, osteoblasts differentiate into osteocytes, which become embedded in the bone matrix. (e) Schematic of a murine skull (E 18.5) stained with Alizarin Red and Alcian Blue. Asterisks: osteogenic fronts. (f-j) Endochondral ossification. (f) Mesenchymal condensations start in a long bone (e.g. humerus). (g) These cells differentiate in chondrocytes whereas cells in the periphery form the perichondrium. (h) Proliferative chondrocytes exit the cell cycle and become hypertrophic. (i) Hypertrophic chondrocytes further mineralize their cartilaginous matrix. Concomitantly, cells from the periosteum invade this region, together with blood vessels and osteoclasts. (j) A mouse humerus stained with Alizarin Red and Alcian Blue (Nakashima and De Crombrugghe, 2003).

In the intramembranous ossification, bone cells are derived directly from mesenchymal cells without the need of an intermediary cartilage template. Mesenchymal condensation is followed by the differentiation of immature osteoblasts resulting in

production of a bone matrix containing collagen type 1α1 (Karsenty et al., 2009). As osteoblast differentiation gradually continues, these cells start to secrete other bone ECM proteins, such as osteopontin and osteonectin, followed by the secretion of alkaline phosphatase, osteocalcin and eventually leading to bone ECM mineralization (Nakashima and De Crombrugghe, 2003). Between the edges of developing dermal bones, in a limited non-mineralized mesenchymal region, pre-osteoblasts are continually proliferating and remain undifferentiated in early post-natal life, composing the calvarial sutures in the skull (**Figure 9, left**).

III.2. Bone matrix mineralization

The overall mechanism of the primary mineralization is similar between mineralized tissues, such as bone, tooth and cartilage, although the inorganic materials and the protein composition vary in each tissue (Golub, 2011). Briefly, in bone formation, the osteoblasts are responsible for the production of organic and inorganic matrices. Firstly, they secrete mainly type 1 collagen, a structural protein crucial to forming a template for future mineral deposition; secondly, they secrete regulatory proteins, such as alkaline phosphatase and osteocalcin, among others, which will control the rate of mineralization. Thirdly, they produce bone apatite crystals, which are secreted via exosomes, thus forming matrix vesicles in the extracellular environment (Shapiro et al., 2015). The preformed hydroxyapatite crystals are deposited in an oriented fashion on a scaffold provided by collagens and regulated by noncollagenous proteins. Finally, due to the activity of osteoblasts and matrix vesicles, the mineralizing bone ECM is enriched in ions such as calcium and phosphate. The amount of these ions is controlled by phosphatases and calcium chelating-proteins, which trigger their incorporation into the hydroxyapatite crystals and the formation of new crystals (Glimcher, 1981). When the bone matrix is completely mineralized, bone cells become osteocytes, which are interconnected via elongated channels called canaliculi (Boskey, 2007; Golub, 2011).

The process of bone and cartilage matrix mineralization can be easily reproduced in vitro when supplementing the culture medium of immature osteoblasts with factors important for proper matrix production. This strategy has been widely used to promote full differentiation of bone and cartilage progenitors from different sources such as mesenchymal cell lines, bone marrow cells (Kamalia et al., 1992), induced-pluripotent stem cells (iPSC) and ESC (Csobonyeiova et al., 2017), as well as NCC (Calloni et al., 2009; Coelho-Aguiar et al., 2013). Among these factors, ascorbic acid, β-glycerolphosphate and dexamethasone are the main components to allow bone matrix formation in vitro. Dexamethasone, a synthetic

glucocorticoid, induces mineralization by several mechanisms as it increases transcriptional activity of various key bone regulators (Shalhoub et al., 1992). Acid ascorbic induces collagen matrix production and activation of osteocalcin (Xiao et al., 1997) while β-glycerolphosphate is the source of phosphate ions when hydrolyzed by alkaline phosphatase (Bellows et al., 1991). Of note, in this Thesis, we used a medium supplemented with these factors to induce terminal differentiation of osteoblasts and chondrocytes in trunk NCC cultures (*see Results section; Article n°2*).

III.3. Molecular aspects of osteogenesis and chondrogenesis

The major transcription factors that act in the commitment of chondrocytes and osteoblasts are Sox9 and Runx2, respectively. *Sox9* (belonging to the SoxE subfamily of transcription factors) is a gene containing a high mobility group box-domain of DNA binding, expressed by premigratory and migratory NCC (Cheung et al., 2005; Cheung, 2003). In later stages, it is restricted to cells of chondrocytic lineage (Haldin and LaBonne, 2010, for a review). Sox9 activates many genes of the chondrogenic pathway as cited above, such as *collagen type 2α1*, *collagen type 11α2* and *aggrecan* (Bridgewater et al., 1998; Lefebvre et al., 1997) and induces *Sox5* and *Sox6* genes, encoding factors that are also involved in chondrogenesis (Akiyama et al., 2002; Mori-Akiyama et al., 2003). *Sox9* appears to be necessary for chondrocyte development, as chondrogenesis is entirely blocked in the absence of this gene (Bi et al., 1999), and osteochondrogenic progenitors are all derived from *Sox9*-expressing cells during mouse embryogenesis (Akiyama et al., 2005). Moreover, mutations in *SOX9* in human lead to a disease called campomelic dysplasia, a semi-lethal skeletal malformation syndrome (Wagner et al., 1994). As Sox9 is a major factor for cartilage formation in general, endochondral ossification is greatly impaired in the absence of this transcription factor. However, during cartilage maturation, *Sox9* should be repressed in hypertrophic chondrocytes as it blocks the expression of genes involved in matrix deposition and blood vessels invasion such as *collagen 10* and *vascular endothelial growth factor* (VEGF) (Hattori et al., 2010; Leung et al., 2011).

Regarding the osteogenic lineage, Runx2 was the first specific transcription factor described (Ducy et al., 1997; Komori et al., 1997) and until now, the earliest known osteogenic-specific marker during embryogenesis. Runx2 is part of the Runt family of transcription factors, which also comprises Runx1, essential for fetal liver-derived hematopoiesis (Wang et al., 1996)

and Runx3, critical for thymopoiesis and neurogenesis in the dorsal root ganglion (Inoue et al., 2002; Levanon et al., 2002). During early skeletal development, *Runx2* is expressed by cells of the osteoblast lineage but not in fully differentiated chondrocytes (Ducy et al., 1997; Ducy, 2000). Thus, *Runx2* expression is restricted to hypertrophic chondrocytes and the osteoprogenitors of the perichondrium region in endochondral bones (Inada et al., 1999; Karsenty et al., 2009). In contrast, in dermal bones, Runx2 is detected until the differentiation of osteoblasts. Particular aspects of the molecular control of *Runx2* expression and craniofacial ossification by NCC will be further discussed in *section IV.3*.

After targeted deletion of *Runx2*, heterozygous mice show skeletal abnormalities, resembling a human disease named cleidocranial dysplasia (Otto and Thornell, 1997). Homozygous mutation led to the total absence of osteoblasts and bone formation whereas development of cartilage was almost normal (Otto and Thornell, 1997; Komori et al., 1997). Therefore, Runx2 appears to be a key regulator for proper osteoblast differentiation. Mesenchymal cells expressing *Runx2* are committed towards an osteoblastic lineage as Runx2 regulates a set of bone marker genes, such as *osteocalcin*, *collagen type 1α1*, *bone sialoprotein* (BSP) and *osteopontin* (Ducy et al., 1997; Ducy and Karsenty, 1995; Sato et al., 1998). As discussed above (*sections III.1 and III.2*), these proteins are necessary for osteoblast and bone matrix maturation. Furthermore, Runx2 appears to act together with Runx3 to regulate the expression of *collagen 10*, *osteopontin*, *BSP2* and *MMP13* in hypertrophic chondrocytes (Komori, 2010). In addition, *VEGF* is upregulated by Runx2 in hypertrophic chondrocytes, thus helping to promote cartilage invasion by blood vessels during endochondral ossification (Zelzer et al., 2001). In summary, Runx2 possesses pleiotropic actions during different events of bone and cartilage formation.

Additionally, a second bone-specific transcription factor, Osterix, reinforces osteoblast lineage commitment in all skeletal elements (Nakashima et al., 2002). It is expressed at later stages when compared with Runx2, mainly in mesenchymal condensations of membranous bones and the perichondrium surrounding the cartilage template during endochondral ossification (Nakashima and De Crombrugghe, 2003). Osteoblast differentiation is completely blocked in *Osterix* knockout mice, despite the presence of Runx2, showing that Osterix acts downstream of Runx2. Interestingly, in *Osterix*-null mice, even in membranous skeletal elements, skeletal progenitors express *Sox9* and *collagen type 2α1*, suggesting a cell fate change towards the chondrocytic lineage (Nakashima et al., 2002). As a result, the combined action of Runx2 and Osterix leads to the specification of pre-osteoprogenitors towards immature osteoblasts. Interestingly, Runx2 dependence of bone differentiation is stage-

dependent, as *Runx2* must be downregulated for full differentiation of osteoblasts (Liu et al., 2001; Geoffroy et al., 2002). Osterix, in turn, is necessary for immature and mature osteoblasts to maintain bone homeostasis (Baek et al., 2010) (**Figure 10**).

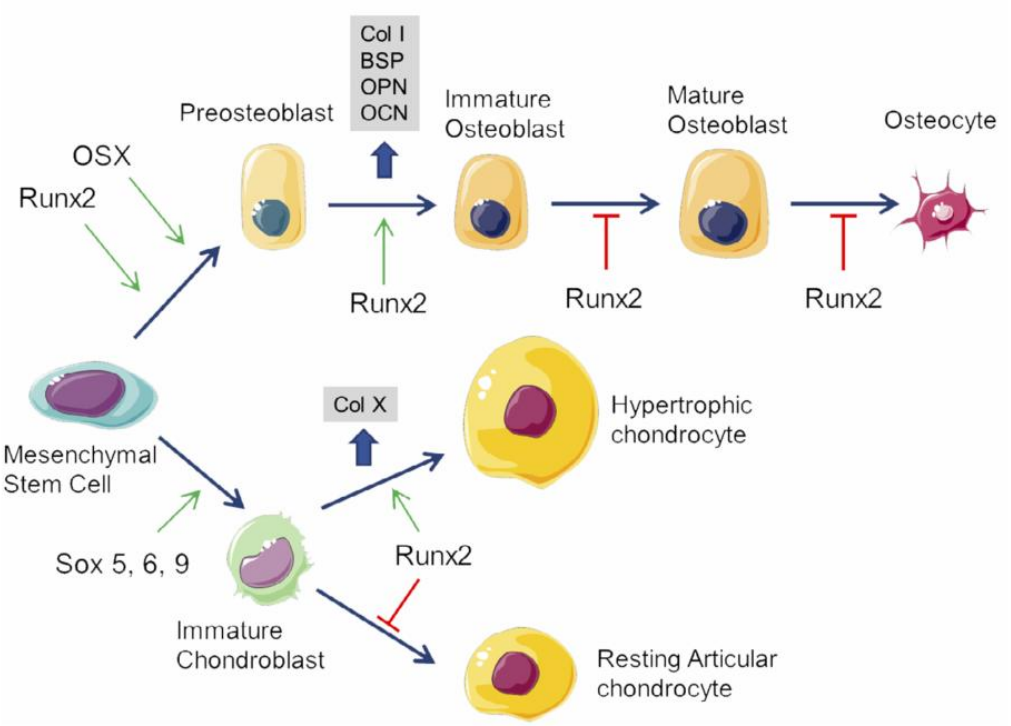

Figure 10: Regulation of osteoblast and chondrocyte differentiation. Runx2 is crucial for the specification of mesenchymal stem cells to the osteoblast lineage and positively influences early stages of osteoblast differentiation. Osterix (OSX) acts downstream of Runx2 to reinforce the commitment of preosteoblasts. Runx2 is also involved in the expression of bone matrix genes *Collagen* (Col) 1, *osteopontin* (OPN), *bone sialoprotein* (BSP), and *osteocalcin* (OCN). For differentiation of mature osteoblasts, *Runx2* needs to be downregulated. Chondrocyte differentiation is initiated by Sox 5/6 and Sox9-mediated mesenchymal condensation. Runx2 induces expression of *ColX* during hypertrophic chondrocyte differentiation whereas it inhibits immature chondrocytes from adopting the phenotype of permanent cartilage (Bruderer et al., 2014).

III.4. Adipogenesis

The adipose tissue has an important function for the storing and mobilization of fat energy in the form of triacylglycerols. Adipose tissues are classified into two types according to their function and the adipose cell types present (Sarjeant and Stephens, 2012, for a review). Firstly, the white adipose tissue (WAT), the predominant fatty tissue in avian and mammals, has essential role in energy homeostasis and production of hormones such as leptin and adiponectin (Zhang et al., 1994; Scherer et al., 1995). WAT is characterized by the presence of

white adipocyte cells, which are morphologically identified by the presence of a unilocular lipid droplet of fat occupying the majority of the cytosol, while the nucleus is usually compressed between the fat and the plasma membrane. Secondly, the brown adipose tissue (BAT), classically described in human neonates and rodents, is important for the thermogenesis mediated by combusting lipids and carbohydrates via uncoupling protein 1 (UCP1) action in the mitochondria. The adipocytes in BAT are morphologically characterized by multilocular lipid droplets (Cannon and Nedergaard, 2004). For many years, it was believed that brown adipocytes exist in human only in the early life; however, recent findings show that adult humans do have BAT, although restricted in some areas such as the neck and the supraclavicular area (Lidell et al., 2013; Cypess et al., 2013; Jespersen et al., 2013). Moreover, another interesting finding is that some brown-like adipocytes are found interspersed in WAT in both human and rodent adults. These cells are called “brite cells” or “beige cells” (Wu et al., 2012; Bartelt and Heeren, 2014; Cereijo et al., 2015, for recent reviews) (**Figure 11**). Both beige and brown adipocytes have similar phenotypic and functional characteristics, expressing proteins controlling nonshivering thermogenesis, such as PRMD16 and UCP1. Nevertheless, the cellular origin of these adipocyte types (i.e. brown, white, and beige) is still poorly known. Brown adipocytic cells are usually associated with the myogenic lineage expressing Myf5 transcription factor, while beige and white adipocytes are Myf5-negative. Beige and white adipocytes can originate from the same bipotent precursors or undergo transdifferentiation depending on the environment conditions (Lee et al., 2012; Rosenwald et al., 2013). Interestingly, in birds, although some avian adipocytes containing multilocular lipid droplets were found in subcutaneous adipose tissues and in vitro limb bud cultures, BAT has never been described in these species (Barré et al., 1986; Saarela et al., 1991; Mezentseva et al., 2008). Nevertheless, the existence of “beige” adipocytes in birds should be examined. Regarding embryonic tissue origin, it is assumed that fat tissues arise from the mesoderm in trunk and limbs, although trunk NCC in culture also can yield adipocytes (Billon et al., 2007; Coelho-Aguiar et al., 2013). In the head, adipocytes can be derived from mesenchymal NCC, present in the face, neck, salivary glands, and ear regions in chick and mouse (Le Lièvre and Le Douarin, 1975; Billon et al., 2007).

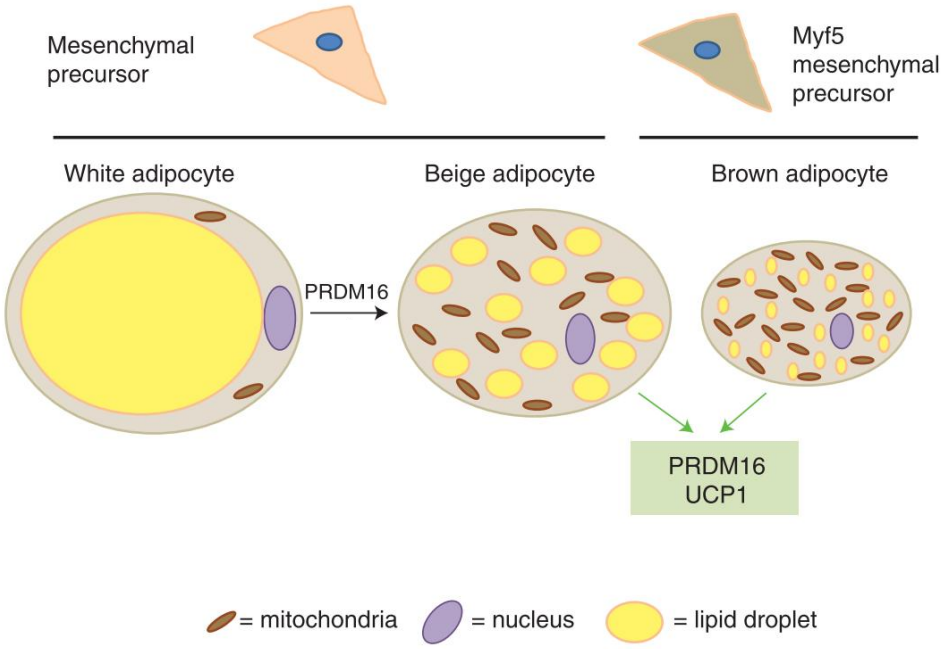

Figure 11: Adipocytic cell types. White and brown adipocytes are derived from distinct precursor cells and have distinct morphological characteristics. Brown adipocytes are derived from Myf5-expressing precursor cells whereas the early marker for white adipocytes is still unknown. Mature brown adipocytes contain multilocular lipid droplets and are mitochondria-rich. PRDM16 is present in both brown and white adipocytes and is a major factor in transforming white adipocytes into beige adipocytes (adapted from Sarjeant and Stephens, 2012).

The early aspects of adipocyte specification from mesenchymal progenitors are still scarcely known. One main reason is the fact that most studies in adipogenesis are performed in vitro, using fibroblast-like preadipocyte cell lines, which are in an already advanced stage of commitment (Green and Meuth, 1974; Green and Kehinde, 1976). Nevertheless, early studies could successfully identify a specific transcription factor, peroxisome proliferator-activated receptor γ (PPARγ), necessary and sufficient for adipogenesis in both brown and white adipocytes (Tontonoz and Spiegelman, 2008). In vivo, PPARγ is required for survival and differentiation of all adipose tissues during development and adult life (Barak et al., 1999; Rosen et al., 1999; Imai et al., 2004; Wang et al., 2013). Therefore, *PPARγ* is considered as a master gene for adipogenesis. Accordingly, a progression of the sequential activation of a set of transcription factors was later described resulting in *PPARγ* expression followed by full adipocyte differentiation (**Figure 12**). Briefly, members of AP-1, KLFs and C/EBP families of transcription factors act to clonally expand the pre-adipocytes and induce activation of *PPARγ*. Afterward, PPARγ and co-activators, such as C/EBPα, STAT5A, KLF and SREBP-1 trigger further steps in adipogenic differentiation, promoting the activity of genes involved in the metabolism of lipids and carbohydrates, like *FAPBP4* (fatty acid binding protein 4), *GLUT4* (responsive

glucose transporter insulin 4) and *GPDH* (glycerolphosphate dehydrogenase) (Sarjeant and Stephens, 2012; Lefterova and Lazar, 2009).

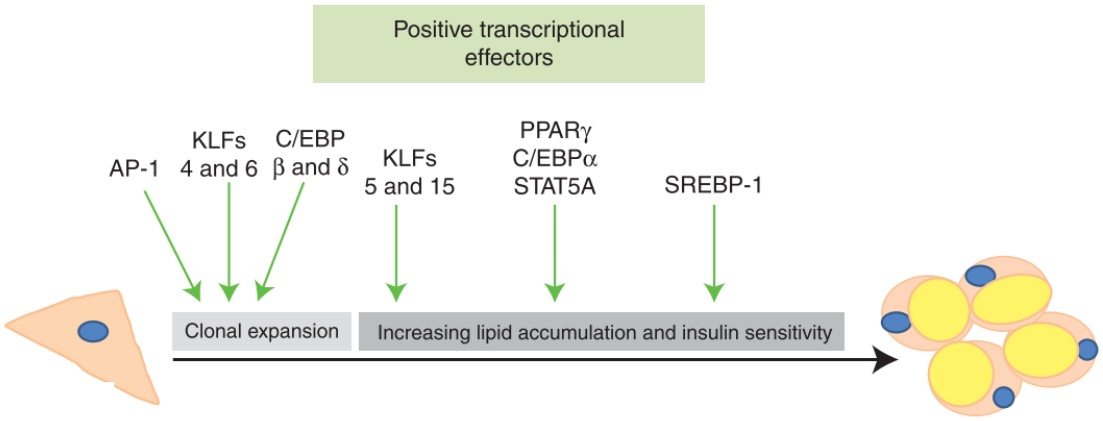

Figure 12: Molecular players in the adipocytic differentiation cascade. Many transcription factors are induced during adipocyte differentiation. Some of these, like members of the AP-1, KLFs and C/EBP families, are induced during clonal expansion. Other transcription factors, like PPARg and its co-activators, promote adipocyte differentiation (adapted from Sarjeant and Stephens, 2012).

IV. The NC and its mesenchymal derivatives

The cephalic NC largely contributes to the head mesenchymal tissues. In avian species, nearly the whole head skeleton is of NC origin, except part of the otic vesicle and the occipital region, which are derived from the somitic and cranial paraxial mesoderm (Le Lièvre and Le Douarin, 1975; Johnston et al., 1973; Couly et al., 1993, 1996; Köntges and Lumsden, 1996) (**Figure 13**). In addition, ocular and periocular structures, such as corneal stroma and endothelium, sclerotic cartilage, choroid membrane and ciliary muscles are NC-derived (Couly et al., 1993, 1996, 1998; Creuzet et al., 2005b) The cephalic NC also yields the dermis of the face and ventral neck, the connective tissue associated with muscle fibers and tendons and the adipocytes (Le Lièvre and Le Douarin, 1975; Billon et al., 2007). It also contributes to the formation of forebrain meninges and many tissues of the cardiovascular system, such as the heart septum and valves, the muscle-connective wall of large arteries, and the pericytes and smooth muscle cells lining blood vessels of the head (Le Lièvre and Le Douarin, 1975; Kirby and Stewart, 1983; Kirby et al., 1983; Etchevers et al., 2001). Finally, the mesenchymal components of the salivary, thyroid and parathyroid glands are of NC origin (Bockman and Kirby, 1984).

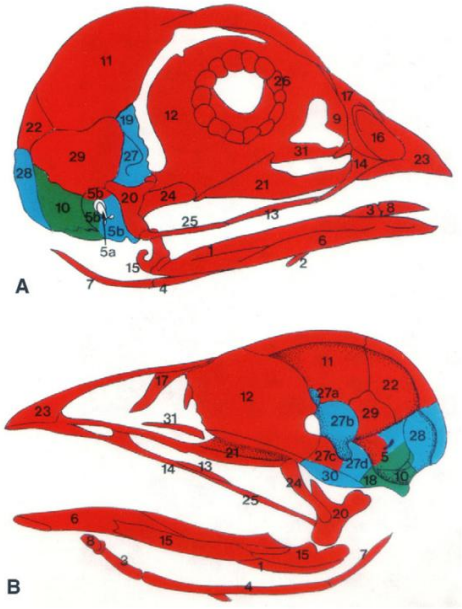

Figure 13: NC contribution to the craniofacial skeleton in avian species. (A) Right external view. (B) Right internal view. Red, skeleton of NC origin; blue, skeleton of cephalic mesoderm origin; green, skeleton of somitic origin (Couly et al., 1993).

In this Chapter, we will briefly discuss the NC and mesoderm interactions during development of mesenchymal tissues in the head, since some of these aspects are discussed in part 1 of this Thesis. In addition, we address some evolutionary aspects related to the

mesenchymal fate of NCC and further discuss the regulatory mechanisms involved in skeletogenesis by NCC, the main topic of part 2 of this Thesis.

IV.1. NC and mesoderm interactions in the cranial mesenchyme: role of *Six1*

Craniofacial development relies on a coordinated growth and differentiation of many embryonic structures, such as the neuroepithelium, the ectodermal placodes, the foregut endoderm and the mesenchymal tissues, which can be either mesoderm- or NC-derived (ectomesenchyme). Since the earliest stages of head development, the cells of the cranial NC and cranial paraxial mesoderm are closely located and they later intermingle and cooperate to the proper differentiation and morphogenesis of many presumptive organs and tissues. How these mesenchymal cells orchestrate their communication, and which tissues depend on this interaction, is briefly debated in this chapter.

According to the fate-mapping of the musculo-skeletal and vascular derivatives in the avian embryo, determined in quail-chick chimeras (Couly et al., 1992, 1993, 1995), the mesoderm contribution to the head tissues arise from three mesoderm subdivisions: first, the somitic mesoderm, which, forms only a part of the otic capsule and cranial base (the baso and exo-occipital bones) and tongue/pharyngeal muscles; second, the cephalic paraxial mesoderm, which also contributes to part of the otic capsule, in addition to the supraoccipital and sphenoid cartilaginous bones and to jaw, extraocular and facial muscles; third, the prechordal mesoderm, anteriorly, giving rise to the extraocular muscles. Moreover, these mesodermal components form additional mesenchymal tissues such as blood vessel endothelia, dermis and connective tissues, mainly in the posterior head and dorsal neck (Noden, 1983; Couly et al., 1992, 1995). In contrast, the cranial NC is at the origin of the same types of tissues, except vascular endothelia, in most head regions, with a remarkable contribution to the skeleton of the entire face and to a large part of the skull. In addition, it provides many ocular (cornea) and periocular structures (Creuzet et al., 2005b).

The development of head mesodermal cells and NCC is deeply connected. For instance, the paraxial mesoderm secretes signals necessary for NC induction and for trunk NCC migration through the rostral part of sclerotome (*see section I.2*). In the posterior head, both NCC and mesodermal cells home to the forming BAs, where they occupy two separate domains inside the BA mesenchyme: the mesodermal cells occupy the core of BAs, whereas

the NCC essentially surround them, resulting in a physical delimitation of the mesodermal domain (presumptive myoblasts) from the NC mesenchyme and surface ectoderm. This first regionalization is probably important for organizing, inside the BAs, the coordinated development of the presumptive skeletal elements and tendons, which are mainly NC-derived, with the muscular and endothelial mesodermal derivatives (Couly et al., 1992, 1993, 1995; Hacker and Guthrie, 1998; Noden and Trainor, 2005; Grenier et al., 2009; Trainor and Tam, 1995). Nevertheless, a significant number of NCC can be found within the mesodermal core of BAs, which intermingle with myogenic precursors to give rise to connective cells, reinforcing the idea of a coordinated development to establish the future muscle and its connective tissues (Grenier et al., 2009).

At later stages of development, NCC yield connective tissue and tendons, helping to assemble the head muscles and promoting adequate insertion of the skeletal elements (Couly et al., 1992; Noden and Trainor, 2005; Grenier et al., 2009). In addition, crosstalk between these cell types has been shown to influence further muscle development. Although NCC are not essential for myoblasts early differentiation, lack of NCC impairs the correct patterning of head muscles, in amphibian, mice and chick embryos (Rinon et al., 2007; Noden and Trainor, 2005). In the absence of NCC, myoblasts are maintained in a proliferative state and failed to undergo full differentiation into myofibers, probably due to the lack of positional cues, which would control the rate of proliferation/differentiation of myoblasts (Rinon et al., 2007).

Regarding the formation of the head skeleton, in bones with both NC and mesoderm origin, in the cranial base (basi-pre and basi-post sphenoid), it has been proposed that NCC and paraxial mesodermal cells not intermingle; instead, what occurs is the fusion of skeletal elements derived from these distinct mesenchymal cells (Noden and Trainor, 2005). Nevertheless, the accurate communication between both tissues is fundamental for the establishment of NC/mesoderm boundaries, such as in mammalian coronal suture, which is formed at the border between NC-derived frontal bone and mesoderm-derived parietal bone. If NC-mesoderm interactions are perturbed, precocious calcification of this suture can happen and generates a form of craniosynostosis, a human congenital disease exhibiting many craniofacial and brain deformities (Morriss-Kay and Wilkie, 2005). Interestingly, it has been shown that the paraxial mesoderm composes the main undifferentiated domain of the coronal suture in mice, and its proper development depends on *Engrailed 1* expression, to avoid invasion by NCC from the frontal osteogenic zone (Deckelbaum et al., 2012). Engrailed 1 transcription factor also controls the activity of *Msx2* and *Twist1*, working jointly to maintain

NC/mesoderm boundary and coronal suture integrity in mammals (Merrill et al., 2006; Ting et al., 2009).

Several molecular players are involved in the coordinated regulation of differentiation of NC- and mesoderm-derived tissues. Tzahor and colleagues (2003) have found that Wnt and BMP signals have repressive effects on myogenesis in the head paraxial mesoderm, while NCC produce their antagonists, such as Frzb and Noggin, thus helping to balance the consequences of these signals in the myogenic population (Tzahor et al., 2003). Moreover, in *Xenopus* embryos, inhibition of FoxN3 transcription factor generates defects in head NC-derived skeleton, with indirect effects on cranial muscle patterning, as shown after NC ablation in the chick embryo (Rinon et al., 2007; Schmidt et al., 2013). In summary, although some molecular players have been described to play a role in the interaction of mesodermal and NC mesenchymal tissues, how these tissues coordinate their development is still poorly known.

In this regard, we aimed to investigate *Six1*, a gene expressed at head mesenchyme in early stages of chick and mice development (Laclef et al., 2003b; a; Sato et al., 2012; Garcez et al., 2014). Six1 belongs to the Six homeobox family of transcription factors, and it is one of the homologs of *Sine Oculis*, a gene required for eye development in *Drosophila* (Kawakami et al., 2000). *Six1* function usually involves the *Pax-Six-Eya-Dach* gene network to control many organ development (Kumar, 2009). In vertebrates, it has been shown that *Six1* gene is important for the development of a variety of tissues and organs, including placodal derivatives, kidney, somitic muscles and several sensory systems (Sato et al., 2012; Kumar, 2009). Besides lack of kidney and thymus, *Six1* null mice exhibit defects in the inner ear, nasal cavity and in various cranial NC and mesoderm derivatives. NC derived skeletal elements such as squamosal, mandibular and maxillary bones are shorter after *Six1* knockout whereas Meckel's cartilage and hyoid bone are disorganized. They also present hypoplasia of the somitic mesoderm-derived tongue muscles (Laclef et al., 2003a; b). In human, *SIX1* haploinsufficiency leads to the branchio-oto-renal syndrome, an autosomal dominant developmental disorder, characterized by hearing loss and branchial arch defects (Kochhar et al., 2008; Ruf et al., 2004).

In chicken embryos, members of the Six family of transcription factors were recently described as playing a significant role in the development of craniofacial NC-derived structures (Garcez et al., 2014). *Six1* depletion, by electroporation of dsRNA targeting *Six1* in early NCC, resulted in smaller NC-derived skeletal elements (e.g. nasal, Meckel and hyoid cartilages), together with defects in pallial and subpallial brain structures. In addition, the combinatory inhibition of *Six* genes (*Six1*, *Six2*, and *Six4*) triggered a strong facial hypoplasia, partially due to

the truncation of craniofacial skeleton, and brain development was greatly impaired. Interestingly, the phenotype of global silencing of *Six* genes resembles the one obtained after *Hoxa2* ectopic expression in premigratory NCC (Creuzet et al., 2002; Garcez et al., 2014). Moreover, electroporation of *Hoxa2* construct in premigratory cephalic NCC led to inhibition of *Six1*, *Six2* and *Six4* expression, suggesting an interaction between these two families of transcription factors during head morphogenesis (Garcez et al., 2014). In this regard, it was previously reported that Hoxa2 interacts with *Six2* promoter, directly inhibiting *Six2* expression in the mouse BA2 (Kutejova et al., 2005, 2008).

In summary, all these data show that *Six1* is a gene expressed in tissues of varied embryonic origins, hence leading to pleiotropic defects when its expression is disrupted. Nevertheless, *Six1* precise function is not completely understood, especially in head mesenchymal tissues. In this regard, since *Six1* appears to be important for both NC- and mesoderm-derived mesenchymal cells, it should be interesting to investigate whether it can play a role in the crosstalk between these cell types during formation of head structures. As a first step in the understanding of this issue, we aimed at better defining the embryonic origin of the *Six1*-expressing cell populations that contribute to the head mesenchyme, to obtain further clues about the functions of *Six1*. In part 1 of this Thesis, we present a study of the spatio-temporal dynamics of *Six1* expression, and the respective contribution of NC versus mesoderm to the generation of *Six1*-expressing territories in the head mesenchyme and its derivatives.

IV.2. Evolutionary aspects

The NC is a structure unique to vertebrates, and its evolution is closely related to the evolution of the vertebrate phylum. Because of this, many current studies focus on a better understanding of the NCC origin. There is a debate about the existence of an ancestral “pre-NC precursor” among chordates, represented by ectodermal cells expressing typical components of the gene regulatory network of the NCC (Delsuc et al., 2006; Jeffery et al., 2008; Abitua et al., 2012). This particular aspect of NC evolution has been reviewed recently by Green and collaborators and will not be further addressed in this Thesis (Green et al., 2015).

The NC generates a remarkable array of cells and tissues overcoming its ectodermal origin and being thus considered as a “fourth germ layer”. The appearance of this structure is the basis for the evolution of critical features specific of vertebrates (Hall, 2000; Le Douarin and Dupin, 2014). Gans and Northcutt, in their seminal article, put forward a hypothesis for

the evolution of the "New Head" in vertebrates (Gans and Northcutt, 1983). They proposed that vertebrate innovations, raised from the rostral ectoderm (i.e anterior brain, NC and placodes), allow the development of a more complex brain associated with sense organs derived from placodes and, finally, the development of a complex masticatory apparatus formed by a NC-derived skeleton. Additionally, Gans and Northcutt suggested that the NC has a central role in this process, by originating novel structures and influencing the development of the forebrain and the placodes. For instance, the vertebrate skull, which is mainly derived from NCC, provided physical protection to encephalic vesicles and, as a consequence, allowed the increase of brain volume during evolution. Interestingly, recent findings show that during development, NCC crucially influence the morphogenesis of the telencephalon, thalamus and optic tectum by secreting factors involved in cell survival and patterning of the forebrain (Creuzet, 2009; Le Douarin et al., 2012; Aguiar et al., 2014). In addition, the proper development of cranial sensory ganglia depends on a close interaction between placodal neurons and NC-derived glia (Fleenor and Begbie, 2014, for a review). In sum, it has been proposed that the appearance of these structures would lead to a switch from the filter-feeding lifestyle of the basal chordates to a predatory way of life, more adapted to the environment and successfully selected during the evolution of the vertebrate phylum (Northcutt and Gans, 1983).

Regarding skeletal evolution, the first evidence of mesenchymal cells derived from the NC in vertebrates is given by the cranial and pharyngeal cartilages in lamprey and hagfish (McCauley and Bronner-Fraser, 2003; Langille and Hall, 1988). After agnathan phylogenetic divergence, mineralized tissues composed of dentin appeared in the odontodes of Conodonts fossils corresponding to the most basal stem of gnathostomes (Donoghue et al., 2006; Baker, 2008, for a review). Dentin is a mineral only produced by NCC in extant vertebrates and, therefore, it is considered that the first mineralized tissues of vertebrates are of NC origin (Sansom et al., 1992). Later on, dentin was found composing the superficial dermal armor of fossilized primitive fish Ostracoderms (Sansom and Albanesi, 2005; Smith, 1991). This finding suggests that, in these animals, the whole exoskeleton was NC-derived, and that early in evolution, the mesenchymal fate was thus present along the entire axial level of the NC, i.e. in both cephalic and trunk NC. Nevertheless, during evolution, the NC-derived skeleton has become restricted to the craniofacial region in amniotes.

In anamniotes, evidence of trunk NC contribution to mesenchymal derivatives has been demonstrated in some species, although some controversies exist. For instance, in zebrafish, some authors argue for a trunk NC origin of the caudal and dorsal fin bony rays

(Smith et al., 1994; Kague et al., 2012), while this ontogeny has been contested by others, defending a mesoderm origin instead (Lee et al., 2013; Kimmel et al., 2001; Mongera and Nüsslein-Volhard, 2013). Similarly, trunk NCC have been suggested to yield the median fin mesenchyme in classical *Xenopus* experiments (Collazo et al., 1993), which has been contradicted by recent findings (Taniguchi et al., 2015). Furthermore, trunk NC contribution to the bony plastron of turtles has been debated, some authors suggesting a NC origin (Clark et al., 2001; Cebra-Thomas et al., 2007, 2013), while others defend a mesoderm origin (Hirasawa et al., 2013). However, even if discordant data were observed regarding the remnant trunk NC contribution to the anamniote skeleton, trunk NCC skeletogenic ability has been clearly revealed by various in vitro assays in avian and mammalian NCC (discussed in *section II.2*), indicating a dormant mesenchymal ability of trunk NCC, which might represent an "evolutionary memory" of trunk NCC.

IV.3. Regulation of the skeletogenesis of NCC

In Chapter III.3, we discussed the key aspects of skeletogenesis and adipogenesis focusing on master genes that sign commitment towards these mesenchymal lineages (*Sox9*, *Runx2*, *Osterix* and *PPARγ* among others). Nevertheless, the upstream factors involved in the molecular control of NCC mesenchymal fate are not completely understood, and some recent findings highlight this issue. In this Chapter, we will focus on the particular signaling pathways, transcription factors and epigenetic mechanisms, which play a role in the early steps of NC skeletogenesis by acting either on the premigratory and migratory NCC or on some NC-derived structures. Finally, we discuss some of the factors specifically involved in the regulation of Runx2 in NC osteoprogenitors.

IV.3.1 Early signals involved in NC mesenchymal fate

Upon delamination and migration, NCC express *Sox10* and *Foxd3*, which are described as NC-specifier genes (*see section I.3*). Nevertheless, at later stages of development, their expression becomes restricted to the neuroglial lineage. In addition, Foxd3 is essential for self-renewal, multipotency and melanogenesis repression in NCC (Kos et al., 2001; Mundell and Labosky, 2011; Nitzan et al., 2013). Regarding NC mesenchymal derivatives, Blentic and colleagues have shown that *Sox10* and *Foxd3* are downregulated in chicken and zebrafish NCC homing to BA, and thus, these cells eventually acquire an ectomesenchymal fate, identified by

expression of *Dlx2* and *Dlx5* genes (Blentic et al., 2008). Dlx2 and Dlx5 are responsible for initiating mesenchyme condensation in cartilage and bone in different species (Gordon et al., 2010; McKeown et al., 2005). In addition, FGF signaling is also involved in *Sox10* and *Foxd3* downregulation in NCC (Blentic et al., 2008). In cultures of mouse NC precursors within the BAs, the choice between neural and mesenchymal fate also involves Sox10 through a mechanism regulated by transforming growth factor (TGF) β1. In these cells, TGFβ1 triggers a switch between SoxE factors leading to *Sox10* downregulation and *Sox9* upregulation (John et al., 2011). Similarly, downregulation of *Foxd3* guides NCC towards a mesenchymal fate in mouse embryos as shown by in vivo analysis and in vitro cloning of NCC (Mundell and Labosky, 2011). Taken together, these findings show that Sox10 and Foxd3 reduction in NCC appear to be a common mechanism to specify the mesenchymal fate. Nevertheless, early post-migratory NCC in the BA still possess broad developmental potentials as shown by in vitro cloning experiments of NCC from the BA in the avian embryo (Sieber-Blum et al., 1993; Ito and Sieber-Blum, 1993) and in Wnt1CreR26R mouse (Zhao et al., 2006). These results suggest that additional signals are essential for a complete commitment of NCC.

Twist1 bHLH-containing transcription factor is expressed by migratory NCC and has also an important role in NC skeletogenesis. *Twist1* conditional deletion in murine NCC impairs survival of NCC migrating to BA and frontonasal mesenchyme (Bildsoe et al., 2009). Patients with heterozygous *TWIST1* null mutations present a craniosynostosis phenotype with increased bone formation in the cranial sutures (El Ghouzzi et al., 1997). In zebrafish embryos, it has been shown that Twist1 potentiates FGF signaling and directly activates *fli1a*, a gene only expressed by mesenchymal lineages. In contrast, Twist1 is inhibited by *Id2a* gene to induce a non-mesenchymal fate via BMP action (Das and Crump, 2012). Furthermore, Twist1 is important for Runx2 regulation at later stages of osteogenesis (see *section III.3*).

As depicted above, FGF and TGFβ signaling regulate *Sox10* and *Foxd3* expression in NCC. Besides the regulation of these genes, TGFβ induces *Sox9* expression in the mandibular arch. Moreover, conditional knockout of *Tgfbr2* in NCC leads to delayed chondrogenesis and tendonogenesis (Oka et al., 2008). In avian cranial NC cultures, FGF2 promotes bone and cartilage differentiation (Sarkar et al., 2001; Abzhanov et al., 2003). Likewise, constitutively active FGFR1 and FGFR2 induce in vitro chondrogenesis in quail NCC (Petiot et al., 2002) and several craniosynostosis syndromes in human (reviewed by Twigg and Wilkie, 2015). FGF8 increases *Sox9* and *Collagen 2* in vivo (Abzhanov and Tabin, 2004) and hypermorphic *Fgfr1* mutant mice display craniofacial defects (Partanen et al., 1998). Recent studies in mouse and

chick embryos have shown that a novel FGF8 co-receptor, named Cubilin, is involved in FGF8 effect on the survival of mesencephalic premigratory NCC (Cases et al., 2013).

Shh is one of the key factors implicated in NC skeletogenesis. Shh ligands are secreted from several head tissues such as the prechordal plate, the forebrain and the pharyngeal endoderm, and Shh signals in a paracrine way to the NC-derived mesenchyme. Consequently, blocking Shh signaling leads to severe head skeleton abnormalities related to NC survival, proliferation and patterning of skeletal elements in mice (Chiang et al., 1996; Jeong et al., 2004; Billmyre and Klingensmith, 2015) and chick (Ahlgren and Bronner-Fraser, 1999; Brito et al., 2006). Recently, Shh binding to CDON dependence receptor appeared to be a mechanism whereby Shh promotes cell survival (Delloye-Bourgeois et al., 2014). In addition, Shh works synergically with FGF8 in promoting chondrogenesis (Abzhanov and Tabin, 2004). Finally, Shh greatly enhances in vitro chondrogenesis by cephalic and trunk NCC (Calloni et al., 2007, 2009). Another member of Hedgehog family, Indian Hedgehog has a strong osteogenic activity during calvarial development, since its loss leads to a reduction in bone size and a delay in matrix mineralization (Lenton et al., 2011).

Members of Six family of transcription factors (Six1, Six2, and Six4) have also been described as important factors during development of craniofacial NC-derived structures (Garcez et al., 2014; Laclef et al., 2003b). This aspect is discussed in more details in *section IV.1*.

IV.3.2 Overview of upstream regulators of Runx2

Runx2 levels are tightly regulated in osteoprogenitors, directly or indirectly, by interactions with many transcription factors.

As main positive regulators, we can cite Dlx factors, Foxo1, Msx1/2, and SATB2. *Dlx* is a family of homeobox genes with crucial roles in BA dorso-ventral patterning (Minoux and Rijli, 2010). *Dlx5* mutant mice exhibit multiple defects in craniofacial structures since Dlx5 activates the expression of a set of osteogenic genes including *Runx2* (Depew et al., 1999; Lee et al., 2005). Interestingly, in calvarial suture mesenchyme, *Dlx5* is induced in osteoblast precursors by BMP2, and thus increases the expression of osteogenic genes in this tissue including *Runx2* (Holleville et al., 2003, 2007). Interestingly, Osterix can act as a co-factor of *Dlx* genes to promote osteogenesis by calvarial osteoblasts (Hojo et al., 2016). Another important factor in *Runx2* regulation is Foxo1, which directly activates *Runx2* expression (Teixeira et al., 2010). Likewise, Msx2 is an upstream factor of *Runx2*, as *Msx2* downregulation leads to a strong

reduction in *Runx2* expression (Aïoub et al., 2007). In vitro, *Msx2* can bypass the action of Runx2 by inducing the expression of *Osterix* in mesenchymal cells deficient for *Runx2* (Matsubara et al., 2008). Also, Msx1 and Dlx5 exert a synergistic action in osteogenesis of the mouse frontal bone (Chung et al., 2010). In contrast, Msx2 inhibits chondrogenesis by repression of *Sox9* in migrating NCC (Semba et al., 2000; Bhatt et al., 2013, for a review) Finally, SATB2 was found to directly interact with Runx2 to enhance its activity (Dobreva et al., 2006).

Some transcription factors are known to inhibit *Runx2* expression like Twist1/2; Twist1 being present in the skull while Twist2 is localized in the limb skeleton. Twist1/2 binds to the Runx2 protein preventing Runx2 access to its target gene promoters and thus inhibiting the early differentiation of osteoblasts (Bialek et al., 2004; Isenmann et al., 2009). Eph-ephrin signaling appears to be an effector of Twist1 to partition osteogenic and non-osteogenic territories in the coronal suture (Ting et al., 2009). Moreover, *Sox9*, the master gene for chondrogenesis, directly interacts with Runx2 to block its activity (Zhou et al., 2006). Although the mechanism of action is not completely understood, other factors such as Sox8, p53, PPARγ and Hoxa2 were shown to reduce *Runx2* expression (Schmidt et al., 2005; Lengner et al., 2006; Lecka-Czernik et al., 1999; Kanzler et al., 1998). In summary, the signaling cascade of the main regulators of NC differentiation into mesenchymal cells is briefly illustrated in **Figure 14**. Finally, *Runx2* expression has been shown to be tightly regulated by epigenetic mechanisms (Vega et al., 2004; Jeon et al., 2006) but also by several microRNAs (reviewed by Lian et al., 2012).

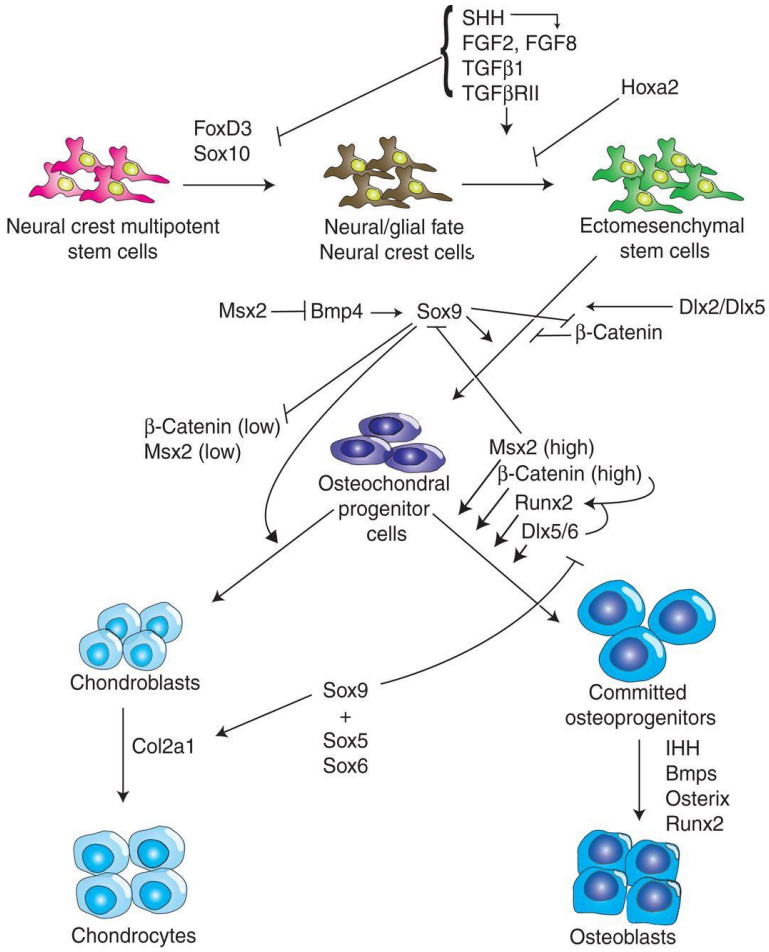

Figure 14: Signaling pathways and transcription factors regulating NC differentiation into osteoblasts and chondrocytes. Schematic representation of signals leading to neural crest cell specification from multipotent progenitors (pink) to neuroglial (brown) or ectomesenchymal (green) cells. This is then followed by differentiation of ectomesenchymal cells into an osteochondral progenitor cell (dark blue) and then bifurcation of potential into chondroblasts or osteoblasts (adapted from Bhatt et al., 2013).

IV.3.3 Epigenetic mechanisms

Emerging body of evidence has shown that post-translational modification and epigenetic mechanisms may play crucial roles in many NCC developmental aspects including mesenchymal fate determination. Recent findings indicate that chromatin modifiers, such as histone deacetylase (Hdac) 8, control accessibility to cis-regulatory sequences of genes such as *Otx2* and *Lhx1*, which are not expressed by mesenchymal NCC (Schmidt et al., 2005): reduction of *Hdac8* in murine NCC leads to abnormal expression of these genes resulting in the loss of cranial specific skeletal elements (Haberland et al., 2009). In addition, another epigenetic mechanism has been identified in zebrafish embryos, which involves the replacement of histone variant H3.3 specifically in the presumptive NCC. Indeed, deficiency in H3.3 significantly reduced the number of mesenchymal NC derivatives. The main hypothesis of this

work is that H3.3-dependent chromatin remodeling triggers either the derepression of enhancers controlling mesenchymal specific genes or the maintenance of chromatin accessibility ("poised state") at these enhancer sequences since the blastula stage. This epigenetic regulation would explain NC notable ability to differentiate into mesenchymal cells (Cox et al., 2012).

Recently, Schwarz and colleagues described a novel role for Ezh2, a core component of polycomb repressive complex 2, which acts as a transcriptional repressor of various target genes by catalyzing the methylation of the lysine 27 of histone 3 (Schwarz et al., 2014). The conditional deletion of this factor in murine premigratory NCC caused many craniofacial defects without affecting NCC migration or homing into BA and nasal bud. Moreover, no defects were identified in neuroglial derivatives. Interestingly, *Ezh2* inhibition led to a massive derepression of *Hox* genes in cephalic NCC supporting *Hox* gene involvement in this phenomenon (Schwarz et al., 2014). A recent paper by Filippo Rijli and colleagues (Minoux et al., 2017) demonstrates an additional role for Ezh2 chromatin modifier in cranial NC development. They discovered that premigratory cranial NCC, from different axial levels of the cephalic NC, for instance, homing to BA or to nasofrontal process, possess a similar state of poised chromatin in cis-regulatory sequences of many positional genes. These results show that the cranial NC is epigenetically equivalent at premigratory stages, which could explain the great NC plasticity. Strikingly, Ezh2 is necessary to maintain this chromatin organization (Minoux et al., 2017).

V. *Hox* genes

V.1. Overview of *Hox* genes effects on development

Hox genes encode a family of homeodomain transcription factors deeply conserved among bilaterians and considered to be fundamental for the evolution of bilaterian body plan. *Hox* genes were originally described in *Drosophila* by the seminal work of Edward Lewis, which described that loss of function mutations of *Bithorax* genes, typically expressed in the posterior segment of the fly embryo, lead to the transformation of the posterior body segment into the anterior one, a phenomenon designated as anterior homeotic transformation (Lewis, 1978). Further studies have shown that *Hox* genes play critical roles in establishing segmental identity along the anteroposterior (AP) axis in vertebrate and invertebrate species (Kessel and Gruss, 1990; McGinnis and Krumlauf, 1992; Carroll, 1995; Duboule and Dollé, 1989; Hrycaj and Wellik, 2016, for a recent review). *Hox* genes are present in a single colinear cluster, designated *Antennapedia* and *Bithorax* complexes, in invertebrates, whereas vertebrates possess multiple *Hox* clusters along different chromosomal territories (**Figure 15**). In amniotes, gene and chromosomal duplications gave rise to 39 *Hox* genes split into four clusters (*HoxA* to *HoxD*). Based on gene sequence similarity and position within the cluster, these genes are subdivided into 13 paralog groups (*Hox1* to *Hox13*) (Scott, 1992; Krumlauf, 1994; Liang et al., 2011).

The most striking characteristics of *Hox* genes, shared by bilaterians, are their spatial and temporal "colinearity". The spatial colinearity is the correspondence between the ordering of a particular *Hox* gene in the chromosome and its regionalized expression pattern along the rostrocaudal axis of the embryo. In other words, the genes located at the 3' extremity of a given *Hox* cluster, such as *Hox* genes from groups 1 and 2, are expressed in the most anterior regions of the embryo, i.e. the hindbrain. Conversely, genes located at the more 5' position in the cluster are expressed in the more posterior regions of the body, such as the tail and the genitalia. The spatial colinearity of successive genes along the cluster thus sharply defines the anterior border of expression of a given *Hox* cluster member (Gaunt et al., 1986; Gaunt, 1988). Additionally, for each *Hox* gene, the timing of activation also follows a sequential order according to its 3'-5'position in the cluster, the *Hox* genes at the 3' end of the cluster being activated first. This principle is called temporal colinearity (Dollé et al., 1989; Izpisúa-Belmonte et al., 1991). As a result of spatial and temporal colinearity, distinct rostrocaudal regions in the

embryo express timely controlled particular combinations of several Hox proteins, or "Hox code", which give the positional identity of a tissue (Duboule, 1994; Hunt et al., 1991).

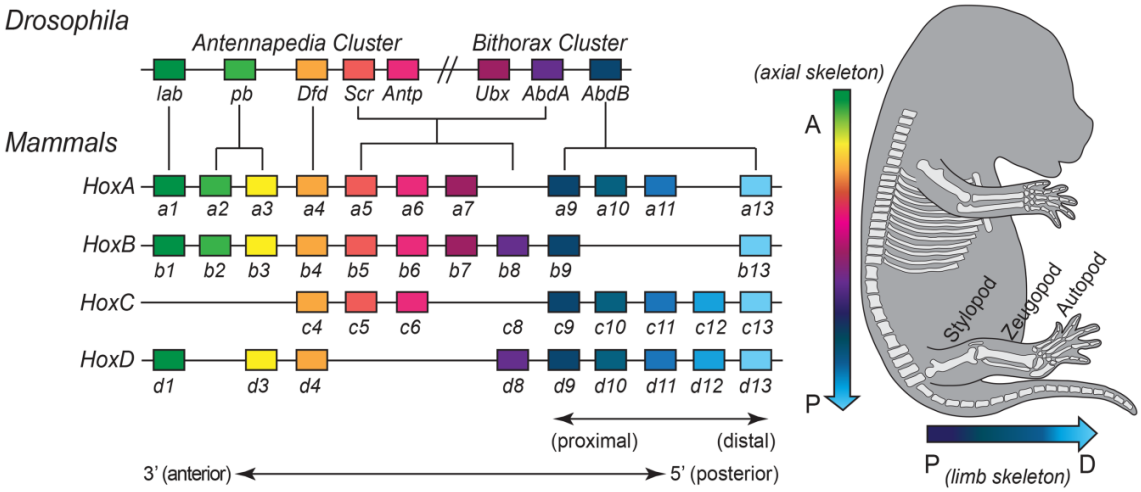

Figure 15: Scheme of *Hox* gene clusters and regional expression in the embryo. Left: Color-coding of *Hox* genes show the conserved relationships between *Drosophila* and mammalian *Hox* genes, and the paralogous relationships within the mammalian cluster. Right: Illustration of the mouse skeleton to evidence the patterning promoted by *Hox* genes at the anterior to posterior (AP) axis of the axial skeleton and the proximal to distal axis (PD) of the limb skeleton (Rux and Wellik, 2016).

As a consequence, the positional information given by combinatorial *Hox* genes is crucial for the patterning of many vertebrate structures. As a well-studied example, in the hindbrain, a nested pattern of *Hox* gene expression is established in every rhombomere, which leads to the specification of unique structures related to each neural segment (Tümpel et al., 2009). This particular Hox code further influences the identity of cranial neuronal subpopulations and nerves, leading to establishment of complex hindbrain neuronal circuits (Narita and Rijli, 2009). In the spinal cord, *Hox* genes are essential for defining motor neuron-muscle specific connectivity (Dasen et al., 2003; Philippidou and Dasen, 2013) whereas, in the vertebral column, a Hox code establishes vertebral specific identities according to the future anatomic organization of the axial skeleton (Kessel and Gruss, 1991; Mallo et al., 2010).

In addition to their highly conserved roles in AP patterning, numerous studies have indicated that *Hox* genes possess pleiotropic functions during development, which may not be associated with the positional information. They are engaged in several processes such as cell survival, autophagy, differentiation and tissue repair (Banreti et al., 2014; Seifert et al., 2015; Rux and Wellik, 2016; Rux et al., 2016).

V.2. *Hox* genes and the NC

In the vertebrate head, the anteriormost limit of *Hox* expression starts at the level of the hindbrain, more specifically at the boundary of rhombomeres r1 and r2 (Prince and Lumsden, 1994). In other words, no *Hox* genes are expressed in the CNS at the levels of the forebrain and the midbrain during development, which are patterned by other homeobox-containing genes such as *Otx* genes (Puelles and Rubenstein, 1993; Boyl et al., 2001). Regarding cephalic NCC, two main domains can be identified with respect to *Hox* genes: a *Hox*-negative domain, which includes the anterior cephalic NCC from posterior diencephalon down to r2 included, homing to the frontonasal process, periocular mesenchyme and first BA; and a *Hox*-positive domain comprising the more caudal cephalic NC, reaching the level of somite 4 in the avian embryo, which includes the NCC homing to the remaining BA (Couly et al., 1996, 2002) (**Figure 16**). Interestingly, the membranous bones in the head exclusively originate from the *Hox*-negative cephalic NCC while endochondral bones are derived from both *Hox*-positive and *Hox*-negative NCC.

Evidence from quail-chick chimera experiments has demonstrated that these two domains of the cephalic NC are not interchangeable, as *Hox*-positive NCC transplanted into anterior *Hox*-negative domain are unable to differentiate into craniofacial skeletal structures such as neurocranium, the nasal capsule, the maxillary bone and the lower jaw, which are produced by *Hox*-negative NCC in normal development. Conversely, after the reverse transplantation, cells of the *Hox*-negative portion of the NC could replace the differentiated tissues of the *Hox*-positive domain. While they formed part of the hyoid cartilage, they kept their *Hox*-negative status (Couly et al., 1998). In addition, after surgical removal of the *Hox*-negative premigratory NC, even a small portion, equivalent to one-third of this NC, could replace the resected NCC region and build a complete facial skeleton (Couly et al., 2002). Thus, these experiments argued for the plasticity of the NCC of the *Hox*-deprived domain and suggested that the cephalic NC mesenchyme potential is limited by their *Hox* gene profile. Indeed, in knockout mice for *Hoxa2*, the most anteriorly expressed *Hox* gene, NCC from the BA2 behave like NCC of the BA1, leading to duplication of a set of BA1 skeletal elements (Rijli et al., 1993; Gendron-Maguire et al., 1993). Further experiments have shown that *Hoxa2* is normally expressed in the BA2 mesenchyme, except in the chondrogenic condensations. However, in *Hoxa2* null embryos, *Sox9* and *Runx2* are upregulated in the entire BA2 (Kanzler et al., 1998).

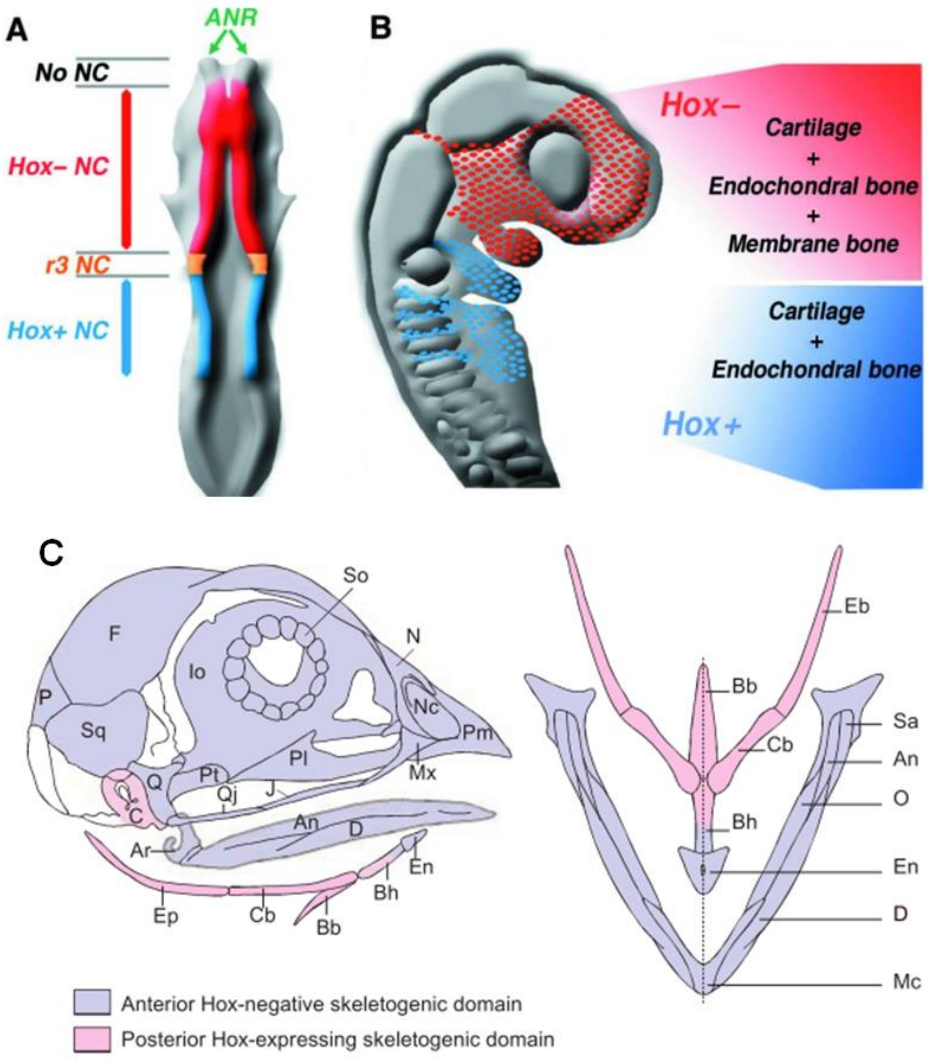

Figure 16: Differential *Hox* gene expression in AP domains of the avian cephalic NC. (A) In a 5ss chick embryo, the cephalic NC is divided into an anterior *Hox*-negative domain (in red) and a posterior, *Hox*-positive domain (in blue). The transition between these two domains corresponds to r3 (in orange). (B) *Hox*-negative NCC (in red) yield cartilages as well as endochondral and dermal bones of the entire upper face and jaws. By contrast, skeletogenic properties of *Hox*-positive NCC (in blue) are limited to chondrogenesis and endochondral ossification in the hyoid structure. (C) The particular contribution of *Hox*-negative and *Hox*-positive NC domains to the craniofacial and hypobranchial skeleton. An, angular; Ar, articular; Bb, basibranchial; Bh, basihyal; C, columella; Cb, ceratobranchial; D, dentary; Eb, epibranchial; En, entoglossum; F, frontal; Io, interorbital septum; J, jugal; Mc, Meckel's cartilage; Mx, maxillary; N, nasal; Nc, nasal capsule; O, opercular; P, parietal; Pl, palate; Pm, premaxilla; Pt, pterygoid; Q, quadrate; Qj, quadratojugal; Sa, supra-angular; So, sclerotic ossicles; Sq, squamosal (Creuzet et al., 2005b; Le Douarin et al., 2004).

On the other hand, forced expression of *Hoxa2* in the whole BA1 led to the reverse homeotic transformation, with BA1 skeletal elements developing into second arch bones in chick (Grammatopoulos et al., 2000) and *Xenopus* embryos (Pasqualetti et al., 2000). Further insights regarding the role of *Hox* genes in NCC came from gain of function studies in which only the NC was selectively targeted. In the chick embryo, ectopic expression of *Hoxa2* in the

Hox-negative domain of cephalic NC resulted in complete loss of the facial skeleton together with severe defects in the brain. Milder effects were observed when *Hoxa3* or and *Hoxb4* were overexpressed in these NCC. Nevertheless, when *Hoxa3* and *Hoxb4* were co-electroporated, the phenotypes obtained were similar to *Hoxa2* overexpression (Creuzet et al., 2002). Interestingly, the effect of ectopic expression of *Hox* genes in cephalic NC resembles the phenotypes obtained when the *Hox*-negative NC domain is surgically removed from the chick embryo (Creuzet et al., 2002, 2005b). A recent report further supports the hypothesis that *Hox* genes regulate the development of mesenchymal-derived NC structures. As cited in Chapter IV.3, conditional removal of *Ezh2* in murine NCC resulted in many craniofacial defects, which is most probably due to the loss of a massive epigenetic repression of *Hox* genes (Schwarz et al., 2014). Furthermore, when *Hoxa2* and *Hoxd10* were transduced in chick mesencephalic NCC cultured in vitro, collagen 2, a marker of chondrogenesis, was significantly reduced (Abzhanov et al., 2003). Similarly, collagen 2 was also diminished after *Hoxd9* overexpression in cultured mouse mesencephalic NCC (Ishikawa and Ito, 2009). Taken together, these results show that *Hox* expression in the anteriormost region of cephalic NCC is incompatible with NCC differentiation into skeletal tissues.

Bearing in consideration the *Hox* influence on the mesenchymal ability of cranial NCC, it has been hypothesized that *Hox* genes, being normally expressed by trunk NCC, could be responsible for the lack of mesenchymal derivatives at this level of NCC in vivo. As discussed in *Chapter II.2*, various experiments have clearly demonstrated that the trunk NCC can generate mesenchymal cell types in vitro indicating that mesenchymal potentiality is present in all NCC. In this regard, some authors have previously suggested that the trunk NC ability to yield chondrocytes in long-term cultures could be related to a reduction of *Hox* gene expression during in vitro culture (Abzhanov et al., 2003; Ido and Ito, 2006). However, Hox effects on other mesenchymal lineages, such as osteoblasts and adipocytes, have never been investigated so far. Therefore, a more detailed study regarding *Hox* gene influence on trunk NC mesenchymal capacity was greatly necessary. Thus, in part 2 of this Thesis, we aimed to investigate whether particular *Hox* genes would affect the production of mesenchymal derivatives by quail trunk NCC.

OBJECTIVES

The NC is a crucial structure for the building of the vertebrate head, mainly due to its capacity to generate a variety of mesenchymal cell types, which provide the craniofacial skeletal, connective and fat tissues. In amniote embryos, this capacity is restricted to the cephalic NCC as opposed to the trunk NCC. Nevertheless, much of the mechanisms involved in the regulation of NCC mesenchymal fate are still poorly known. In this Thesis, we aimed to uncover some of the molecular players involved in the emergence of mesenchymal phenotypes in cephalic and trunk NCC, focusing on Six and Hox families of transcription factors.

Part 1:

Our first aim was to determine the spatio-temporal dynamics of Six1 transcription factor in head mesenchymal cell types, and the respective contribution of cranial NCC and mesoderm to Six1-expressing territories during head development in the avian embryo.

Specific objectives:

-To identify the expression profile of *Six1* gene at distinct stages of avian development; by using in situ hybridization and immunostaining;

-To idenfify differential expression of *Six1* gene in the cephalic NC and mesoderm; by using quail-chick chimera experiments;

-To determine which NC-derived differentiated cell types express *Six1* gene in cephalic tissues.

The results are described in chapter I of Results (Article 1, in preparation)

Part 2:

In this part of the Thesis, our objective was to investigate the molecular mechanisms underlying the acquisition of mesenchymal fate by trunk and cephalic NCC, focusing on the Hox family of transcription factors. We aimed at testing the hypothesis that *Hox* gene inhibition could be part of a regulatory program for mesenchymal lineages differentiation, shared by cephalic and trunk NCC in culture.

Specific objectives:

-To determine the profile of *Hox* genes expressed in trunk premigratory and early migratory NCC, comparing with cephalic NCC as a negative control;

-To evaluate the expression profile of *Hox* genes during time course of trunk NCC differentiation in vitro, in order to identify candidate *Hox* genes specifically downregulated during osteoblast formation in culture;

-To investigate whether individual *Hox* genes are involved in controlling trunk NC mesenchymal potential in vitro using gain of function approaches;

-To investigate whether selected *Hox* genes influence neural, melanocytic and myofibroblastic differentiation;

-To compare the effects of selected *Hox* genes on cephalic NCC development in vitro;

-To investigate the influence of *Hox* overexpression on the stemness properties of trunk NCC.

Results are mainly described in chapter II of Results (Article 2, in preparation). Additional findings are described in chapter III of Results.

RESULTS

I. Article I

Respective contribution of the cephalic neural crest and mesoderm to Six1-expressing head territories in the avian embryo

Barbara F. Fonseca[1], Gérard Couly[1,2] and Elisabeth Dupin[1]*

Affiliations

[1]Sorbonne Universités, UPMC Univ Paris 06, INSERM, CNRS, Institut de la Vision, 17 rue Moreau, 75012 Paris, France.

[2]Université Descartes, Necker, 75015 Paris, France.

Authors

Barbara F. Fonseca: <barbara.da-fonseca@inserm.fr>
Gérard Couly: <gerard.couly@gmail.com>
Elisabeth Dupin: <elisabeth.dupin@inserm.fr>

* Corresponding author:
Elisabeth Dupin: elisabeth.dupin@inserm.fr
Phone: 33+153 462 537 ; Telecopy: 33+153 462 600

Abbreviations: neural crest (NC); neural crest cells (NCC); branchial arch (BA); somite-stage (ss); Hamburger and Hamilton (HH); peripheral nervous system (PNS)

Abstract

Vertebrate head development depends on a series of interactions between many cell populations of distinct embryological origins. Cranial mesenchymal tissues have a dual embryonic source: - the neural crest (NC), which generates most of craniofacial skeleton, dermis, pericytes, fat cells, and tenocytes; and - the mesoderm, which yields muscles, blood vessel endothelia and some posterior cranial bones. The molecular players that orchestrate co-development of cephalic NC and mesodermal cells to properly construct the head of vertebrates remain poorly understood. In this regard, *Six1* gene, a vertebrate homolog of *Drosophila Sine Oculis*, is known to be required for development of ear, nose, tongue and cranial skeleton. However, the embryonic origin and fate of *Six1*-expressing cells have remained unclear. In this work, we addressed these issues in the avian embryo model by using quail-chick chimeras, cephalic NC cultures and immunostaining for Six1. Our data show that, at early NC migration stages, *Six1* is expressed by mesodermal cells but excluded from the NC cells. Then, *Six1* becomes widely expressed in NC cells that colonize the pre-otic mesenchyme. In contrast, in the branchial arches, Six1 is present only in mesodermal cells that give rise to jaw muscles. At later developmental stages, the distribution of Six1-expressing cells in mesoderm-derived tissues is consistent with a possible role of this factor in the myogenic program of all types of head muscles, including pharyngeal, extraocular and tongue muscles. In NC derivatives, Six1 is notably expressed in perichondrium and cartilage areas of the nasal septum, jaw, and sclera. Moreover, in cephalic NC cultures, chondrocytes and myofibroblasts, not the neural and melanocytic cells express Six1. In sum, these results point to a dynamic tissue-specific expression of *Six1* in a variety of cephalic NC- and mesoderm-derived cell types and tissues, opening the way for further analysis of *Six1* function in the development of these two cellular populations during vertebrate head formation.

Keywords : Six1; neural crest; mesoderm; quail-chick chimera; branchial arch

Introduction

The head of vertebrates is built during development through the growth and differentiation of specialized structures and cell types which derive from distinct embryological primordia: the neural plate, yielding the brain while the ectodermal placodes are at the origin of most of the cephalic sense organs, in collaboration with the cells migrating from the neural crest (NC) to form cranial sensory ganglia. Besides the CNS and peripheral nervous system (PNS), most tissues in the head of amniote vertebrates develop from mesenchymal progenitors that ensure the production of the cranial dermis, bones, cartilages and blood vessels as well as tendons, muscles, fat and connective tissues. These mesenchymal cranial tissues are derived from two main embryological sources, the mesoderm and the NC, whereas, in the trunk, they have a unique mesodermal origin. It is well recognized that most of the cephalic mesenchyme arises from the NC. As theorized by Gans and Northcutt in a seminal article published in 1983, the “new head” that vertebrates acquired during evolution is mainly due to the production of NC derivatives rostral to the notochord (Gans and Northcutt, 1983). Thus, the NC cells (NCC) provided a skull and facial tissues to accompany the expansion of the prosencephalon and, in cooperation with ectodermal placodes, they participated in the addition of sophisticated sensory modalities, resulting in the complex head structures and brain, which allowed successful radiation of modern vertebrates.

Regarding head skeletogenesis, a triple origin of the craniofacial skeleton has been defined in the avian embryo thanks to quail-chick chimera experiments (Couly et al., 1993); thus, the head skeleton is formed by concerted development of the anteriormost NC mostly yielding facial structures, the cranial paraxial mesoderm and, for its caudalmost part, the somitic mesoderm (Creuzet et al., 2005a). How the various bone and cartilage rudiments arising from mesodermal and NC precursors develop in concert to form the head skeleton, and how they assemble with muscles and tendons for example, are main issues in craniofacial biology. The establishment of the vertebrate head vascularization represents another striking example of the cooperation between the developing NCC and mesodermal cells: the cephalic vascular system is established from both the mesoderm, - for the endothelia of blood vessels - and the NC, - for the smooth muscle cells and pericytes lining these endothelia (Couly et al., 1995; Etchevers et al., 2001). It is therefore clear that the building of most of the distinct mesenchymal tissues of the head depends on tightly coordinated interactions between the cranial NC and mesoderm.

Molecular regulation of commitment and differentiation of mesenchymal tissues is mediated in part, by the action of transcription factors that control the downstream activity of the genes encoding the specialized proteins needed for the generation of the distinct types of differentiated mesenchymal cells. Among these transcription factors, the *Six* homeobox family of transcription factor genes are homologs of genes required for eye development in *Drosophila* (Kawakami et al., 2000). Three subgroups of *Six* genes have been characterized in vertebrates, including *Six1/Six2*, homologs to *Drosophila Sine Oculis*, *Six3/Six6* homologs to *Optix* and *Six4/Six5* homologs of *Dsix4* (for references, Kumar, 2009). While *Six3* mainly functions in eye and rostral CNS development (Lagutin et al., 2003; Oliver et al., 1995a; Lavado et al., 2008; Jeong et al., 2008), differential expression and effects of the other *Six* genes have been described in a number of tissues distinct from the brain, such as muscles, kidney, the auditory system, genitalia, several sensory organs and craniofacial structures (Kumar, 2009). *Six1* is well known as a pan-placodal marker, labeling the pre-placodal domain at presomitic stages and, later on, all the placodes (except the lens) and most of their derivatives (for references, Baker and Bronner-Fraser, 2001; Schlosser, 2010). With respect to the development of mesenchymal tissues, *Six1* and *Six2* are expressed in the developing limb and somitic mesenchyme (Oliver et al., 1995b; Laclef et al., 2003a; Bonnin et al., 2005), as well as in the head and branchial arch (BA) mesenchyme, and in kidney nephrogenic chords (Laclef et al., 2003b). *Six1* is required for early steps of myogenesis (Heanue et al., 1999; Laclef et al., 2003a). Its inactivation in mice also causes defects in kidney, thymus, inner ear and craniofacial development (Laclef et al., 2003b). In human, *Six1* gene haploinsufficiency results in the branchio-oto-renal syndrome, an autosomal dominant developmental disorder characterized by hearing loss and branchial defects (Ruf et al., 2004; Kochhar et al., 2008) while defects in human *Six2* cause conductive hearing loss (Guan et al., 2016) and mild forms of frontal dysplasia (Hufnagel et al., 2016).

Several notable effects of the loss of *Six* gene function on cranial NC development have been reported. *Six1* mutant fetuses in the mouse exhibit shorter squamosal, mandibular and maxillary bones, Meckel's cartilage and hyoid bone, which are formed by NCC of BA1, BA2 and BA3 (Laclef et al., 2003b). In contrast, invalidation of *Six2* in the mouse specifically affects the formation of the endochondral skeleton of the cranial base, including the basisphenoid bone (He et al., 2010), which has a dual origin, from the NC, anteriorly, and from the cranial mesoderm, in its posterior part (Couly et al., 1993; Chai et al., 2000; Jiang et al., 2002; Santagati and Rijli, 2003). *Six2*-null newborn mice display premature bone fusion due to abnormal chondrocyte differentiation, although initial migration and skeletogenic differentiation of NCC appeared unaffected (He et al., 2010). In mouse BA2 NCC, *Six2* has been

shown to be a direct target of *Hoxa2*, the most anteriorly expressed *Hox* gene, which is present in BA2 and represses *Six2* (Kutejova et al., 2005, 2008). The more rostral NC (from mid-diencephalon to rhombomere-2 included), is endowed with a characteristic *Hox*-free status that is required for the formation of the NC-derived facial skeleton, and, indirectly, for anterior brain development (Couly et al., 1998, 2002; Creuzet et al., 2002; Creuzet, 2009). In the chick embryo, Garcez et al. (2014) have reported that the silencing of *Six2, Six1* and *Six4* genes in the early NC, by in ovo electroporation of double-strand RNAs, results in severe hypoplasia of the facial skeleton and atrophy of the anterior dorsal brain (Garcez et al., 2014). Moreover, when the three *Six* genes are silenced simultaneously, the skeletal and brain defects are exaggerated and phenocopy those obtained after ectopic expression of *Hoxa2* in the premigratory cephalic NC (Creuzet et al., 2002). According to rescue experiments, these authors concluded that *Six* genes, expressed in the anterior cephalic NCC from the migratory stage, can be negatively regulated by *Hoxa2* and likely function to control proliferation and cell death in the developing cranial NC mesenchyme (Garcez et al., 2014).

Taken together, the data described above, argue that, among pleiotropic expression and effects on the vertebrate embryo, *Six1*/*Six2* genes are crucial for the development of head mesenchymal tissues, although their precise dynamics of expression and their respective role in the NC and mesodermal cells remains unclear. In order to address this issue, we have used the avian embryo model to investigate the detailed spatial-temporal pattern of expression of *Six1* gene, particularly regarding the fate of mesoderm- and NC-derived cells in the developing head. By using in vivo quail-chick transplantations of the NC and mesoderm as well as in vitro cranial NC cell cultures, the present study highlights the respective contribution of NC and mesodermal cells to the deployment and differentiation of Six1-expressing cells in head mesenchymal tissues.

Materials and Methods

- Chicken embryos handling and cryosectioning

Fertilized eggs of *Gallus gallus* chicken were obtained from a commercial source (EARL Les Bruyères, France) and incubated at 38.5 °C in humidified conditions. Embryos were collected at different developmental time points. Stage determination was done according to Hamburger and Hamilton (1951) (HH stage) and, in embryos until 2 days of incubation (E2), by counting the number of somite pairs, here referred to somite-stage (ss). Embryos were fixed in 4% formaldehyde for 2 hours at room temperature or overnight at 4 °C, washed in PBS 1X,

embedded in 30% sucrose overnight, and frozen in isopentane at -50°C (temperature stabilized with dry ice). Frozen sections were cut at 18µm with a cryostat (Leica).

- Construction of quail-chick chimeras of the cranial neural crest and mesoderm

Quail (*Coturnix coturnix japonica*) and chicken *Gallus gallus* fertilized eggs were obtained from commercial sources (Cailles de Chanteloup and EARL Les Bruyères, France) and incubated at 38.5 °C in humidified conditions for about 30 hours in order to obtain embryos at stage 8 of Hamburger and Hamilton (HH8), with 5 somite-stage (5ss). The NC chimeras were constructed by isotopic and isochronic replacement of the chick cranial neural fold (i.e. the premigratory neural crest) by its quail counterpart, according to previous experiments of NCC fate mapping (Couly and Le Douarin, 1987; Couly et al., 1993). The graft of neural fold encompassed the rostrocaudal level from the midbrain to anterior rhombencephalon. Cranial mesoderm quail-chick chimeras were prepared as previously described (Couly et al., 1992, 1995): a portion of the quail paraxial cephalic mesoderm was microsurgically isolated after opening of the superficial ectoderm lateral to the mesencephalon at stage HH8 (5ss); the excised cranial mesoderm was then grafted in an identical position in a stage-matched chick host embryo. All the quail to chicken grafts were performed unilaterally. Twenty-four hours after surgery, the host embryos (of stage HH15) were sacrificed and handled for cryosectioning as described above.

-In situ hybridization and immunohistochemistry on sections

Chicken *Six1* riboprobes were prepared from a cDNA plasmid encoding full-length coding sequence of chicken *Six1* (GenBank AB199734.1), which was kindly provided by Dr. Atsushi Kuroiwa (Nagoya University). The *cSix1* template was linearized with HindIII endonuclease and transcribed with a T3 polymerase in the presence of digoxigenin-11-D-UTP (Roche Diagnostics) to synthesize the antisense riboprobe. In situ hybridization on frozen sections was performed as previously described (Marillat et al., 2002). Briefly, after proteinase K treatment (10ug/ml, Invitrogen) and postfixation in 4% PFA, slides were pre-hybridized for 2 hours at room temperature in hybridization buffer (50% formamide, 5× SSC, 1× Denhardt's, 50 µg/ml yeast tRNA, and 500 µg/ml salmon testes ssDNA, pH7.4; all reagents from Sigma) Hybridization took place overnight at 72°C, in the same buffer, with *Six1* riboprobe diluted at 1:200. Detection of the hybridization involved anti-DIG-AP antibody (1:5000, Roche Diagnostics) followed by color substrate reaction with nitroblue tetrazolium chloride (337.5 µg/ml) and 5-bromo-4-chloro-3-indolyl phosphate (175 µg/ml) (Roche Diagnostics). Cryosections were mounted in Mowiol (Calbiochem Darmstadt, Germany).

For the immunostaining, tissue cryosections were permeabilized for 1h in PBS containing 5% fetal bovine serum, 1% bovine serum albumin and 0.1% Triton X-100, before overnight incubation with the following primary antibodies: anti-Six1 (1:200; Sigma, HPA001893), anti-Sox10 (1:250; Santa Cruz, sc-17342), anti-Sox9 (1:500; Millipore, AB5535) anti-chondroitin sulfate (1:1600; Sigma, C8035), anti-βIII tubulin TUJ1 (1:500; Covance, MMS435P). Supernatants from mouse hybridoma against QCPN (quail, non chick perinuclear marker) and MF-20 (chicken myosin heavy chain) were purchased from DSHB (Developmental Studies Hybridoma Bank, University of Iowa, Iowa City, IA) and used undiluted. HNK1 antigen labeling was performed using 1:3 diluted supernatants from cultured hybridoma cells (HNK1, ATCC TIB-200). All secondary antibodies used were Alexa Fluor 488, 546 and 647-conjugated antibodies (ThermoFisher Scientific). Cryosections were counterstained with 4′,6-diamidino-2-phenylindole (DAPI) (10 mg/mL; Sigma) and mounted in Mowiol (Calbiochem Darmstadt, Germany). Analysis and imaging were performed with a fluorescence microscope (DM6000, Leica) coupled to a CoolSnapHQ camera (Roper Scientific) or whole section images were captured with a Nanozoomer 2.0 slide scanner (Hamamatsu).

-Quail cephalic neural crest culture and immunostaining

Quail cephalic NCC were obtained from 6-7 ss embryos (equivalent to stage HH9) and cultured essentially as previously described (Calloni et al., 2007, 2009). Briefly, the neural primordium at the level of midbrain-anterior rhombencephalon, which includes the premigratory NC at this early stage, was isolated and plated in explant culture for 15-18 hours; during this in vitro period, the NCC exit from the dorsal neural primordium and migrate on the substrate, similar to their behavior in vivo (Le Douarin and Kalcheim, 1999). Approximately one-to-two thousands of NCC per neural tube fragment thus can be harvested in such migratory cell outgrowth (after discarding the neural explant that remained epithelial) (Calloni et al., 2007, 2009). Cranial NCC were then seeded on a 3T3 fibroblast feeder layer in 96-well plates (400 NCC per well) in DMEM containing 10% FCS and 2% chicken embryo extract (80ng/ml). Cultures were maintained at 37°C in a humidified 5% CO2 incubator and the medium changed every 3 days. After 6 days of culture, the cells were fixed in 4% formaldehyde for 30 min and then immunolabeled with anti-Six1, anti-chondroitin sulfate and HNK1 antibodies, as detailed above for cryosections. Cultures were also analyzed using an antibody to α-smooth muscle actin (αSMA clone 1A4; 1:800 Sigma, A5228) and mouse anti-quail tyrosine hydroxylase hybridoma (undiluted supernatant) (Fauquet and Ziller, 1989). The cultures were counterstained with 4′,6-diamidino-2-phenylindole (DAPI) to mark cell nuclei, which led quail cephalic NCC to be easily distinguished from mouse 3T3 fibroblasts by their distinct nuclei size

(Baroffio et al., 1988). Imaging and automatic quantification of labeled fluorescent cells in the cultures was carried out with an Arrayscan High-Content system (Thermo Fisher Scientific).

Results

Expression pattern of *Six1* gene and Six1 protein at early stages of avian cranial development

Six1 early expression pattern in the chick has been described by Mootoosamy and Dietrich (2002) and Sato et al. (2012): *Six1* transcripts were detected as soon as stage 8 of Hamburger and Hamilton (1951) (stage HH8) in the cranial mesenchyme and otic vesicle, and later on, became widespread in the cranial mesenchyme. A recent report indicated that *Six1*, as well as *Six2* and *Six4* genes, are expressed in the craniofacial NCC population at 10 ss (HH10) in chicken embryos (Garcez et al., 2014). However, at similar NC early migratory stages, Sato et al. (2012) found no overlap between GFP reporter expression, driven by *Six1* enhancers electroporated in the chick, and immunoreactivity to the NC marker HNK1, thus conflicting with the results from in situ hybridization in whole chicken embryos reported before (Garcez et al., 2014). The precise origin of Six1-positive mesenchymal cells, from the cranial NC or the mesoderm, therefore, remains unclear.

In order to better define the tissue-specific expression of Six1 transcription factor in the developing embryonic head, we first analyzed the distribution of *Six1* RNA and Six1 protein in sections of chicken embryos of stage HH11, when migration of cranial NCC takes place (Fig. 1). Delamination of NCC from the dorsalmost region of the neural primordium begins at the level of posterior diencephalon-mesencephalon then progresses caudally (Couly and Le Douarin, 1987). In stage HH11 embryos, equivalent to the stage of 13 somites (13ss), (Fig. 1a), *Six1* transcripts were detected in the mesenchyme ventral to the mesencephalon and in the anterior foregut endoderm while no transcripts were found more dorsally, near the neural primordium (Fig. 1b). A similar, ventral expression pattern was obtained after Six1 immunostaining (Fig. 1d). Immunolabeling with Sox10, a recognized marker of NCC at this early developmental stage (Cheng et al., 2000), marked the NCC migrating under the ectoderm towards the pharyngeal regions and did not overlap with Six1 expression (Fig. 1d-f). At the rhombencephalic level, both *Six1* transcripts (Fig. 1g) and Six1 immunoreactivity (Fig. 1i) were strongly expressed laterally and ventrally to the neural primordium, in the non-neural ectoderm, the mesenchyme and the foregut endoderm. As shown in Fig.1 j-k, Sox10-positive NCC that started to migrate from the dorsal rhombencephalon did not express Six1.

We further investigated Six1 expression at a later stage, when the NCC have spread into the growing head and the branchial arches (BAs) and become intermingled with paraxial mesodermal cells (Noden and Trainor, 2005). In the head of E2.5 chick embryos, at HH15 stage, *Six1*-expressing cells were distributed under the ectoderm lateral to the mesencephalon (Fig.2a,b), where Six1-immunoreative cell nuclei were also detected, in the vicinity and within the forming trigeminal ganglion (Fig. 2c-d and c'-d'); the latter ganglion contained Sox10-positive non-neuronal cells of NC origin and Tuj1-immunoreactive neurons (Fig. 2 e-f and e'-f'). We did not observe colocalization of Six1-positive and Sox10-positive nuclei, while Six1 was co-expressed with Tuj1 in a subset of ganglion neurons (Fig. 2g and g'). This result is in agreement with recent findings showing that the Six1-positive sensory neurons in the trigeminal ganglia are mainly of placodal origin in the mouse and chick embryos (Sato et al., 2012; Karpinski et al., 2016). At the level of the anterior rhombencephalon, *Six1* transcripts were highly expressed in otic vesicles, pharynx and the periocular and pharyngeal mesenchyme (Fig.2h). Interestingly, nuclei labeled with Six1 antibody occupied the core of BA2, a region that will later differentiate into jaw muscles (Fig. 2i and j). In a more posterior section of the same embryo, at the level of the first somites, Six1-positive nuclei were detected in the dermomyotome whereas Sox10 antibody stained the NCC migrating ventrally to the cardiac region (Fig. 2 l and m).

Taken together, these results indicate that the early expression pattern of *Six1* in the chick embryonic head varies with time and is not restricted to only one developmental source (NC, placode or mesoderm), neither to a unique fate (mesenchymal or neural). Of note, however, at early NC migratory stages (HH11), Six1 expression appears excluded from the cranial NCC while broadly distributed in non-neural tissues, particularly the cranial mesenchyme.

Cephalic NC and mesoderm origins of Six1 expression domains analyzed in avian quail-chick chimeras

Our data (Fig.1) suggested a complex and dynamic expression of Six1 during early cranial development in the chick embryo, when NCC migration and deployment of mesodermal cells led to their mixing and co-organization in the forming head. In an attempt to clarify the distribution of Six1 transcription factor in cells derived from the cephalic NC and paraxial mesoderm in the early head mesenchymal tissues, we have performed quail-chick transplantations in ovo, of either the cephalic NC or the cranial paraxial mesoderm. According to previous work by Couly and collaborators (for references, Le Douarin and Kalcheim, 1999;

Creuzet et al., 2005a), such transplantations allowed to establish the precise fate map of these two cell populations in the avian model.

The first type of transplantation involved the isotopic grafting of the premigratory cephalic NC, taken from a quail embryo at the 5 somite-stage (stage HH8), into a chick host embryo of the same stage (Fig. 3 a), as published previously (Couly and Le Douarin, 1988; Couly et al., 1993). Analysis of quail-chick chimeras was performed approximately 24-30 hr after the graft at stage HH15 (25ss), using both the QCPN antibody to identify the grafted quail cells and immunostaining for Six1. Sections of the anterior head of the host embryo showed the presence of numerous Six1-positive cells in the presumptive nasal region (Fig. 3c), both in the olfactory placode and in the underlying mesenchyme near the prosencephalon; the grafted quail cells from the rostral cranial NC populated this mesenchymal area (Fig. 3 d) and, in many cases, they coexpressed Six1 (Fig. 3 e, e'). In addition, the periocular mesenchyme (Fig. 3 f-i) comprised a high density of Six1- and QCPN-immunoreactive cells; colocalization of these markers revealed that a subset of the engrafted NCC, homing towards the eye, expressed Six1 transcription factor (Fig. 3g'-i'). More caudally (Fig. 3j-m), Six1 labeling was found in the BAs, as already described (Fig. 2 I,j), in the pharyngeal endoderm and mesenchyme, where Six1-positive nuclei were clustered in the center of the BA2 (Fig. 3k). In contrast, the QCPN-positive NCC settled in the periphery of the BA mesenchyme and were distinct from Six1-expressing chicken cells in the arch core (Fig. 3l, m). These data, therefore, showed at least a subpopulation of the grafted cranial NCC, which populated the nasal and periocular mesenchyme, expressed Six1, while Six1 appeared excluded from the mesenchymal NCC in the BAs.

The cranial mesoderm, located lateral to the mes-metencephalon, is known to yield various mesenchymal derivatives, including part of the chondrocranium and otic capsule, mandibular and dorsolateral extraocular muscles, meninges and blood vessel endothelium, which have been precisely mapped by quail-chick transplantations (Couly et al., 1992, 1993, 1995). By performing the same type of cranial paraxial mesoderm transplantation, from quail to chicken embryos at stage HH8 (5ss) (Fig. 4a), we have explored the extent of Six1 expression in the grafted mesodermal cells that developed in the chick host (stage HH15; 25ss) 24-30h after the transplantation. In cryosections at the level of the mesencephalon (Fig. 4 b-f), Six1-immunoreactive cell nuclei were widely distributed in the region of the forming trigeminal sensory ganglia and nerves, detected by expression of the NC marker HNK1 (Fig.4 e, e'). Ventrally to the ganglion, a subset of engrafted quail mesodermal cells (QCPN+; Fig. 4 d, d') coexpressed Six1 (Fig. 4 f'). More caudally, Six1-positive cells occupied the core of BA2, where

myogenic precursors will differentiate (Fig. 4 h); on the same section, the engrafted quail mesodermal cells were located in a similar central position in the arch, and most of them exhibited Six1-labeled nuclei (Fig. 4 j, j').

From these quail-chick grafting experiments we can conclude that, in the BA, the central location of Six1+ mesodermal cells is complementary to the peripheral distribution displayed by Six1-negative NCC (see Fig. 3 m). In more rostral head mesenchyme, deployment of Six1 expression targeted mesenchymal cells derived either from the mesoderm, such as in the vicinity of the trigeminal ganglion or from the NC, e.g., in the nasal and periocular regions.

Six1 expression in differentiated cephalic neurosensory and mesenchymal structures

We further studied the distribution of Six1-expressing cells in the developing neural, sensory and mesenchymal structures of the head of chicken embryos of 3 days of incubation (E3) and E7. Fig.5 (a-j) shows a vertical section of an E3 (stage HH19) chicken head, where the otic vesicle exhibited strong Six1 immunoreactivity (Fig.5 c), except in its dorsal part close to the rhombencephalon, which was labeled with Sox10 antibody (Fig.5 d), in agreement with the previously reported activity of a chicken *Sox10* enhancer in early otic development (Betancur et al., 2010). In the mesencephalic region at the same stage (E3), Six1 was abundantly expressed in the trigeminal ganglion (Fig.5 g), which was positive for Sox10 and Tuj1, markers of the non-neuronal and neuronal cells of the ganglion, respectively (Fig.5h and i). In the core of the trigeminal ganglion, we did not observe a colocalization of Six1 and Sox10 labeling in the cell nuclei (Fig.5 j, j'), while Six1 appeared to be expressed in the sensory neurons (Fig.5 j''), in agreement with previous data showing that Six1 is present in the sensory neurons of cranial ganglia and dorsal root ganglia (Laclef et al., 2003b; Sato et al., 2012; Karpinski et al., 2016).

At a later stage of development, in the E7 chicken head (Fig. 5 k-o), Six1 was detected in placodal derivatives, such as the olfactory epithelium (Fig. 5 m) and the adenohypophysis (Fig. 5 n). In the region dorsal to the mesencephalon, dispersed Six1-positive cell nuclei were identified in the mesenchyme between the neuroepithelium and the epidermis (Fig. 5 l, l'), where meninges and skull bones later develop. In addition, the Six1 protein was widely expressed in the forming ear, both in the epithelium of the inner ear (Fig. 5 o) and in the ventral part of the otic capsule, which contained differentiating chondrocytes (that expressed chondroitin sulfate) (Fig. 5 o, o'). These results are consistent with the well-documented role of *Six1* gene in the induction and maintenance of the ectodermal placodes, including its

requirement for the formation of the middle and inner ear (Laclef et al., 2003b; Zheng et al., 2003; Schlosser, 2010; Grocott et al., 2012).

We then focused on differentiated cephalic muscles and facial skeletal elements in the E7 chicken embryo and we examined the distribution of Six1-positive cells in these tissues. Coronal section at the ocular level presented numerous cell nuclei labeled with Six1 antibody in the nasal, maxillary and periocular mesenchyme (Fig. 6 a-c), and in the region of the extraocular muscles (labeled with MF20 antibody; Fig. 6 d,e). Detailed views of the same section showed that Six1 is expressed in dispersed cells, close to outer eye surface (Fig. 6f, g), in the region wherein the scleral cartilage is forming (Fig. 6g', g'') as well as in numerous cells within the extraocular muscles (medial rectus and inferior oblique muscles, Fig. 6g', g''). The nasal cartilage, which expressed Sox9 transcription factor and synthesized chondroitin sulfate (Fig. 6n and l), comprised sparse Six1-immunoreactive cells; in contrast, these cells were highly enriched in the surrounding perichondrium and in the nasofrontal mesenchyme (Fig. 6k, m). More posteriorly, Six1 expression was found in tongue muscles (Fig. 6 o, p-p'') and lining Meckel's cartilage in the lower jaw (Fig. 6 q-q''). In the throat, Six1 labeling was recorded within laryngeal muscles (Fig. 6 r-u), at the periphery of the trachea (Fig. 6 t) and surrounding laryngeal cartilages (Fig. 6v-w). These data show that head muscles, including extraocular muscles, pharyngeal and laryngeal muscles, and tongue muscles, exhibit strong expression of Six1, indicating that this factor could be a crucial regulator of cranial myogenesis in the avian embryo, as described in zebrafish (Lin et al., 2009) and in the limb and trunk skeletal muscles of the chick and mouse (Heanue et al., 1999; Laclef et al., 2003a; Grifone et al., 2005, 2007).

Differentiation of Six1-expressing cells in cranial NCC cultures

To gain further insights on the pattern of expression of *Six1* in the cephalic NCC, we have investigated whether the Six1 protein is present in the distinct cell types that these NCC can produce, when cultured in vitro in conditions previously shown to be appropriate for the development of multipotent NC progenitors (Calloni et al., 2007, 2009; Coelho-Aguiar et al., 2013). For this purpose, early cephalic NCC were obtained after their emigration from mes-metencephalon explanted from quail embryos at the stage of 6-7 somites and cultured for 18 hr; isolated NCC were thereafter subcultured and maintained for six days in vitro, according to our previously published protocol (Calloni et al., 2007). Phenotype analysis with cell type-specific antibodies indicated the differentiation of neurons and glial cells, melanoblasts, myofibroblasts and chondrocytes, as expected. Simultaneous detection of Six1-

immunoreactivity in the cephalic NCC cultures revealed that two differentiated NC-derived cell types expressed Six1: myofibroblasts positive for the smooth muscle marker αSMA (Fig. 7 a-d) and chondrocytes, within cartilage nodules that synthesized chondroitin sulfate (Fig. 7 e-h). The other, neural and melanocytic, cells derived from the NCC, were negative for Six1 (not shown). In addition to labeling mesenchymal cells (myofibroblasts and chondrocytes), Six1 was also expressed in the nuclei of a subset of NCC with an undefined phenotype (since these cells were also negative for markers of the neuronal, glial and melanocytic lineages). Cell quantification indicated that the majority of Six1-positive cells were myofibroblasts (Fig. 7 i). In fact, we found that Six1-expressing cells represented a very small subpopulation of the NCC (approximately 1%) in these 6 day-cultures, while Six1 was not detected at the earlier time of culture. Therefore, at least in these in vitro conditions, expression of Six1 was acquired during the differentiation of myofibroblasts and chondrocytes. The latter result is in agreement with the expression of Six1 in vivo at E7 in several cartilages of NC origin (Fig. 6). The in vitro expression of Six1 in αSMA+ cells is rather puzzling since we did not observe Six1-immunoreactivity in blood vessels and in the NC-derived pericytes and smooth muscle cells lining cephalic vascular endothelia in E7 chicken head (Fig. Supplem. 1). However, αSMA is rather a versatile marker in vitro, marking a population of fibroblastic-like cells that develop in cultures of avian and mouse NCC, particularly under stimulation by TGFβ (for references, Dupin and Coelho-Aguiar, 2013). Further analyses are required to assign a definitive identity, of connective or smooth muscle cells, to this particular subset of Six1-positive cells differentiating in cephalic NCC cultures.

Discussion

The development of the head of vertebrates relies upon a series of morphogenetic movements, which trigger coordinated interactions of cell populations of distinct embryonic origins. It is particularly evidenced in the mesenchymal tissues of the head, which are composed of cells from a dual embryonic source: mesoderm and NC. Some examples of the importance of coordinated communication between mesenchymal tissues are: the definition of mesoderm/NC boundary in cranial bone sutures, particularly the coronal suture of mammals (Merrill et al., 2006; Ting et al., 2009; Deckelbaum et al., 2012); the recruitment of NC-derived pericytes and vascular smooth muscle cells to the endothelium in the forming blood vessels (of mesoderm origin) (Etchevers et al., 2001); the coordination between mesoderm and NC-derived cartilage precursors for the correct development of otic capsule,

and the patterning of head muscles, due to interactions between mesodermal myogenic cells and connective cells/tenocytes of NC origin (Couly et al., 1992; Noden and Trainor, 2005; Grenier et al., 2009).

Here we have considered the respective contribution of cranial NC and mesoderm to the territories that express *Six1* gene in the developing avian head. We first observe Six1 expression in many ectodermal derivatives, such as the olfactory, otic and epibranchial placodes. This corroborates current literature, which classifies *Six1* gene as a pan-placodal marker (Baker and Bronner-Fraser, 2001; Schlosser, 2010). Six1 is also broadly expressed in head mesenchymal tissues (Laclef et al., 2003b; Garcez et al., 2014; Sato et al., 2012). In early avian developmental stages (HH11), during NCC migration, we found that Six1 is mainly present in the cranial mesenchyme, of non-NC origin. This is attested by the lack of colocalization with Sox10, a NC specifier gene expressed in these NCC migratory stages. This result contradicts a previous report of *Six1* mRNA expression in premigratory and migratory cranial NCC in whole-mount preparations of the chick embryo (Garcez et al., 2014). However, a recent detailed study of gene expression during formation of the neural fold shows that only a subtle set of early cranial NCC express *Six1* transiently at this stage, when *Six1* expression is mainly observed in the future placodal region (Roellig et al., 2017).

At late migratory NC stages, in E2.5 chicken embryos, Six1 has a broad expression in the head mesenchyme, especially in the periocular mass and surrounding the developing forebrain. By fate analyses performed in quail-chick chimeras, we can definitely distinguish between NC and mesoderm mesenchymal populations. After quail neural fold transplantation into the chick embryo, we could identify that Six1-expressing NCC populate the periocular, perinasal and periotic mesenchyme. After the transplantation of quail cranial paraxial mesoderm into the chick embryo of the same stage, we observed that a subset of mesodermal cells in the preotic mesenchyme, closely located to the developing trigeminal ganglion, is also Six1+. Therefore, Six1 is expressed in cells originating from both the NC and mesoderm, at this stage of development, and does not represent a reliable marker of the origin of cranial mesenchymal cells. Intriguingly, in the BAs, Six1 is mostly expressed in the core of the mesenchyme, known to be mesoderm-derived (Couly et al., 1992, 1993; Grenier et al., 2009), which suggests that Six1 is an early marker of jaw muscles. Our grafting experiments clearly show that Six1-expressing cells, in the center of BAs, are derived from the mesoderm and clearly distinct from the NC-derived cells in the arch periphery. Nevertheless, it is rather puzzling that we did not identify Six1-expressing cells in the pharyngeal NC-mesenchyme since *Six1* null mice exhibit some craniofacial anomalies related with NC-derived skeletal elements of

the BAs. Whether this could be due to an indirect effect of *Six1* loss in the presumptive muscles, or from loss of *Six1* expression in these skeletal tissues at later stages remains to be investigated. Nevertheless, our data show that Six1 expression in NC-derived tissues, at these early stages, appears to be restricted to the preotic mesenchyme.

We also described Six1 expression at later stages, in E3 and E7 chicken. At E3, Six1 is expressed in the ventral otic placode, where it is essential for cochlear and vestibular development (Ozaki et al., 2004). Moreover, Six1 is present in neurons of the trigeminal ganglion, but not in Sox10+ glial progenitors. Similar results have been described in mouse embryos (Karpinski et al., 2016). Regarding mesenchymal cell types, at E7, Six1 is present in the nasal and periocular mesenchyme and in cartilage components of the developing eye, such as the scleral cartilage, which are of NC origin, (Creuzet et al., 2005b). Interestingly, Six1 is expressed both in chondrocytes and perichondrium, although its expression is stronger in the perichondrium, such as in the nasal septum. Of note, no expression of Six1 was detected in eye structures such as the retina, lens, cornea and optic nerve. These results corroborate previous findings showing that *Six1*, and the closely-related gene *Six2*, are not involved in the development of eye neuroepithelium in vertebrates, although they have an evolutionary homology with *Sine oculis* of *Drosophila* (Kawakami et al., 2000). Furthermore, Six1 expression by the chondrocytes derived from NCC was found in cultures of cephalic NCC, albeit the total number of Six1-positive cells in these cultures was rather limited (about 1%). Finally, we observed Six1-expressing cells dispersed in the mesenchyme adjacent to the dorsal surface of the mesencephalon, which suggests Six1 expression in precursors of the meninges, which are mesodermal-derived in this brain region (Couly et al., 1992).

Regarding mesodermal derivatives, Six1 is mainly expressed in several head muscles, for instance in the extraocular muscles, in the branchiomeric muscles of the pharyngeal and laryngeal regions, and in tongue muscles. Indeed, in *Six1* null mice, these muscles are greatly impaired, together with an extensive hypoplasia of the trunk and limb muscles, which require *Six1* function at several steps of myogenesis (Laclef et al., 2003a; b). These findings suggest a common dependence on *Six1* gene for a general skeletal muscle developmental program. The exact role of *Six1* gene in head muscles should be further investigated, since genetic networks regulating patterning and differentiation are distinct between developing head and trunk muscles (Sambasivan et al., 2011). Finally, at least in the head, Six1 appears to be deprived of any contribution to the vascular system: we did not observe Six1 expression in head blood vessels at all stages analyzed neither in NC-derived vascular smooth muscle cells and pericytes at E7.

In summary, the careful examination of *Six1* expression in mesenchymal tissues of the developing avian embryo from stage HH11 to E7 shows that this gene is expressed in cells derived from both cranial NC and mesoderm, in a tissue- and stage- dependent manner. These results open the way to investigate Six1 downstream targets and further decipher *Six1* gene function in the establishment of the diverse mesenchymal cranial tissues. Future experiments in which one could selectively knockdown *Six1*, in a temporal and tissue-specific way, would be beneficial for a further understanding of its role in mesoderm and NC patterning and differentiation, and to investigate whether this gene acts in the coordinated development of these two cellular populations during vertebrate head morphogenesis.

Acknowledgements

The authors thank Anais Potey and Stéphane Fouquet for their technical assistance (High-throughput Screening Facility and Imaging Core Facility, Vision Institute, France). We also thank Dr. Atsushi Kuroiwa (Nagoya University) for providing chicken *Six1* plasmid. This work was supported by the Centre National de la Recherche Scientifique (CNRS; France). B.F.F was supported by a Ph.D. fellowship from "Ciências sem Fronteiras" program (CNPq; Brazil).

References

Baker, C. V, and M. Bronner-Fraser. 2001. Vertebrate cranial placodes I. Embryonic induction. *Dev. Biol.* 232:1–61.

Baroffio, A., E. Dupin, and N.M. Le Douarin. 1988. Clone-forming ability and differentiation potential of migratory neural crest cells. *Neurobiology*. 85:5325–5329.

Betancur, P., M. Bronner-Fraser, and T. Sauka-Spengler. 2010. Genomic code for Sox10 activation reveals a key regulatory enhancer for cranial neural crest. *Proc. Natl. Acad. Sci. USA*. 107:3570–5.

Bonnin, M.A., C. Laclef, R. Blaise, S. Eloy-Trinquet, F. Relaix, P. Maire, and D. Duprez. 2005. Six1 is not involved in limb tendon development, but is expressed in limb connective tissue under Shh regulation. *Mech. Dev.* 122:573–585.

Calloni, G.W., N.M. Le Douarin, and E. Dupin. 2009. High frequency of cephalic neural crest cells shows coexistence of neurogenic, melanogenic, and osteogenic differentiation capacities. *Proc. Natl. Acad. Sci. USA*. 106:8947–8952.

Calloni, G.W., C. Glavieux-Pardanaud, N.M. Le Douarin, and E. Dupin. 2007. Sonic Hedgehog promotes the development of multipotent neural crest progenitors endowed with both mesenchymal and neural potentials. *Proc. Natl. Acad. Sci. USA*. 104:19879–19884.

Chai, Y., X. Jiang, Y. Ito, P. Bringas, J. Han, D.H. Rowitch, P. Soriano, a P. McMahon, and H.M. Sucov. 2000. Fate of the mammalian cranial neural crest during tooth and mandibular morphogenesis. *Development*. 127:1671–1679.

Cheng, Y., M. Cheung, M.M. Abu-Elmagd, A. Orme, and P.J. Scotting. 2000. Chick sox10, a transcription factor expressed in both early neural crest cells and central nervous system. *Brain Res. Dev. Brain Res.* 121:233–241.

Coelho-Aguiar, J.M., N.M. Le Douarin, and E. Dupin. 2013. Environmental factors unveil dormant developmental capacities in multipotent progenitors of the trunk neural crest. *Dev. Biol.* 384:13–25.

Couly, G., P. Coltey, A. Eichmann, and N.M. Le Douarin. 1995. The angiogenic potentials of the cephalic mesoderm and the origin of brain and head blood vessels. *Mech. Dev.* 53:97–112.

Couly, G., S. Creuzet, S. Bennaceur, C. Vincent, and N.M. Le Douarin. 2002. Interactions between Hox-negative cephalic neural crest cells and the foregut endoderm in patterning the facial skeleton in the vertebrate head. *Development*. 1073:1061–1073.

Couly, G., and N.M. Le Douarin. 1988. The fate map of the cephalic neural primordium at the presomitic to the 3-so mite stage in the avian embryo. *Development*. 103:101–113.

Couly, G., A. Grapin-botton, P. Coltey, B. Ruhin, and N.M. Le Douarin. 1998. Determination of the identity of the derivatives of the cephalic neural crest : incompatibility between Hox gene expression and lower jaw development. *Development*. 3459:3445–3459.

Couly, G.F., P.M. Coltey, and N.M. Le Douarin. 1992. The developmental fate of the cephalic mesoderm in quail-chick chimeras. *Development*. 114:1–15.

Couly, G.F., P.M. Coltey, and N.M. Le Douarin. 1993. The triple origin of skull in higher vertebrates: a study in quail-chick chimeras. *Development*. 117:409–429.

Couly, G.F., and N.M. Le Douarin. 1987. Mapping of the early neural primordium in quail-chick chimeras. II. The prosencephalic neural plate and neural folds: Implications for the genesis of cephalic human congenital abnormalities. *Dev. Biol.* 120:198–214.

Creuzet, S., G. Couly, and N.M. Le Douarin. 2005a. Patterning the neural crest derivatives during development of the vertebrate head: insights from avian studies. *J. Anat.* 207:447–459.

Creuzet, S., G. Couly, C. Vincent, and N.M. Le Douarin. 2002. Negative effect of Hox gene expression on the development of the neural crest-derived facial skeleton. *Development*. 129:4301–4313.

Creuzet, S., C. Vincent, and G. Couly. 2005b. Neural crest derivatives in ocular and periocular structures. *Int. J. Dev. Biol.* 49:161–171.

Creuzet, S.E. 2009. Neural crest contribution to forebrain development. *Semin. Cell Dev. Biol.* 20:751–9.

Deckelbaum, R.A., G. Holmes, Z. Zhao, C. Tong, C. Basilico, and C.A. Loomis. 2012. Regulation of cranial morphogenesis and cell fate at the neural crest-mesoderm boundary by engrailed 1. *Development*. 139:1346–1358.

Le Douarin, N.M., and C. Kalcheim. 1999. The Neural Crest. Second Edi. Cambridge University Press, New York. 472 pp.

Dupin, E., and J.M. Coelho-Aguiar. 2013. Isolation and differentiation properties of neural crest

stem cells. *Cytometry. A*. 83:38–47.

Etchevers, H.C., C. Vincent, N.M. Le Douarin, and G.F. Couly. 2001. The cephalic neural crest provides pericytes and smooth muscle cells to all blood vessels of the face and forebrain. *Development*. 128:1059–1068.

Fauquet, M., and C. Ziller. 1989. A monoclonal antibody directed against quail tyrosine hydroxylase: description and use in immunocytochemical studies on differentiating neural crest cells. *J. Histochem. Cytochem.* 37:1197–1205.

Gans, C., and R.G. Northcutt. 1983. Neural Crest and the Origin of Vertebrates: A New Head. *Science*. 220:268–273.

Garcez, R.C., N.M. Le Douarin, and S.E. Creuzet. 2014. Combinatorial activity of Six1-2-4 genes in cephalic neural crest cells controls craniofacial and brain development. *Cell. Mol. Life Sci.* 71:2149–2164.

Grenier, J., M.A. Teillet, R. Grifone, R.G. Kelly, and D. Duprez. 2009. Relationship between neural crest cells and cranial mesoderm during head muscle development. *PLoS One*. 4:1–15.

Grifone, R., J. Demignon, J. Giordani, C. Niro, E. Souil, F. Bertin, C. Laclef, P.X. Xu, and P. Maire. 2007. Eya1 and Eya2 proteins are required for hypaxial somitic myogenesis in the mouse embryo. *Dev. Biol.* 302:602–616.

Grifone, R., J. Demignon, C. Houbron, E. Souil, C. Niro, M.J. Seller, G. Hamard, and P. Maire. 2005. Six1 and Six4 homeoproteins are required for Pax3 and Mrf expression during myogenesis in the mouse embryo. *Development*. 132:2235–2249.

Grocott, T., M. Tambalo, and A. Streit. 2012. The peripheral sensory nervous system in the vertebrate head: a gene regulatory perspective. *Dev. Biol.* 370:3–23.

Guan, J., D. Wang, W. Cao, Y. Zhao, R. Du, H. Yuan, Q. Liu, L. Lan, L. Zong, J. Yang, Z. Yin, B. Han, F. Zhang, and Q. Wang. 2016. SIX2 haploinsufficiency causes conductive hearing loss with ptosis in humans. *J. Hum. Genet.* 61:917–922.

Hamburger, V., and H.L. Hamilton. 1951. A series of normal stages in the development of the chick embryo. *J. Morphol.* 88:49–92.

He, G., S. Tavella, K.P. Hanley, M. Self, G. Oliver, R. Grifone, N. Hanley, C. Ward, and N. Bobola. 2010. Inactivation of Six2 in mouse identifies a novel genetic mechanism controlling development and growth of the cranial base. *Dev. Biol.* 344:720–730.

Heanue, T.A., R. Reshef, R.J. Davis, G. Mardon, G. Oliver, S. Tomarev, A.B. Lassar, and C.J. Tabin. 1999. Synergistic regulation of vertebrate muscle development by Dach2, Eya2, and Six1, homologs of genes required for Drosophila eye formation. *Genes Dev.* 13:3231–3243.

Hufnagel, R.B., S.L. Zimmerman, L.A. Krueger, P.L. Bender, Z.M. Ahmed, and H.M. Saal. 2016. A new frontonasal dysplasia syndrome associated with deletion of the SIX2 gene. *Am. J. Med. Genet. Part A*. 170A:487–491.

Jeong, Y., F.C. Leskow, K. El-Jaick, E. Roessler, M. Muenke, A. Yocum, C. Dubourg, X. Li, X. Geng, G. Oliver, and D.J. Epstein. 2008. Regulation of a remote Shh forebrain enhancer by the

Six3 homeoprotein. *Nat. Genet.* 40:1348–1353.

Jiang, X., S. Iseki, R.E. Maxson, H.M. Sucov, and G.M. Morriss-Kay. 2002. Tissue Origins and Interactions in the Mammalian Skull Vault. *Dev. Biol.* 241:106–116.

Karpinski, B.A., C. A. Bryan, E.M. Paronett, J.L. Baker, A. Fernandez, A. Horvath, T.M. Maynard, S.A. Moody, and A.S. LaMantia. 2016. A cellular and molecular mosaic establishes growth and differentiation states for cranial sensory neurons. *Dev. Biol.* 415:228–241.

Kawakami, K., S. Sato, H. Ozaki, and K. Ikeda. 2000. Six family genes--structure and function as transcription factors and their roles in development. *Bioessays*. 22:616–626.

Kochhar, A., D.J. Orten, J.L. Sorensen, S.M. Fischer, C.W.R.J. Cremers, W.J. Kimberling, and R.J.H. Smith. 2008. SIX1 mutation screening in 247 branchio-oto-renal syndrome families: A recurrent missense mutation associated with BOR. *Hum. Mutat.* 29:565.

Kumar, J.P. 2009. The sine oculis homeobox (SIX) family of transcription factors as regulators of development and disease. *Cell. Mol. Life Sci.* 66:565–583.

Kutejova, E., B. Engist, M. Mallo, B. Kanzler, and N. Bobola. 2005. Hoxa2 downregulates Six2 in the neural crest-derived mesenchyme. *Development*. 132:469–478.

Kutejova, E., B. Engist, M. Self, G. Oliver, P. Kirilenko, and N. Bobola. 2008. Six2 functions redundantly immediately downstream of Hoxa2. *Development*. 135:1463–1470.

Laclef, C., G. Hamard, J. Demignon, E. Souil, C. Houbron, and P. Maire. 2003a. Altered myogenesis in Six1-deficient mice. *Development*. 130:2239–2252.

Laclef, C., E. Souil, J. Demignon, and P. Maire. 2003b. Thymus, kidney and craniofacial abnormalities in Six1 deficient mice. *Mech. Dev.* 120:669–679.

Lagutin, O. V, C.C. Zhu, D. Kobayashi, J. Topczewski, K. Shimamura, L. Puelles, H.R.C. Russell, P.J. McKinnon, L. Solnica-Krezel, and G. Oliver. 2003. Six3 repression of Wnt signaling in the anterior neuroectoderm is essential for vertebrate forebrain development. *Genes Dev.* 17:368–79.

Lavado, A., O. V. Lagutin, and G. Oliver. 2008. Six3 inactivation causes progressive caudalization and aberrant patterning of the mammalian diencephalon. *Development*. 135:441–450.

Lin, C.Y., W.T. Chen, H.C. Lee, P.H. Yang, H.J. Yang, and H.J. Tsai. 2009. The transcription factor Six1a plays an essential role in the craniofacial myogenesis of zebrafish. *Dev. Biol.* 331:152–166.

Marillat, V., O. Cases, K.T. Nguyen-Ba-Charvet, M. Tessier-Lavigne, C. Sotelo, and A. Chedotal. 2002. Spatiotemporal expression patterns of slit and robo genes in the rat brain. *J. Comp. Neurol.* 442:130–155.

Merrill, A.E., E.G. Bochukova, S.M. Brugger, M. Ishii, D.T. Pilz, S.A. Wall, K.M. Lyons, A.O.M. Wilkie, and R.E. Maxson. 2006. Cell mixing at a neural crest-mesoderm boundary and deficient ephrin-Eph signaling in the pathogenesis of craniosynostosis. *Hum. Mol. Genet.* 15:1319–1328.

Mootoosamy, R.C., and S. Dietrich. 2002. Distinct regulatory cascades for head and trunk myogenesis. *Development*. 129:573–583.

Noden, D.M., and P.A. Trainor. 2005. Relations and interactions between cranial mesoderm and neural crest populations. *J. Anat.* 207:575–601.

Oliver, G., A. Mailhos, R. Wehr, N. Copeland, N. Jenkins, and P. Gruss. 1995a. Six3, a murine homologue of the sine oculis gene, demarcates the most anterior border of the developing neural plate and is expressed during eye development. *Development*. 121:4045–4055.

Oliver, G., R. Wehr, N.A. Jenkins, N.G. Copeland, B.N. Cheyette, V. Hartenstein, S.L. Zipursky, and P. Gruss. 1995b. Homeobox genes and connective tissue patterning. *Development*. 121:693–705.

Ozaki, H., K. Nakamura, J.I. Funahashi, K. Ikeda, G. Yamada, H. Tokano, H. Okamura, K. Kitamura, S. Muto, H. Kotaki, K. Sudo, R. Horai, Y. Iwakura, and K. Kawakami. 2004. Six1 controls patterning of the mouse otic vesicle. *Development*. 131:551–562.

Roellig, D., J. Tan-Cabugao, S. Esaian, and M.E. Bronner. 2017. Dynamic transcriptional signature and cell fate analysis reveals plasticity of individual neural plate border cells. *Elife*. 6:1–24.

Ruf, R.G., P.-X. Xu, D. Silvius, E.A. Otto, F. Beekmann, U.T. Muerb, S. Kumar, T.J. Neuhaus, M.J. Kemper, R.M. Raymond, P.D. Brophy, J. Berkman, M. Gattas, V. Hyland, E.-M. Ruf, C. Schwartz, E.H. Chang, R.J.H. Smith, C.A. Stratakis, D. Weil, C. Petit, and F. Hildebrandt. 2004. SIX1 mutations cause branchio-oto-renal syndrome by disruption of EYA1-SIX1-DNA complexes. *Proc. Natl. Acad. Sci. USA*. 101:8090–8095.

Sambasivan, R., S. Kuratani, and S. Tajbakhsh. 2011. An eye on the head: the development and evolution of craniofacial muscles. *Development*. 138:2401–2415.

Santagati, F., and F.M. Rijli. 2003. Cranial neural crest and the building of the vertebrate head. *Nat. Rev. Neurosci.* 4:806–18.

Sato, S., K. Ikeda, G. Shioi, K. Nakao, H. Yajima, and K. Kawakami. 2012. Regulation of Six1 expression by evolutionarily conserved enhancers in tetrapods. *Dev. Biol.* 368:95–108.

Schlosser, G. 2010. Making Senses. Development of Vertebrate Cranial Placodes. *Int. Rev. Cell Mol. Biol.* 283:129–234.

Ting, M.-C., N.L. Wu, P.G. Roybal, J. Sun, L. Liu, Y. Yen, and R.E. Maxson. 2009. EphA4 as an effector of Twist1 in the guidance of osteogenic precursor cells during calvarial bone growth and in craniosynostosis. *Development*. 136:855–864.

Zheng, W., L. Huang, Z.-B. Wei, D. Silvius, B. Tang, and P.-X. Xu. 2003. The role of Six1 in mammalian auditory system development. *Development*. 130:3989–4000.

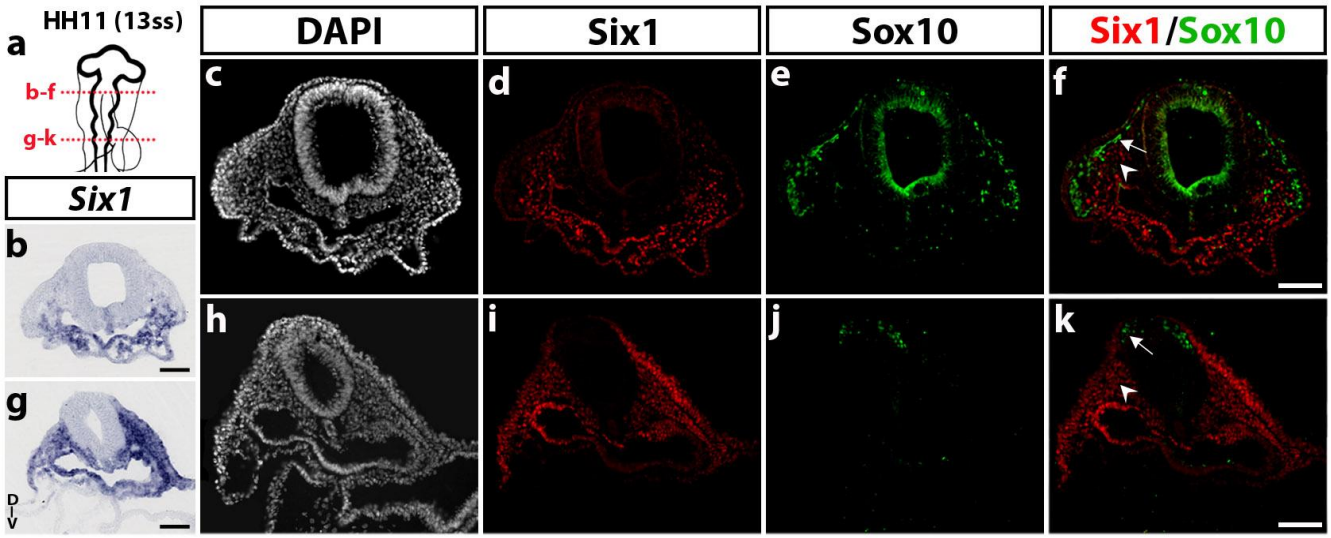

Fig. 1 Six1 expression pattern in the head of HH11 (13ss) chicken embryo. **a** Schematic representation of a HH11 (13ss) chicken embryonic head; red dotted lines indicate the position and orientation of the sections shown in **b-f** (mesencephalic level) and **g-k** (rhombencephalic level). **b and g** *Six1* gene transcripts are detected in the foregut endoderm and in the cranial mesenchyme, located ventral to the mesencephalon (in **b)** and more laterally, at the rhombencephalic level (in **g**). **c-f** Transversal section, showing immunoreactivity to Six1 (**d**) and Sox10 (**e**), with no apparent overlap (See merge stainings in **f**). **d** and **i** Adjacent sections to **b** and **g**, respectively, after Six1 immunostaining show an expression pattern of Six1 similar to that observed after in situ hybridization. **e** and **j** Co-immunostaining with Sox10 antibody labels the NCC, which migrate from the mesencephalon dorsolaterally under the ectoderm in **e** and are starting to migrate from the rhombencephalon in **j** . **f** and **k** Merge of Six1 and Sox10 stainings (arrows: migratory neural crest cells; arrowheads: cranial paraxial mesodermal cells). D-V, dorso-ventral orientation; f, foregut; nt, neural tube; h, heart. Scale bars: 100µm.

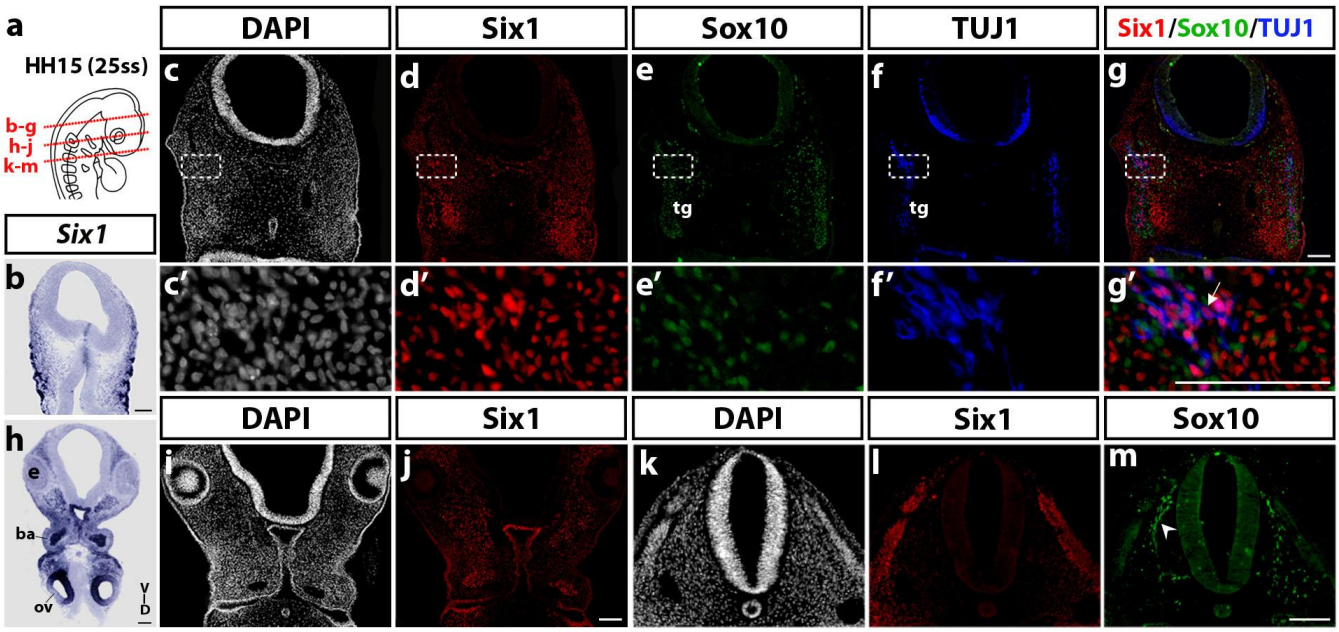

Fig. 2 Six1 expression pattern in the head of HH15 (25ss) chicken embryo. **a** Schematic representation of a HH15 chicken embryo; red dotted lines indicate the position and orientation of sections shown in **b-g, h-j** and **k-m** images. **b** and **h** *Six1* transcripts expression in the lateral mesenchyme of the anterior head (hm in **b**), and, in a more caudal section (**h**), in the periocular mesenchyme, foregut (f), branchial arch (ba) mesenchyme and superficial ectoderm and otic vesicles (ov) (e, eye). **c-g** Horizontal section (D-V dorso-ventral orientation), Six1, Sox10 and Tuj1 immunostainings (the box area is magnified in **c'-g')**: Six1 is expressed in the mesenchyme surrounding the trigeminal ganglion (tg) and in the trigeminal ganglion and nerves, where it labels a subset of Tuj1-positive neurons, not Sox10-positive non-neuronal cells (**c'-g'**); arrow in **g'** indicates a Six1-positive neuron. **i, j** section at the level of the eye, showing Six1 expression in the periocular cranial mesenchyme, the branchial arch mesenchyme and the endoderm lining the pouch, **k-m** Section at the anterior somitic level, Six1 is strongly expressed in the dermomyotome **(l**) while Sox10 labels the migratory NCC, indicated by an arrowhead (**m**). Scale bars: 100µm.

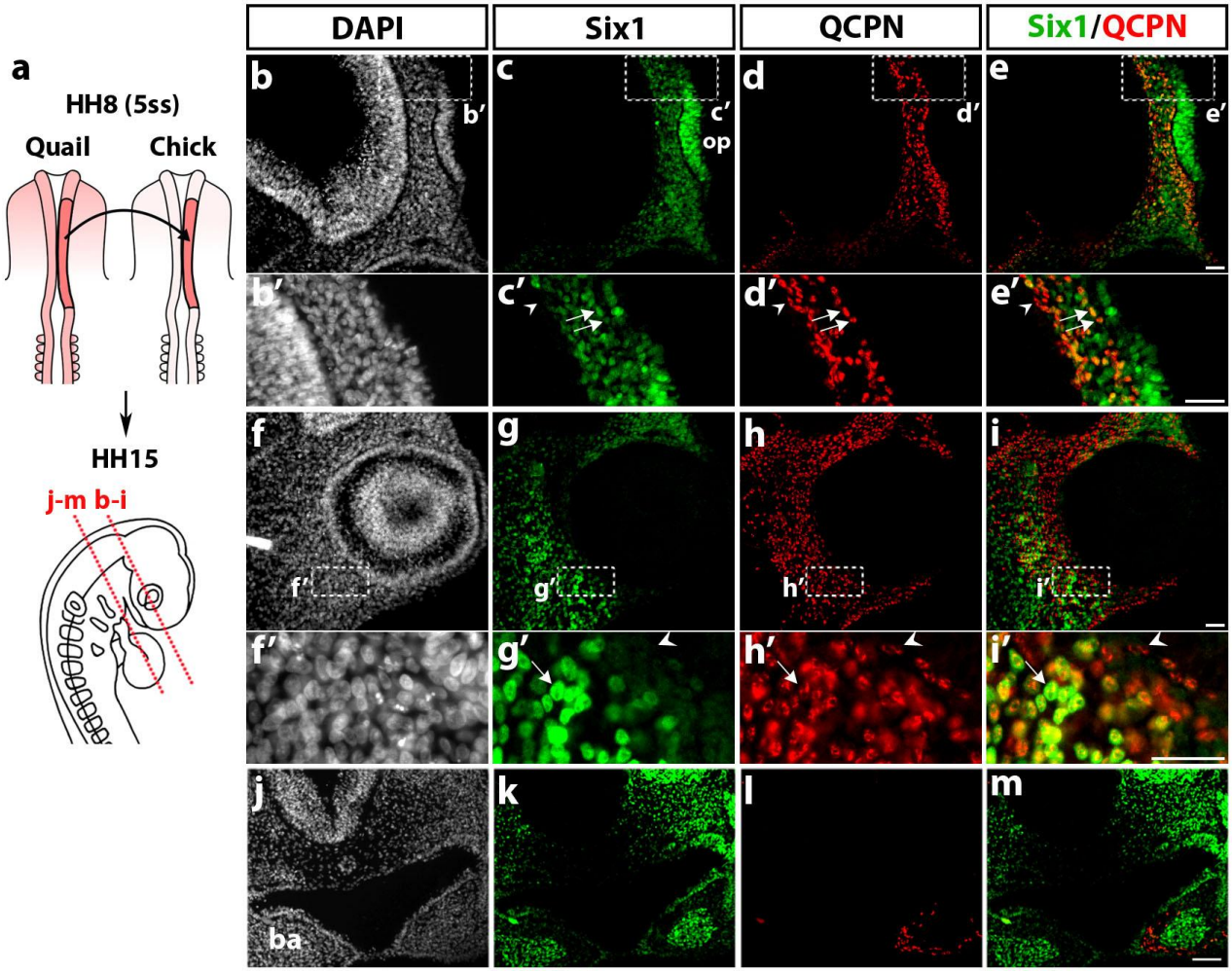

Fig. 3 Six1 expression in quail-chick chimeras of the cephalic NC. **a** Schematic representation of the cranial NC grafting procedure. The chick neural fold/premigratory NC from midbrain to anterior rhombencephalic level was unilaterally replaced by its quail counterpart (in red) at HH8 (5ss) stage; the resulting chimeras were analyzed at HH15 (25ss) for Six1 immunoreactivity, nuclear staining (DAPI) and the presence of QCPN+ quail cells (red dotted lines indicate orientation and position of the sections shown in **b-i** and **j-m**). **b-e** In the prosencephalic region, 9Six1 (**c**) is expressed in the olfactory placode (op) and the adjacent cranial mesenchyme surrounding the prosencephalon, in which quail NCC positive for QCPN are located (**d**); **b'-e'** Highlighting of the area boxed in b-e, showing engrafted quail cells that are either positive (arrows) or negative (arrowhead) for Six1. **f-i** Six1 and QCPN are both expressed in the head mesenchyme around the eye. **f'-i'** (magnified region indicated by a boxed area in **f-i)** Some NCC engrafted in the periocular mesenchyme co-stain with Six1 and QCPN (arrow), while others do not express Six1 protein (arrowhead). **j-m** In the maxillary region, Six1 expression (**k**) is present in the mesenchyme dorsal to the foregut, in the foregut endoderm and the core region of the first BA (ba in **j**) whereas the grafted QCPN+ cells (**l**) are located in the peripheral mesenchyme of the BA and do not express Six1 (**m** Merge of Six1 and QCPN). Scale bars 25µm (**b-i**) and (**b'-i'**); scale bars 50µm (**j-m**).

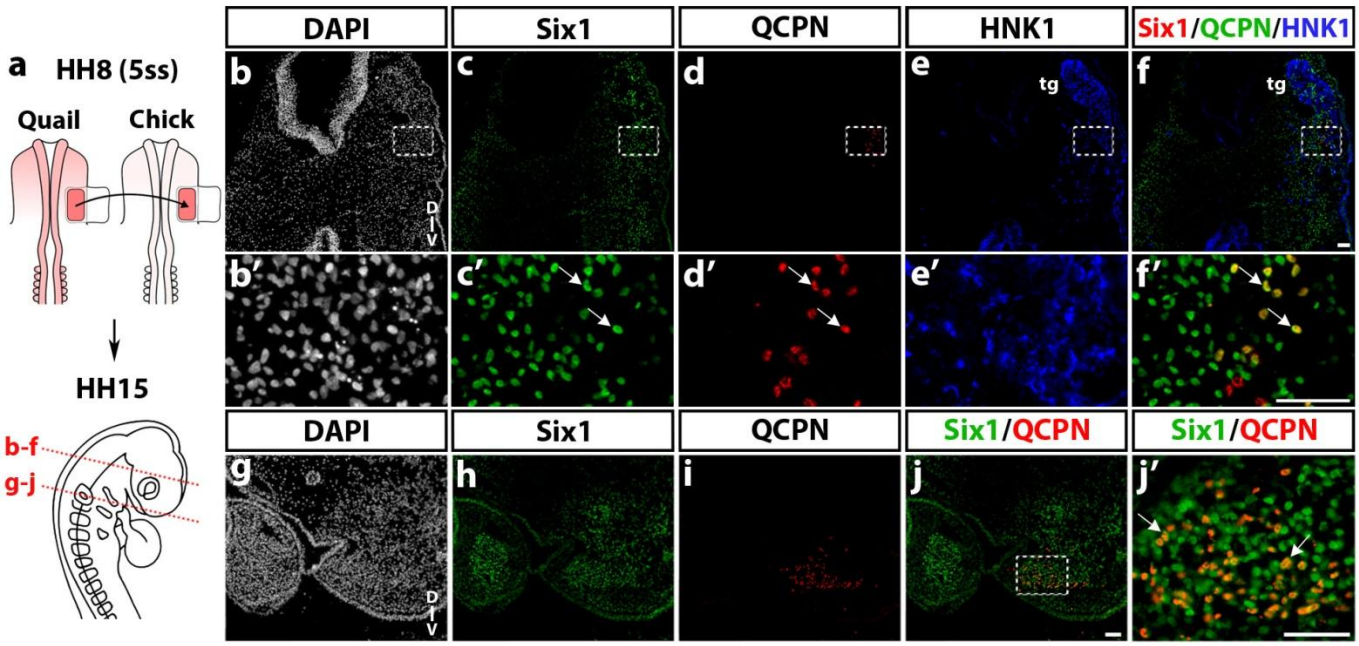

Fig. 4 Six1 expression in quail-chick chimeras of the cephalic mesoderm. **a** Schematic representation of the grafting procedure. Part of the chick lateral paraxial mesoderm was unilaterally replaced by its quail counterpart (in red) at HH8 stage, and the chimeras were analyzed at HH15 (red dotted lines: position and orientation of the sections shown in **b-f** and **g-j**). **b-f** and **b'-f'** At the level of the trigeminal ganglion (tg) and nerves, detected by HNK1 staining (**e-e'**), engrafted quail mesodermal cells, co-stained with Six1 and QCPN, are found in the host lateral mesoderm near the trigeminal ganglion (arrows in **b'-f'**). **g-j** In the region of BA2, quail cells from the grafted mesoderm are present in the core mesenchyme of the BA, which strongly expresses Six1. **j'** Magnification of the boxed area indicated in **j**, showing grafted mesodermal cells that express both Six1 and QCPN (arrows). D-V, dorso-ventral orientation. Scale bars 50µm.

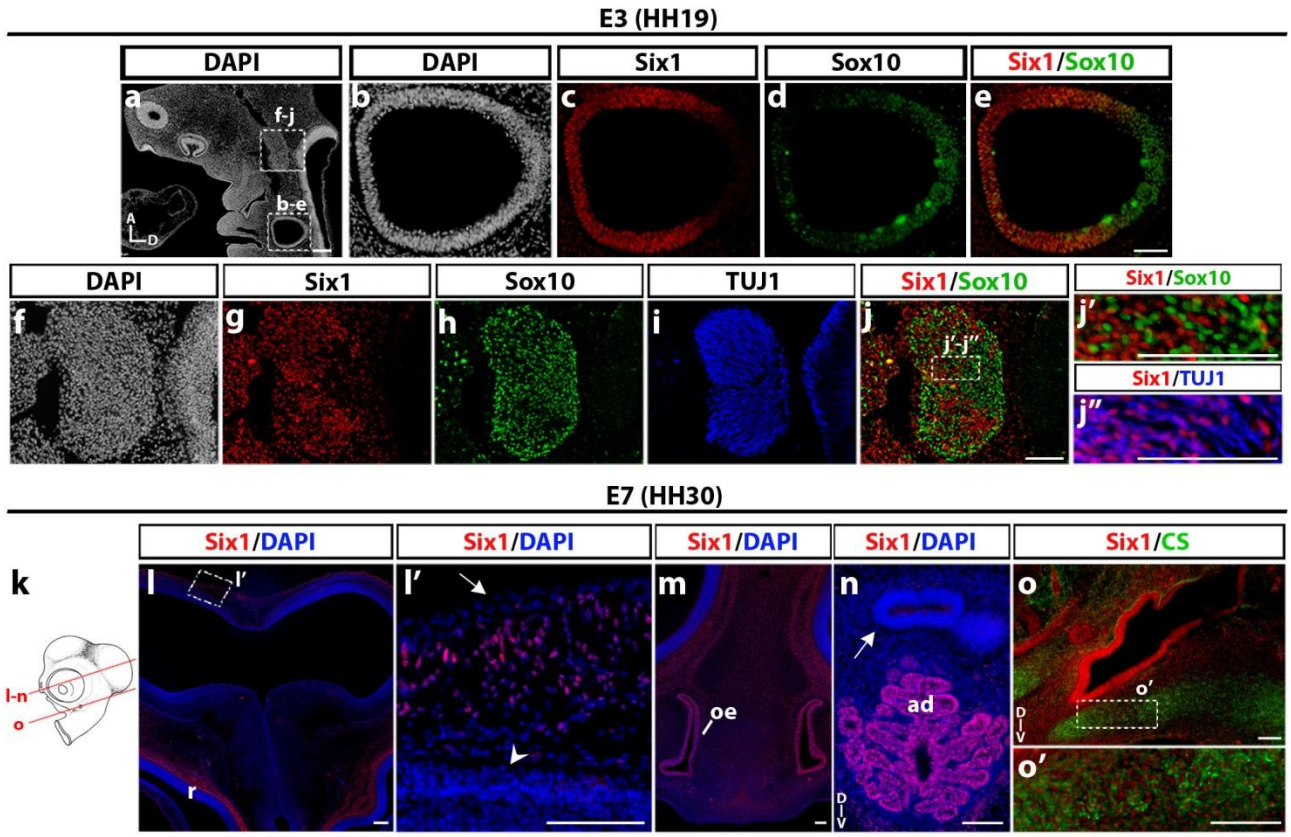

Fig. 5 Six1 expression in head neural structures of E3 and E7 chicken embryos. **a** DAPI staining of E3 (HH19) chicken head longitudinal section (A and D, anterior and dorsal orientations). Boxed areas indicate regions of the otic vesicle and trigeminal ganglion magnified in **b-e** and **f-j**, respectively. **c-e** Six1 immunoreactivity (**c**) is located in the ventrolateral region of the E3 otic vesicle, whereas Sox10 antibody labels its dorsal region (**d** and **e**). **f-j** More rostrally in the same section, Six1-immunoreactive nuclei (**g**) exhibit a dense pattern in the trigeminal ganglion and surrounding mesenchyme; the trigeminal ganglion is positive for Sox10 (**h**) and Tuj1 (**i**) markers; **j** Merge of Six1 and Sox10; **j'-j"** (magnifications of the boxed area indicated in **j**) Six1-positive nuclei mostly correspond to Sox10-negative, Tuj1-positive neuronal cells in the trigeminal ganglion. **k** Schematic representation of a chick embryonic head at E7 (HH30); red lines indicate position and orientation of the sections shown in **l-n** and **o**. **l** In midbrain, Six1-expressing cells are found lining the dorsal mesencephalon and more ventrally, adjacent to the retina. **l'** highlights the dorsal region boxed in **l,** showing Six1-positive cells scattered in the mesenchyme between the surface ectoderm (arrows) and the neuroepithelium in the mesencephalon (arrowheads). **m** and **n** More ventrally in the same section, Six1 is expressed in the olfactory epithelium (oe, in **m**), and adenohypophysis (ad, in **n**) whereas the neurohypophysis is Six1-negative (arrow in **n**). **o** Six1 and CS immunostaining in the otocyst region: Six1 is expressed in the ventrolateral otic epithelium and adjacent cartilages, detected with antibody against chondroitin sulfate (CS). **o'** (magnification of the region boxed in **o)** highlights partial overlap of Six1 and CS markers in the cartilage adjacent to the otic vesicle. (D and V indicate dorsal and ventral orientations). Scale bars: 100µm, except for **a** and **l**, 200µm.

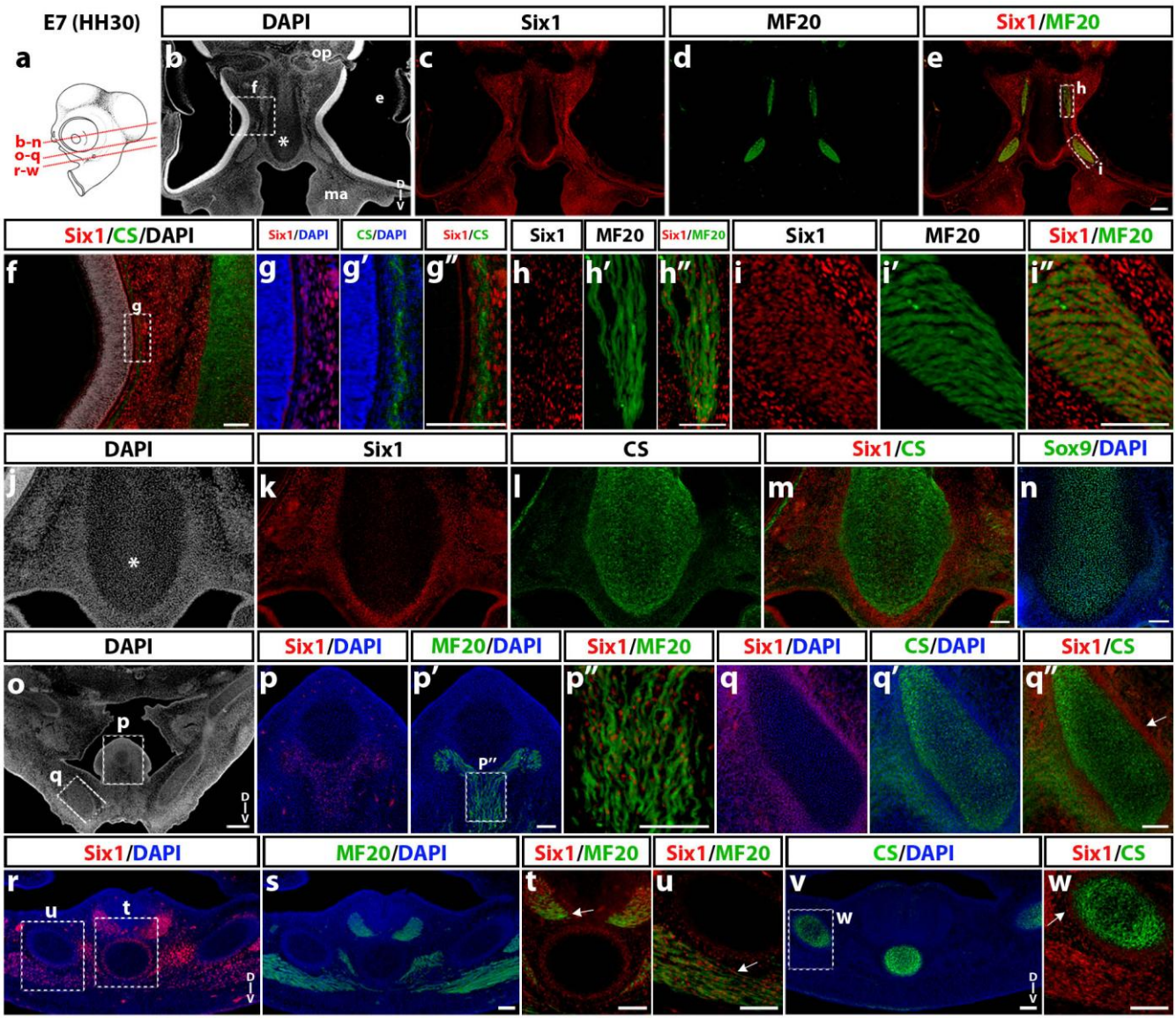

Fig. 6. Six1 expression in mesenchymal cephalic structures in E7 chicken. **a** Schematic representation of an E7 (HH30) chick embryo; red lines indicate cryosections shown in **b-n**, **o-q** and **r-w**. **b-e** At the level of the eyes (e), Six1 immunoreactivity (**c**) is widely detected in the periocular mesenchyme, nasal septum (* in **b**), maxillary bud (ma), and in the extraocular muscles, positive for anti-myosin MF20 (**d**, **e**) **f** (Magnification of the area boxed in **b)** Six1 expression pattern is dense in the periocular mesenchyme and scattered in the adjacent nasal septum, stained with the chondrocytic marker CS. **g-g"** Highlights of the region boxed in **f**, showing Six1 expression in the CS-positive scleral cartilage. **h** and **i** Magnifications of the areas boxed in **e**, showing Six1 expression in medial rectus (**h-h''**) and inferior oblique (**i-i''**) extraocular muscles. **j-n** Six1 labeling is strong in the perinasal mesenchyme and more scattered in the nasal septum (*), which is immunoreactive to CS (**l-m**) and Sox9 (**n**). **m** Note dense Six1 expression in the nasal perichondrium. **o-q** (boxed areas in **o** indicate regions magnified in **p** and **q**) At BA1 level, Six1 and MF20 (**p-p'**) are co-expressed in tongue muscles (magnified in **p"**). **q-q"** In jaw rudiment, both Six1 and CS label Meckel's cartilage, while Six1 also marks the perichondrium (arrow in **q"**). **r-w** Six1, MF20 and CS stainings in BA2: Six1 in expressed in laryngeal muscles (**r-u)**, including ceratoglossus (**t**; arrow) and constrictor and dilatator glottidis (**u**; arrow) (**t** and **u**, magnifications of regions boxed in **r**). **v** CS-labeled ceratobranchial and basibranchial cartilages, the latter magnified in **w,** showing Six1-expressing perichondrium (arrow in **w).** D-V, dorso-ventral orientation; optic nerve (op). Scale bars: 100µm, except for **b-e** and **o,** 300µm.

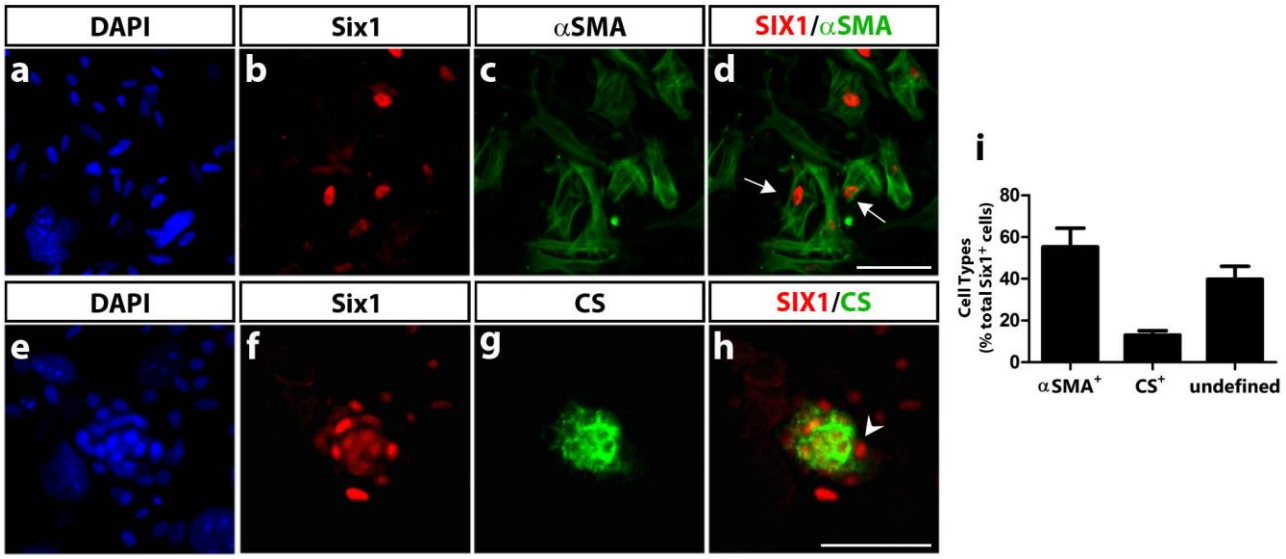

Fig. 7. Six1 expression in cephalic NCC differentiating in culture. After 6 days of culture, cephalic quail NCC were assayed for expression of Six1 and various NC-derived phenotypic markers (see Methods section). Six1-positive nuclei were recorded in approximately 1% of the NCC population. **a-d** Co-staining of nuclear Six1 and cytoplasmic αSMA shows expression of Six1 in myofibroblastic cells (arrows in **d**). **e-h** DAPI, Six1 and CS stainings identify Six1-expressing chondrocytes, positive for CS and forming a tridimensional nodule; Six1-immunoreactive cells are also present in the perichondrial region (arrowhead in **h**). **i** Quantification of cell phenotypes in the Six1-positive cell subpopulation identified in 6 day-NCC cultures. Approximately 55% of Six1-labeled NCC are of myofibroblastic (αSMA+) and 13% of chondrocytic (CS+), phenotypes. The remaining Six1-expressing cells (i.e., negative for CS and αSMA) were not labeled with HNK1 and tyrosine hydroxylase (markers of PNS precursor cells and adrenergic neurons, respectively); these cells are thus designated of undefined phenotype. Scale bars: 50µm.

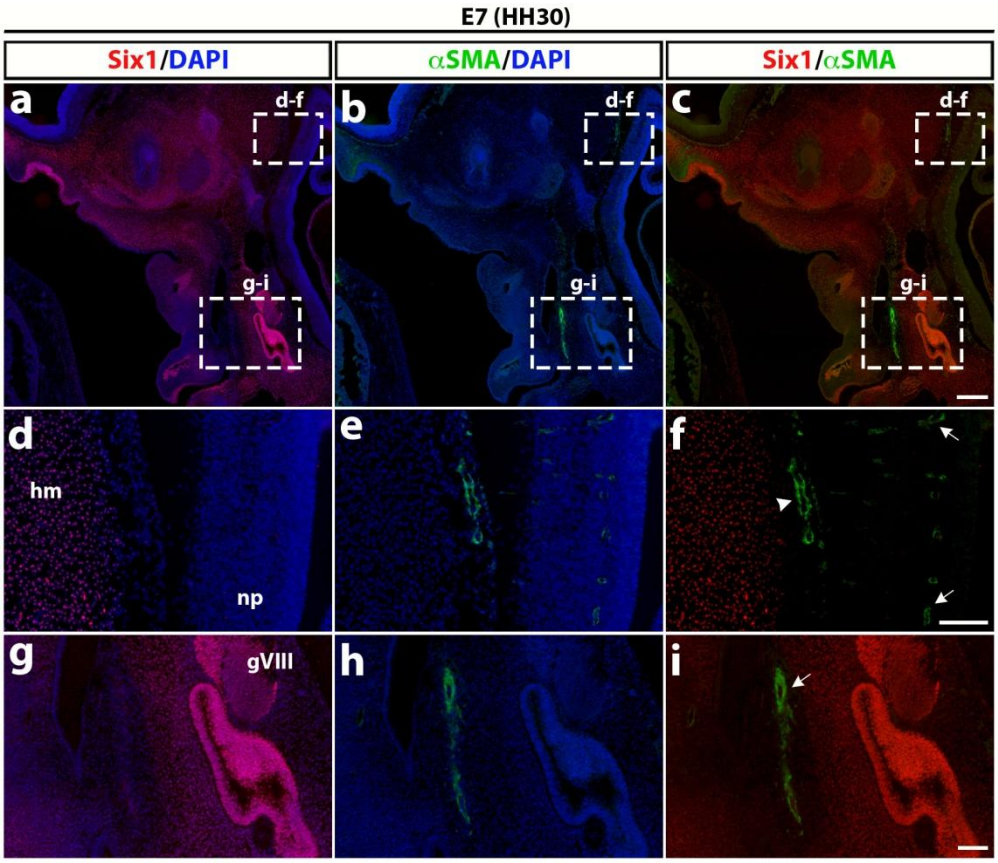

Supplementary Fig. 1: Absence of Six1-immunoreactive cells in head blood vessels at E7. (**a,d,g**) Six1 immunostaining in sections of the E7 chicken head, counterstained with DAPI. (**b,e,h**) αSMA immunostaining and DAPI. (**c,f,i**) Merge of Six1 and αSMA labeling. (**d-f**) Magnification of the area depicted in (**a-c**) Note Six1 expression in head mesenchyme (hm) but not in the wall of blood vessels adjacent to the neuroepithelium (np) (arrowhead in **f**), neither in αSMA+ pericytes within the brain epithelium (arrows in **f**) (**d-f**). (**g-i**) Magnification of the area depicted in (**a-c**): Observe Six1 staining (**g**), in the inner ear epithelium and associated vestibulo-acoustic (gVIII) ganglion whereas αSMA+ smooth muscle cells lining blood vessels lack Six1 expression (arrow in **i**). Scale bar: 100µm; except in **a-c** (300µm).

II. Article II

Regulation of neural crest mesenchymal differentiation potentials by *Hox* genes

Barbara F. Fonseca[1] and Elisabeth Dupin[1*]

[1] Sorbonne Universités, Institut de la Vision, Centre de Recherche UMR INSERM S968/ CNRS 7210/ UPMC

* Correspondence to:
Elisabeth Dupin, PhD.
Institut de la Vision Centre de Recherche
Département de Biologie du Développement
Equipe Rôle des molécules de guidage axonal
17 rue Moreau
75012 Paris France
elisabeth.dupin@inserm.fr

Abbreviations: NC: neural crest; NCC: neural crest cells

Abstract

The Neural Crest (NC) is a unique stem cell population that contributes to the formation of the main craniofacial skeletal structures of vertebrates. In amniotes, the NC ability to yield mesenchymal cell types (e.g. chondrocytes, adipocytes and osteocytes) is restricted to the cranial level, since the trunk NC does not generate these mesenchymal derivatives in vivo. However, recent findings have shown that mesenchymal cell differentiation by trunk NCC can be disclosed by in vitro permissive environments, suggesting that the trunk NC is not completely devoid of mesenchymal potentiality. The molecular mechanisms, involved in trunk NCC mesenchymal fate inhibition in vivo, are currently unknown. Here, we investigated whether *Hox* genes, which can prevent the formation of head NC skeletal structures, could also impair trunk NC differentiation into bone, cartilage, and adipocytes. We observed that trunk NCC maintained in culture in pro-mesenchyme conditions, downregulated a set of *Hox* genes, concomitantly with the onset of *Runx2,* an early marker of osteogenesis. Moreover, overexpression of *Hoxa2*, not of more posteriorly expressed *Hox* genes, like *Hoxc10*, reduced the number of *Runx2* osteoprogenitors in trunk NC culture, without affecting the differentiation into other NC derivatives, such as neurons, melanocytes, glia and myofibroblasts. The loss of osteoprogenitors in early trunk NC cultures led to a significant reduction in the full differentiation of osteoprogenitors, since smaller mineralized bone regions were later on, identified after *Hoxa2* overexpression. Interestingly, *Hoxa2* forced expression concomitantly impaired in vitro adipogenesis and chondrogenesis. In cephalic NCC cultured in vitro, the number of *Runx2* osteoprogenitors was also diminished after forced expression of *Hoxa2*. In conclusion, inhibition of *Hoxa2* appears to be a common mechanism shared by both cephalic and trunk NCC, in order to promote the differentiation of mesenchymal cell types.

Keywords: neural crest; avian embryo; Hox; mesenchymal fate; Runx2; skeletogenesis; adipogenesis; chondrogenesis

Introduction

The Neural Crest (NC) formed in the dorsal aspect of the neural primordium in vertebrate embryos. Concomitantly with neural tube closure, the NC cells (NCC) start to migrate, to later occupy distant regions in the embryo where they differentiate into diverse cell types such as melanocytes, neurons/glia and various types of mesenchymal cells (cartilage, bone and fat cells) (Le Douarin and Kalcheim, 1999). However, despite a broad array of derivatives, NCC mesenchymal fate differs between the rostrocaudal levels of the neural tube from which they emigrate. For instance, the NCC from the trunk region (caudal to somite 4) of amniote vertebrates do not have a skeletogenic or adipocytic fate and thus mainly produce neural cells of the peripheral nervous system (PNS) and melanocytes, together with endocrine adrenomedullary cells (Billon et al., 2007; Couly and Le Douarin, 1988; Couly et al., 1993; Le Douarin et al., 2004). Moreover, in quail-chick chimeras, when the cephalic pre-migratory NC was replaced by its trunk counterpart, the formation of the NC-derived head skeleton was impaired: the implanted quail trunk NCC produced only a small population of fibroblasts and pericytes covering blood vessels in the host cranial tissues (Nakamura and Ayer-le Lièvre, 1982). Similar observations of the differential NCC contributions to mesenchymal tissues along the neural axis were raised in mammals, by fate analyses of NCC in transgenic mice (Yamauchi et al., 1999; Chai et al., 2000; Jiang et al., 2002; Matsuoka et al., 2005; Danielian et al., 1998; Jiang et al., 2000). Together, these results show that the mesenchymal fate is absent in the trunk NC of amniote vertebrates.

Nonetheless, a possible mesenchyme production by trunk NCC earlier in vertebrate evolution is currently being discussed. As some evidence in the fossils of early primitive vertebrates (Ostracoderms) has suggested, the trunk and cephalic NCC in these animals would have yielded the primitive exoskeleton that covered their whole body length. This hypothesis was put forward because the skeletal armor of these primitive fish contained dentine, a mineral produced only by NC-derived tissues (Smith and Hall, 1990; Smith, 1991). Moreover, although still debated (Mongera and Nüsslein-Volhard, 2013; Lee et al., 2013), some contributions of the trunk NC to mesenchymal derivatives in vivo can be found in extant anamniote vertebrate species, particularly in distal bony rays of the caudal and dorsal fins of teleost fish (Smith et al., 1994; Kague et al., 2012). Moreover, in the mouse, Joseph and colleagues have shown that the endoneurial fibroblasts in the sciatic nerve are also trunk NC-derived (Joseph et al., 2004). Thus, apart from these few studies, the trunk NC mesenchymal derivatives in extant vertebrates are

quite restricted in vivo, when compared to the variety of mesenchymal tissues produced by the cephalic NC. However, when avian trunk NCC were cultured in vitro, they could yield mesenchymal/skeletal cell types, as reported in several studies (McGonnell and Graham, 2002; Abzhanov et al., 2003; Billon et al., 2007; Calloni et al., 2007). Recently, our group has shown that trunk NCC under specific culture conditions give rise to fully differentiated cartilage, bone, and fat cells. Moreover, in single NCC cultures, it was found that the vast majority of trunk NCC are neural-mesenchymal progenitors, which suggested that most of the trunk NCC would be able to generate mesenchymal derivatives (Coelho-Aguiar et al., 2013). Therefore, as do cephalic NCC, trunk NCC possess a noteworthy mesenchymal lineage potential, although it is almost completely silenced in vivo.

The molecular mechanisms underlying the expression, or silencing, of mesenchymal potential in trunk NCC is still unknown. Recent findings from Simões-Costa and Bronner (2016) helped to shed light on this issue. They have shown that, in early stages of development, the cephalic, not the trunk, NC, expresses a specific combination of transcription factors, which is essential for cranial NCC differentiation into mesenchymal lineages. Moreover, after ectopic expression of these genes and thereafter grafting the “reprogrammed” trunk NCC into the developing head, an cranial-like differentiation of trunk NCC into skeletal elements could be elicited in vivo in the host branchial arch (Simoes-Costa and Bronner, 2016). These results suggest that a small set of three transcription factors enables to confer mesenchymal fate in both trunk and cephalic NCC, reinforcing the possibility that similar molecular programs could regulate NC mesenchymal potentiality along the entire neural axis.

Regarding these molecular pathways, the *Hox* family of transcription factors has been shown to dramatically influence the formation of mesenchymal derivatives by the cephalic NC. None of the *Hox* genes are expressed by the anterior cephalic NCC (down to rhombomere-2 included); strikingy, ectopic *Hox* expression resulted in lack of bone and cartilage derivatives from cephalic NCC in vivo and in a reduction of their differentiation into collagen-2-expressing chondrocytes in vitro (Couly et al., 2002; Creuzet et al., 2002; Abzhanov et al., 2003). Moreover, *Ezh2*, a known epigenetic repressor of *Hox* gene expression, was recently described as crucial for the skeletogenic program of the cephalic NCC in the mouse (Schwarz et al., 2014).

In the present work, we investigated the role of *Hox* genes regarding the ability of avian trunk NCC to generate mesenchymal cell types, using the in vitro culture system previously

devised by our group to study osteogenic and adipogenic NC progenitors (Coelho-Aguiar et al., 2013). We first showed that a particular subset of *Hox* genes, including *Hoxa2*, is downregulated in cultured trunk NCC, concurrently with the emergence of *Runx2*-positive skeletal progenitors. Then, by performing gain of function experiments in early NCC in vitro, we found that *Hoxa2* overexpression reduced the number of *Runx2*+ osteoprogenitors, produced by both cephalic and trunk NCC. *Hoxa2* also impaired the terminal differentiation into main mesenchymal cell types. These results, therefore, suggest that the expression of mesenchymal potentialities by trunk NCC in vitro could, at least partially, rely upon downregulation of *Hoxa2*, which thus could help to disclose trunk NC dormant mesenchymal fate.

Materials and Methods

NC cultures and transfection procedure

Quail (*Coturnix coturnix japonica*) fertilized eggs were obtained from a commercial source (Cailles de Chanteloup, France) and incubated at 38.5 °C. For trunk NC cultures, thoracic neural tubes from embryos of 2 days of incubation, 20-25 somite-stage (20-25ss), were dissected and cultured as described (Calloni et al., 2007; Coelho-Aguiar et al., 2013). After for 15-18 hours (h) of culture, explanted neural tubes were detached and discarded. Isolated NCC, which had migrated from these explanted tubes, were detached, centrifuged and counted before transfection. About 80,000 trunk NCC were transfected with 100ng DNA plasmid using Lipofectamine 2000 (ThermoFisher Scientific) at a 1:2 DNA-reagent ratio. Immediately after DNA delivery, NCC were seeded as 12 µl-droplets per well (5,000 cells per drop) in collagen-1 coated wells (4-well and 24-well culture plates; Nunc). Three hours after plating, the wells were filled with culture medium containing DMEM (Sigma), 10% FBS (Invitrogen) and 2% chicken embryo extract (80ng/ml).

For cephalic NC cultures, mesencephalic neural primordia, including the pre-migratory neural crest, were isolated from 6-7ss embryos and cultured essentially as previously described (Calloni et al., 2007, 2009). Briefly, approximately 25 neural primordia were isolated and cultured in collagen-1 coated 35-mm dishes. After 15 h, the cultures were transfected with 1.5 µg of DNA constructs using Lipofectamine 2000 (ThermoFisher Scientific). Three hours later, the migratory NCC were isolated from the explants of mesencephalon, then seeded on a 3T3 fibroblast feeder-layer (Calloni et al., 2007). About 200 NCC were plated per well in 96-well plates (TPP) in DMEM

containing 10% FCS and 2% chicken embryo extract (80ng/ml). Cephalic and trunk NCC cultures were maintained at 37°C in a humidified 5% CO2 incubator and the medium was changed every three days.

Expression plasmids

We isolated chicken *Hoxa2* and *Hoxc10* DNA constructs by PCR amplification of cDNA sequences, followed by subcloning into the EcoRI-NotI site of pCX expression plasmid (Niwa et al., 1991). In-Fusion HD Cloning Kit (Clontech) was used for PCR amplification and thermocycling conditions were set up according to the manufacturer's instructions. All constructs were sequenced for accuracy. The pCX-EGFP plasmid (Okabe et al., 1997) was used in all experiments as a control. All constructs were amplified in endotoxin-free condition (MaxiPrep kit, Qiagen).

Quantitative RT-PCR

Total RNA was isolated using a RNeasy Micro kit with a DNase digestion step (Qiagen). cDNA was synthesized with a reverse transcription kit (iScript; Bio-Rad Laboratories) in a PTX-100 thermal cycler (Bio-Rad Laboratories, Hercules, CA, USA). For real-time quantitative PCR (RT-qPCR), cDNA, Power SYBR Green PCR master mix and 0.6µM/well of specific primers were mixed in a 96-well optical reaction plate (all from Applied Biosystems; see TableS1 for primer sequences). Cycling conditions included an initial denaturation step at 95°C for 10 min, followed by 40 cycles consisting of 15 sec denaturation at 95°C and 1 min at 60°C for annealing and primer extension. GAPDH (glyceraldehyde-3-phosphate dehydrogenase) was used as a housekeeping gene for normalization, and amplification of its cDNA was done in parallel with the genes of interest. PCR products were subjected to melting curve analysis, and threshold cycle (Ct) values were determined using the Applied Biosystems software. Relative fold changes were calculated using the ΔΔCt method.

In situ hybridization and immunostaining

Riboprobes were prepared from a cDNA plasmid encoding the chicken *Runx2* coding sequence (GenBank NM_204128.1), according to an already described procedure (Calloni et al., 2007). Digoxygenin-labeled antisense RNA probes were used to perform in situ hybridization on trunk NC cultures, according to a detailed protocol described elsewhere (Calloni et al., 2007, 2009).

For immunostaining, 6-day cultures of trunk and cephalic NCC were fixed in 4% formaldehyde for 30 min and immunolabeled with anti-Runx2 (1:100, Sigma, HPA022040), antibody to α-smooth muscle actin (αSMA, clone 1A4; 1:800, Sigma, A5228), and the following hybridoma supernatants (used undiluted): mouse anti-quail tyrosine hydroxylase (Fauquet and Ziller, 1989), melanoblast/melanocyte early marker (MelEM) (Nataf et al., 1993) and HNK1 (ATCC TIB-200). All secondary antibodies used were Alexa Fluor 488-, 546- and 647-conjugated antibodies (ThermoFisher Scientific), except for Runx2 immunostaining, which was detected using HRP-labeled goat anti-rabbit and signal amplification with Cy3-tyramide (Tyramide System Amplification, Perkin-Elmer). Cultures were counterstained with 4',6-diamidino-2-phenylindole (DAPI) to mark cell nuclei, which enables quail cephalic NCC to be easily distinguished from mouse 3T3 fibroblasts by their distinct nuclear sizes (Baroffio et al., 1988).

Imaging and quantifications were carried out automatically with an Arrayscan High-Content system (Thermo Fisher Scientific), in which at least 49 fields of each replicate culture were analyzed. In cephalic NC cultures, specific protocols were designed to exclude the 3T3 cell nuclei from nuclei quantification. Representative pictures were obtained in every experiment with an inverted fluorescence microscope (Nikon-Eclipse Ti-E).

Terminal differentiation in NCC cultures and histological staining

To promote full differentiation of NCC into mesenchymal lineages, long-term culture of trunk NCC was performed essentially as previously described (Coelho-Aguiar et al., 2013). After 7 days of culture in DMEM, 2%FBS and 2% chicken embryo extract, the medium was supplemented with 85nM insulin, 1 nM tri-iodo-thyronine (T3), 0.5 µM rosiglitazone, 0.05 µM dexamethasone, 25 µg/ml ascorbic acid and 5 mM β-glycerol phosphate (all from Sigma). This specific medium composition promoted terminal differentiation of skeletogenic and adipogenic cells derived from trunk NCC in vitro (Coelho-Aguiar et al., 2013). To assess for mineralized bone areas, cartilage nodules and lipid-storing adipocytes, 25-day-cultures were fixed with 4% formaldehyde for 1h at room temperature, and sequential histological staining was performed as follows. First, the cultures were stained for 5 min with 2% Alizarin Red S (Sigma), washed with H2O and the stained mineralized bone matrix was imaged. Next, to detect cartilaginous matrix, Alcian Blue (Sigma) solution (1% in 0.1M HCl pH 1.0) was applied overnight, washed and then imaged. Finally, triglyceride lipid accumulation in adipocytes was identified by Oil Red O staining (0.5% in isopropanol, Sigma). Image acquisition was performed with an inverted microscope (Nikon-Eclipse

Ti-E) and the total area of stained regions was quantified using Fiji software (Schindelin et al., 2012).

Statistical Analyses

All data are presented as mean values ± SEM of at least three independent experiments and analyzed with GraphPad Prism 5.03 (GraphPad Software Inc.). Statistical significance was tested by a one-way ANOVA with Dunnett's correction for multiple comparisons (for data from RT-qPCR, in situ hybridization and immunostaining; Figure 2 and 4), Mann-Whitney test (for areas of stained regions, Figure 3) and Unpaired t-test (for analyses of cephalic NCC, Figure 5). Significance was set as follows: $P < 0.05$ (*), $P < 0.01$ (**), or $P < 0.001$ (***).

Results

A defined set of *Hox* genes are downregulated in trunk NC cultures maintained in pro-mesenchyme culture conditions

Given that trunk multipotent NCC display mesenchymal potentials in vitro as do cephalic NCC in vivo and in vitro (Le Douarin and Kalcheim, 1999; Calloni et al., 2007; Billon et al., 2007; Coelho-Aguiar et al., 2013), we aimed to investigate if the onset of mesenchymal progenitors in trunk NCC in vitro cultures could, to some extent, operate according to a similar mechanism as in the cephalic NCC. We thus hypothesized that *Hox* gene inhibition could play a role in the expression of these mesenchymal capacities. As a first step to investigate this possibility, we aimed at identifying the *Hox* genes expressed by the trunk NC before and during in vitro differentiation. For this purpose, we evaluated the repertoire of *Hox* genes expressed in the quail neural tube, at the level and stage of development used in prepare NC cultures (Figure 1A), corresponding to the thoracic neural tube of E2 quail embryos (22-25 ss stage), wherein the *Hox* paralog groups 6 to 9 are expected to be expressed (Burke et al., 1995; Nolte and Krumlauf, 2007, for a review). As the neural tube explants also comprised portions of the most posterior cervical domain (between 18 to 19 ss) and of the most anterior lumbar domain (pre-somitic mesoderm, 26 ss), we included *Hox* genes from paralog groups 5 and 10 in the analyses. In addition, *Hoxa2* gene expression was also investigated, due to previous findings showing its inhibitory effect on the formation of NC-derived craniofacial structures in vivo (Creuzet et al., 2002; Kanzler et al., 1998). By RT-qPCR, we found

that, from the *Hox* genes mentioned above, 10 defined *Hox* members were highly expressed in isolated trunk NCC cultures at day 0 (Table S1 and Figure S1): *Hoxa2*, *Hoxb5*, *Hoxc6*, *Hoxa7*, *Hoxb8, Hoxc8, Hoxb9, Hoxc9, Hoxc10* and *Hoxd10*) showed at least 50-fold higher mRNA expression levels compared with mesencephalic NCC, which represented a negative control for *Hox* gene expression.

We then investigated the time-course of the expression profile of these selected *Hox* genes during in vitro culture of trunk NCC, isolated from trunk neural tube explants as illustrated in Figure 1A, and maintained for 8 days in culture conditions wherein NCC differentiate into a large array of NC derivatives, including several mesenchymal cell types (Coelho-Aguiar et al., 2013). In this regard, *Runx2*, a transcription factor gene necessary for bone cell specification, was significantly detected by RT-qPCR as soon as 2 days of culture and thereafter was continuously present, with a peak of increased transcription levels at 4 days of culture (Figure 1B). These results suggest that the onset of bone specification in trunk NCC occurs during the early culture period. As a consequence, we analyzed the dynamics of the expression of the selected set of *Hox* genes during the first week of culture. A first subset of these *Hox* genes, namely *Hoxa2*, *Hoxc9* and *Hoxc10* was significantly downregulated at day-2, (by approximately 5.7, 5.5 and 9.7-fold, respectively), compared with day-0 cultures (Figure 1C). These three *Hox* genes then were continuously downregulated (up to 20.3, 28.4 and 42.2 fold at day-8, respectively, compared with day-0 cultures). Two other genes, *Hoxc6* and *Hoxc8,* showed only moderate reduction of mRNA levels at day-8 and day-6, respectively (Figure 1C). In contrast, the remaining five other tested *Hox* genes (*Hoxb5, Hoxa7, Hoxb8, Hoxb9 and Hoxd10*) did not significantly change in this temporal analysis, although *Hoxb9* exhibited a modest upregulation at day-2 (Figure 1D). Together, these results show that the onset of *Runx2*-expressing osteoblasts in trunk NCC cultures (between day-2 and day-4 of culture) is temporally linked with a downregulation of a specific set (*Hoxa2*, *Hoxc9* and *Hoxc10)* of the *Hox* gene repertoire initially expressed in the trunk NC.

Hoxa2 forced expression reduces the number of osteoprogenitors and terminal differentiation of trunk NCC into bone, cartilage and fat cells

The results shown in Figure 1 pointed out that *Hoxa2*, *Hoxc9* and *Hoxc10* were significantly downregulated concomitantly with in vitro differentiation of osteoblasts by trunk NCC. To investigate if this change in *Hox* gene activity could be functionally related to the mesenchymal differentiation of NCC, we aimed to evaluate the consequences of forced expression of these

genes on the development of Runx2+ cells in trunk NC cultures. Firstly, we decided to investigate *Hoxa2*, due to its established negative effect on the formation of the NC craniofacial mesenchyme in vivo and in vitro (Creuzet et al., 2002; Kanzler et al., 1998; Abzhanov et al., 2003). Additionally, we forced the expression of *Hoxc10*, the most posterior *Hox* gene expressed by the cultured trunk NCC, which was, similarly to *Hoxa2*, significantly downregulated during in vitro progression towards mesenchymal differentiation. As shown in Figure 2A, after isolation of NCC from NT explants, we transfected the NCC suspension (day-0 of culture) with pCX plasmids, which resulted in approximately 45-70% of the NCC successfully expressing *Hox* or *GFP* reporter (Figure Suppl 2). When we examined the amount of Runx2+ cells in day-6 culture, identified by *in situ* hybridization and immunostaining, we observed that forced expression of *Hoxa2*, but not *Hoxc10*, reduced the number of *Runx2*-expressing cells (Figure 2 B-M): *Runx2* transcripts were present in 12.5% of the cells in control GFP plasmid condition, while this percentage decreased to 5% after *Hoxa2* overexpression, indicating a 60% reduction (Figure 2N). At the protein level, 11% of trunk NCC expressed Runx2 in control GFP cultures versus 4% in *Hoxa2*-transfected cultures, showing, again, a 60% decrease of the number of Runx2-expressing cells (Figure 2O).

We next asked whether *Hoxa2* forced expression could impair the progression towards terminal differentiation of bone progenitors, due to its influence on the number of Runx2+ cells. Trunk NCC cultures were transfected as described previously and further grown in the presence of “mesenchymal differentiation factors” (MDF) (see Materials and Methods; Figure 3A), which enhanced terminal differentiation of cultured NCC into bone, cartilage and fat cells (Coelho-Aguiar et al., 2013). This experimental procedure allowed analyses of *Hoxa2* effects on additional mesenchymal lineages, such as chondrocytes and adipocytes. As shown in Figure 3, MDF treatment promoted mineral deposition in the matrix surrounding osteoblasts in culture, easily observed after Alizarin Red staining in 25-day cultures (Figure 3 B,E). Cartilaginous matrix deposition and lipid-storing adipocytes could be detected with Alcian Blue and Oil Red O histological staining, respectively (Figure 3C,F and 3D,G). We noted that the transfection procedure at day-0 did not interfere with terminal differentiation of these mesenchymal derivatives, which were present in 25-day cultures transfected with control GFP plasmid (Figure 3 B-D). However, after *Hoxa2* overexpression, the regions stained with Alizarin Red, Alcian Blue and Oil Red O were much smaller and less frequent (Figure 3 E-G), suggesting an impairment of the terminal differentiation process. The number of cultures containing mineralized bone areas drops down after *Hoxa2* overexpression (11 in 61) when compared to GFP-transfected NC cultures (25 in

61). Regarding cartilage differentiation, 28 cultures in 46 and only 16 cultures in a total of 46 contained cartilage nodules in control and *Hoxa2* conditions, respectively. Similarly, 34 in 46 cultures had differentiated adipocytes versus 29 in 46 after *Hoxa2* gain of function. A quantification of the total area of the cultures occupied by the differentiated mesenchymal cells was also performed to better evaluate the effect of *Hoxa2* (Figure 3H-J). The total surface area in each culture was normalized by the total cell number in the cultures, detected after DAPI nuclei staining. We could then observe that, compared to *GFP, Hoxa2* gain of function decreased approximately by 85% the total area occupied by mineralized ossified regions, by 70% the area of cartilaginous matrix and by 70% the total surface of adipocytes (Figure 3H-J).

Taken together, these results show that *Hoxa2* strongly reduces the number of Runx2+ osteoblastic cells, further preventing terminal differentiation of bone cells in trunk NCC cultures. Moreover, *Hoxa2* gain of function also impaired the production of differentiated chondrogenic and adipogenic cells, indicating that *Hoxa2* exerts inhibitory effects on the in vitro differentiation of mesenchymal lineages in trunk NCC.

Hoxa2 and _Hoxc10_ did not influence trunk NCC differentiation into myofibroblasts and non-mesenchymal cell types

We also investigated whether *Hoxa2* and *Hoxc10* overexpression in day-0 cultures could influence the differentiation of NCC into other cell types, such as neural and melanocytic cells. Figure 4 shows the distinct cell phenotypes analyzed at day-6 in the transfected cultures: catecholaminergic neurons (TH+), melanocytes (MelEM+), myofibroblasts (αSMA+) and undifferentiated cells/neural progenitors (HNK1+). We found that the trunk NCC population in control cultures that overexpressed *GFP* was composed of about 40% HNK1+ cells, 22% αSMA+, 3,5% MelEM+ and a small population of TH+ neurons (0.4%) (Figure 4M). The percentages of these cell phenotypes did not change significantly after *Hoxa2* and *Hoxc10* overexpression (Figure 4M).

In cephalic NCC cultures, _Hoxa2_ ectopic expression reduced Runx2 osteoprogenitors, without effect on other NC derivatives

Taken into account the above results of *Hoxa2* gain of function in trunk NCC cultures, we next investigated whether similar events could be observed in cephalic NCC. In vitro, *Hoxa2* viral transduction decreased the production of chondrocytes expressing collagen-2 in avian mesencephalic neural fold cultures (Abzhanov et al., 2003). However, a possible action of *Hoxa2*

on Runx2-positive progenitors has not been examined, especially in an isolated NCC culture environment. Therefore, we carried out pCX plasmids deliveries to mesencephalic NT explants containing the premigratory NCC, followed by culturing these cells until differentiation in vitro (see Materials and Methods). With this transfection strategy, approximately 40-50% of NCC successfully expressed GFP driven by the pCX-GFP construct (data not shown). As shown in Figure 5A-H, in day-6 cultures, Runx2 labeled cells accounted for approximately 22% of the cranial NCC transfected with control pCX-GFP. This percentage was remarkably decreased after *Hoxa2* ectopic expression in cranial NCC: about 10% expressed Runx2, resulting in a reduction of 55% compared to GFP control condition (Figure 5G). Interestingly, *Hoxa2* ectopic expression was also associated with a 40% decrease of the total cell number per culture, as depicted by DAPI cell nuclei quantification (Figure 5H). Moreover, similarly to trunk NCC experiments, we investigated if *Hoxa2* could alter differentiation into multiple NC derivatives, including catecholaminergic neurons (TH+), melanocytes (MelEM+), myofibroblasts (αSMA+) and undifferentiated cells/neural progenitors (HNK1+). In control GFP-transfected cells, the cephalic NCC population comprised about 60% HNK1+ cells, 7% αSMA+, 3% MelEM+ and 0.3% TH+ neurons (Figure 5I-P). No differences were observed in the relative amount of these NC derivatives after *Hoxa2* gain of function. Therefore, these results point toward an effect of ectopic *Hoxa2* in cephalic NCC, specifically on the development of Runx2-expressing osteoprogenitors.

Discussion

In vertebrates, mesenchymal cell types (e.g., chondrocytes, bone cells and adipocytes) originate from two embryonic tissues: the mesoderm and the NC. In the latter, mesenchymal fate is essentially restricted to the NC cephalic domain. Apart from a modest contribution of trunk NCC to endoneurial fibroblasts in the sciatic nerve of mammals and, although controversial, to the caudal and dorsal fin bony rays of teleost fish (Joseph et al., 2004; Smith et al., 1994; Mongera and Nüsslein-Volhard, 2013; Lee et al., 2013), the trunk NC does not produce other mesenchymal derivatives. Nevertheless, when challenged by a permissive in vitro environment, avian trunk NCC can differentiate into skeletogenic and adipogenic cell types, showing that the trunk NC of amniotes is not devoid of mesenchymal differentiation potential (Baroffio et al., 1988, 1991, Calloni et al., 2007, 2009; Billon et al., 2007; Coelho-Aguiar et al., 2013).

Hox proteins might be candidate factors underlying the differential regulation of mesenchymal fate between trunk and cephalic NCC. *Hox* genes are expressed by the trunk NCC whereas the skeletogenic cephalic NCC belong to the *Hox*-negative anteriormost domain of the vertebrate body. Furthermore, the expression of *Hox* genes ectopically induced in the cranial NCC, severely impairs the generation of NC facial mesenchyme (Couly et al., 1996, 1998, 2002; Creuzet et al., 2002; Kanzler et al., 1998; Kitazawa et al., 2015). It is therefore plausible that *Hox* genes in the trunk NC may have a role in the inability of these cells to execute a mesenchymal developmental program in vivo. Along this line, we have here investigated the possible influence of *Hox* genes on NC mesenchymal fate, using in vitro culture models that allow to monitor differentiation of avian cephalic and trunk NCC .

Selected *Hox* genes are downregulated concomitantly with trunk NCC osteoblast differentiation in vitro

Given that trunk NCC display mesenchymal potentials in vitro as do cephalic NCC in vivo and in vitro, we hypothesized that the capacity of trunk NCC to differentiate into mesenchymal derivatives in vitro could involve a downregulation of *Hox* genes during the culture, when trunk NCC are maintained in pro-mesenchymal conditions. By RT-qPCR analyses at different culture time points, we found that a particular subset of *Hox* genes, (namely, *Hoxa2*, *Hoxc6*, *Hoxc8*, *Hoxc9,* and *Hoxc10*), were negatively regulated by trunk NCC, concomitantly with the onset and upregulation of the bone specification gene, *Runx2*, the earliest mesenchymal lineage marker gene expressed in these cultures. Interestingly, it has been previously demonstrated that expression of *Hoxb4* and genes of the *Hox9* paralog group was downregulated in long-term trunk NC cultures giving rise to chondrocytes (Abzhanov et al., 2003; Ido and Ito, 2006). Nonetheless, whether *Hox* genes could act on other NC-derived mesenchymal cell lineages, such as osteoblasts and adipocytes, has not been studied. To address these issues, we investigated whether particular *Hox* genes have the capacity of inhibiting mesenchymal cell fate in trunk NCC cultured in vitro. We focused in this work on two *Hox* genes: *Hoxa2*, due to the deleterious effects on cephalic development observed when this gene is expressed ectopically in the cranial NC (Creuzet et al., 2005, for a review) and *Hoxc10*, since we found that, similarly to *Hoxa2*, this gene was strongly downregulated during in vitro bone differentiation of trunk NCC.

Hoxa2, not _Hoxc10_ gain of function in trunk NCC exerts negative effects on early skeletogenic cells

With the aim to investigate whether *Hoxa2* and *Hoxc10* can inhibit mesenchymal differentiation of trunk NCC in vitro, we forced the expression of these genes at the beginning of the culture period, before the onset of Runx2 expression. Following *Hoxa2* overexpression, we detected a drastic reduction in the number of Runx2-labeled osteoprogenitors, suggesting that *Hoxa2* influences the emergence of bone progenitors in the NC cultures. Indeed, in murine embryos, *Hoxa2* gene inactivation led to increase of *Runx2* expression by postmigratory NCC in the branchial arches (Kanzler et al., 1998). Conversely, ectopic expression of *Hoxa2* resulted in downregulation of *Runx2* and *Sox9* in cephalic NC-derived skeletal elements (Grammatopoulos et al., 2000; Garcez et al., 2014; Kitazawa et al., 2015). These results suggest that *Hoxa2* causes alterations of *Runx2* activity in cephalic NCC in vivo, and in trunk NCC in vitro. Interestingly, our data also showed that forced expression of *Hoxc10* did not significantly reduce Runx2 expression by trunk NCC, suggesting that not all the *Hox* genes could account for the same effects as *Hoxa2*; hence, a specific downregulation of *Hoxa2*, instead of a global *Hox* gene reduction, might play a role in NCC differentiation.

The molecular mechanism by which *Hoxa2* could influence Runx2 expression in NCC is not yet understood. A direct action of Hoxa2 transcription factor on *Runx2* transcriptional activity may be a possible mechanism, since putative Hox-binding consensus sequences have been characterized in the *Runx2* gene promoter (Hassan et al., 2007). Nevertheless, a specific binding of Hoxa2 protein to the *Runx2* promoter has never been described. Alternatively, Hoxa2 could downregulate other genes, which mediate induction of main molecular players in bone differentiation by NCC, including *Runx2*. In this regard, the *Six2* gene could be involved, since it has been described as a direct downstream factor of *Hoxa2* in the NC-derived mesenchyme of BA2 in the mouse (Kutejova et al., 2005, 2008). In addition, *Six2* gene inhibition in the anterior cranial NCC resulted in hypoplasia of the craniofacial skeleton in mouse and chick embryos, a phenotype opposite to *Hoxa2* overexpression (He et al., 2010; Garcez et al., 2014). However, at least in our culture system, an involvement of *Six2* during in vitro mesenchymal differentiation of avian trunk NCC seems unlikely, since we did not detect expression of *Six2* and closely related *Six1* genes, in untransfected and transfected cultures (data not shown).

Notably, activation of *Runx2* gene by individual *Hox* genes, instead of its repression, has been previously reported. In mesoderm-derived tissues, some of the posteriorly expressed *Hox* genes can activate *Runx2*, *Sox9,* and other bone master genes, thus allowing the progression of endochondral ossification (Hassan et al., 2007, 2009; Gross et al., 2012; Neufeld et al., 2014). In this line, it should be interesting to understand which are the factors involved in impairment of skeletogenesis by *Hox*, specifically in the NCC.

Hoxa2 gain of function influences the terminal differentiation of trunk NC-derived bone, cartilage and fat cells

By using a culture protocol previously devised by our group to assess the mesenchymal differentiation capacities of trunk NCC in vitro (Coelho-Aguiar et al., 2013), we investigated if *Hoxa2* forced expression in early trunk NCC could affect the formation of mature differentiated bone, cartilage and adipose tissue cells in long-term cultures. For this purpose, trunk NCC were transfected on the first day of culture with *Hoxa2* plasmid and further analyzed after 25 days in culture, when differentiated bone and cartilage matrices, and lipid-storing adipocytes were identified. We observed a significant reduction in the surface area occupied by mineralized bone after *Hoxa2* forced expression, thus suggesting that early effects of *Hoxa2* on Runx2-positive osteoprogenitors could have prevented, later on, the maturation of bone cells derived from trunk NC progenitors.

Furthermore, *Hoxa2* gain of function significantly decreased chondrocyte mineralization by approximately 70% as compared with the GFP-control plasmid. Previous reports have shown that avian trunk NCC in long-term cultures can produce cartilage (McGonnell and Graham, 2002), and the onset of collagen-2 expression by chondrocytes was correlated with downregulation of *Hoxb4* and *Hox9* in avian and murine trunk NCC (Abzhanov et al., 2003; Ido and Ito, 2006). Our present data provide a first evidence that *Hoxa2* overexpression affects cartilage full differentiation by trunk NCC in vitro. Interestingly, in vivo *Hoxa2* gain of function in immature chondrocytes expressing *collagen 2a1* gene, resulted in overall chondrodysplasia and delayed endochondral ossification in transgenic mouse embryos (Massip et al., 2007). Taken together, these results suggest a robust negative effect of *Hoxa2* on trunk NC skeletogenic potential and differentiation.

Our protocol to obtain fully differentiated mesenchymal cells derived from quail trunk NCC in culture also permited the study of the differentiation of adipocytes (Coelho-Aguiar et al., 2013).

In this way, we could address, for the first time, whether *Hoxa2* could influence adipogenesis by trunk NCC. Notably, *Hoxa2* gain of function significantly reduced the surface area containing lipid-storing adipocytes, suggesting that, not only bone and cartilage, but also adipocytic cell differentiation in vitro is impaired following *Hoxa2* overexpression in trunk NCC. Regarding adipose tissue formation, particular *Hox* genes are involved in mesoderm-derived adipocyte differentiation (Seifert et al., 2015). For instance, *Hoxa4*, *Hoxa7*, and *Hoxd4* were upregulated during in vitro adipogenesis of 3T3-L1 pre-adipocytic cells, although a specific function of these genes was not studied (Cowherd et al., 1997). Furthermore, Pbx1, which acts as cofactor of several *Hox* genes (Mann et al., 2009; Capellini et al., 2011), was recently described as required for early steps of adipogenesis in neuralized mouse ES cells, a model of NC-derived adipogenesis (Billon et al., 2007) and in human multipotent adipose-derived stem cells (Monteiro et al., 2011). Whether, in trunk NC cultures, *Hoxa2* negative regulation of the adipogenic fate could have a relationship with Hoxa2 binding to Pbx1, remains to be investigated.

Ectopic expression of *Hoxa2* in cephalic NCC reduces in vitro development of Runx2 progenitors

Hoxa2 effects on cranial NCC development have been extensively described in avian and murine models (Couly et al., 1996, 1998, 2002; Creuzet et al., 2002; Kanzler et al., 1998; Kitazawa et al., 2015). Nonetheless, a direct effect of *Hoxa2* forced expression on osteoblasts has never been described in isolated cephalic NCC. Thus, in order to be able to compare *Hoxa2* effects between cranial and trunk NCC, we performed quail cephalic NC cultures on 3T3 feeder layers, using a protocol previously established by our group (Calloni et al., 2007, 2009), and we transfected these cells with the same *Hox* and *GFP* constructs used for trunk NC cultures. In the *Hoxa2*-overexpressing cultures, we found a significant reduction of the number of *Runx2*+ osteoprogenitors, in comparison with the GFP control condition. We also noticed a decrease in the total cell number per culture, indicating that *Hoxa2* could act on the survival or the proliferation rates of the whole NCC population, possibly also including progenitors for chondrocytes and adipocytes, which differentiated in cephalic NC in vitro cultures (Calloni et al., 2007, 2009; Billon et al., 2007). In vivo, ectopic expression of *Hoxa2* in chicken cranial NCC leads to a reduction in cell proliferation and increase in cell death at early postmigratory NC stages, later on resulting in hypoplasia of nasal and mandibular buds (Creuzet et al., 2002; Garcez et al., 2014). However, in a genetic mouse model wherein *Hox* genes were globally upregulated in the whole NC after targeted deletion of the epigenetic repressor *Ezh2*, Schwarz et al. (2014) did not find differences in cranial

NCC proliferation and apoptosis; yet, these *Ezh2* mutant mice exhibited severe defects in the NC-derived craniofacial mesenchyme (Schwarz et al., 2014). As of note, in the present trunk NC in vitro experiments, the reduction of the total NCC number after *Hoxa2* gene transfection was highly variable (ranging from 5 to 20%) compared with the GFP control condition (data not shown). Therefore, *Hoxa2* may have an additional role in cephalic NCC, probably controlling cell death and/or cell division. Interestingly, *Hox* genes have been associated with autophagy control in *Drosophila* and vertebrate cells (Banreti et al., 2014; Yang et al., 2016). Moreover, recent findings suggest that integrity of the autophagy process is required during induction and delamination of chick NCC (Wang et al., 2015, 2017). Nevertheless, whether the action of *Hox* genes on NC mesenchymal progenitor development could involve regulation of autophagy is currently unknown.

Myofibroblasts and neural cell types are not affected by *Hoxa2* gain of function in cephalic and trunk NCC

Besides mesenchymal derivatives, the NCC give rise to a broad array of cell types in vivo and in vitro, including melanocytes, myofibroblasts, and PNS neural (glial and neuronal) cells. Moreover, cephalic and trunk NCC comprise similar multipotent precursors endowed with neuro-mesenchymal fate, that is, precursors capable of yielding both neural and mesenchymal cell types in vitro (Dupin et al., 2010; Dupin and Le Douarin, 2014). Considering the presence of multipotent cells in early NCC, we examined the influence of *Hoxa2* on the differentiation of main NC-derived cell types, i.e., myofibroblasts, TH+ neurons, melanocytes and HNK1+ neuroglial precursors. Strikingly, *Hoxa2* overexpression did not significantly alter the percentage of myofibroblasts and neural cells obtained in cephalic NC cultures. These results corroborate previous in vivo findings, which showed that *Hox*-positive rhombencephalic NCC, if grafted into a more anterior *Hox*-negative domain of the NC, were still able to yield neural derivatives and vascular smooth muscle cells, not skeletal cells, in the host cranial territories, while maintaining their *Hox* status (Couly et al., 1998; Creuzet et al., 2002; Couly et al., 2002). Similar conclusions regarding neuronal and glial differentiation ability were obtained in *Ezh2* mutant mouse embryos, wherein multiple *Hox* genes are derepressed in the cephalic NCC (Schwarz et al., 2014). In summary, our results support the hypothesis that *Hoxa2* exerts a negative, lineage-specific effect on cephalic and trunk NCC mesenchymal fate in vitro. In contrast, as already observed for Runx2+ osteoprogenitors, the

production of myofibroblasts and neural cell types by cultured trunk NCC was not significantly modified after *Hoxc10* gain of function.

Concluding remarks

In this work, we have shown that the in vitro mesenchymal differentiation capacity of trunk NCC is partially impaired by *Hoxa2*, not by *Hoxc10*, after overexpression of these genes in early trunk NCC. In addition, *Hoxa2* decreased terminal differentiation of bone cells, chondrocytes and adipocytes in long-term trunk NC cultures. In cephalic NCC, *Hoxa2* gain of function also reduced the number of NC-derived bone progenitors in vitro. Altogether, these data suggest a similar dependence of trunk and cephalic NCC on a *Hoxa2*-negative status in order to allow the outcome of *Runx2*-expressing osteoblasts.

It has been proposed that, in primitive vertebrates, both cephalic and trunk NC may have been at the origin of skeletal cells that formed the superficial dermal bone covering the whole body of these extinct animals (Smith, 1991; Smith and Hall, 1990; Le Douarin and Dupin, 2012). From our data, which reveal that *Hoxa2* acts on both cephalic and trunk NC to prevent their mesenchymal outcome, we hypothesize that this regulation by *Hoxa2* may represent a common mechanism to restrict NC mesenchymal fate, shared by NCC along the entire neural axis. Nonetheless, recent findings suggested that the mesenchymal molecular program of avian cephalic NCC relies upon the expression of a defined set of three cranial-specific transcription factors (Simoes-Costa and Bronner, 2016). Strikingly, Simoes-Costa and Bronner (2016) could reprogram the fate of trunk NCC in an in vivo context, when, after ectopic expression of the selected set of genes, the trunk NCC were grafted in the cephalic NC migratory stream of a host embryo (Simoes-Costa and Bronner, 2016). Therefore, these and our present data illustrate that multiple regulatory pathways might be necessary to control the expression of the diverse mesenchymal fates in the NCC: potentially inhibitory factors include *Hox* genes, particularly *Hoxa2*, while cranial NC-specific positive regulators would reinforce mesenchymal fate in the cephalic NCC. Whether *Hox* genes could act upstream of these cranial NC-specific regulatory genes, to prevent their expression in trunk NCC, is an interesting issue for future investigation.

Acknowledgements

The authors thank Anaïs Potey and Stéphane Fouquet for their technical assistance (High-Throughput Screening and Imaging Core Facilities, Vision Institute, France). This work was supported by the Centre National de la Recherche Scientifique (CNRS; France). B.F.F was supported by a Ph.D fellowship from "Ciências sem Fronteiras" program (CNPq; Brazil).

References

Abzhanov, A., E. Tzahor, A.B. Lassar, and C.J. Tabin. 2003. Dissimilar regulation of cell differentiation in mesencephalic (cranial) and sacral (trunk) neural crest cells in vitro. *Development*. 130:4567–4579.

Banreti, A., B. Hudry, M. Sass, A. Saurin, and Y. Graba. 2014. Hox Proteins Mediate Developmental and Environmental Control of Autophagy. *Dev. Cell*. 28:56–69.

Baroffio, A., E. Dupin, and N.M. Le Douarin. 1988. Clone-forming ability and differentiation potential of migratory neural crest cells. *Neurobiology*. 85:5325–5329.

Baroffio, A., E. Dupin, and N.M. Le Douarin. 1991. Common precursors for neural and mesectodermal derivatives in the cephalic neural crest. *Development*. 112:301–305.

Billon, N., P. Iannarelli, M.C. Monteiro, C. Glavieux-Pardanaud, W.D. Richardson, N. Kessaris, C. Dani, and E. Dupin. 2007. The generation of adipocytes by the neural crest. *Development*. 134:2283–2292.

Burke, A.C., C.E. Nelson, B.A. Morgan, and C.J. Tabin. 1995. Hox genes and the evolution of vertebrate axial morphology. *Development*. 121:333–346.

Calloni, G.W., N.M. Le Douarin, and E. Dupin. 2009. High frequency of cephalic neural crest cells shows coexistence of neurogenic, melanogenic, and osteogenic differentiation capacities. *Proc. Natl. Acad. Sci. USA*. 106:8947–8952.

Calloni, G.W., C. Glavieux-Pardanaud, N.M. Le Douarin, and E. Dupin. 2007. Sonic Hedgehog promotes the development of multipotent neural crest progenitors endowed with both mesenchymal and neural potentials. *Proc. Natl. Acad. Sci. USA*. 104:19879–19884.

Capellini, T.D., V. Zappavigna, and L. Selleri. 2011. Pbx homeodomain proteins: TALEnted regulators of limb patterning and outgrowth. *Dev. Dyn.* 240:1063–86.

Chai, Y., X. Jiang, Y. Ito, P. Bringas, J. Han, D.H. Rowitch, P. Soriano, a P. McMahon, and H.M. Sucov. 2000. Fate of the mammalian cranial neural crest during tooth and mandibular morphogenesis. *Development*. 127:1671–1679.

Coelho-Aguiar, J.M., N.M. Le Douarin, and E. Dupin. 2013. Environmental factors unveil dormant developmental capacities in multipotent progenitors of the trunk neural crest. *Dev. Biol.* 384:13–25.

Couly, G., S. Creuzet, S. Bennaceur, C. Vincent, and N.M. Le Douarin. 2002. Interactions between Hox-negative cephalic neural crest cells and the foregut endoderm in patterning the facial skeleton in the vertebrate head. *Development*. 1073:1061–1073.

Couly, G., and N.M. Le Douarin. 1988. The fate map of the cephalic neural primordium at the presomitic to the 3-so mite stage in the avian embryo. *Development*. 103:101–113.

Couly, G., A. Grapin-botton, P. Coltey, B. Ruhin, and N.M. Le Douarin. 1998. Determination of the identity of the derivatives of the cephalic neural crest : incompatibility between Hox gene expression and lower jaw development. *Development*. 3459:3445–3459.

Couly, G., a Grapin-Botton, P. Coltey, and N.M. Le Douarin. 1996. The regeneration of the cephalic neural crest, a problem revisited: the regenerating cells originate from the contralateral or from the anterior and posterior neural fold. *Development*. 122:3393–3407.

Couly, G.F., P.M. Coltey, and N.M. Le Douarin. 1993. The triple origin of skull in higher vertebrates: a study in quail-chick chimeras. *Development*. 117:409–429.

Cowherd, R.M., R.E. Lyle, C.P. Miller, and R.E. Mcgehee. 1997. Developmental profile of homeobox gene expression during 3T3-L1 adipogenesis. *Biochem. Biophys. Res. Commun.* 237:470–5.

Creuzet, S., G. Couly, and N.M. Le Douarin. 2005. Patterning the neural crest derivatives during development of the vertebrate head: insights from avian studies. *J. Anat.* 207:447–459.

Creuzet, S., G. Couly, C. Vincent, and N.M. Le Douarin. 2002. Negative effect of Hox gene expression on the development of the neural crest-derived facial skeleton. *Development*. 129:4301–4313.

Danielian, P.S., D. Muccino, D.H. Rowitch, S.K. Michael, and A.P. McMahon. 1998. Modification of gene activity in mouse embryos in utero by a tamoxifen-inducible form of Cre recombinase. *Curr. Biol.* 8:1323-S2.

Le Douarin, N.M., S. Creuzet, G. Couly, and E. Dupin. 2004. Neural crest cell plasticity and its limits. *Development*. 131:4637–4650.

Le Douarin, N.M., and E. Dupin. 2012. The neural crest in vertebrate evolution. *Curr. Opin. Genet. Dev.* 22:381–9.

Le Douarin, N.M., and C. Kalcheim. 1999. The Neural Crest. Second Edi. Cambridge University Press, New York. 472 pp.

Dupin, E., G.W. Calloni, and N.M. Le Douarin. 2010. The cephalic neural crest of amniote vertebrates is composed of a large majority of precursors endowed with neural, melanocytic, chondrogenic and osteogenic potentialities. *Cell Cycle*. 9:238–249.

Dupin, E., and N.M. Le Douarin. 2014. The neural crest, A multifaceted structure of the vertebrates. *Birth Defects Res. Part C - Embryo Today Rev.* 102:187–209.

Fauquet, M., and C. Ziller. 1989. A monoclonal antibody directed against quail tyrosine hydroxylase: description and use in immunocytochemical studies on differentiating neural crest cells. *J. Histochem. Cytochem.* 37:1197–1205.

Garcez, R.C., N.M. Le Douarin, and S.E. Creuzet. 2014. Combinatorial activity of Six1-2-4 genes in cephalic neural crest cells controls craniofacial and brain development. *Cell. Mol. Life Sci.* 71:2149–2164.

Grammatopoulos, G.A., E. Bell, L. Toole, A. Lumsden, and A.S. Tucker. 2000. Homeotic transformation of branchial arch identity after Hoxa2 overexpression. *Development*.

127:5355–5365.

Gross, S., Y. Krause, M. Wuelling, and A. Vortkamp. 2012. Hoxa11 and Hoxd11 Regulate Chondrocyte Differentiation Upstream of Runx2 and Shox2 in Mice. *PLoS One*. 7:e43553.

Hassan, M.Q., S. Saini, J.A.R. Gordon, A.J. Van Wijnen, M. Montecino, J.L. Stein, G.S. Stein, and J.B. Lian. 2009. Molecular Switches Involving Homeodomain Proteins, HOXA10 and RUNX2 Regulate Osteoblastogenesis. *Cells Tissues Organs*. 189:122–125.

Hassan, M.Q., R. Tare, S.H. Lee, M. Mandeville, B. Weiner, M. Montecino, A.J. van Wijnen, J.L. Stein, G.S. Stein, and J.B. Lian. 2007. HOXA10 controls osteoblastogenesis by directly activating bone regulatory and phenotypic genes. *Mol. Cell. Biol.* 27:3337–52.

He, G., S. Tavella, K.P. Hanley, M. Self, G. Oliver, R. Grifone, N. Hanley, C. Ward, and N. Bobola. 2010. Inactivation of Six2 in mouse identifies a novel genetic mechanism controlling development and growth of the cranial base. *Dev. Biol.* 344:720–730.

Ido, A., and K. Ito. 2006. Expression of chondrogenic potential of mouse trunk neural crest cells by FGF2 treatment. *Dev. Dyn.* 235:361–367.

Jiang, X., S. Iseki, R.E. Maxson, H.M. Sucov, and G.M. Morriss-Kay. 2002. Tissue Origins and Interactions in the Mammalian Skull Vault. *Dev. Biol.* 241:106–116.

Jiang, X., D.H. Rowitch, P. Soriano, A.P. McMahon, and H.M. Sucov. 2000. Fate of the mammalian cardiac neural crest. *Development*. 127:1607–1616.

Joseph, N.M., Y. Mukouyama, J.T. Mosher, M. Jaegle, S.A. Crone, E.-L. Dormand, K.-F. Lee, D. Meijer, D.J. Anderson, and S.J. Morrison. 2004. Neural crest stem cells undergo multilineage differentiation in developing peripheral nerves to generate endoneurial fibroblasts in addition to Schwann cells. *Development*. 131:5599–5612.

Kague, E., M. Gallagher, S. Burke, M. Parsons, T. Franz-Odendaal, and S. Fisher. 2012. Skeletogenic Fate of Zebrafish Cranial and Trunk Neural Crest. *PLoS One*. 7:e47394.

Kanzler, B., S.J. Kuschert, Y.-H. Liu, and M. Mallo. 1998. Hoxa-2 restricts the chondrogenic domain and inhibits bone formation during development of the branchial area. *Development*. 125:2587–2597.

Kitazawa, T., K. Fujisawa, N. Narboux-Neme, Y. Arima, Y. Kawamura, T. Inoue, Y. Wada, T. Kohro, H. Aburatani, T. Kodama, K.S. Kim, T. Sato, Y. Uchijima, K. Maeda, S. Miyagawa-Tomita, M. Minoux, F.M. Rijli, G. Levi, Y. Kurihara, and H. Kurihara. 2015. Distinct effects of Hoxa2 overexpression in cranial neural crest populations reveal that the mammalian hyomandibular-ceratohyal boundary maps within the styloid process. *Dev Biol*. 402:162–174.

Kutejova, E., B. Engist, M. Mallo, B. Kanzler, and N. Bobola. 2005. Hoxa2 downregulates Six2 in the neural crest-derived mesenchyme. *Development*. 132:469–478.

Kutejova, E., B. Engist, M. Self, G. Oliver, P. Kirilenko, and N. Bobola. 2008. Six2 functions redundantly immediately downstream of Hoxa2. *Development*. 135:1463–1470.

Lee, R.T.H., J.P. Thiery, and T.J. Carney. 2013. Dermal fin rays and scales derive from mesoderm, not neural crest. *Curr. Biol.* 23:R336-7.

Mann, R.S., K.M. Lelli, and R. Joshi. 2009. Hox specificity unique roles for cofactors and

collaborators. *Curr. Top. Dev. Biol.* 88:63–101.

Massip, L., F. Ectors, P. Deprez, M. Maleki, C. Behets, B. Lengele, P. Delahaut, J. Picard, and R. Rezsohazy. 2007. Expression of Hoxa2 in cells entering chondrogenesis impairs overall cartilage development. *Differentiation*. 75:256–267.

Matsuoka, T., P.E. Ahlberg, N. Kessaris, P. Iannarelli, U. Dennehy, W.D. Richardson, A.P. McMahon, and G. Koentges. 2005. Neural crest origins of the neck and shoulder. *Nature*. 436:347–355.

McGonnell, I.M., and A. Graham. 2002. Trunk Neural Crest Has Skeletogenic Potential. *Curr. Biol.* 12:767–771.

Mongera, A., and C. Nüsslein-Volhard. 2013. Scales of fish arise from mesoderm. *Curr. Biol.* 23:338–9.

Monteiro, M.C., M. Sanyal, M.L. Cleary, C. Sengenès, A. Bouloumè, C. Dani, and N. Billon. 2011. PBX1: A novel stage-specific regulator of adipocyte development. *Stem Cells*. 29:1837–1848.

Nakamura, H., and C.S. Ayer-le Lièvre. 1982. Mesectodermal capabilities of the trunk neural crest of birds. *J Embryol Exp Morphol*. 70:1–18.

Nataf, V., P. Mercier, C. Ziller, and N.M. Le Douarin. 1993. Novel Markers of Melanocyte Differentiation in the Avian Embryo. *Exp. Cell Res.* 207:171–182.

Neufeld, S.J., F. Wang, and J. Cobb. 2014. Genetic Interactions Between Shox2 and Hox Genes During the Regional Growth and Development of the Mouse Limb. *Genetics*. 198:1117–1126.

Niwa, H., K. Yamamura, and J. Miyazaki. 1991. Efficient selection for high-expression transfectants with a novel eukaryotic vector. *Gene*. 108:193–199.

Nolte, C., and R. Krumlauf. 2006. Expression of Hox genes in the nervous system of vertebrates. *In* HOX gene expression. ed Papageorgiou S, editor. Landes Bioscience and Springer, Austin, TX. 14–41.

Okabe, M., M. Ikawa, K. Kominami, T. Nakanishi, and Y. Nishimune. 1997. “Green mice” as a source of ubiquitous green cells. *FEBS Lett.* 407:313–319.

Schindelin, J., I. Arganda-Carreras, E. Frise, V. Kaynig, M. Longair, T. Pietzsch, S. Preibisch, C. Rueden, S. Saalfeld, B. Schmid, J.-Y. Tinevez, D.J. White, V. Hartenstein, K. Eliceiri, P. Tomancak, and A. Cardona. 2012. Fiji: an open-source platform for biological-image analysis. *Nat. Methods*. 9:676–682.

Schwarz, D., S. Varum, M. Zemke, A. Schöler, A. Baggiolini, K. Draganova, H. Koseki, D. Schübeler, and L. Sommer. 2014. Ezh2 is required for neural crest-derived cartilage and bone formation. *Development*. 141:867–877.

Seifert, A., D.F. Werheid, S.M. Knapp, and E. Tobiasch. 2015. Role of Hox genes in stem cell differentiation. *World J. Stem Cells*. 7:583–595.

Simoes-Costa, M., and M.E. Bronner. 2016. Reprogramming of avian neural crest axial identity and cell fate. *Science*. 352:1570–3.

Smith, M., A. Hickman, D. Amanze, A. Lumsden, and P. Thorogood. 1994. Trunk Neural Crest Origin of Caudal Fin Mesenchyme in the Zebrafish Brachydanio rerio. *Proc. R. Soc. London B Biol. Sci.*

256:137–145.

Smith, M.M. 1991. Putative skeletal neural crest cells in early late ordovician vertebrates from colorado. *Science*. 251:301–303.

Smith, M.M., and B.K. Hall. 1990. Development and evolutionary origins of vertebrate skeletogenic and odontogenic tissues. *Biol. Rev. Camb. Philos. Soc.* 65:277–373.

Wang, G., E.-N. Chen, C. Liang, J. Liang, L.-R. Gao, M. Chuai, A. Münsterberg, Y. Bao, L. Cao, and X. Yang. 2017. Atg7-Mediated Autophagy Is Involved in the Neural Crest Cell Generation in Chick Embryo. *Mol Neurobiol*. 1–14.

Wang, X.-Y., S. Li, G. Wang, Z.-L. Ma, M. Chuai, L. Cao, and X. Yang. 2015. High glucose environment inhibits cranial neural crest survival by activating excessive autophagy in the chick embryo. *Sci. Rep.* 5:18321.

Yamauchi, Y., K. Abe, A. Mantani, Y. Hitoshi, M. Suzuki, F. Osuzu, S. Kuratani, and K. Yamamura. 1999. A Novel Transgenic Technique That Allows Specific Marking of the Neural Crest Cell Lineage in Mice. *Dev. Biol.* 212:191–203.

Yang, L., X. Zhang, H. Li, and J. Liu. 2016. The long noncoding RNA HOTAIR activates autophagy by upregulating ATG3 and ATG7 in hepatocellular carcinoma. *Mol. BioSyst.* 12:2605–2612.

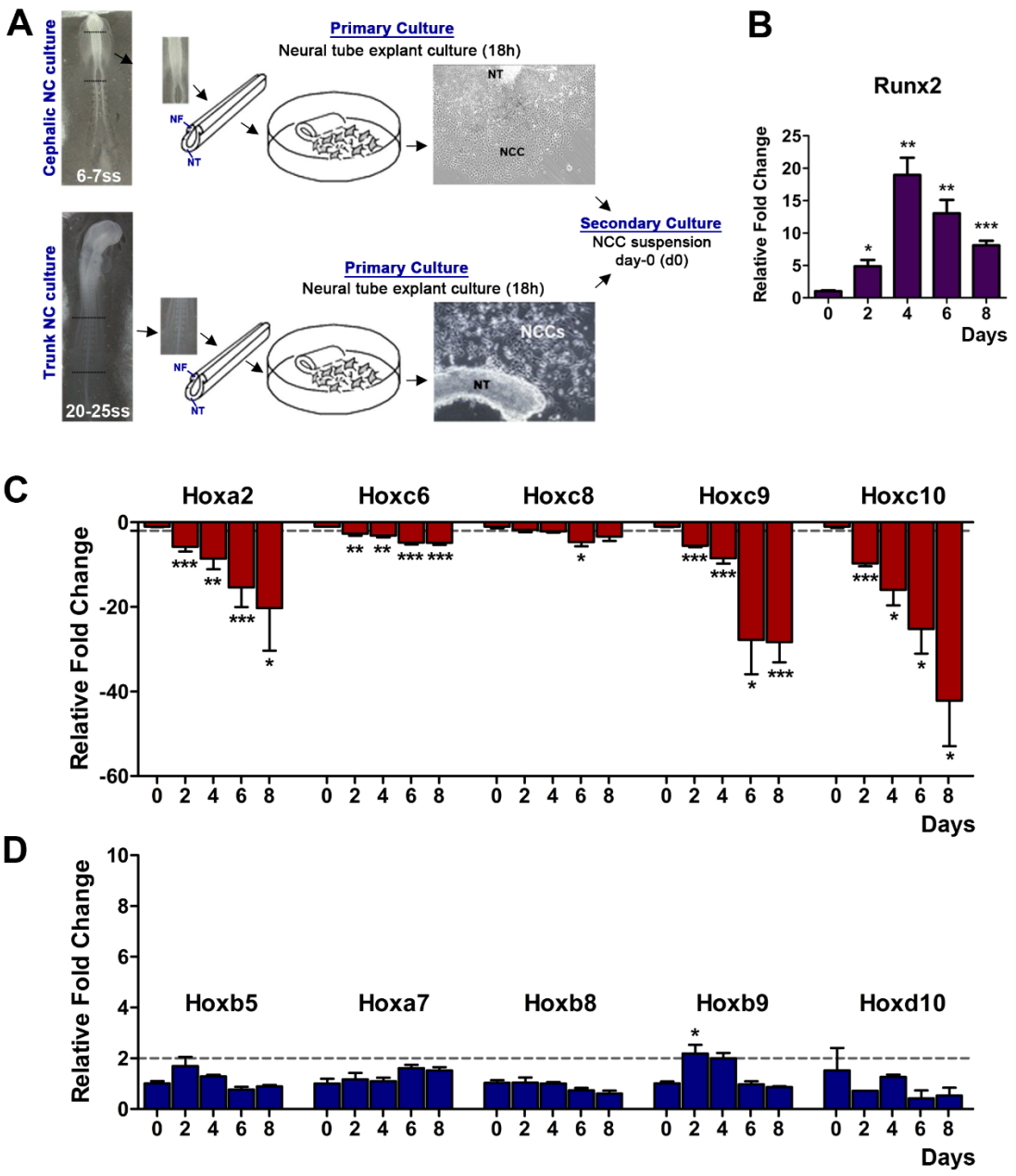

Figure 1: Temporal expression pattern of *Runx2* and *Hox* genes in trunk NCC cultures. (A) Schematic representation of NC isolation and culture procedure. Briefly, trunk neural tubes (from the level corresponding to 20-25 somites) were cultured for 18h (primary culture) after isolation from quail embryos of 2 days of incubation. Then, the NCC that had migrated from the explanted neural primordia were detached and sub-cultured (secondary culture) in specific medium conditions as described in Materials and Methods. The same procedure was applied to prepare cephalic NCC cultures from mesencephalon-anterior rhombencephalon isolated from 6-7ss quail embryos. (B, C and D). Data from RT-qPCR analysis of trunk NCC between day-0 and day-8 of secondary culture are shown as fold change of gene expression at different time-points relative to

day-0 (corresponding to the initial plating of the NCC). (B) An upregulation of *Runx2* gene expression was concomitant with downregulation of particular *Hox* genes, namely *Hoxa2*, *Hoxc6*, *Hoxc8*, *Hoxc9* and *Hoxc10* (C). (D) Expression of another set of *Hox* genes (*Hoxb5*, *Hoxa7*, *Hoxb8*, and *Hoxd10*) remains unchanged during the culture period, while *Hoxb9* expression slightly increased at d day-2. Values were normalized in all samples with *GAPDH* control gene. *p<0.05; **p<0.01, ***p<0,001.

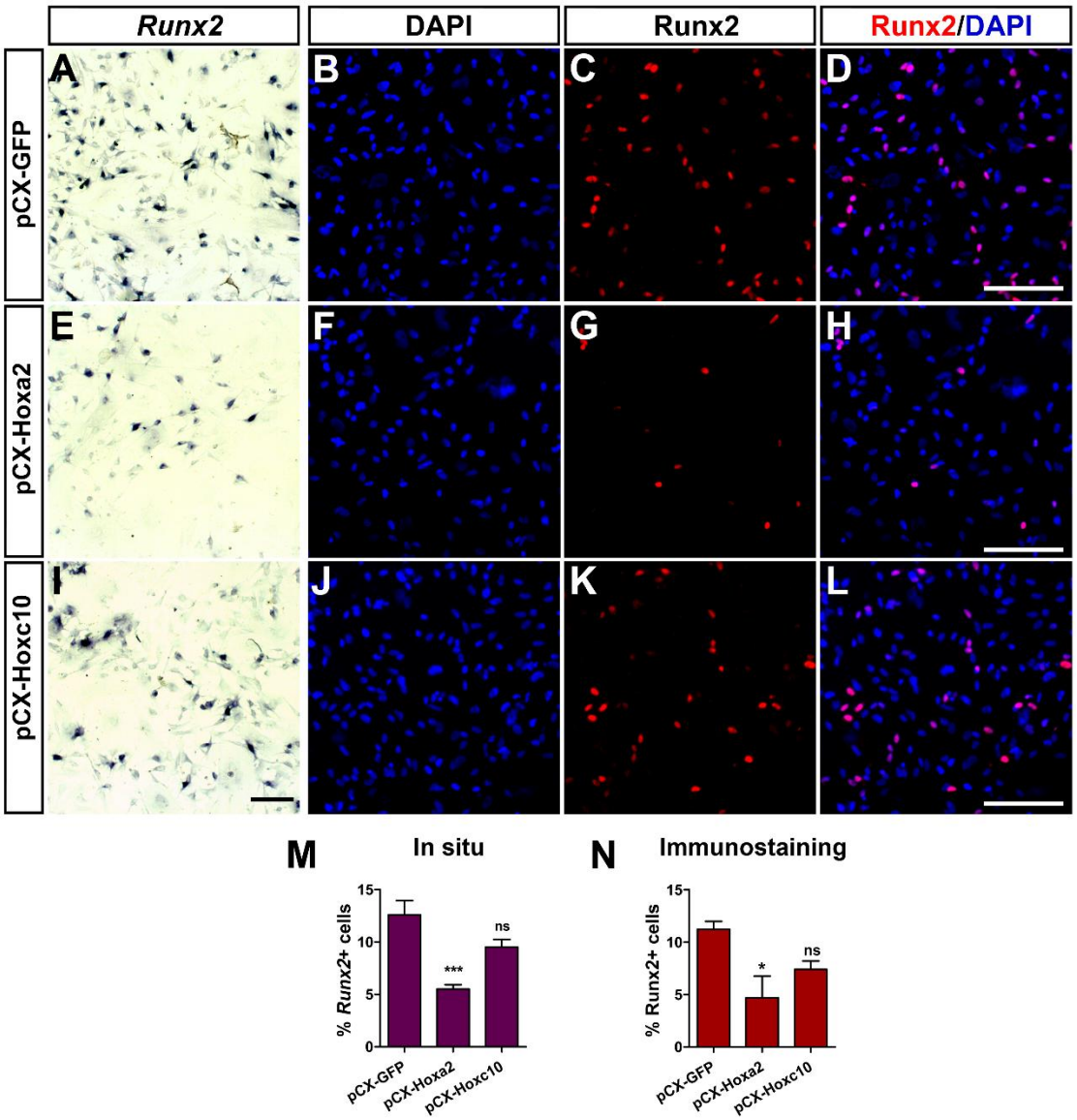

Figure 2: Forced expression of *Hoxa2* in early trunk NCC decreases the number of Runx2-positive osteoprogenitors. At day-0, trunk NCC were transfected at time of plating in secondary culture with either pCX-Hoxa2, pCX-Hoxc10 or control pCX-GFP plasmids. After 6 days in culture, Runx2-positive cells were detected by in situ hybridization (A, E, I) or immunostaining (C, G, K). (B, F, J) DAPI nuclear staining; (D, H, L) Merge of Runx2 and DAPI. As compared with control cultures (pCX-GFP) (A-D), fewer NCC expressing *Runx2* transcripts and Runx2 protein were detected after gain of function of *Hoxa2* (E-H), not *Hoxc10* (I-L). Quantification of cells expressing *Runx2* transcripts (M) and protein (N) (percentage of DAPI positive cells) in day-6-cultures showed that *Hoxa2* decreased the total number of osteoprogenitors by approximately 60%. Scale bar: 100µm (immunofluorescence images); 200µm (in situ hybridization). ns= not significant, *p<0.05; **p<0.01, ***p<0,001.

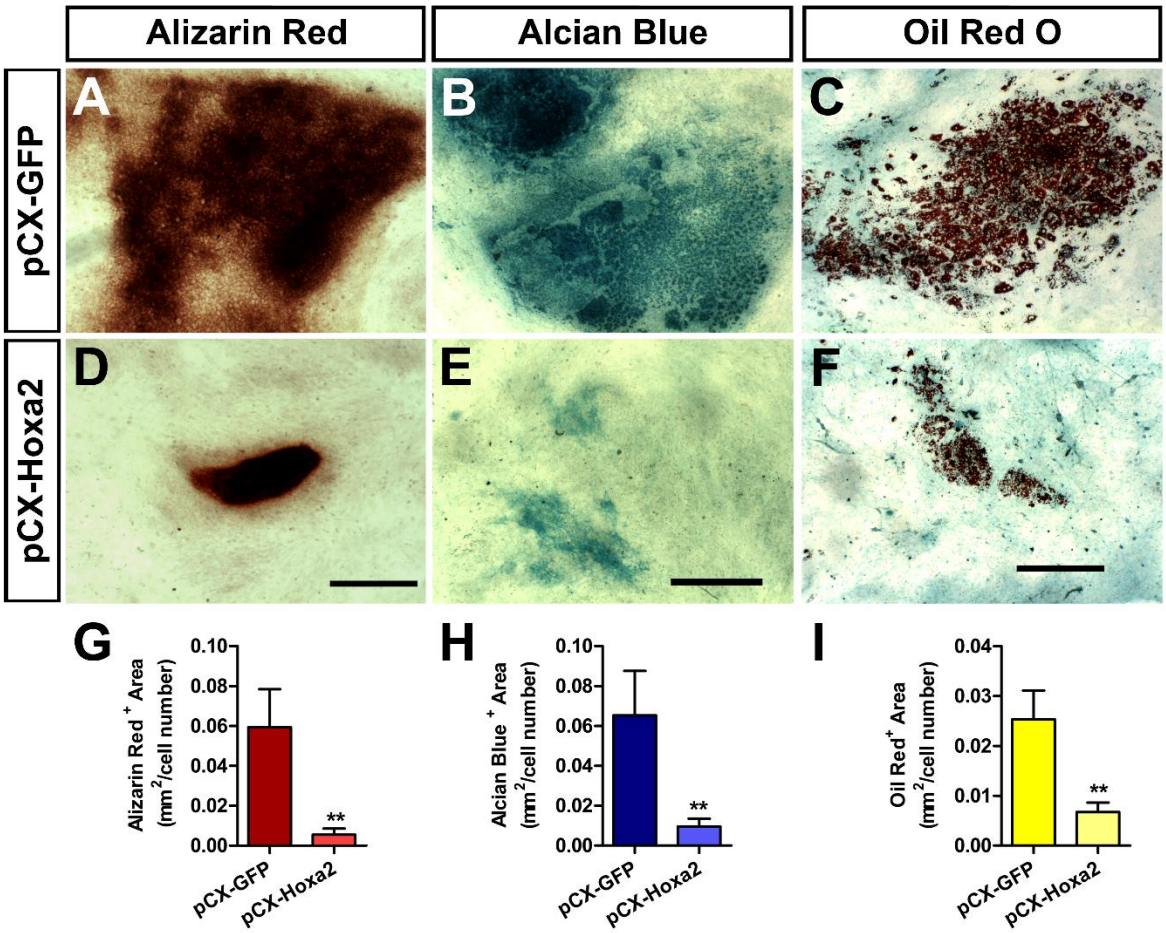

Figure 3: Osteoblastic, chondrocytic and adipocytic terminal differentiation of trunk NCC in vitro is reduced after gain of function of *Hoxa2*. Trunk NCC were transfected with pCX-GFP or pCX-Hoxa2 at day-0 and further maintained until day-25 of culture before staining with Alizarin Red (A, D), Alcian Blue (B, E) and Oil Red O (C, F) to identify bone calcified matrix, cartilaginous matrix and lipid-storing adipocytes, respectively. Compared with GFP control plasmid (A-C), *Hoxa2* forced expression (D-F) resulted in smaller regions of NC cultures containing differentiated bone, cartilage and fat cells. (G-I) Quantification of the total area of staining for Alizarin Red (G), Alcian Blue (H) and Oil Red O (I) after transfection with *Hoxa2* or *GFP* plasmids; data are expressed as the mean area of staining normalized by the total cell number per culture (Alizarin red: n= 61 cultures in 4 independent experiments; Alcian Blue and Oil Red O: n=46 cultures in 3 independent experiments). Scale bar: 500µm, ***p<0,001.

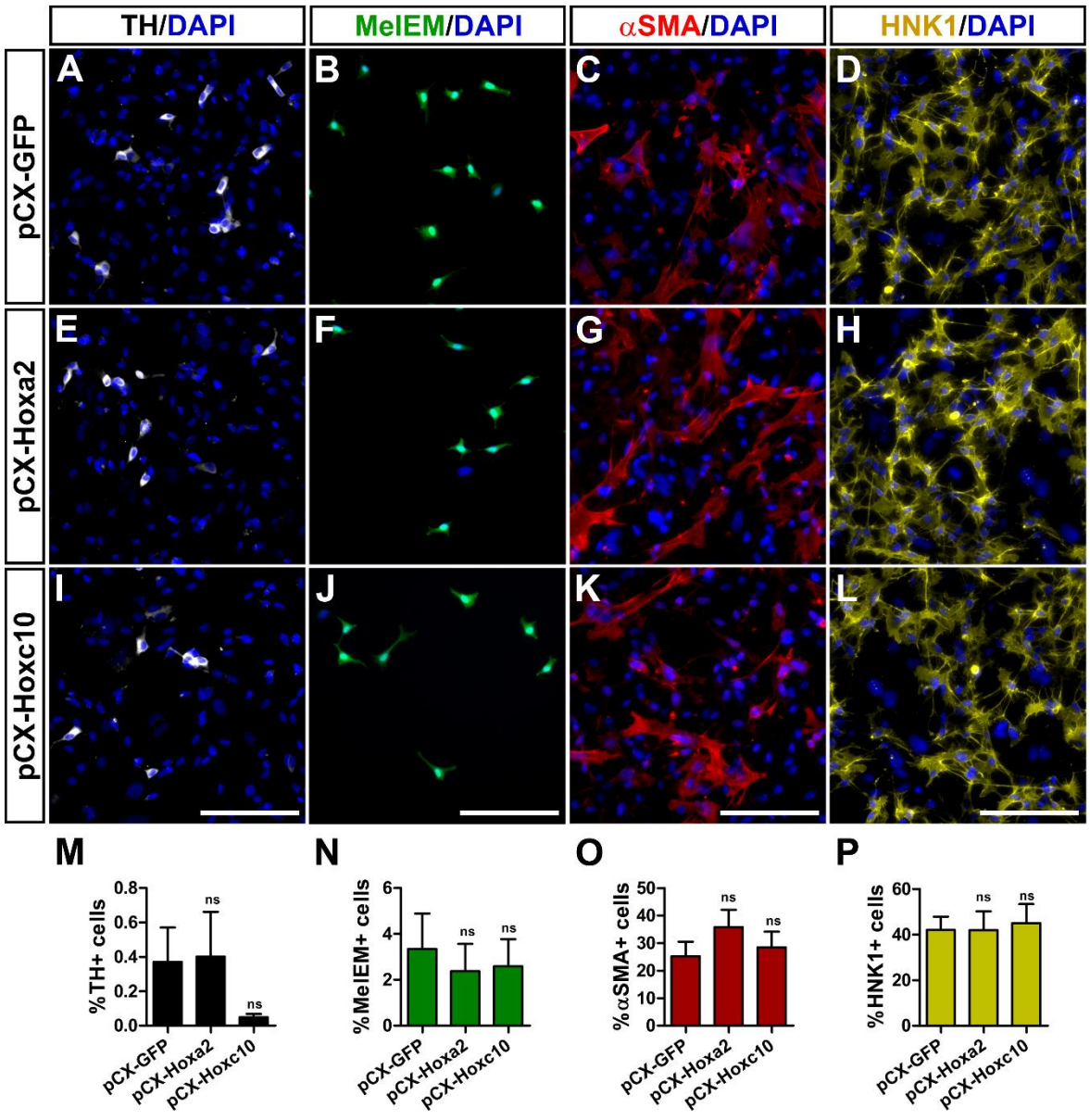

Figure 4: Myofibroblasts and neural-melanocytic cells are not affected by *Hoxa2* and *Hoxc10* forced expression in trunk NCC. Immunolabeling of TH+ neurons (A-I), MelEM+ melanocytes (B-J), αSMA+ myofibroblasts (C-K) and HNK1+ neural progenitors (D-L) in day-6 trunk NCC cultures after overexpression of *Hoxa2*, *Hoxc10* or *GFP* at day-0. (M-P) For each phenotypic marker, the total number of immunoreactive cells is expressed as the percentage of total cell nuclei per culture; no significant differences are observed between *Hoxa2*, *Hoxc10* and *GFP* transfected cultures (n=6 cultures in 3 independent experiments; for all markers). (M-P). Scale bar: 100µm. ns= not significant, *p<0.05; **p<0.01, ***p<0,001.

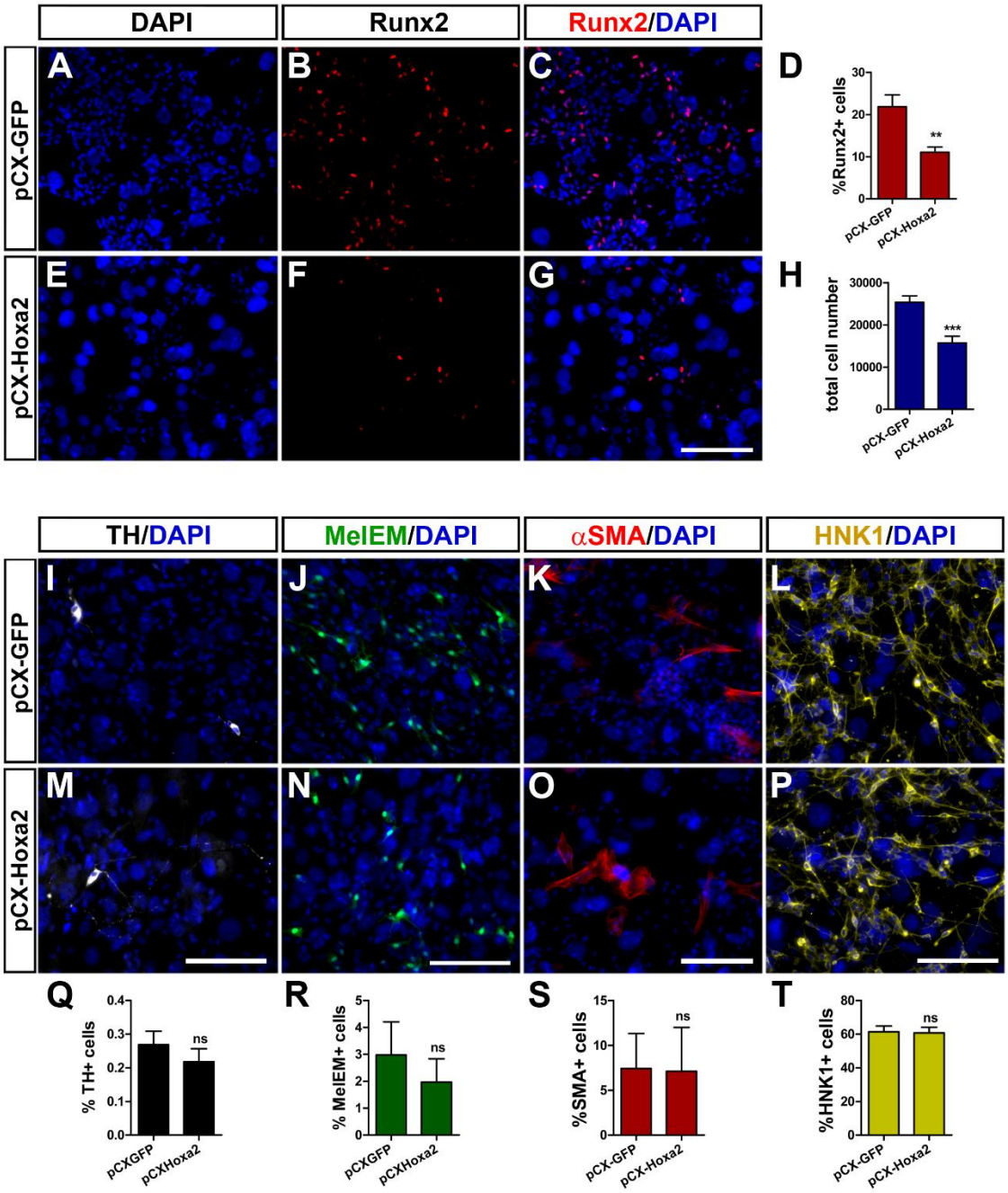

Figure 5: Forced expression of *Hoxa2* in cephalic NCC reduced the differentiation of osteoprogenitors, but not the other differentiated cell types.

Mesencephalic NCC isolated as described in Materials and Methods were transfected at day-0 of culture with either pCX-Hoxa2 or control pCX-GFP plasmids. DAPI nuclear staining and expression of differentiation markers were analyzed after 6 days of culture on a 3T3 feeder-layer as described previously (Calloni et al., 2009). DAPI staining (A, B) shows the presence of small nuclei of quail

NCC surrounding the large nuclei of mouse 3T3 cells; Runx2 immunoreactivity (B, F) and merge of Runx2 and DAPI (C, G); *Hoxa2* forced expression led to 55% reduction of the percentage of Runx2+ cells per culture (D) and to 40% reduction of the total number of nuclei per culture (H), as compared with control *GFP* (n=15 cultures analyzed for both *GFP* and *Hoxa2*). No differences were observed in the relative cell number of other NC derivatives, including TH+ neurons (I, M, Q), MelEM+ melanocytes (J, N, R), αSMA+ myofibroblasts (K, O, S) and HNK1+ neural progenitors (L, P, T); quantifications are expressed as a percentage of DAPI positive nuclei in each condition (n=17, 6, 10, and 11 cultures in 3 independent experiments, for analysis of TH, MelEM, αSMA and HNK1, respectively). Scale bar: 100µm. ns= not significant, ***p<0,001.

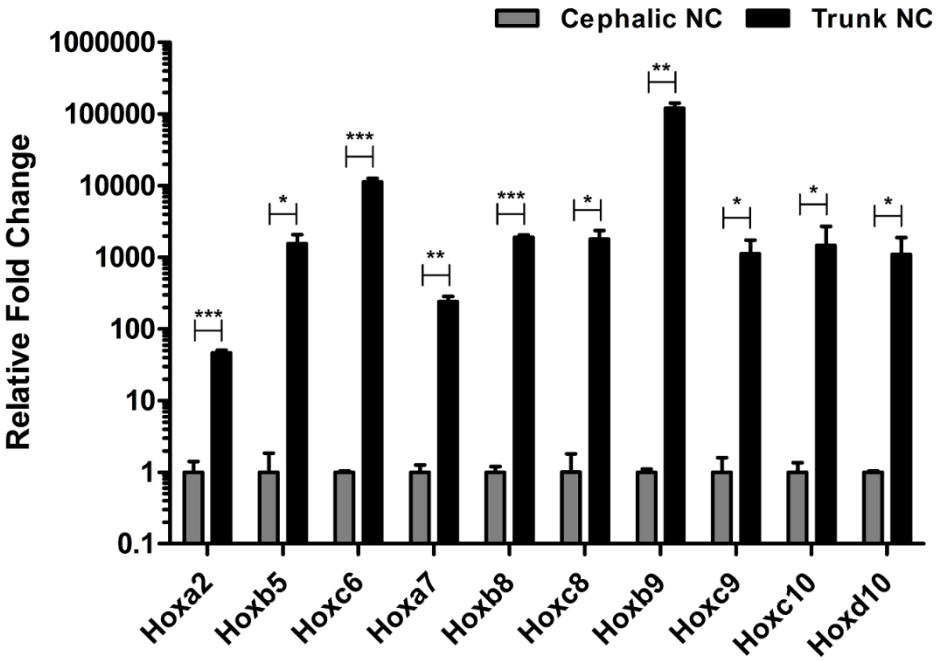

Supplementary Figure 1: Repertoire of *Hox* genes expressed in early trunk NCC cultures. RT-qPCR analysis of *Hox* gene expression was performed on trunk NCC after 18h of in vitro migration from explanted neural tubes (day-0). Data are shown as fold-change relative to *Hox* expression in cephalic migratory NCC (isolated at midbrain level from 10ss quail embryos). Ten *Hox* genes (i.e., *Hoxa2*, *Hoxb5*, *Hoxc6*, *Hoxa7*, *Hoxb8*, *Hoxc8*, *Hoxb9*, *Hoxc9*, *Hoxc10* and *Hoxd10*) were highly amplified in trunk NCC, as compared to mesencephalic NCC. Values were normalized in all samples with *GAPDH* control gene. *p<0.05; **p<0.01, ***p<0,001.

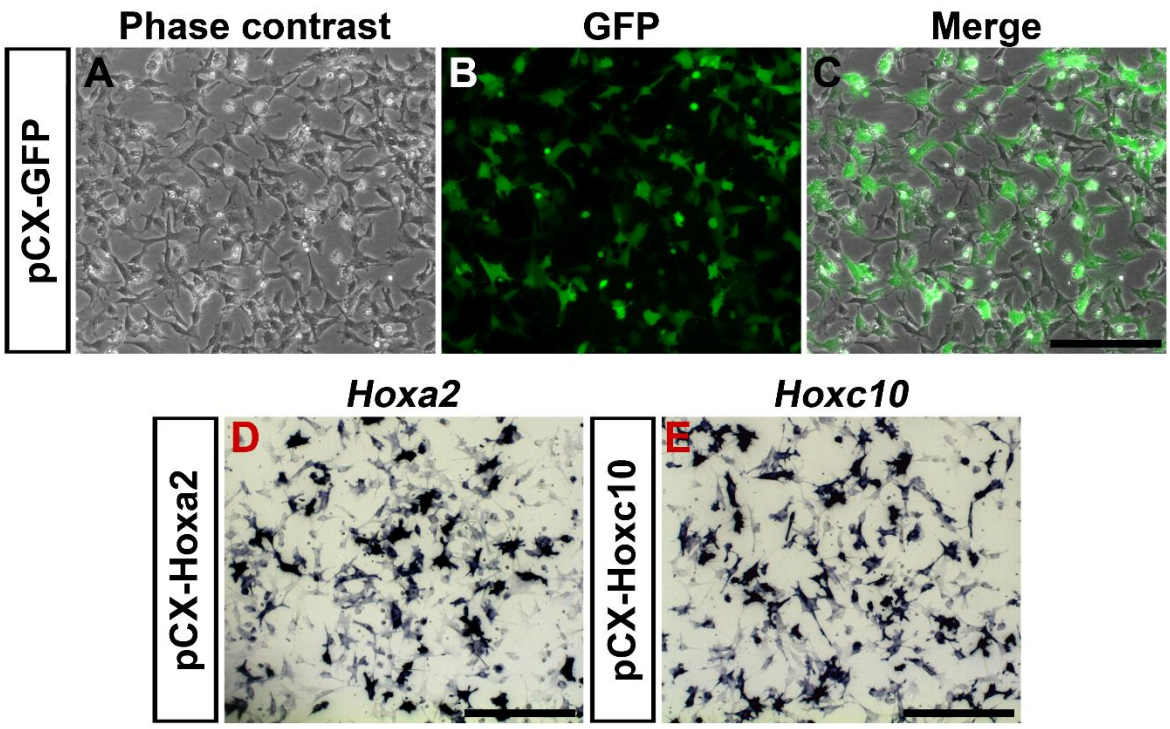

Supplementary Figure 2: Expression of GFP, *Hoxa2* and *Hoxc10* after transfection in trunk NCC. (A-C) Trunk NCC transfected at day-0 with pCX-GFP plasmid (A) Phase contrast; (B) GFP fluorescence (C) Merge of GFP and phase contrast. Note that the majority of trunk NCC express GFP. (D) *Hoxa2* mRNA expression 24h after pCX-Hoxa2 transfection at day-0. (E) *Hoxc10* mRNA expression 24h after pCX-Hoxc10 transfection at day-0. Transfected trunk NCC strongly expressed these *Hox* genes (purple cells). Scale bar: 200µm.

Table S1: RT-qPCR primer sequences

Gene	Forward Primer	Reverse Primer	Insert (bp)	Accession Number
Hoxa2	CCACAAAGACCCCCTTGAAATC	CAAGAGCTGCGTGTTGGTGTA	85	NM_205150.2
Hoxb5	GGACCTTAGCATCAACCGCT	ACGCCTGTCTAAACCTGCTC	107	AY875647.1
Hoxc6	TGCAGCGTATGAACTCCCAC	TCCAACGTTTGGTAACGGGA	88	XM_003643454.2
Hoxa7	GCTCCTTTGCAAGCAACTCC	CGGAAGAGAACGGGCTTTGA	120	NM_204595.1
Hoxb8	ACCCGAGCAACTTCTATGGC	GTGTACTGCACCAAGTCCGA	82	NM_204911.1
Hoxc8	CCATCACACCACGTCCAAGA	GCACGGGTTTTGCTGGTATC	78	NM_204893.1
Hoxb9	TCCAATCAAAGGCCCAGCTT	GCTGGGTTGGTTTGATCTGTTC	83	XM_001233690.3
Hoxc9	CAGAGCAGCGCAGACAATTC	TTCGCGACGGGATTGTTAGG	102	NM_001277282.1
Hoxc10	ACCCAAGGAACGAGCATCTG	AACTCACTTTAGCCACCGGG	81	XM_001233805.3
Hoxd10	GAGGCATCCGCAATTACACG	GCAGGAGAGCTGTTGGGAAA	113	XM_001234538.3
Runx2	ACAGGACTTCCAGCCATCAC	GCTTGTGAACTGCCTGGGAT	90	NM_204128.1

III. Additional results

Clonal analyses of trunk NC progenitors after *Hoxa2* ectopic expression

In a previous study of the in vitro developmental potentials of quail trunk NCC, it was shown that multipotent neural-mesenchymal progenitors are at the origin of osteoblasts and adipocytes (Coelho-Aguiar et al., 2013). In order to understand further the influence of *Hoxa2* on NCC mesenchymal fate and multipotency, we have investigated this issue at single-cell resolution, by in vitro cloning analyses of trunk NCC that overexpressed *Hoxa2*. For this purpose, we constructed a plasmid in which the chicken *Hoxa2* gene is expressed together with a GFP reporter ("Hoxa2-GFP"). This plasmid also contains transposon-responsive elements, to stably introduce this exogenous construct in NCC by Tol2-mediated gene transfer (*see below*) (Sato et al., 2007). Moreover, we tested different cloning strategies aiming to achieve the best cloning efficiencies to permit the analyses of the variety of trunk NC derivatives.

In this Chapter, we present these additional results, which complement our analyses of *Hoxa2* effects on trunk NCC, described in Article n°2.

Materials and Methods

Expression plasmids

We isolated full-length chicken *Hoxa2* by PCR amplification of cDNA sequence, followed by subcloning into the *XbaI-MfeI* site of pT2K-CAGGS-H2B-EGFP expression plasmid (a gift from X. Morin) (Sato et al., 2007). This new plasmid (pT2K-CAGGS-Hoxa2-H2B-EGFP) is hereafter named "Hoxa2-GFP". Clontech's In-Fusion HD Cloning Kit (Clontech) was used for PCR amplification and thermocycling conditions were programmed according to the manufacturer's instructions. All constructs were further sequenced for accuracy. The pT2K-CAGGS-H2B-EGFP was utilized in all experiments as a control plasmid, hereafter named "control-GFP". All constructs were amplified in endotoxin-free condition (MaxiPrep kit, Qiagen). For genome integration, we used a pCAGGS-T2TP plasmid, which encodes a transposase sequence, under control of a CAGGS promoter (a gift from J. Livet). The

transposase is responsible for the excision of the construct flanked by Tol2 sequences in the "control-GFP" and "Hoxa2-GFP" plasmids, and then subsequently integrate these constructs into the host genome (**Figure 17**).

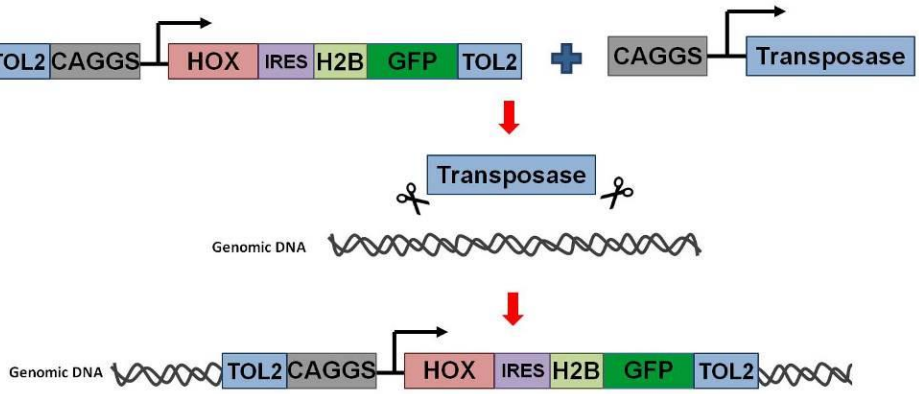

Figure 17: Scheme of Hoxa2-GFP and Transposase vectors used to mediate permanent transfection of Hoxa2-GFP in trunk NCC

Trunk NCC culture, transfection procedure and clonal analyses

For trunk NC cultures, we obtained thoracic neural tubes, dissected and cultured as previously described by Calloni et al. (2007), Coelho-Aguiar et al. (2013) and described in details in the *Materials and Methods section of Article 2*. To obtain GFP-expressing cells before cloning, NCC were co-transfected with a pCAGGS-T2TP plasmid (0.35 µg) together with "control-GFP" or "Hoxa2-GFP" plasmids (0.65 µg), during NCC primary culture, that is, in cultures containing NCC undergoing delamination and migration from the trunk neural primordia. After 18 hours of culture, explanted neural tubes were detached and discarded. The outgrowth NCC were then trypsinized, centrifuged and the percentage of GFP+ cells was quantified with an inverted fluorescence microscope (Nikon-Eclipse Ti-E). The mixed cell suspension (containing 5-10% of GFP+ cells) was used for the cloning experiments. We attempted three different cloning methods, briefly described below (for *more details, see next sections*):

The first strategy consisted in manually selecting single GFP+ NCC, under the control of an inverted fluorescence microscope, and plating them individually using a glass micropipette as previously described (Baroffio et al., 1988, 1991; Real et al., 2006). Second, we attempted to automatically clone GFP+ cells, by fluorescence activated cell sorting (FACS). NCC were resuspended in DMEM without FCS, filtered through a 30µm nylon membrane (MACS, Miltenyl

Biotec) and kept on ice before sorting using a MoFlo Astrios sorter (Beckman-Counter). The gates for GFP+ and GFP- cells were determined using an equivalent non-transfected trunk NCC suspension. Finally, we performed GFP+ NCC cloning by limiting dilution as follows: we quantified the proportion of GFP+ per total cell number in the NCC suspension (transfection efficiency), followed by appropriate dilution of this initial cell suspension in order to obtain 0.5 GFP+ cells per well. For instance, in the experiments with 10% transfection efficiency, we plated 5 NCC per well (for expected 0.5 GFP+ and 4.5 GFP-cells).

In all in vitro cloning experiments, further culturing and phenotypic analyses were performed with a similar protocol. Briefly, trunk NCC were seeded on a growth-arrested 3T3 feeder-layer in 96-well plates (TPP) and cultured with DMEM medium containing 10% FCS and 2% chicken embryo extract (80ng/ml). Clonal cultures were maintained at 37°C in a humidified 5% CO2 incubator and the medium was changed every three days. To identify the different cell types in individual clones, cells were fixed with 4% formaldehyde for 30min at day-10 and immunostained with lineage-specific markers (Runx2, TH, SMA and HNK1 antibodies, as previously described in *Materials and Methods section of Article 2*). Melanocytes were identified in the colonies by the presence of melanin.

Results

- Forced expression of Hoxa2-GFP plasmid reduces the number of Runx2+ progenitors in trunk NC cultures

Before starting the clonal analyses, we tested whether the overexpression of "Hoxa2-GFP" plasmid enabled to trigger the same effects on Runx2-expressing cells in mass cultures of trunk NCC, as we observed previously with the pCX-Hoxa2 construct (*see Results Article 2*). We found a reduced number of Runx2-positive cells, also stained with GFP, in NCC transfected with Hoxa2-GFP, in comparison with control cultures (control-GFP) (**Figure X**). The quantification allowed us to detect a similar level of Runx2 inhibition, as recorded with the pCX-Hoxa2 construct. These results allowed us to proceed to clonal analyses.

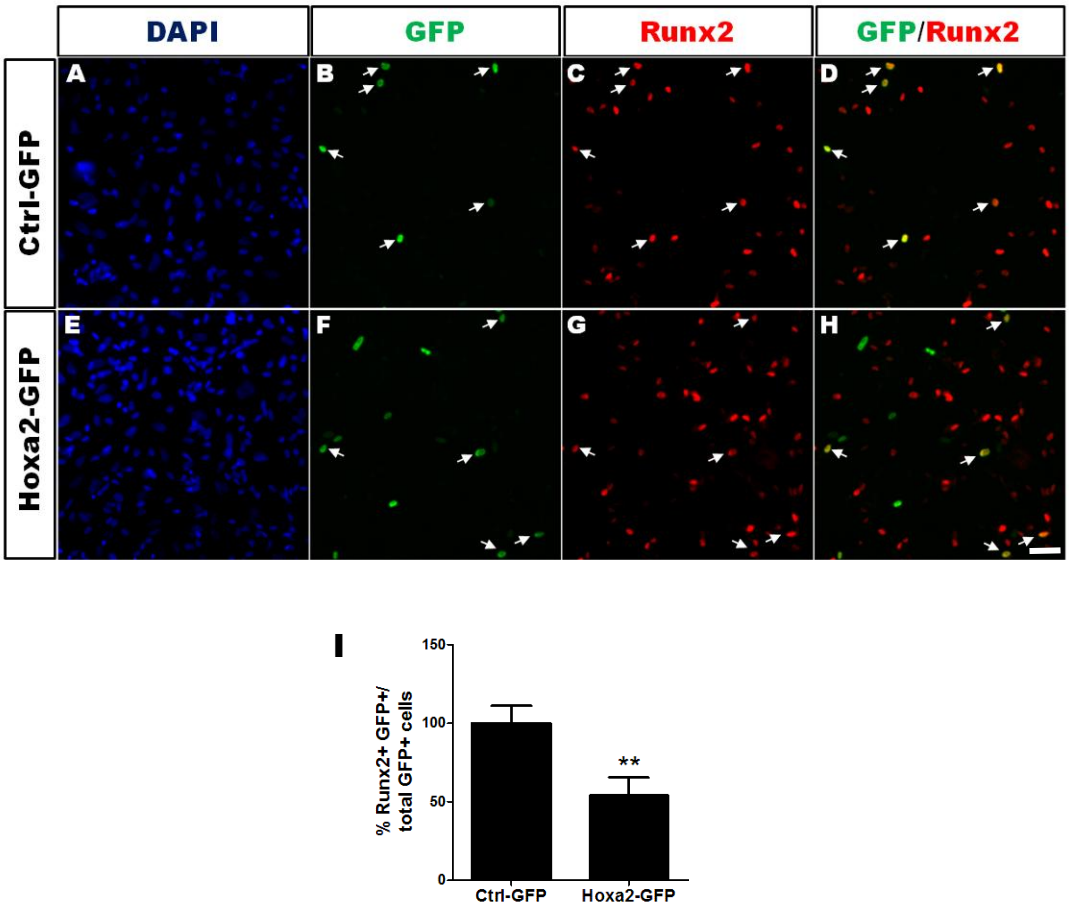

Figure 18: Runx2 expression after NCC transfection with integrative plasmids. Trunk NCC cultures after overexpression of either Hoxa2-GFP or control-GFP (Ctrl-GFP) integrative plasmids. (A,E) DAPI nuclear staining; (B,F) GFP expression driven by Hox or ctrl plasmids. (C,G) Runx2 immunostaining; (D,H) Merge GFP and Runx2. Arrows indicate Runx2+ GFP+ cells. (I) Quantification of double-stained NCC is given by the ratio of Runx2+GFP+ cells per total number of GFP+ cells. Bar:50µm; Unpaired t-test, **p<0.01; n=3.

- Set up of an ideal protocol for individually plating GFP+ trunk NCC

We tried three different strategies in order to get clonal seeding of GFP+ cells. The first one consisted in manually cloning GFP+ cells, with a similar protocol used by our group (Baroffio et al., 1988, 1991, Calloni et al., 2007, 2009; Trentin et al., 2004; Coelho-Aguiar et al., 2013; Real et al., 2006). For this purpose, we manually picked GFP+ cells from a trunk NCC suspension 24h after transfection, by using a thin glass micropipette. However, since the transfection efficiency with integrative plasmids was very low (below 10%), it became challenging and time-consuming to manually select fluorescent these cells in order to get clonal cultures in a proper amount to allow further investigations.

Secondly, we decided to use FACS to purify GFP+ NCC and immediately clone them by automatic single-cell plating, which ensured that only one GFP+ cell was plated. This strategy led to a high efficiency of clone formation, since at least 30% of the wells contained GFP+ colonies on the day of analysis (day 10). Nevertheless, almost none of the clones contained Runx2+ osteoblasts in these conditions, assessed in three independent experiments. In fact, in these clones, even those transfected with the control plasmid, the NCC differentiated mainly into melanocytes and HNK1+ cells. Such unexpected results indicate that, after FACS sorting and cloning, the NCC population does not behave as unsorted NCC in terms of differentiation. One possible explanation is that multipotent NC progenitors either do not survive or "lose" their multipotency when submitted to an automatic sorting technique. Indeed, only the most frequent NC derivatives (HNK1+ neuroglial progenitors and melanocytes), which are known as a resistant cell population in culture, originated from clones plated using this technique.

To overcome these technical difficulties, we finally decided to clone these cells by a limiting dilution method, adapted from NCC cloning protocols published by Sieber-Blum and colleagues (Sieber-Blum and Cohen, 1980; Ito and Sieber-Blum, 1991). Briefly, we manually plated a mixed cell suspension (GFP+/GFP- NCC) at a dilution in order to obtain 0.5 GFP+ cell per well in average. Albeit the probability to get wells without GFP+ cells increased with this method, this procedure helped to ensure that GFP+ colonies detected on day-10 originated from a single GFP+ cell. However, we obtained a rather limited number of GFP+ colonies at day-10, in four different experiments, since the cloning efficiency was really low (about 3%). This is strikingly different compared to the clonal efficiency obtained by manual or automatic single-cell plating, which was of at least 30% (Trentin et al., 2004; Calloni et al., 2007, 2009; Coelho-Aguiar et al., 2013; and our data). Nevertheless, the limiting dilution strategy allowed us to analyze, at least in a preliminary way, the effects of *Hoxa2* on trunk NCC differentiation at the single-cell level.

- Single cell analyses of *Hoxa2* effects on trunk NCC multipotency (*preliminary results*)

The results obtained in four independent experiments of NCC cloning in vitro by limiting dilution are depicted in **Table 1**. In addition, some examples of transfected colonies observed at day-10 are shown in **Figures 19** and **20**.

The first notable result obtained in these experiments was the difference in the total number of cells per clone between control-GFP and Hoxa2-GFP NCC colonies. This number

reduced approximately by 65% in Hoxa2-GFP condition, in comparison with GFP control plasmid (**Table 1**). This finding indicates that *Hoxa2* impairs the overall survival and/or proliferation of cloned NCC. Secondly, the analysis of cell phenotypes revealed several differences between the two NCC population: unipotent clones (colonies with only one cell type) represented approximately 11.5% of the clones in the GFP-control condition, whereas this number reaches 35.3% of those expressing Hoxa2-GFP plasmid, suggesting that *Hoxa2* overexpression increased the generation of clones with a restricted progeny. In addition, we could observe a slight reduction in the number of colonies with mesenchymal derivatives in *Hoxa2* condition: the number of colonies with Runx2+ cells and αSMA+ myofibroblasts decreased by 25% and 48%, respectively, compared to control colonies. In contrast, *Hoxa2* forced expression promoted the formation of a higher number of clones containing melanocytes (**Table 1**).

In summary, these data, although preliminary, have shown that *Hoxa2* forced expression reduced the size of the progeny and the production of mesenchymal derivatives by single NCC while increasing the clones containing melanocytes. Although these results confirm the negative influence of Hoxa2 on osteoblasts, they also slightly contrast with our previous data obtained in mass cultures with pCX-plasmids, where no effects on the differentiation of neural-melanocytic cell types were observed after transient *Hoxa2* overexpression.

Nevertheless, these clonal experiments shall be interpreted carefully. Albeit the significant reduction in the *Hoxa2* colony size was highly reproducible between four independent experiments, the limited total number of colonies analyzed (26 in control and 34 in *Hoxa2*), precluded an analysis representative of the diversity of trunk NCC multipotent progenitors, which was previously described by our group (Coelho-Aguiar et al., 2013). Further experiments and analysis of a larger number of clones are needed to allow us to assess all the possible effects of *Hoxa2* on the in vitro development of single trunk NCC.

Trunk NC Clones	Control-GFP	Hoxa2-GFP	
Number of clones	26	34	
Cloning efficiency (%)	2.7	3.4	
Number of cells per clone	941.2 ± 279.7	331.3 ± 136.3	p<0.01
HNK1+ clones	24	28	
HNK1+ clones (%)	92.3	82.4	
Runx2+ clones	16	16	
Runx2+ clones (%)	61.5	47.1	#
TH+ clones	9	12	
TH+ clones (%)	34.6	35.3	
αSMA+ clones	15	10	
αSMA+ clones (%)	57.7	29.4	#
Melanocytes+ clones	2	6	
Melanocytes+ clones (%)	7.7	17.7	#
Unipotent clones	3	12	
Unipotent clones (%)	11.5	35.3	#
Bipotent clones	8	9	
Bipotent clones (%)	30.8	26.5	
Tripotent clones	12	10	
Tripotent clones (%)	46.2	29.4	
Quadripotent clones	3	3	
Quadripotent clones (%)	11.5	8.8	

Table 1: Quantification of clonal efficiency, number of cells per clone and clone phenotypes derived from trunk NCC after control-GFP and Hoxa2-GFP overexpression.

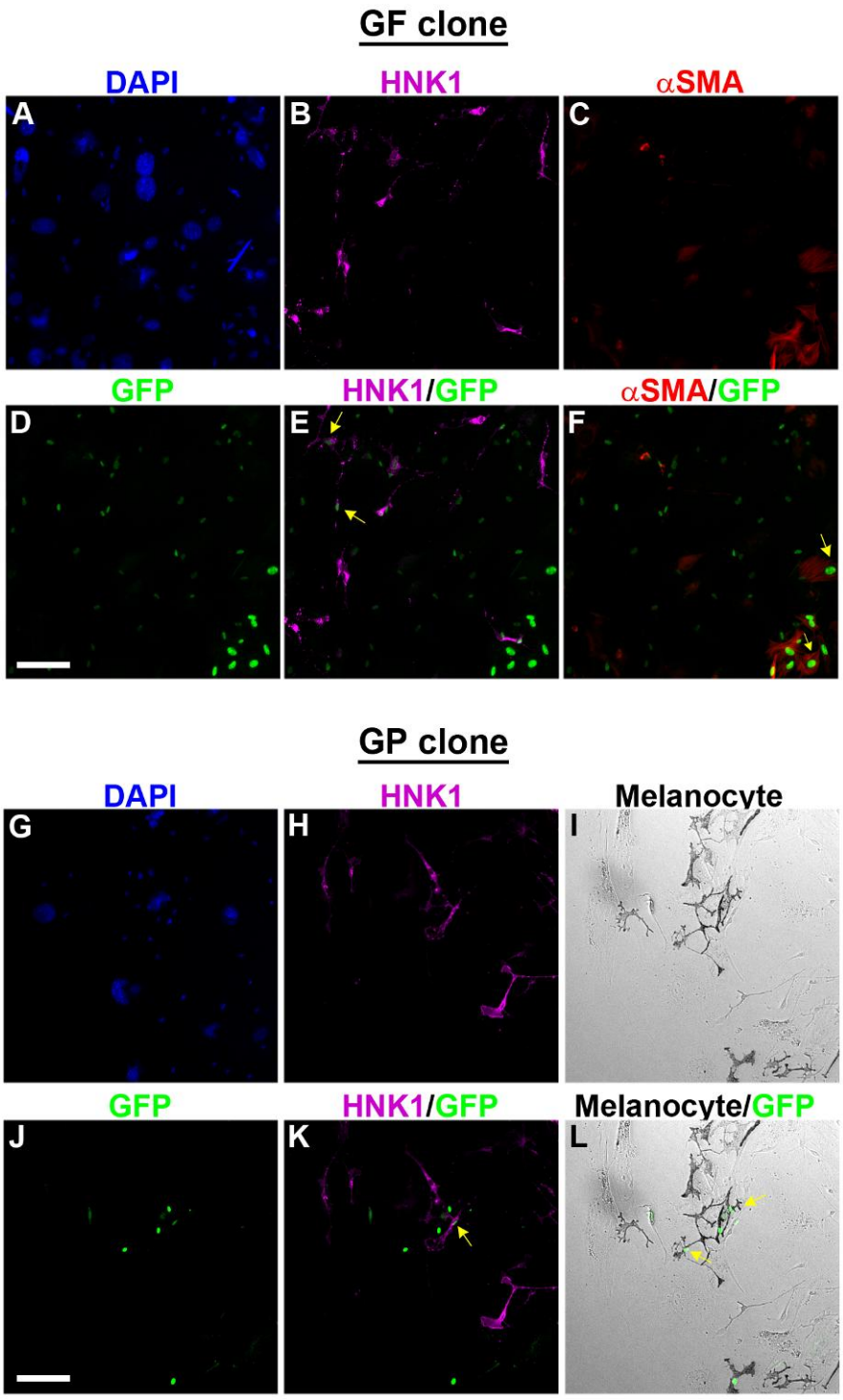

Figure 19: Examples of GFP+ bipotent clones obtained in limiting dilution clonal analyses. (A-F) Same region of a glial-fibroblast (GF) bipotent colony showing fluorescent labelings as indicated. Observe co-localization of nuclear GFP in HNK1+ and SMA+ cells (arrows in E and F, respectively). (G-L) Views of the same region of a bipotent GFP+ clone containing both HNK1+ glial/neuroglial progenitors and pigmented melanocytes (GP colony). Observe co-localization of nuclear GFP with HNK1 and with melanin (arrows in K and L, respectively). Bar 100µm.

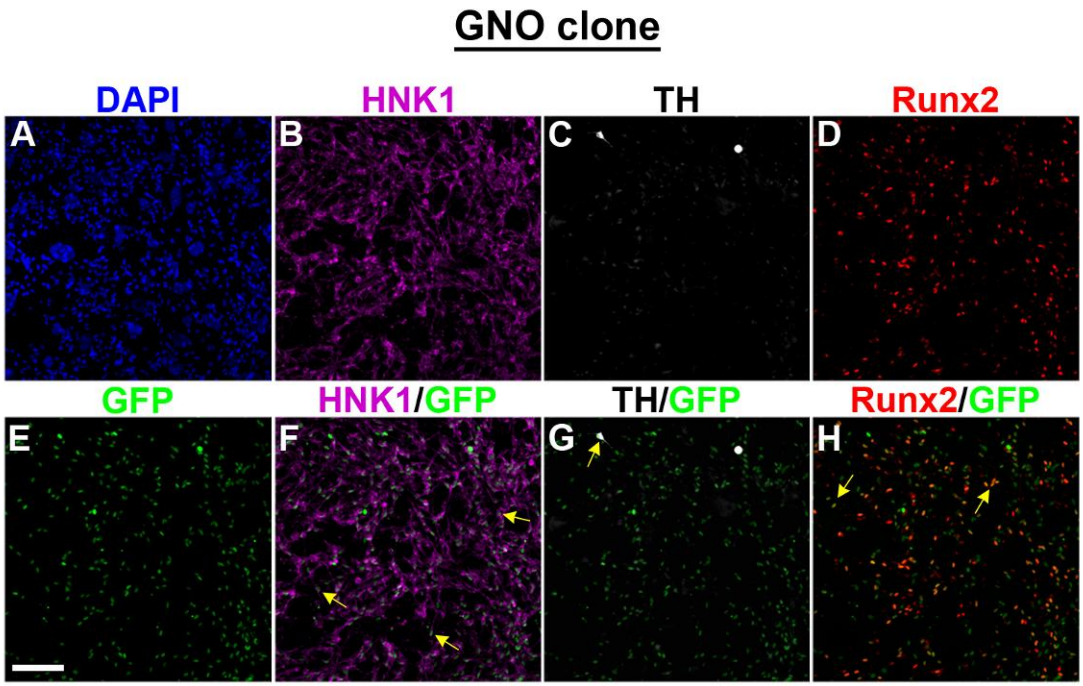

Figure 20: Example of a tripotent clone obtained in limiting dilution clonal analyses. Same region of a tripotent colony derived from transfected NCC, showing distinct fluorescent labelings as indicated. Note the presence of neuroglial progenitors (HNK1+), adrenergic neurons (TH+) and osteoblasts (Runx2+), and co-localization of nuclear GFP+ with each lineage specific marker (arrows in F, G, H). Bar 100µm.

DISCUSSION

I. *Six1* expression in NC and mesoderm-derived craniofacial territories of the avian embryo

The development of the head of vertebrates involves morphogenetic movements, differentiation and growth of mesenchyme-derived tissues and organs, which result from coordinated interactions between two main cellular populations of distinct embryonic sources: the mesoderm and the NC. On one hand, the contribution of the cephalic NC to a large part of head mesenchymal tissues, including bones, cartilage, dermis and adipose deposits in the entire face and the ventral neck, is a unique characteristic of vertebrates. On the other hand, the cranial mesoderm is responsible for the development and organization of the head muscles and blood vessel endothelia; it also yields bones of the posterior head and participates, with the NCC, to the genesis of the otic capsule and to the formation of the basisphenoid bone of cranial base. It is thus crucial to understand the regulatory cellular and molecular mechanisms whereby these two cell populations develop in concert and properly assemble in order to produce the diverse mesenchymal tissues that construct the complex head of the vertebrates.

Much remains to be known regarding the regulatory genes that control orchestrated co-development of cells derived from the NC and mesoderm in the forming head. In this line, we have investigated, in this Thesis, the germ-layer origin and differential fate of the cranial cells that express the transcription factor Six1 during head formation in the avian embryo. Six1 belongs to the Six homeobox family of transcription factors (Kawakami et al., 2000), known to control many organ development in vertebrates (Kumar, 2009), including craniofacial bones, the ear and tongue muscles (Laclef et al., 2003b; a). In human branchio-oto-renal syndrome, hearing loss and branchial defects result from *Six1* haploinsufficiency (Kochhar et al., 2008; Ruf et al., 2004). During mammalian and avian development, *Six1* exhibits broad expression in cranial mesenchymal tissues and ectodermal placode derivatives (Laclef et al., 2003b; Garcez et al., 2014; Sato et al., 2012). Nevertheless, in head development, the precise distribution of *Six1*-expressing cells, and *Six1* function in the NC and mesoderm, are still unclear.

In this work (*see Article 1*), we have presented the spatial-temporal expression of Six1 protein in the head of the chick embryo in vivo; in addition, by using quail-chick transplantations in ovo, we have determined the respective contribution of cephalic NC and paraxial mesoderm to Six1-expressing cell populations in early head development. We observed Six1 expression in many ectodermal derivatives, such as the olfactory, otic and

epibranchial placodes. These findings corroborate current literature regarding *Six1* gene as a general placodal marker (Schlosser, 2010; Baker and Bronner-Fraser, 2001). Here we will focus on the main results concerning the differential expression of Six1 in mesenchymal tissues of NC and mesoderm origin.

Our analysis of *Six1* mRNA and Six1 protein expression at early stages of chick embryo development (E1.5 to E3), and in quail-chick chimeras, first provides new information on the initial distribution of Six1-positive NCC and mesodermal cells. At early migratory stages, mesencephalic and rhombencephalic NCC did not express Six1 while this factor was widely expressed in the early cephalic mesoderm. Thus, Six1 did not colocalize with Sox10, a NC "specifier" expressed during NCC migration. When we examined cephalic NCC cultured in vitro after 17hours of migration from explanted mesencephalon, we similarly did not detect Six1-immunoreactive cells (data not shown). These results contradict a previous report describing *Six1* mRNA expression at early cranial NC migration stages in whole-mount preparations of the chick embryo (Garcez et al., 2014). Nevertheless, our data are in agreement with the analysis of *Six1* expression in embryonic sections by Sato and colleagues (2012); moreover, these authors did not find any activity of *Six1* enhancers in the HNK1+ cranial NCC, after electroporation of genomic constructs in the chick embryo. Furthermore, during formation of the neural fold in the chick, *Six1* expression was mainly observed in the lateral neural plate border, i.e. the future placodal region, and only transiently in a subtle set of early cranial NCC close to this region (Roellig et al., 2017).

Despite apparent absence of significant expression of Six1 at early migatory stages, we found that, when NCC deploy in the cephalic mesenchyme of E2 and E3 chick embryo, they start to broadly express Six1, particularly in the periocular, perinasal and periotic regions, as illustrated by the presence of numerous Six1-immunoreactive quail cells after cranial NC transplantation. In contrast, in the pre-otic regions, a modest contribution of mesodermal cells to the mesenchyme located in the vicinity of the trigeminal ganglion was observed after cranial mesoderm transplantations. Whether these Six1-expressing cells correspond to future muscle precursors or presumptive skeletogenic mesodermal cells remains to be investigated. A quite different distribution of Six1 was found in the cells engrafted into the BA mesenchyme of the host embryos: only mesodermal cells populating the core of the arch were positive for Six1 whereas the NCC that settled in the BA periphery were negative. Since mesodermal cells located in the core of BAs are known to comprise myogenic precursors (Grenier et al., 2009; Couly et al., 1993), it is quite plausible that Six1 is involved in myogenesis in the jaw, similarly to its action on somitic-derived muscle precursors in the trunk (Laclef et al., 2003a).

At later stages, in E7 chicken, Six1 expression was detected in several tissues and cell populations derived from the cranial NC. PNS neural derivatives expressing Six1 appeared limited to a subset of neurons in the trigeminal ganglion while NC-derived Sox10+ glial progenitors did not express Six1. The possibility that Six1-positive trigeminal neurons belong to the placodal-derived neuronal populations of the ganglion is supported by previous work in the chick and mouse that have identified Six1 as an important factor in development of PNS sensory neurons (Karpinski et al., 2016; Sato et al., 2012).

Regarding mesenchymal cell types of NC origin, at E7, Six1 was present in cells of the nasal septum and mesenchyme, and in periocular mesenchymal tissues. In the eye proper, Six1 was not detected in the retina, lens, cornea and optic nerve. These results support previous findings showing that *Six1*, and the closely-related gene *Six2*, are not involved in the development of the eye in vertebrates, despite evolutionary homology of *Six1* with *Drosophila Sine oculis* (Kawakami et al., 2000; Laclef and Maire, 2004). However, Six1-positive cells were clearly detected in differentiating periocular structures, such as the scleral cartilage and the presumptive choroid, which both are of NC origin in the chick (Creuzet et al., 2005a). Interestingly, in the nasal septum, Six1 was expressed both in chondrocytes and in perichondrium, although its expression was stronger in the perichondrium. Furthermore, Six1 expression by chondrocytes derived from the cephalic NC was further verified in cultures of cephalic NCC, albeit the total number of Six1-positive cells in these cultures was rather limited (about 1%). Finally, we observed Six1-expressing cells dispersed in the mesenchyme adjacent to the dorsal mesencephalon, which suggests Six1 expression in precursors of the meninges, which are mesodermal-derived in this brain region (Couly et al., 1992).

Concerning mesodermal derivatives, our data reveal that Six1 is mainly expressed in the head skeletal muscles, which are formed by distinct components of the mesoderm (i.e., prechordal and cranial paraxial mesoderm for extraocular muscles, cranial paraxial mesoderm for BA muscles and somitic mesoderm for laryngeal and tongue muscles). These different types of muscles depend upon distinct regulatory gene networks for their specification (Sambasivan et al., 2011). Therefore, a common dependence on *Six1* gene activity is likely a feature of the molecular program controlling myogenesis both in trunk and head.

In the auditory system, Six1 plays multiple roles and its deletion in mice severely affects the outer, middle and inner ear structures (Laclef et al., 2003b; Ozaki et al., 2004). Our data showing Six1-expressing cells in the chick ventral otic placode at E3 and the inner ear epithelium at E7, are consistent with its known essential action in cochlear and vestibular

development. We also found a contribution of Six1-positive cells to the formation of ventral cartilage of the otic capsule. Due to the triple origin of the otic capsule in the avian embryo, from the NC, the cranial and somitic mesoderm (Couly et al., 1993), further experiments are needed to delineate the tissular origin and the fate of this subset of Six1-expressing mesenchymal cells.

Finally, at least in the head, Six1 seems to be deprived of any contribution to mesodermal and NC-derived components of the vascular system: we did not observe Six1 expression in blood vessel endothelia at all stages analyzed, and the NC-derived vascular smooth muscle cells and pericytes did not express Six1 in E7 chicken embryo. However, in cultures of isolated quail cephalic NCC, we identified the presence of a small subset of NCC that expressed both Six1 and αSMA, an early marker of myofibroblasts and smooth muscle cells, which develop in mouse and avian NC cultures (Shah et al., 1996; Trentin et al., 2004; Calloni et al., 2007, 2009).

In sum, the careful examination of *Six1* expression and the use of fate mapping of Six1-expressing cells in quail-chick chimeras have shown that, in mesenchymal tissues, this gene exhibits a complex and dynamic expression pattern in cells derived from both the cranial NC and mesoderm. In particular Six1-expressing cells of NC origin contribute to the formation of periocular structures and facial cartilages, whereas Six1 in mesodermal cells has an important distribution in skeletal myogenic cells of the head. Our results therefore open the way to further improve the understanding of *Six1* function in head tissue morphogenesis. In contrast to placodal development regulation by *Six1* gene (Neilson et al., 2010; Yan et al., 2015), *Six1* downstream targets in mesenchymal tissues are still poorly known. Further experiments involving the selective knockdown of *Six1* gene, in a temporal and NC- or mesoderm-specific manner, would be beneficial for a further understanding of the roles of *Six1* in the differentiation, patterning and assembly of mesenchymal cell subpopulations from the NC and mesoderm, during development of the vertebrate head.

II. Regulation of NC mesenchymal differentiation potentials by *Hox* genes

The capacity to differentiate into mesenchymal cell types is a remarkable feature of the cephalic NCC, which contribute to the formation of the main mesenchymal-derived structures in the head of vertebrates (for references, Dupin and Le Douarin, 2014). Mesenchymal fate appears to be restricted to this anterior axial level of the NC, since the trunk NC contribution to mesenchymal tissues is limited to a few particular examples in the mouse and zebrafish, far from representing the same variety of mesenchymal cell types as those generated by cephalic NCC (Joseph et al., 2004; Kague et al., 2012). Nevertheless, the mesenchymal potentiality of trunk NCC might be actually not so much restricted, since recent findings from our laboratory have shown that quail trunk NCC comprise multipotent progenitors that are able, under permissive environmental conditions, to generating a vast array of mesenchymal cell types in vitro, including osteoblasts, chondrocytes, and adipocytes (Calloni et al., 2007; Coelho-Aguiar et al., 2013). The in vitro clonal analysis performed in these studies also revealed that the trunk NC stem cell population is mainly composed of progenitors with a dual neural-mesenchymal differentiation capacity, similarly to the cephalic NCC (Calloni et al., 2007, 2009). These findings suggest that the differentiation of mesenchymal multipotent NC progenitors could probably rely on similar molecular mechanisms, along the whole neural axis. In this aspect, *Hox* genes, particularly *Hoxa2*, have been described as transcription factors that can prevent head mesenchyme formation if ectopically expressed in the Hox-free domain of the cranial NC (Couly et al., 2002; Creuzet et al., 2002, 2004).

In part 2 of this Thesis manuscript, we have presented experiments aimed at investigating how and to which extent *Hox* genes can affect the production of mesenchymal derivatives by the cephalic and trunk NCC, using in vitro culture systems that proved to be appropriate for the characterization of avian NC mesenchymal progenitors.

II.1 Selected *Hox* genes are downregulated concomitantly with trunk NCC differentiation in vitro

Previous work by our group has shown that trunk NCC display mesenchymal potentials in vitro as do cephalic NCC in vivo and in vitro (Le Douarin and Kalcheim, 1999; Calloni et al., 2007; Billon et al., 2007; Coelho-Aguiar et al., 2013). In this Thesis work, we hypothesized that the ability of trunk NCC to differentiate into mesenchymal derivatives in vitro could involve a

downregulation of *Hox* genes when cultured trunk NCC are maintained in pro-mesenchymal conditions. A first strategy was to detect, by RT-qPCR, which members of the *Hox* genes were modulated in culture. It has been shown that expression of *Hoxb4* and genes of the *Hox9* paralog group decreases in long-term NC cultures giving rise to cartilage (Abzhanov et al., 2003; Ido and Ito, 2006). Nevertheless, other mesenchymal cell lineages, such as osteoblasts and adipocytes, have not yet been investigated. In the present work, we investigated *Hox* genes from paralog groups 5 to 10, which are expressed at the level of the neural tube used in our experiments to perform NC cultures (Burke et al., 1995 and our data). We additionally investigated the expression of *Hoxa2*, the first *Hox* gene to be described as involved in mesenchymal differentiation of the cephalic NCC in vivo in chick and mouse embryos (Creuzet et al., 2002; Kanzler et al., 1998). By RT-qPCR, we thus identified a particular subset of *Hox* genes, i.e., *Hoxa2*, *Hoxc6*, *Hoxc8*, *Hoxc9* and *Hoxc10*, significantly downregulated during the progression of trunk NCC development in vitro. Interestingly, their downregulation occurred with the same time-course as the onset of expression of *Runx2*, the earliest mesenchymal lineage marker gene expressed in these cultures. This result supports our hypothesis that a downregulation of a subset of *Hox* genes could be involved in the regulation of mesenchymal potentialities of trunk NCC. Of note, not all the different *Hox* genes analyzed were downregulated in trunk NCC in vitro, most of them maintaining a rather constant expression level at all times analyzed (between day-0 and day-8 of culture). Our results thus argue that individual *Hox* genes, rather than global Hox gene reduction, might play a role in NCC differentiation. However, whether the expression profile of *Hox* genes can change at later times of culture, such as the case of *Hoxb4* in Abzhanov and colleagues work (Abzhanov et al., 2003), remains to be further investigated.

II.2 *Hoxa2* and *Hoxc10* gain of function in cultured trunk NCC: effects on early skeletogenesis

To investigate whether *Hox* genes are capable of affecting mesenchymal differentiation of trunk NCC in vitro, we focused on two *Hox* genes that we found to be downregulated in PCR analyses: *Hoxa2* and *Hoxc10*. We performed gain of function experiments, using transfections of early NCC with pCX plasmids, before the onset of *Runx2* expression. After six days in culture, we observed a drastic reduction in the number of Runx2-expressing osteoprogenitors formed after *Hoxa2* overexpression in the NCC, suggesting that Hoxa2 negatively influences the onset of bone progenitors in the cultures. Indeed, when *Hoxa2* was depleted in murine embryos, *Runx2* expression was increased in the BAs (Kanzler et

al., 1998). On the other hand, ectopic expression of *Hoxa2* specifically in cephalic NCC resulted in downregulation of *Runx2* and *Sox9* (Kitazawa et al., 2015; Garcez et al., 2014; Grammatopoulos et al., 2000). These results suggest that *Hoxa2* alters *Runx2* regulation in both cephalic and trunk NCC. Interestingly, our data also showed that forced expression of *Hoxc10* did not significantly reduce *Runx2* expression by trunk NCC, suggesting that not all the *Hox* genes could account for the same effects of *Hoxa2*.

The molecular mechanism by which Hoxa2 could influence *Runx2* expression in NCC remains somewhat elusive. One possibility is that Hoxa2 directly modulates *Runx2* transcription, as putative Hox consensus sequences have been already characterized in mouse *Runx2* promoter (Hassan et al., 2007). Nevertheless, one of these Hox-binding sequences was related to activation by *Hoxa10* of *Runx2* transcriptional activity in mammalian long bones and vertebra, and not with *Runx2* repression, as it seems to be the case in mesenchymal progenitors derived from the avian NCC. Interestingly, this putative sequence displayed a strong affinity with Hoxa10, not with other Hox factors, such as Hoxa9, Hoxa11, and Hoxa13 (Hassan et al., 2007).

These results allow us to address some considerations about the specificity of Hox and Runx2 interactions:

Firstly, although Hox transcription factors have similar homeodomains and apparently low DNA-binding specificity (Hrycaj and Wellik, 2016), in the case of *Runx2* regulation, it appears that distinct *Hox* genes possess different binding affinities to the *Runx2* promoter. In fact, the presence of specific Hox co-factors, also expressed in Hox-positive tissues, help in DNA-binding site selection and in conferring functional specificity to individual *Hox* genes (Mann et al., 2009).

Secondly, besides their crucial role in vertebral and limb bone identity and patterning (Kessel and Gruss, 1991; Mallo et al., 2010), particular *Hox* genes are necessary for activation of *Runx2* gene, instead of a repression of this gene. Indeed, in mesoderm-derived tissues, some of the posterior *Hox* genes can activate *Runx2*, *Sox9,* and other bone master genes, allowing the progression of endochondral ossification (Hassan et al., 2007, 2009; Gross et al., 2012; Neufeld et al., 2014). In this line, it should be interesting to understand which are the factors involved in *Hox* inhibition during bone formation, specifically in the NCC.

Alternatively to a possible direct action on *Runx2* transcription, Hoxa2 could downregulate other genes, which mediate induction of *Runx2* and/or other molecular effector genes in bone differentiation by NCC. In this regard, *Six2* gene was recently described as

encoding a direct downstream factor of *Hoxa2* in the NC-derived BA2 mesenchyme in the mouse (Kutejova et al., 2008, 2005). Moreover, *Six2* inhibition in the head mesenchyme led to hypoplasia of the craniofacial skeleton in mouse and chick embryos, opposite to the phenotype resulting from *Hoxa2* overexpression (He et al., 2010; Garcez et al., 2014). Nevertheless, Six2 downstream factors involved in bone differentiation are currently unknown. Importantly, in avian trunk NCC, our preliminary data argue against the possibility that *Hoxa2* effects could be mediated by an inhibition of *Six2*, since this latter gene, and its closely related *Six1*, were not found to be expressed during trunk NC mesenchymal differentiation in our in vitro model (data not shown). In summary, the genetic regulatory cascade involving *Hoxa2* and *Runx2* in cephalic and trunk NCC needs to be further investigated.

II.3 *Hoxa2* gain of function influences the terminal differentiation of trunk NC mesenchymal cells

By using a culture protocol previously devised by our group to assess the mesenchymal differentiation capacities of trunk NCC (Coelho-Aguiar et al., 2013), we aimed to investigate if *Hoxa2* forced expression could affect, after *Runx2* reduction, the formation of mature differentiated bone cells in trunk NC long-term cultures. In addition, this culture protocol, which is permissive for osteogenic, chondrogenic and adipogenic full differentiation, allowed us to investigate *Hoxa2* effects on the main mesenchymal lineages derived from trunk NCC in vitro. After trunk NCC transfection on the first day of culture with *Hoxa2* plasmid, the analysis of bone and cartilage mineralized regions, and lipid storing adipocytes identified in 25 day-cultures showed that overexpression of *Hoxa2* led to several alterations in the late development of NC mesenchymal cells, as discussed below.

First, we observed a significant reduction in the number and the area occupied by mineralized bone regions after *Hoxa2* forced expression, in comparison with the control condition transfected with a GFP plasmid. These results suggest that early effects of *Hoxa2* on Runx2-positive osteoprogenitors could have prevented, later on, the formation of bone matrix structures derived from these trunk NC progenitors. It would be interesting to overexpress *Hoxa2* at later stages and to examine its influence on bone matrix formation, for instance, after the appearance of Runx2 osteoprogenitors; nevertheless, transfection of trunk NCC at late stages of culture turned out to be inefficient to target a considerable number of cells, at least with the expression plasmids used in these experiments (data not shown). The high heterogeneity of the differentiated NC cell types that develop in late cultures, also probably

precluded efficient targeting of bone progenitors by *Hoxa2* plasmids. To overcome this issue, one strategy would be to isolate Runx2-positive cells by FACS and overexpress *Hoxa2* in a purified Runx2-positive population in culture. Another possibility would be to induce *Hoxa2* expression under the control of *Runx2* promoter sequences, as done by Massip and colleagues to investigate *Hoxa2* effects in committed chondrocytes in vivo (Massip et al., 2007). These strategies would allow us to further address the downstream effects of Hoxa2 on *Runx2* specified progenitors.

Furthermore, we observed that *Hoxa2* gain of function significantly decreased cartilage mineralization by approximately 70% as compared with the GFP-control plasmid. The onset of cartilage ECM in long-term avian trunk NC cultures has been previously reported (McGonnell and Graham, 2002), and induction of cartilage-specific collagen 2 was associated with *Hoxb4* and *Hox9* downregulation in chick and mouse long-term trunk NC cultures (Abzhanov et al., 2003; Ido and Ito, 2006). However, our data revealed, for the first time, a direct effect of *Hoxa2* on the production of fully differentiated cartilage by trunk NCC in vitro. In vivo, endochondral ossification and cartilage formation in the whole body were greatly impaired in mouse embryos where *Hoxa2* was ectopically expressed in immature chondrocytes expressing *collagen 2a1*. In these mice, *Hoxa2* overexpression resulted in overall chondrodysplasia and delayed cartilage hypertrophy and mineralization (Massip et al., 2007). As of note, in trunk quail NC cultures, the majority of cartilage regions (Alcian Blue-positive) were likewise labeled with Alizarin Red, suggesting an endochondral-like ossification process in vitro, as previously described (Coelho-Aguiar et al., 2013).

In long-term cultures of quail trunk NCC, we could also observe an effect of *Hoxa2* on adipogenesis. *Hoxa2* gain of function notably reduced the surface area containing lipid-storing adipocytes (OilRed O positive). To our knowledge, it is the first time that *Hoxa2* forced expression is associated with impairment of adipogenesis, especially in trunk NCC. Other *Hox* genes, however, have been previously related to adipogenesis regulation, and it is known that the particular *Hox* genes involved in this process depend on the anteroposterior position of fat deposits in the body (Seifert et al., 2015). Some reports suggested that *Hoxa4*, *Hoxa7*, and *Hoxd4* were upregulated during in vitro adipogenesis of 3T3-L1 pre-adipocytic cells, although a specific function of these genes was not described (Cowherd et al., 1997). Regarding adipocytic cell types, the expression of *Hox* from paralogous group 4 appears to be associated with a fate decision between white and brown adipose tissues (Cantile et al., 2003). Moreover, Hoxc8 inhibition, via miR-196a action, is very likely required for the specification of beige adipocytes, which are induced upon cold exposure in mouse white adipose tissue (Trajkovski and Lodish,

2013). Finally, the transcription factor Pbx1 was recently described as a required factor for early steps of adipogenesis in neuralized mouse ESC and human multipotent adipose-derived stem cells (Monteiro et al., 2011). Notably, Pbx1 is a member of TALE family of transcription factors, which acts as co-factor of several *Hox* genes, helping to activate or repress many *Hox* target genes, in multiple contexts (Mann et al., 2009; Capellini et al., 2011). Whether Hoxa2 regulation of the adipogenic fate could have a relationship with its binding to Pbx1, in trunk NCC cultures, is not known.

II.4 Ectopic expression of *Hoxa2* reduces the number of Runx2 progenitors in cephalic NCC

Since we showed that *Hoxa2* overexpression significantly reduces Runx2+ cells and impairs terminal differentiation of mesenchymal derivatives in trunk NC cultures, we decided to evaluated the effect of *Hoxa2* ectopic expression on cephalic NCC in culture. To our knowledge, *Hoxa2* effects on Runx2 expression have never been investigated in isolated cephalic NCC. With this objective, we performed cephalic NC cultures with a specific protocol previously established by our laboratory (Calloni et al., 2009). In this experimental approach, cephalic NCC were cultured on 3T3 feeder layers, which allows the differentiation of numerous Runx2-expressing cells in the culture. Moreover, this procedure permits the initial plating of a small number of cephalic NCC, which represents a significant advantage, due to the difficulty to obtain a high amount of cephalic NCC in primary cultures (around 10,000 cells per experiment). With the aim to target only the NCC, but not the feeder-layer cells, we carried out the transfections in primary cultures (i.e. containing explanted neural tubes and migratory NCC), three hours before harvesting and replating the NCC. Although the amount of cephalic NCC expressing these plasmids barely exceeded 50% of the total cell population, we still observed a significant reduction of Runx2 osteoprogenitors, in comparison with GFP control condition. Interestingly, we also noticed a decrease in the total cell number, indicating that we cannot exclude an effect of *Hoxa2* on the whole NCC population, possibly including other mesenchymal progenitors, for chondrocytes and adipocytes, obtained from cephalic NCC in vitro (Calloni et al., 2007, 2009; Billon et al., 2007). Notably, when *Hoxa2* was ectopically expressed in the cephalic NC of chicken embryos, nasal and mandibular buds failed to develop, and this was partially associated with a reduction of cell proliferation and an increase of apoptosis in early NCC (Creuzet et al., 2002; Garcez et al., 2014). Conversely, when *Hox* genes were upregulated in mouse cephalic NCC, due to the loss of *Ezh2*, no clear differences in NCC proliferation and cell death rates were observed (Schwarz et al., 2014). In trunk NC

experiments, we also observed a reduction in the total cell number after *Hoxa2* transfection. However, this was highly variable between different experiments, ranging from 5 to 20% of reduction compared with the control condition (data not shown). Therefore, the effects on NCC death and proliferation after *Hoxa2* overexpression remain to be clarified.

II.5 Myofibroblasts and neural cell types are not affected by *Hoxa2* gain of function in cephalic and trunk NCC

As previously shown by our group, avian cephalic and trunk NCC comprise multipotent precursors, generating a similar vast array of NC-derived cell types in vitro (Dupin et al., 2010; Dupin and Le Douarin, 2014). Taking this into consideration, we aimed to evaluate *Hoxa2* effects on NC derivatives other than bone cells, such as SMA+ myofibroblasts, TH+ neurons, Melem+ melanocytes and HNK1+ neuroglial precursors. In this regard, the phenotypic analysis of cephalic NC 6 day-cultures following *Hoxa2* gain of function, did not show any significant differences in the percentage of these cell types. In vivo, avian Hox-positive NCC transplanted anteriorly into a Hox-negative environment, although they cannot yield skeleton, are still able to generate neural derivatives and musculo-connective cells in the wall of head blood vessels (Couly et al., 1998, 2002; Nakamura and Ayer-le Lièvre, 1982). Interestingly, in the recent paper by Schwarz and colleagues (Schwarz et al., 2014), where a wide range of *Hox* genes have been derepressed by *Ezh2* deletion in murine NCC, glial and neuronal differentiation were not affected. These results indicate that *Hox* genes predominantly act on cranial NC-derived mesenchymal cell types. Similarly, in quail trunk NCC, gain of function of *Hoxa2* did not modify the generation of these cell types in vitro. Taken together, these results reinforce the hypothesis that *Hoxa2* has a more pronounced, if not exclusive, effect on cephalic and trunk NCC mesenchymal derivatives in vitro. In contrast, it is noteworthy that *Hoxc10* gain of function did not significantly affect the production of Runx2-positive osteoprogenitors, myofibroblasts and neural cell types derived from trunk NCC, therefore emphasizing the differential action of individual *Hox* genes in NCC fate.

II.6 Single cell analyses of *Hoxa2* effects on trunk NCC multipotency (preliminary results)

Previous experiments have shown that osteoblasts derive from several types of multipotent trunk NCC in vitro (Coelho-Aguiar et al., 2013). How Hoxa2 regulates

mesenchymal potentials in these progenitors is currently unknown. To be able to analyze Hoxa2 influence on trunk NC multipotent progenitors at single cell resolution, we performed NCC clonal analysis in vitro. As described in Additional Results Chapter (*Results*, *section III*), we generated a genetic construct to be able to permanently express chicken *Hoxa2* gene together with a *GFP* reporter ("Hoxa2-GFP"). In this way, we could identify Hoxa2-expressing cells using GFP expression.

Among different tested methods for preparing single GFP+ NCC cultures, we obtained highest clonal efficiency with a protocol based on the limiting dilution technique. However, after analysis at 10 days of culture, only approximately 3% of single plated GFP+ cells generated a colony. This efficiency is really low, compared with previous in vitro clonal analyses from our group, in which NCC exhibited a clonal efficiency of at least 30% (Trentin et al., 2004; Calloni et al., 2007, 2009; Coelho-Aguiar et al., 2013). Although the basic culture conditions were similar, some particularities of the present experiments might have contributed to this weak outcome: - the low transfection efficiency with "ctrl-GFP" and "Hoxa2-GFP" plasmids, which was below 10%, - the initial plating of 0.5% GFP+ cells per well, which helped to ensure clonality, but increased the probability to yield wells without GFP+ cells, and finally, - the intrinsic characteristics of the transposon vector system, in which we can not guarantee that all transfected cells will, later on, integrate the insert and produce a progeny with a stable expression of the construct. As a consequence, the total number of clones we have obtained, in four independent experiments, is not large enough to enable us to draw firm conclusions about the cellular mechanisms whereby Hoxa2 influences trunk NC multipotency. Nonetheless, these preliminary results allow us to prepare some hypotheses, as discussed below.

Firstly, although the cloning efficiency was similar between "Hoxa2-GFP" and "GFP-control" conditions, the number of cells per clone was significantly reduced after *Hoxa2* forced expression, suggesting an effect of this gene on single NCC survival or proliferation. Secondly, we detected more clones yielding only a single cell type in Hoxa2-GFP compared with control condition. This result indicates that Hoxa2 could trigger a restriction of fate diversification in trunk NC progenitors. The reduction in the variety of cell types in NCC progeny could also be a secondary effect, resulting from Hoxa2 influence on the total cell number of NCC progeny. In that case, all progenitor types would be equally reduced. In contrast, we observed that clones containing TH+ neurons, for instance, accounted for 30% of clones in both Hoxa2-treated and GFP-control colonies. Thus, it is likely that the decrease in the diversity of cell types results from the regulation of NCC fate by Hoxa2, independently of its effects on total cell number.

Moreover, a clear correlation between colony size and diversity of cell types within a colony has never been recorded in previous in vitro NCC clonal analyses performed by our group (Calloni et al., 2007 and unpublished data), meaning that highly multipotent cells can yield colonies of variable sizes. Finally, we could also observe that the number of clones containing pigment cells were over-represented whereas clones containing mesenchymal NC derivatives, such as osteoblasts and myofibroblasts, were mildly reduced in *Hoxa2*-expressing clones. These preliminary results suggest that Hoxa2 could negatively regulate the commitment of trunk NC multipotent progenitors towards a mesenchymal fate.

II.7 Concluding remarks

In the present work, we first determined that a set of *Hox* genes, including *Hoxa2* and *Hoxc10*, is downregulated in trunk NCC, when grown in culture conditions appropriate to disclose their differentiation into mesenchymal cell types. Next, we showed that the mesenchymal differentiation capacity of trunk NCC is partially inhibited following overexpression of *Hoxa2*, but not *Hoxc10*, at early stages of culture. This effect was associated later on with impairment of terminal differentiation of bone cells, chondrocytes, and adipocytes in long-term trunk NC cultures. Moreover, in cephalic NCC, *Hoxa2* reduced the number of bone progenitors formed in vitro. Our data therefore suggest a similar dependence on a *Hoxa2*-negative status for the outcome of Runx2-positive osteoblasts in both trunk and cephalic NCC.

The precise role of *Hoxa2* gene on NC mesenchymal progenitors remains to be elucidated. One possibility is that *Hoxa2* acts on cell survival or proliferation, which is supported by our preliminary data from single NCC cultures (*see Results, section III*), and by in vivo experiments of *Hoxa2* gain of function in the chicken NCC (Creuzet et al., 2002; Garcez et al., 2014). Recently, *Hox* gene regulation has been associated with autophagy control in *Drosophila* and vertebrate cells (Banreti et al., 2014; Yang et al., 2016). Interestingly, some reports have suggested that a tight regulation of autophagy may be crucial during early steps of chick NC development, by playing a dual role in early NCC proliferation and death (Wang et al., 2015, 2017). Thus, it should be interesting to investigate whether *Hox* effects on NC mesenchymal progenitors involve a possible regulation of autophagy.

Nevertheless, other possibilities cannot be excluded, since no clear effect on cell division and apoptosis was reported in early murine ectomesenchymal NCC that failed to generate proper skeletal structures when overexpressing *Hox* genes (Schwarz et al., 2014). We

cannot rule out the possibility that *Hox* genes could also have an impact on NCC fate decision, since ectopic expression of *Hoxa2* in BA1 reduced *Sox9* and *Runx2* expression in transgenic mice (Kanzler et al., 1998; Kitazawa et al., 2015). In our preliminary in vitro clonal analyses, we observed an increase of fate-restricted clones after *Hoxa2* forced expression in trunk NCC. A possible role of *Hox* genes in NC stem cell fate decision has to be further clarified in cephalic and trunk NCC.

Finally, since *Hoxa2* produces similar effects on cephalic and trunk NC mesenchymal derivatives in vitro, we can speculate about the possibility that this regulation could represent an ancient mechanism shared by NCC all along the neural axis, since it is argued that, in primitive vertebrates, both cephalic and trunk NCC have played a role in the ontogeny of skeletal cells (Smith, 1991; Smith and Hall, 1990; Le Douarin and Dupin, 2012 for a review). Nonetheless, a recent study has shown that, as opposed to trunk NCC, cephalic NCC express specific transcription factors, which act to promote their mesenchymal fate (Simoes-Costa and Bronner, 2016). These findings suggest that, during evolution, either cephalic NCC have acquired new factors that were necessary to reinforce and regulate their mesenchymal fate, or the trunk NCC may have lost these factors, which could explain why the trunk NC of amniotes is virtually devoid of mesenchymal derivatives in vivo. Strikingly, avian trunk NCC can be partially reprogrammed in vivo to a cephalic NC-like identity by ectopic expression of these factors, followed by grafting into a permissive environment, that is, in cephalic NC migratory stream (Simoes-Costa and Bronner, 2016). It should be interesting to investigate whether *Hox* genes could act upstream of these transcription factors, for example by preventing their expression in trunk NCC. Taken together, in view of the remarkable multipotency of NCC and their astonishing role in skeletogenesis of the “New Head” of vertebrates (Gans and Northcutt, 1983), multiple regulatory networks might be necessary to endow NCC with their various mesenchymal fate.

REFERENCES

Abitua, P.B., E. Wagner, I.A. Navarrete, and M. Levine. 2012. Identification of a rudimentary neural crest in a non-vertebrate chordate. *Nature*. 492:104–107.

Abzhanov, A., and C.J. Tabin. 2004. Shh and Fgf8 act synergistically to drive cartilage outgrowth during cranial development. *Dev. Biol.* 273:134–148.

Abzhanov, A., E. Tzahor, A.B. Lassar, and C.J. Tabin. 2003. Dissimilar regulation of cell differentiation in mesencephalic (cranial) and sacral (trunk) neural crest cells in vitro. *Development*. 130:4567–4579.

Adameyko, I., F. Lallemend, J.B. Aquino, J.A. Pereira, P. Topilko, T. Müller, N. Fritz, A. Beljajeva, M. Mochii, I. Liste, D. Usoskin, U. Suter, C. Birchmeier, and P. Ernfors. 2009. Schwann Cell Precursors from Nerve Innervation Are a Cellular Origin of Melanocytes in Skin. *Cell*. 139:366–379.

Adameyko, I., F. Lallemend, A. Furlan, N. Zinin, S. Aranda, S.S. Kitambi, A. Blanchart, R. Favaro, S. Nicolis, M. Lubke, T. Muller, C. Birchmeier, U. Suter, I. Zaitoun, Y. Takahashi, and P. Ernfors. 2012. Sox2 and Mitf cross-regulatory interactions consolidate progenitor and melanocyte lineages in the cranial neural crest. *Development*. 139:397–410.

Aguiar, D.P., S. Sghari, and S. Creuzet. 2014. The facial neural crest controls fore- and midbrain patterning by regulating Foxg1 expression through Smad1 activity. *Development*. 141:2494–505.

Ahlgren, S.C., and M. Bronner-Fraser. 1999. Inhibition of sonic hedgehog signaling in vivo results in craniofacial neural crest cell death. *Curr. Biol.* 9:1304–1314.

Aïoub, M., F. Lézot, M. Molla, B. Castaneda, B. Robert, G. Goubin, J.R. Néfussi, and A. Berdal. 2007. Msx2-/- transgenic mice develop compound amelogenesis imperfecta, dentinogenesis imperfecta and periodental osteopetrosis. *Bone*. 41:851–859.

Akbareian, S.E., N. Nagy, C.E. Steiger, J.D. Mably, S.A. Miller, R. Hotta, D. Molnar, and A.M. Goldstein. 2013. Enteric neural crest-derived cells promote their migration by modifying their microenvironment through tenascin-C production. *Dev. Biol.* 382:446–456.

Akiyama, H., M.C. Chaboissier, J.F. Martin, A. Schedl, and B. De Crombrugghe. 2002. The transcription factor Sox9 has essential roles in successive steps of the chondrocyte differentiation pathway and is required for expression of Sox5 and Sox6. *Genes Dev.* 16:2813–2828.

Akiyama, H., J.-E. Kim, K. Nakashima, G. Balmes, N. Iwai, J.M. Deng, Z. Zhang, J.F. Martin, R.R. Behringer, T. Nakamura, and B. de Crombrugghe. 2005. Osteo-chondroprogenitor cells are derived from Sox9 expressing precursors. *Proc. Natl. Acad. Sci. USA*. 102:14665–14670.

Ayer-Le Lievre, C.S., and N.M. Le Douarin. 1982. The early development of cranial sensory ganglia and the potentialities of their component cells studied in quail-chick chimeras. *Dev. Biol.* 94:291–310.

Baek, W.-Y., B. de Crombrugghe, and J.-E. Kim. 2010. Postnatally induced inactivation of Osterix in osteoblasts results in the reduction of bone formation and maintenance. *Bone*. 46:920–928.

Baggiolini, A., S. Varum, J.M. Mateos, D. Bettosini, N. John, M. Bonalli, U. Ziegler, L. Dimou, H. Clevers, R. Furrer, and L. Sommer. 2015. Premigratory and Migratory Neural Crest Cells

Are Multipotent In Vivo. *Cell Stem Cell*. 16:314–322.

Baker, C. V, and M. Bronner-Fraser. 2001. Vertebrate cranial placodes I. Embryonic induction. *Dev. Biol.* 232:1–61.

Baker, C. V, M. Bronner-Fraser, N.M. Le Douarin, and M.A. Teillet. 1997. Early- and late-migrating cranial neural crest cell populations have equivalent developmental potential in vivo. *Development*. 124:3077–3087.

Baker, C.V. 2008. The evolution and elaboration of vertebrate neural crest cells. *Curr. Opin. Genet. Dev.* 18:536–543.

Banreti, A., B. Hudry, M. Sass, A. Saurin, and Y. Graba. 2014. Hox Proteins Mediate Developmental and Environmental Control of Autophagy. *Dev. Cell*. 28:56–69.

Barak, Y., M.C. Nelson, E.S. Ong, Y.Z. Jones, P. Ruiz-Lozano, K.R. Chien, A. Koder, and R.M. Evans. 1999. PPARγ is required for placental, cardiac, and adipose tissue development. *Mol. Cell*. 4:585–595.

Baroffio, A., E. Dupin, and N.M. Le Douarin. 1988. Clone-forming ability and differentiation potential of migratory neural crest cells. *Neurobiology*. 85:5325–5329.

Baroffio, A., E. Dupin, and N.M. Le Douarin. 1991. Common precursors for neural and mesectodermal derivatives in the cephalic neural crest. *Development*. 112:301–305.

Barrandon, Y., and H. Green. 1985. Cell size as a determinant of the clone-forming ability of human keratinocytes. *Proc. Natl. Acad. Sci. USA*. 82:5390–5394.

Barraud, P., A.A. Seferiadis, L.D. Tyson, M.F. Zwart, H.L. Szabo-Rogers, C. Ruhrberg, K.J. Liu, and C.V.H. Baker. 2010. Neural crest origin of olfactory ensheathing glia. *Proc. Natl. Acad. Sci. USA*. 107:21040–21045.

Barré, H., F. Cohen-Adad, C. Duchamp, and J.-L. Rouanet. 1986. Multilocular adipocytes from muscovy ducklings differentiated in response to cold acclimation. *J Physiol*. 375:27–38.

Bartelt, A., and J. Heeren. 2014. Adipose tissue browning and metabolic health. *Nat. Rev. Endocrinol*. 10:24–36.

Basch, M.L., M. Bronner-Fraser, and M.I. García-Castro. 2006. Specification of the neural crest occurs during gastrulation and requires Pax7. *Nature*. 441:218–222.

De Bellard, M.E., Y. Rao, and M. Bronner-Fraser. 2003. Dual function of Slit2 in repulsion and enhanced migration of trunk, but not vagal, neural crest cells. *J. Cell Biol.* 162:269–279.

Bellmeyer, A., J. Krase, J. Lindgren, and C. LaBonne. 2003. The protooncogene c-Myc is an essential regulator of neural crest formation in Xenopus. *Dev. Cell*. 4:827–839.

Bellows, C.G., J.E. Aubin, and J.N.M. Heersche. 1991. Initiation and progression of mineralization of bone nodules formed in vitro: the role of alkaline phosphatase and organic phosphate. *Bone Miner.* 14:27–40.

Belmadani, A. 2005. The Chemokine Stromal Cell-Derived Factor-1 Regulates the Migration of Sensory Neuron Progenitors. *J. Neurosci.* 25:3995–4003.

Bhatt, S., R. Diaz, and P.A. Trainor. 2013. Signals and Switches in Mammalian Neural Crest Cell Differentiation Signals and Switches in Mammalian Neural Crest Cell Differentiation. *Cold Spring Harb. Perspect. Biol.* 5:1–20.

Bi, W., J.M. Deng, Z. Zhang, R.R. Behringer, and B. de Crombrugghe. 1999. Sox9 is required for

cartilage formation. *Nat. Genet.* 22:85–89.

Bialek, P., B. Kern, X. Yang, M. Schrock, D. Sosic, N. Hong, H. Wu, K. Yu, D.M. Ornitz, E.N. Olson, M.J. Justice, and G. Karsenty. 2004. A twist code determines the onset of osteoblast differentiation. *Dev. Cell*. 6:423–435.

Bildsoe, H., D.A.F. Loebel, V.J. Jones, Y.T. Chen, R.R. Behringer, and P.P.L. Tam. 2009. Requirement for Twist1 in frontonasal and skull vault development in the mouse embryo. *Dev. Biol.* 331:176–188.

Billmyre, K.K., and J. Klingensmith. 2015. Sonic hedgehog from pharyngeal arch 1 epithelium is necessary for early mandibular arch cell survival and later cartilage condensation differentiation. *Dev. Dyn.* 244:564–576.

Billon, N., P. Iannarelli, M.C. Monteiro, C. Glavieux-Pardanaud, W.D. Richardson, N. Kessaris, C. Dani, and E. Dupin. 2007. The generation of adipocytes by the neural crest. *Development*. 134:2283–2292.

Bittencourt, D.A., M.C. da Costa, G.W. Calloni, M. Alvarez-Silva, and A.G. Trentin. 2013. Fibroblast growth factor 2 promotes the self-renewal of bipotent glial smooth muscle neural crest progenitors. *Stem Cells Dev.* 22:1241–1251.

Bixby, S., G.M. Kruger, J.T. Mosher, N.M. Joseph, and S.J. Morrison. 2002. Cell-intrinsic differences between stem cells from different regions of the peripheral nervous system regulate the generation of neural diversity. *Neuron*. 35:643–656.

Blanco, M.J., A. Barrallo-Gimeno, H. Acloque, A.E. Reyes, M. Tada, M.L. Allende, R. Mayor, and M.A. Nieto. 2007. Snail1a and Snail1b cooperate in the anterior migration of the axial mesendoderm in the zebrafish embryo. *Development*. 134:4073–4081.

Blentic, A., P. Tandon, S. Payton, J. Walshe, T. Carney, R.N. Kelsh, I. Mason, and A. Graham. 2008. The emergence of ectomesenchyme. *Dev. Dyn.* 237:592–601.

Bockman, D., and M. Kirby. 1984. Dependence of thymus development on derivatives of the neural crest. *Science*. 223:498–500.

Bolande, R.P. 1974. The neurocristopathies. A unifying concept of disease arising in neural crest maldevelopment. *Hum. Pathol.* 5:409–429.

Bolande, R.P. 1997. Neurocristopathy: its growth and development in 20 years. *Pediatr. Pathol. Lab. Med.* 17:1–25.

Boskey, A.L. 2007. Mineralization of Bones and Teeth. *Elements*. 3:387–393.

Boyl, P.P., M. Signore, A. Annino, J.P. Barbera, D. Acampora, and A. Simeone. 2001. Otx genes in the development and evolution of the vertebrate brain. *Int. J. Dev. Neurosci.* 19:353–63.

Bradley, T., W. Robinson, and D. Metcalf. 1967. Colony production in vitro by normal polycythaemic and anaemic bone marrow. *Nature*. 214:511.

Brandl, C., C. Florian, O. Driemel, B.H.F. Weber, and C. Morsczeck. 2009. Identification of neural crest-derived stem cell-like cells from the corneal limbus of juvenile mice. *Exp. Eye Res.* 89:209–217.

Bridgewater, L.C., V. Lefebvre, and B. De Crombrugghe. 1998. Chondrocyte-specific enhancer elements in the Col11a2 gene resemble the Col2a1 tissue-specific enhancer. *J. Biol. Chem.* 273:14998–15006.

Brito, J.M., M.-A. Teillet, and N.M. Le Douarin. 2006. An early role for sonic hedgehog from foregut endoderm in jaw development: ensuring neural crest cell survival. *Proc. Natl. Acad. Sci. USA*. 103:11607–11612.

Bronner-Fraser, M. 1986. Analysis of the early stages of trunk neural crest migration in avian embryos using monoclonal antibody HNK-1. *Dev. Biol.* 115:44–55.

Bronner-Fraser, M., and S. Fraser. 1989. Developmental potential of avian trunk neural crest cells in situ. *Neuron*. 3:755–766.

Bronner-Fraser, M., and S.E. Fraser. 1988. Cell lineage analysis reveals multipotency of some avian neural crest cells. *Nature*. 335:161–164.

Bronner, M. 2015. Confetti Clarifies Controversy: Neural Crest Stem Cells Are Multipotent. *Cell Stem Cell*. 16:217–218.

Bruderer, M., R. Richards, M. Alini, and M. Stoddart. 2014. Role and Regulation of Runx2 in Osteogenesis. *Eur. Cells Mater.* 28:269–286.

Brugmann, S. 2004. Six1 promotes a placodal fate within the lateral neurogenic ectoderm by functioning as both a transcriptional activator and repressor. *Development*. 131:5871–5881.

Burke, A.C., C.E. Nelson, B.A. Morgan, and C.J. Tabin. 1995. Hox genes and the evolution of vertebrate axial morphology. *Development*. 121:333–346.

Burstyn-Cohen, T., J. Stanleigh, D. Sela-Donenfeld, and C. Kalcheim. 2004. Canonical Wnt activity regulates trunk neural crest delamination linking BMP/noggin signaling with G1/S transition. *Development*. 131:5327–5339.

Calloni, G.W., N.M. Le Douarin, and E. Dupin. 2009. High frequency of cephalic neural crest cells shows coexistence of neurogenic, melanogenic, and osteogenic differentiation capacities. *Proc. Natl. Acad. Sci. USA*. 106:8947–8952.

Calloni, G.W., C. Glavieux-Pardanaud, N.M. Le Douarin, and E. Dupin. 2007. Sonic Hedgehog promotes the development of multipotent neural crest progenitors endowed with both mesenchymal and neural potentials. *Proc. Natl. Acad. Sci. USA*. 104:19879–19884.

Cannon, B., and J. Nedergaard. 2004. Brown adipose tissue: function and physiological significance. *Physiol. Rev.* 84:277–359.

Cantile, M., A. Procino, M. D'Armiento, L. Cindolo, and C. Cillo. 2003. HOX gene network is involved in the transcriptional regulation of in vivo human adipogenesis. *J. Cell. Physiol.* 194:225–236.

Capellini, T.D., V. Zappavigna, and L. Selleri. 2011. Pbx homeodomain proteins: TALEnted regulators of limb patterning and outgrowth. *Dev. Dyn.* 240:1063–86.

Caplan, A.I., and D.G. Pechak. 1987. The cellular and molecular embryology of bone formation. *In* Bone and Mineral Research. W. Peck, editor. 117–183.

Carmona-Fontaine, C., H.K. Matthews, S. Kuriyama, M. Moreno, G.A. Dunn, M. Parsons, C.D. Stern, and R. Mayor. 2008. Contact inhibition of locomotion in vivo controls neural crest directional migration. *Nature*. 456:957–961.

Carmona-Fontaine, C., E. Theveneau, A. Tzekou, M. Tada, M. Woods, K.M. Page, M. Parsons, J.D. Lambris, and R. Mayor. 2011. Complement Fragment C3a Controls Mutual Cell Attraction during Collective Cell Migration. *Dev. Cell*. 21:1026–1037.

Carney, T.J., K.A. Dutton, E. Greenhill, M. Delfino-Machin, P. Dufourcq, P. Blader, and R.N. Kelsh. 2006. A direct role for Sox10 in specification of neural crest-derived sensory neurons. *Development*. 133:4619–4630.

Carroll, S. 1995. Homeotic genes and the evolution of arthropods and chordates. *Nature*. 376:479–485.

Cases, O., A. Perea-Gomez, D.P. Aguiar, A. Nykjaer, S. Amsellem, J. Chandellier, M. Umbhauer, S. Cereghini, M. Madsen, J. Collignon, P. Verroust, J.-F. Riou, S.E. Creuzet, and R. Kozyraki. 2013. Cubilin, a high affinity receptor for fibroblast growth factor 8, is required for cell survival in the developing vertebrate head. *J. Biol. Chem.* 288:16655–16670.

Cebra-Thomas, J.A., E. Betters, M. Yin, C. Plafkin, K. McDow, and S.F. Gilbert. 2007. Evidence that a late-emerging population of trunk neural crest cells forms the plastron bones in the turtle Trachemys scripta. *Evol. Dev.* 9:267–277.

Cebra-Thomas, J.A., A. Terrell, K. Branyan, S. Shah, R. Rice, L. Gyi, M. Yin, Y. Hu, G. Mangat, J. Simonet, E. Betters, and S.F. Gilbert. 2013. Late-emigrating trunk neural crest cells in turtle embryos generate an osteogenic ectomesenchyme in the plastron. *Dev. Dyn.* 242:1223–1235.

Cereijo, R.É.N., M. Giralt, and F. Villarroya. 2015. Thermogenic brown and beige/brite adipogenesis in humans. *Ann. Med.* 47:169–177.

Chai, Y., X. Jiang, Y. Ito, P. Bringas, J. Han, D.H. Rowitch, P. Soriano, a P. McMahon, and H.M. Sucov. 2000. Fate of the mammalian cranial neural crest during tooth and mandibular morphogenesis. *Development*. 127:1671–1679.

Chalpe, A.J., M. Prasad, A.J. Henke, and A.F. Paulson. 2010. Regulation of cadherin expression in the chicken neural crest by the Wnt/β-catenin signaling pathway. *Cell Adhes. Migr.* 4:431–438.

Chappell, J., and S. Dalton. 2013. Roles for MYC in the establishment and maintenance of pluripotency. *Cold Spring Harb. Perspect. Med.* 3:1–9.

Cheung, M. 2003. Neural crest development is regulated by the transcription factor Sox9. *Development*. 130:5681–5693.

Cheung, M., M.-C.C. Chaboissier, A. Mynett, E. Hirst, A. Schedl, and J. Briscoe. 2005. The transcriptional control of trunk neural crest induction, survival, and delamination. *Dev. Cell*. 8:179–192.

Chiang, C., Y. Litingtung, E. Lee, K.E. Young, J.L. Corden, H. Westphal, and P.A. Beachy. 1996. Cyclopia and defective axial patterning in mice lacking Sonic hedgehog gene function. *Nature*. 383:407–413.

Chibon, P. 1967. Nuclear labelling by tritiated thymidine of neural crest derivatives in the amphibian Urodele Pleurodeles waltlii Michah. *J. Embryol. Exp. Morph.* 18:343–358.

Chung, I.H., J. Han, J. Iwata, and Y. Chai. 2010. Msx1 and Dlx5 function synergistically to regulate frontal bone development. *Genesis*. 48:645–655.

Clark, K., G. Bender, B. Patrick Murray, K. Panfilio, S. Cook, R. Davis, K. Murnen, R.S. Tuan, and S.F. Gilbert. 2001. Evidence for the neural crest origin of turtle plastron bones. *Genesis*. 31:111–117.

Coelho-Aguiar, J.M., N.M. Le Douarin, and E. Dupin. 2013. Environmental factors unveil dormant developmental capacities in multipotent progenitors of the trunk neural crest.

Dev. Biol. 384:13–25.

Cohen, A.M., and I.R. Konigsberg. 1975. A clonal approach to the problem of neural crest determination. *Dev. Biol.* 46:262–280.

Collazo, A., M. Bronner-Fraser, and S. Fraser. 1993. Vital dye labelling of Xenopus laevis trunk neural crest reveals multipotency and novel pathways of migration. *Development*. 118:363–376.

Couly, G., P. Coltey, A. Eichmann, and N.M. Le Douarin. 1995. The angiogenic potentials of the cephalic mesoderm and the origin of brain and head blood vessels. *Mech. Dev.* 53:97–112.

Couly, G., S. Creuzet, S. Bennaceur, C. Vincent, and N.M. Le Douarin. 2002. Interactions between Hox-negative cephalic neural crest cells and the foregut endoderm in patterning the facial skeleton in the vertebrate head. *Development*. 1073:1061–1073.

Couly, G., A. Grapin-botton, P. Coltey, B. Ruhin, and N.M. Le Douarin. 1998. Determination of the identity of the derivatives of the cephalic neural crest : incompatibility between Hox gene expression and lower jaw development. *Development*. 3459:3445–3459.

Couly, G., a Grapin-Botton, P. Coltey, and N.M. Le Douarin. 1996. The regeneration of the cephalic neural crest, a problem revisited: the regenerating cells originate from the contralateral or from the anterior and posterior neural fold. *Development*. 122:3393–3407.

Couly, G.F., P.M. Coltey, and N.M. Le Douarin. 1992. The developmental fate of the cephalic mesoderm in quail-chick chimeras. *Development*. 114:1–15.

Couly, G.F., P.M. Coltey, and N.M. Le Douarin. 1993. The triple origin of skull in higher vertebrates: a study in quail-chick chimeras. *Development*. 117:409–429.

Cowherd, R.M., R.E. Lyle, C.P. Miller, and R.E. Mcgehee. 1997. Developmental profile of homeobox gene expression during 3T3-L1 adipogenesis. *Biochem. Biophys. Res. Commun.* 237:470–5.

Cox, S.G., H. Kim, A.T. Garnett, D.M. Medeiros, W. An, and J.G. Crump. 2012. An essential role of variant histone H3.3 for ectomesenchyme potential of the cranial neural crest. *PLoS Genet.* 8:1–16.

Creuzet, S., G. Couly, and N.M. Le Douarin. 2005a. Patterning the neural crest derivatives during development of the vertebrate head: insights from avian studies. *J. Anat.* 207:447–459.

Creuzet, S., G. Couly, C. Vincent, and N.M. Le Douarin. 2002. Negative effect of Hox gene expression on the development of the neural crest-derived facial skeleton. *Development*. 129:4301–4313.

Creuzet, S., B. Schuler, G. Couly, and N.M. Le Douarin. 2004. Reciprocal relationships between Fgf8 and neural crest cells in facial and forebrain development. *Proc. Natl. Acad. Sci. USA*. 101:4843–7.

Creuzet, S., C. Vincent, and G. Couly. 2005b. Neural crest derivatives in ocular and periocular structures. *Int. J. Dev. Biol.* 49:161–171.

Creuzet, S.E. 2009. Regulation of pre-otic brain development by the cephalic neural crest. *Proc. Natl. Acad. Sci. USA*. 106:15774–15779.

Csobonyeiova, M., S. Polak, R. Zamborsky, and L. Danisovic. 2017. iPS cell technologies and their prospect for bone regeneration and disease modeling: A mini review. *J. Adv. Res.* 8:321–327.

Cypess, A.M., A.P. White, C. Vernochet, T.J. Schulz, R. Xue, C.A. Sass, T.L. Huang, C. Roberts-Toler, L.S. Weiner, C. Sze, A.T. Chacko, L.N. Deschamps, L.M. Herder, N. Truchan, A.L. Glasgow, A.R. Holman, A. Gavrila, P.-O. Hasselgren, M.A. Mori, M. Molla, and Y.-H. Tseng. 2013. Anatomical localization, gene expression profiling and functional characterization of adult human neck brown fat. *Nat. Med.* 19:635–639.

Danielian, P.S., D. Muccino, D.H. Rowitch, S.K. Michael, and A.P. McMahon. 1998. Modification of gene activity in mouse embryos in utero by a tamoxifen-inducible form of Cre recombinase. *Curr. Biol.* 8:1323-S2.

Das, A., and J.G. Crump. 2012. Bmps and id2a act upstream of Twist1 to restrict ectomesenchyme potential of the cranial neural crest. *PLoS Genet.* 8:e1002710.

Dasen, J.S., J.-P. Liu, and T.M. Jessell. 2003. Motor neuron columnar fate imposed by sequential phases of Hox-c activity. *Nature*. 425:926–933.

David, N.B., D. Sapède, L. Saint-Etienne, C. Thisse, B. Thisse, C. Dambly-Chaudière, F.M. Rosa, and A. Ghysen. 2002. Molecular basis of cell migration in the fish lateral line: role of the chemokine receptor CXCR4 and of its ligand, SDF1. *Proc. Natl. Acad. Sci. USA*. 99:16297–16302.

Deckelbaum, R.A., G. Holmes, Z. Zhao, C. Tong, C. Basilico, and C.A. Loomis. 2012. Regulation of cranial morphogenesis and cell fate at the neural crest-mesoderm boundary by engrailed 1. *Development*. 139:1346–1358.

Delloye-Bourgeois, C., N. Rama, J. Brito, N. Le Douarin, and P. Mehlen. 2014. Sonic Hedgehog promotes the survival of neural crest cells by limiting apoptosis induced by the dependence receptor CDON during branchial arch development. *Biochem. Biophys. Res. Commun.* 452:655–660.

Delsuc, F., H. Brinkmann, D. Chourrout, and H. Philippe. 2006. Tunicates and not cephalochordates are the closest living relatives of vertebrates. *Nature*. 439:965–968.

Depew, M.J., J.K. Liu, J.E. Long, R. Presley, J.J. Meneses, R.A. Pedersen, and J.L. Rubenstein. 1999. Dlx5 regulates regional development of the branchial arches and sensory capsules. *Development*. 126:3831–3846.

Dobreva, G., M. Chahrour, M. Dautzenberg, L. Chirivella, B. Kanzler, I. Fari??as, G. Karsenty, and R. Grosschedl. 2006. SATB2 Is a Multifunctional Determinant of Craniofacial Patterning and Osteoblast Differentiation. *Cell*. 125:971–986.

Dollé, P., J.-C. Izpisúa-Belmonte, H. Falkenstein, A. Renucci, and D. Duboule. 1989. Coordinate expression of the murine Hox-5 complex homoeobox-containing genes during limb pattern formation. *Nature*. 342:767–772.

Donoghue, P.C.J., I.J. Sansom, and J.P. Downs. 2006. Early evolution of vertebrate skeletal tissues and cellular interactions, and the canalization of skeletal development. *J. Exp. Zool. B. Mol. Dev. Evol.* 306:278–94.

Dooley, D., P. Vidal, and S. Hendrix. 2014. Immunopharmacological intervention for successful neural stem cell therapy: New perspectives in CNS neurogenesis and repair. *Pharmacol. Ther.* 141:21–31.

Dottori, M., M.K. Gross, P. Labosky, and M. Goulding. 2001. The winged-helix transcription factor Foxd3 suppresses interneuron differentiation and promotes neural crest cell fate. *Development*. 128:4127–4138.

Le Douarin, N.M. 1969. Particularités du noyau interphasique chez la caille japonaise (Coturnix coturnix japonica). Utilisation de ces particularités comme “marquage biologique” dans les recherches sur les interactions tissulaires et les migrations cellulaires au cours de l’ont. *Bull. Biol. Fr. Belg.* 103:435–452.

Le Douarin, N.M. 1982. The Neural Crest. Cambridge, UK: Cambridge University Press.

Le Douarin, N.M., G. Couly, and S.E. Creuzet. 2012. The neural crest is a powerful regulator of pre-otic brain development. *Dev. Biol.* 366:74–82.

Le Douarin, N.M., S. Creuzet, G. Couly, and E. Dupin. 2004. Neural crest cell plasticity and its limits. *Development*. 131:4637–4650.

Le Douarin, N.M., and E. Dupin. 2012. The neural crest in vertebrate evolution. *Curr. Opin. Genet. Dev.* 22:381–9.

Le Douarin, N.M., and E. Dupin. 2014. The Neural Crest, a Fourth Germ Layer of the Vertebrate Embryo: Significance in Chordate Evolution. *In* Neural Crest Cells: Evolution, Development and Disease. P.A. Trainor, editor. Elsevier. 3–26.

Le Douarin, N.M., and C. Kalcheim. 1999. The Neural Crest. Second Edi. Cambridge University Press, New York. 472 pp.

Le Douarin, N.M., D. Renaud, M.A. Teillet, and G.H. Le Douarin. 1975. Cholinergic differentiation of presumptive adrenergic neuroblasts in interspecific chimeras after heterotopic transplantations. *Proc. Natl. Acad. Sci. USA*. 72:728–732.

Le Douarin, N.M., and M. Teillet. 1973. The migration of neural crest cells to the wall of the digestive tract in avian embryo. *J. Embryol. Exp. Morph.* 30:31–48.

Le Douarin, N.M., and M.-A.M. Teillet. 1974. Experimental Analysis of the Migration and Differentiation of Neuroblasts of the Autonomic Nervous System and of Neuroectodermal Mesenchymal Derivatives, using a Biological Cell Marking Technique. *Dev. Biol.* 41:162–184.

Duband, J.-L. 2010. Diversity in the molecular and cellular strategies of epithelium-to-mesenchyme transitions: Insights from the neural crest. *Cell Adh. Migr.* 4:458–482.

Dubaud, J., and J. Thiery. 1987. Distribution of laminin and collagens during avian neural crest development. *Development*. 10:461–478.

Duboule, D. 1994. Temporal colinearity and the phylotypic progression: a basis for the stability of a vertebrate Bauplan and the evolution of the morphologies through heterochrony. *Development*. Supplement:135–142.

Duboule, D., and P. Dollé. 1989. The structural and functional organization of the murine HOX gene family resembles that of Drosophila homeotic genes. *EMBO J.* 8:1497–1505.

Ducy, P. 2000. Cbfa1: A molecular switch in osteoblast biology. *Dev. Dyn.* 219:461–471.

Ducy, P., and G. Karsenty. 1995. Two distinct osteoblast-specific cis-acting elements control expression of a mouse osteocalcin gene. *Mol. Cell. Biol.* 15:1858–1869.

Ducy, P., R. Zhang, V. Geoffroy, A.L. Ridall, and G. Karsenty. 1997. Osf2/Cbfa1: A Transcriptional Activator of Osteoblast Differentiation. *Cell*. 89:747–754.

Dupin, E. 1984. Cell division in the ciliary ganglion of quail embryos in situ and after back-transplantation into the neural crest migration pathways of chick embryos. *Dev. Biol.* 105:288–299.

Dupin, E., A. Baroffio, C. Dulac, P. Cameron-Curry, and N.M. Le Douarin. 1990. Schwann-cell differentiation in clonal cultures of the neural crest, as evidenced by the anti-Schwann cell myelin protein monoclonal antibody. *Proc. Natl. Acad. Sci. USA*. 87:1119–1123.

Dupin, E., G.W. Calloni, and N.M. Le Douarin. 2010. The cephalic neural crest of amniote vertebrates is composed of a large majority of precursors endowed with neural, melanocytic, chondrogenic and osteogenic potentialities. *Cell Cycle*. 9:238–249.

Dupin, E., and J.M. Coelho-Aguiar. 2013. Isolation and differentiation properties of neural crest stem cells. *Cytometry. A*. 83:38–47.

Dupin, E., S. Creuzet, and N.M. Le Douarin. 2006. The contribution of the neural crest to the vertebrate body. *Adv. Exp. Med. Biol.* 589:96–119.

Dupin, E., and N.M. Le Douarin. 2014. The neural crest, A multifaceted structure of the vertebrates. *Birth Defects Res. Part C - Embryo Today Rev.* 102:187–209.

Dupin, E., C. Glavieux, P. Vaigot, and N.M. Le Douarin. 2000. Endothelin 3 induces the reversion of melanocytes to glia through a neural crest-derived glial-melanocytic progenitor. *Proc. Natl. Acad. Sci. USA*. 97:7882–7887.

Dupin, E., C. Real, C. Glavieux-Pardanaud, P. Vaigot, and N.M. Le Douarin. 2003. Reversal of developmental restrictions in neural crest lineages: transition from Schwann cells to glial-melanocytic precursors in vitro. *Proc. Natl. Acad. Sci. USA*. 100:5229–5233.

Dupin, E., and L. Sommer. 2012. Neural crest progenitors and stem cells: from early development to adulthood. *Dev. Biol.* 366:83–95.

Dyachuk, V., A. Furlan, M.K. Shahidi, M. Giovenco, N. Kaukua, C. Konstantinidou, V. Pachnis, F. Memic, U. Marklund, T. Muller, C. Birchmeier, K. Fried, P. Ernfors, and I. Adameyko. 2014. Parasympathetic neurons originate from nerve-associated peripheral glial progenitors. *Science*. 345:82–87.

Eisen, J.S., and J. a Weston. 1993. Development of the neural crest in the zebrafish. *Dev. Biol.* 159:50–59.

El-Helou, V., P.C. Beguin, J. Assimakopoulos, R. Clement, H. Gosselin, R. Brugada, A. Aumont, J. Biernaskie, L. Villeneuve, T.K. Leung, K.J.L. Fernandes, and A. Calderone. 2008. The rat heart contains a neural stem cell population; role in sympathetic sprouting and angiogenesis. *J. Mol. Cell. Cardiol.* 45:694–702.

Endo, Y., N. Osumi, and Y. Wakamatsu. 2002. Bimodal functions of Notch-mediated signaling are involved in neural crest formation during avian ectoderm development. *Development*. 129:863–873.

Erickson, C.A., T.D. Duong, and K.W. Tosney. 1992. Descriptive and experimental analysis of the dispersion of neural crest cells along the dorsolateral path and their entry into ectoderm in the chick embryo. *Dev. Biol.* 151:251–272.

Escot, S., C. Blavet, E. Faure, S. Zaffran, J.-L. Duband, and C. Fournier-Thibault. 2016. Disruption of CXCR4 signaling in pharyngeal neural crest cells causes DiGeorge syndrome-like malformations. *Development*. 143:582–588.

Escot, S., C. Blavet, S. Härtle, J.L. Duband, and C. Fournier-Thibault. 2013. Misregulation of

SDF1-CXCR4 signaling impairs early cardiac neural crest cell migration leading to conotruncal defects. *Circ. Res.* 113:505–516.

Espinosa-Medina, I., E. Outin, C. a Picard, Z. Chettouh, S. Dymecki, G.G. Consalez, E. Coppola, and J.-F. Brunet. 2014. Neurodevelopment. Parasympathetic ganglia derive from Schwann cell precursors. *Science*. 345:87–90.

Etchevers, H. 2011. Primary culture of chick, mouse or human neural crest cells. *Nat. Protoc.* 6:1568–1577.

Etchevers, H.C. 2014. Hiding in Plain Sight: Molecular Genetics Applied to Giant Congenital Melanocytic Nevi. *J. Invest. Dermatol.* 134:879–882.

Etchevers, H.C., J. Amiel, and S. Lyonnet. 2006. Molecular bases of human neurocristopathies. *Adv. Exp. Med. Biol.* 589:213–234.

Etchevers, H.C., C. Vincent, N.M. Le Douarin, and G.F. Couly. 2001. The cephalic neural crest provides pericytes and smooth muscle cells to all blood vessels of the face and forebrain. *Development*. 128:1059–1068.

Faure, S., M.A. Lee, T. Keller, P. ten Dijke, and M. Whitman. 2000. Endogenous patterns of TGFbeta superfamily signaling during early Xenopus development. *Development*. 127:2917–2931.

Faure, S., P. de Santa Barbara, D.J. Roberts, and M. Whitman. 2002. Endogenous Patterns of BMP Signaling during Early Chick Development. *Dev. Biol.* 244:44–65.

Fernandes, K.J.L., I.A. McKenzie, P. Mill, K.M. Smith, M. Akhavan, F. Barnabé-Heider, J. Biernaskie, A. Junek, N.R. Kobayashi, J.G. Toma, D.R. Kaplan, P.A. Labosky, V. Rafuse, C.-C. Hui, and F.D. Miller. 2004. A dermal niche for multipotent adult skin-derived precursor cells. *Nat. Cell Biol.* 6:1082–1093.

Fernández-Garre, P., L. Rodríguez-Gallardo, V. Gallego-Díaz, I.S. Alvarez, and L. Puelles. 2002. Fate map of the chicken neural plate at stage 4. *Development*. 129:2807–2822.

Ferronha, T., M.A. Rabadán, E. Gil-Guiñon, G. Le Dréau, C. de Torres, and E. Martí. 2013. LMO4 is an essential cofactor in the Snail2-mediated epithelial-to-mesenchymal transition of neuroblastoma and neural crest cells. *J. Neurosci.* 33:2773–2783.

Fleenor, S.J., and J. Begbie. 2014. Neural Crest Cell and Placode Interactions in Cranial PNS Development. *In* Neural Crest Cells: Evolution, Development and Disease. P.A. Trainor, editor. Elsevier. 153–165.

Fontaine-Perus, J.C., M. Chanconie, and N.M. Le Douarin. 1982. Differentiation of peptidergic neurones in quail-chick chimaeric embryos. *Cell Differ.* 11:183–193.

Forni, P.E., C. Taylor-Burds, V.S. Melvin, T. Williams, and S. Wray. 2011. Neural Crest and Ectodermal Cells Intermix in the Nasal Placode to Give Rise to GnRH-1 Neurons, Sensory Neurons, and Olfactory Ensheathing Cells. *J. Neurosci.* 31:6915–6927.

Gammill, L.S. 2006. Guidance of trunk neural crest migration requires neuropilin 2/semaphorin 3F signaling. *Development*. 133:99–106.

Gammill, L.S., C. Gonzalez, and M. Bronner-Fraser. 2007. Neuropilin 2/semaphorin 3F signaling is essential for cranial neural crest migration and trigeminal ganglion condensation. *Dev. Neurobiol.* 67:47–56.

Gans, C., and R.G. Northcutt. 1983. Neural Crest and the Origin of Vertebrates: A New Head.

Science. 220:268–273.

Garcez, R.C., N.M. Le Douarin, and S.E. Creuzet. 2014. Combinatorial activity of Six1-2-4 genes in cephalic neural crest cells controls craniofacial and brain development. *Cell. Mol. Life Sci.* 71:2149–2164.

Garcia-Castro, M.I., C. Marcelle, and M. Bronner-Fraser. 2002. Ectodermal Wnt function as a neural crest inducer. *Science*. 297:848–851.

Gaunt, S.J. 1988. Mouse homeobox gene transcripts occupy different but overlapping domains in embryonic germ layers and organs: a comparison of Hox-3.1 and Hox-1.5. *Development*. 103:135–144.

Gaunt, S.J., J.R. Miller, D.J. Powell, and D. Duboule. 1986. Homoeobox gene expression in mouse embryos varies with position by the primitive streak stage. *Nature*. 324:662–664.

Gendron-Maguire, M., M. Mallo, M. Zhang, and T. Gridley. 1993. Hoxa-2 mutant mice exhibit homeotic transformation of skeletal elements derived from cranial neural crest. *Cell*. 75:1317–1331.

Geoffroy, V., M. Kneissel, B. Fournier, A. Boyde, and P. Matthias. 2002. High Bone Resorption in Adult Aging Transgenic Mice Overexpressing Cbfa1/Runx2 in Cells of the Osteoblastic Lineage. *Mol. Cell. Biol.* 22:6222–6233.

El Ghouzzi, V., M. Le Merrer, F. Perrin-Schmitt, E. Lajeunie, P. Benit, D. Renier, P. Bourgeois, A.L. Bolcato-Bellemin, A. Munnich, and J. Bonaventure. 1997. Mutations of the TWIST gene in the Saethre-Chotzen syndrome. *Nat. Genet.* 15:42–46.

Gilbert, S.F. 2000. Developmental biology. Sinauer Associates. 749 pp.

Glimcher, M.J. 1981. The chemistry and biology of mineralized connective tissues. Elsevier.

Golub, E.E. 2011. Biomineralization and matrix vesicles in biology and pathology. *Semin Immunopathol*. 33:409–417.

Gordon, J.A.R., M.Q. Hassan, S. Saini, M. Montecino, A.J. van Wijnen, G.S. Stein, J.L. Stein, and J.B. Lian. 2010. Pbx1 represses osteoblastogenesis by blocking Hoxa10-mediated recruitment of chromatin remodeling factors. *Mol. Cell. Biol.* 30:3531–3541.

Grammatopoulos, G.A., E. Bell, L. Toole, A. Lumsden, and A.S. Tucker. 2000. Homeotic transformation of branchial arch identity after Hoxa2 overexpression. *Development*. 127:5355–5365.

Green, H., and O. Kehinde. 1976. Spontaneous heritable changes leading to increased adipose conversion in 3T3 cells. *Cell*. 7:105–113.

Green, H., and M. Meuth. 1974. An established pre-adipose cell line and its differentation in culture. *Cell*. 3:127–133.

Green, S. a., M. Simoes-Costa, and M.E. Bronner. 2015. Evolution of vertebrates as viewed from the crest. *Nature*. 520:474–482.

Grenier, J., M.A. Teillet, R. Grifone, R.G. Kelly, and D. Duprez. 2009. Relationship between neural crest cells and cranial mesoderm during head muscle development. *PLoS One*. 4:1–15.

Gross, S., Y. Krause, M. Wuelling, and A. Vortkamp. 2012. Hoxa11 and Hoxd11 Regulate Chondrocyte Differentiation Upstream of Runx2 and Shox2 in Mice. *PLoS One*. 7:e43553.

Groves, A.K., and C. LaBonne. 2014. Setting appropriate boundaries: Fate, patterning and competence at the neural plate border. *Dev. Biol.* 389:2–12.

Guillory, G., and M. Bronner-Fraser. 1986. An in vitro assay for neural crest cell migration through the somites. *J. Embryol. Exp. Morphol.* 98:85–97.

Haberland, M., M.H. Mokalled, R.L. Montgomery, and E.N. Olson. 2009. Epigenetic control of skull morphogenesis by histone deacetylase 8. *Genes Dev.* 23:1625–1630.

Hacker, A., and S. Guthrie. 1998. A distinct developmental programme for the cranial paraxial mesoderm in the chick embryo. *Development*. 125:3461–3472.

Haldin, C.E., and C. LaBonne. 2010. SoxE factors as multifunctional neural crest regulatory factors. *Int. J. Biochem. Cell Biol.* 42:441–444.

Hall, B. 2000. The neural crest as a fourth germ layer and vertebrates as quadroblastic not triploblastic. *Evol Dev.* 2:3–5.

Hall, B.K. 2009. The Neural Crest and Neural Crest Cells in Vertebrate Development and Evolution. Springer. 400 pp.

Hassan, M.Q., S. Saini, J.A.R. Gordon, A.J. Van Wijnen, M. Montecino, J.L. Stein, G.S. Stein, and J.B. Lian. 2009. Molecular Switches Involving Homeodomain Proteins, HOXA10 and RUNX2 Regulate Osteoblastogenesis. *Cells Tissues Organs*. 189:122–125.

Hassan, M.Q., R. Tare, S.H. Lee, M. Mandeville, B. Weiner, M. Montecino, A.J. van Wijnen, J.L. Stein, G.S. Stein, and J.B. Lian. 2007. HOXA10 controls osteoblastogenesis by directly activating bone regulatory and phenotypic genes. *Mol. Cell. Biol.* 27:3337–52.

Hattori, Y., N. Kanamoto, K. Kawano, H. Iwakura, M. Sone, M. Miura, A. Yasoda, N. Tamura, H. Arai, T. Akamizu, K. Nakao, and Y. Maitani. 2010. Molecular characterization of tumors from a transgenic mouse adrenal tumor model: Comparison with human pheochromocytoma. *Int. J. Oncol.* 37:695–705.

He, G., S. Tavella, K.P. Hanley, M. Self, G. Oliver, R. Grifone, N. Hanley, C. Ward, and N. Bobola. 2010. Inactivation of Six2 in mouse identifies a novel genetic mechanism controlling development and growth of the cranial base. *Dev. Biol.* 344:720–730.

Hirasawa, T., H. Nagashima, and S. Kuratani. 2013. The endoskeletal origin of the turtle carapace. *Nat. Commun.* 4:1–7.

His, W. 1868. Untersuchungen über die erste Anlage des Wirbeltierleibes. Die erste Entwicklung des Hühnchens. Vogel, Leipzig.

Hockman, D., A.J. Burns, G. Schlosser, K.P. Gates, B. Jevans, A. Mongera, S. Fisher, G. Unlu, E.W. Knapik, C.K. Kaufman, C. Mosimann, L.I. Zon, J.J. Lancman, P.D.S. Dong, H. Lickert, A.S. Tucker, and C.V. Baker. 2017. Evolution of the hypoxia-sensitive cells involved in amniote respiratory reflexes. *Elife*. 6:e21231.

Hojo, H., S. Ohba, X. He, L.P. Lai, and A.P. McMahon. 2016. Sp7/Osterix Is Restricted to Bone-Forming Vertebrates where It Acts as a Dlx Co-factor in Osteoblast Specification. *Dev. Cell*. 37:238–253.

Holleville, N., S. Matéos, M. Bontoux, K. Bollerot, and A.-H. Monsoro-Burq. 2007. Dlx5 drives Runx2 expression and osteogenic differentiation in developing cranial suture mesenchyme. *Dev. Biol.* 304:860–874.

Holleville, N., A. Quilhac, M. Bontoux, and A.-H. Monsoro-Burq. 2003. BMP signals regulate

Dlx5 during early avian skull development. *Dev. Biol.* 257:177–189.

Horstadius, S. 1950. The Neural Crest: Its Properties and Derivatives in the Light of Experimental Research. Oxford University Press, London.

Horton, W.A. 1993. Cartilage morphology. *In* Extracellular matrix and heritable disorders of connective tissue. P. Royce and B. Steinmann, editors. Liss, New York. 73–84.

Hrycaj, S.M., and D.M. Wellik. 2016. Hox genes and evolution. *F1000Research*. 5:859.

Hunt, P., M. Gulisano, M. Cook, M.-H. Sham, A. Faiella, D. Wilkinson, E. Boncinelli, and R. Krumlauf. 1991. A disctinct Hox Code for the branchial region of the vertebrate head. *Nature*. 353:861–864.

Ido, A., and K. Ito. 2006. Expression of chondrogenic potential of mouse trunk neural crest cells by FGF2 treatment. *Dev. Dyn.* 235:361–367.

Ikenouchi, J., M. Matsuda, M. Furuse, and S. Tsukita. 2003. Regulation of tight junctions during the epithelium-mesenchyme transition: direct repression of the gene expression of claudins/occludin by Snail. *J. Cell Sci.* 116:1959–1967.

Imai, T., R. Takakuwa, S. Marchand, E. Dentz, J.M. Bornert, N. Messaddeq, O. Wendling, M. Mark, B. Desvergne, W. Wahli, P. Chambon, and D. Metzger. 2004. Peroxisome proliferator-activated receptor gamma is required in mature white and brown adipocytes for their survival in the mouse. *Proc. Natl. Acad. Sci. USA*. 101:4543–4547.

Inada, M., T. Yasui, S. Nomura, S. Miyake, K. Deguchi, M. Himeno, M. Sato, H. Yamagiwa, T. Kimura, N. Yasui, T. Ochi, N. Endo, Y. Kitamura, T. Kishimoto, and T. Komori. 1999. Maturational disturbance of chondrocytes in Cbfa1-deficient mice. *Dev. Dyn.* 214:279–290.

Inoue, K., S. Ozaki, T. Shiga, K. Ito, T. Masuda, N. Okado, T. Iseda, S. Kawaguchi, M. Ogawa, S.-C. Bae, N. Yamashita, S. Itohara, N. Kudo, and Y. Ito. 2002. Runx3 controls the axonal projection of proprioceptive dorsal root ganglion neurons. *Nat. Neurosci.* 5:946–954.

Isenmann, S., A. Arthur, A.C.W. Zannettino, J.L. Turner, S. Songtao, C.A. Glackin, and S. Gronthos. 2009. TWIST family of basic helix-loop-helix transcription factors mediate human mesenchymal stem cell growth and commitment. *Stem Cells*. 27:2457–2468.

Ishikawa, S., and K. Ito. 2009. Plasticity and regulatory mechanisms of Hox gene expression in mouse neural crest cells. *Cell Tissue Res.* 337:381–391.

Ito, K., and M. Sieber-Blum. 1991. In vitro clonal analysis of quail cardiac neural crest development. *Dev. Biol.* 148:95–106.

Ito, K., and M. Sieber-Blum. 1993. Pluripotent and Developmentally restricted neural-crest derived cells in posterior visceral arches. *Dev. Biol.* 156:191–200.

Izpisúa-Belmonte, J.C., H. Falkenstein, P. Dollé, A. Renucci, and D. Duboule. 1991. Murine genes related to the Drosophila AbdB homeotic genes are sequentially expressed during development of the posterior part of the body. *EMBO J.* 10:2279–2289.

Janebodin, K., O. V. Horst, N. Ieronimakis, G. Balasundaram, K. Reesukumal, B. Pratumvinit, and M. Reyes. 2011. Isolation and characterization of neural crest-derived stem cells from dental pulp of neonatal mice. *PLoS One*. 6:e27526.

Jeffery, W.R., T. Chiba, F.R. Krajka, C. Deyts, N. Satoh, and J.S. Joly. 2008. Trunk lateral cells are neural crest-like cells in the ascidian Ciona intestinalis: Insights into the ancestry and

evolution of the neural crest. *Dev. Biol.* 324:152–160.

Jeon, E.J., K.Y. Lee, N.S. Choi, M.H. Lee, H.N. Kim, Y.H. Jin, H.M. Ryoo, J.Y. Choi, M. Yoshida, N. Nishino, B.C. Oh, K.S. Lee, H.L. Yong, and S.C. Bae. 2006. Bone morphogenetic protein-2 stimulates Runx2 acetylation. *J. Biol. Chem.* 281:16502–16511.

Jeong, J., J. Mao, T. Tenzen, A.H. Kottmann, and A.P. McMahon. 2004. Hedgehog signaling in the neural crest cells regulates the patterning and growth of facial primordia. *Genes Dev.* 18:937–951.

Jespersen, N.Z., T.J. Larsen, L. Peijs, S. Daugaard, P. Homøe, A. Loft, J. De Jong, N. Mathur, B. Cannon, J. Nedergaard, B.K. Pedersen, K. Møller, and C. Scheele. 2013. A classical brown adipose tissue mrna signature partly overlaps with brite in the supraclavicular region of adult humans. *Cell Metab.* 17:798–805.

Jia, L., L. Cheng, and J. Raper. 2005. Slit/Robo signaling is necessary to confine early neural crest cells to the ventral migratory pathway in the trunk. *Dev. Biol.* 282:411–421.

Jiang, X., S. Iseki, R.E. Maxson, H.M. Sucov, and G.M. Morriss-Kay. 2002. Tissue Origins and Interactions in the Mammalian Skull Vault. *Dev. Biol.* 241:106–116.

John, N., P. Cinelli, M. Wegner, and L. Sommer. 2011. Transforming growth factor β-mediated Sox10 suppression controls mesenchymal progenitor generation in neural crest stem cells. *Stem Cells*. 29:689–699.

Johnson, M. 1966. A radioautographic study of the migration and fate of cranial neural crest in the chick embryo. *Anat. Rec.* 156:143–156.

Johnston, M., A. Bhakdinaronk, and Y. Reid. 1973. An expanded role of the neural crest in oral and pharyngeal development. *Symp Oral Sens Percept.* 4:37–52.

Johnston, M.C. 1966. A radioautographic study of the migration and fate of cranial neural crest cells in the chick embryo. *Anat. Rec.* 156:143–155.

Joseph, N.M., Y. Mukouyama, J.T. Mosher, M. Jaegle, S.A. Crone, E.-L. Dormand, K.-F. Lee, D. Meijer, D.J. Anderson, and S.J. Morrison. 2004. Neural crest stem cells undergo multilineage differentiation in developing peripheral nerves to generate endoneurial fibroblasts in addition to Schwann cells. *Development*. 131:5599–5612.

Kague, E., M. Gallagher, S. Burke, M. Parsons, T. Franz-Odendaal, and S. Fisher. 2012. Skeletogenic Fate of Zebrafish Cranial and Trunk Neural Crest. *PLoS One*. 7:e47394.

Kalcheim, C., and T. Burstyn-Cohen. 2005. Early stages of neural crest ontogeny: Formation and regulation of cell delamination. *Int. J. Dev. Biol.* 49:105–116.

Kaltschmidt, B., C. Kaltschmidt, and D. Widera. 2012. Adult Craniofacial Stem Cells: Sources and Relation to the Neural Crest. *Stem Cell Rev. Reports*. 8:658–671.

Kamalia, N., C. a McCulloch, H.C. Tenebaum, and H. Limeback. 1992. Dexamethasone recruitment of self-renewing osteoprogenitor cells in chick bone marrow stromal cell cultures. *Blood*. 79:320–326.

Kanzler, B., S.J. Kuschert, Y.-H. Liu, and M. Mallo. 1998. Hoxa-2 restricts the chondrogenic domain and inhibits bone formation during development of the branchial area. *Development*. 125:2587–2597.

Karpinski, B.A., C. A. Bryan, E.M. Paronett, J.L. Baker, A. Fernandez, A. Horvath, T.M. Maynard, S.A. Moody, and A.S. LaMantia. 2016. A cellular and molecular mosaic establishes growth

and differentiation states for cranial sensory neurons. *Dev. Biol.* 415:228–241.

Karsenty, G., H.M. Kronenberg, and C. Settembre. 2009. Genetic Control of Bone Formation. *Annu. Rev. Cell Dev. Biol.* 25:629–648.

Karsenty, G., and E.F. Wagner. 2002. Reaching a genetic and molecular understanding of skeletal development. *Dev. Cell*. 2:389–406.

Kasemeier-Kulesa, J.C., R. McLennan, M.H. Romine, P.M. Kulesa, and F. Lefcort. 2010. CXCR4 Controls Ventral Migration of Sympathetic Precursor Cells. *J. Neurosci.* 30:13078–13088.

Kaucka, M., E. Ivashkin, D. Gyllborg, T. Zikmund, M. Tesarova, J. Kaiser, M. Xie, J. Petersen, V. Pachnis, S.K. Nicolis, T. Yu, P. Sharpe, E. Arenas, H. Brismar, H. Blom, H. Clevers, U. Suter, A.S. Chagin, K. Fried, A. Hellander, and I. Adameyko. 2016. Analysis of neural crest-derived clones reveals novel aspects of facial development. *Sci. Adv.* 2:e1600060.

Kaukua, N., M.K. Shahidi, C. Konstantinidou, V. Dyachuk, M. Kaucka, A. Furlan, Z. An, L. Wang, I. Hultman, L. Ährlund-Richter, H. Blom, H. Brismar, N.A. Lopes, V. Pachnis, U. Suter, H. Clevers, I. Thesleff, P. Sharpe, P. Ernfors, K. Fried, and I. Adameyko. 2014. Glial origin of mesenchymal stem cells in a tooth model system. *Nature*. 513:551–554.

Kawakami, K., S. Sato, H. Ozaki, and K. Ikeda. 2000. Six family genes--structure and function as transcription factors and their roles in development. *Bioessays*. 22:616–626.

Kelsh, R.N., M.L. Harris, S. Colanesi, and C.A. Erickson. 2009. Stripes and belly-spots -- a review of pigment cell morphogenesis in vertebrates. *Semin. Cell Dev. Biol.* 20:90–104.

Kerosuo, L., and M. Bronner-Fraser. 2012. What is bad in cancer is good in the embryo: Importance of EMT in neural crest development. *Semin. Cell Dev. Biol.* 23:320–332.

Kerosuo, L., and M.E. Bronner. 2016. cMyc Regulates the Size of the Premigratory Neural Crest Stem Cell Pool. *Cell Rep.* 17:2648–2659.

Kerosuo, L., S. Nie, R. Bajpai, and M.E. Bronner. 2015. Crestospheres: Long-Term Maintenance of Multipotent, Premigratory Neural Crest Stem Cells. *Stem Cell Reports*. 5:499–507.

Kessel, M., and P. Gruss. 1990. Murine developmental control genes. *Science*. 249:374–379.

Kessel, M., and P. Gruss. 1991. Homeotic transformations of murine vertebrae and concomitant alteration of Hox codes induced by retinoic acid. *Cell*. 67:89–104.

Keyte, A., and M.R. Hutson. 2012. The neural crest in cardiac congenital anomalies. *Differentiation*. 84:25–40.

Kimmel, C.B., C.T. Miller, and C.B. Moens. 2001. Specification and Morphogenesis of the Zebrafish Larval Head Skeleton. *Dev. Biol.* 233:239–257.

Kirby, M.L., T.F. Gale, and D.E. Stewart. 1983. Neural crest cells contribute to normal aorticopulmonary septation. *Science*. 220:1059–1061.

Kirby, M.L., and D.E. Stewart. 1983. Neural crest origin of cardiac ganglion cells in the chick embryo: Identification and extirpation. *Dev. Biol.* 97:433–443.

Kitazawa, T., K. Fujisawa, N. Narboux-Nême, Y. Arima, Y. Kawamura, T. Inoue, Y. Wada, T. Kohro, H. Aburatani, T. Kodama, K.S. Kim, T. Sato, Y. Uchijima, K. Maeda, S. Miyagawa-Tomita, M. Minoux, F.M. Rijli, G. Levi, Y. Kurihara, and H. Kurihara. 2015. Distinct effects of Hoxa2 overexpression in cranial neural crest populations reveal that the mammalian hyomandibular-ceratohyal boundary maps within the styloid process. *Dev. Biol.* 402:162–174.

Kochhar, A., D.J. Orten, J.L. Sorensen, S.M. Fischer, C.W.R.J. Cremers, W.J. Kimberling, and R.J.H. Smith. 2008. SIX1 mutation screening in 247 branchio-oto-renal syndrome families: A recurrent missense mutation associated with BOR. *Hum. Mutat.* 29:565.

Komori, T. 2010. Regulation of bone development and extracellular matrix protein genes by RUNX2. *Cell Tissue Res.* 339:189–195.

Komori, T., H. Yagi, S. Nomura, A. Yamaguchi, K. Sasaki, K. Deguchi, Y. Shimizu, R.. Bronson, Y.-H. Gao, M. Inada, M. Sato, R. Okamoto, Y. Kitamura, S. Yoshiki, and T. Kishimoto. 1997. Targeted Disruption of Cbfa1 Results in a Complete Lack of Bone Formation owing to Maturational Arrest of Osteoblasts. *Cell*. 89:755–764.

Köntges, G., and A. Lumsden. 1996. Rhombencephalic neural crest segmentation is preserved throughout craniofacial ontogeny. *Development*. 122:3229–3242.

Kos, R., M. V Reedy, R.L. Johnson, and C.A. Erickson. 2001. The winged-helix transcription factor FoxD3 is important for establishing the neural crest lineage and repressing melanogenesis in avian embryos. *Development*. 128:1467–1479.

Kozhemyakina, E., A.B. Lassar, and E. Zelzer. 2015. A pathway to bone: signaling molecules and transcription factors involved in chondrocyte development and maturation. *Development*. 142:817–831.

Krispin, S., E. Nitzan, Y. Kassem, and C. Kalcheim. 2010. Evidence for a dynamic spatiotemporal fate map and early fate restrictions of premigratory avian neural crest. *Development*. 137:585–595.

Kronenberg, H.M. 2003. Developmental regulation of the growth plate. *Nature*. 423:332–336.

Krull, C.E., R. Lansford, N.W. Gale, A. Collazo, C. Marcelle, G.D. Yancopoulos, S.E. Fraser, and M. Bronner-Fraser. 1997. Interactions of Eph-related receptors and ligands confer rostrocaudal pattern to trunk neural crest migration. *Curr. Biol.* 7:571–580.

Krumlauf, R. 1994. Hox genes in vertebrate development. *Cell*. 78:191–201.

Kulesa, P.M., and S.E. Fraser. 1998. Neural crest cell dynamics revealed by time-lapse video microscopy of whole embryo chick explant cultures. *Dev. Biol.* 204:327–344.

Kulesa, P.M., M.C. McKinney, and R. McLennan. 2013. Developmental imaging: the avian embryo hatches to the challenge. *Birth Defects Res. C. Embryo Today*. 99:121–33.

Kumar, J.P. 2009. The sine oculis homeobox (SIX) family of transcription factors as regulators of development and disease. *Cell. Mol. Life Sci.* 66:565–583.

Kuo, B.R., and C.A. Erickson. 2010. Regional differences in neural crest morphogenesis. *Cell Adh. Migr.* 4:567–585.

Kutejova, E., B. Engist, M. Mallo, B. Kanzler, and N. Bobola. 2005. Hoxa2 downregulates Six2 in the neural crest-derived mesenchyme. *Development*. 132:469–478.

Kutejova, E., B. Engist, M. Self, G. Oliver, P. Kirilenko, and N. Bobola. 2008. Six2 functions redundantly immediately downstream of Hoxa2. *Development*. 135:1463–1470.

Kwon, H.J., N. Bhat, E.M. Sweet, R.A. Cornell, and B.B. Riley. 2010. Identification of early requirements for preplacodal ectoderm and sensory organ development. *PLoS Genet.* 6:e1001133.

Laclef, C., G. Hamard, J. Demignon, E. Souil, C. Houbron, and P. Maire. 2003a. Altered myogenesis in Six1-deficient mice. *Development*. 130:2239–2252.

Laclef, C., and P. Maire. 2004. Redéploiement des gènes Six au cours de l'evolution. *Medecine/Sciences*. 20:1085–1090.

Laclef, C., E. Souil, J. Demignon, and P. Maire. 2003b. Thymus, kidney and craniofacial abnormalities in Six1 deficient mice. *Mech. Dev.* 120:669–679.

Lahav, R., E. Dupin, L. Lecoin, C. Glavieux, D. Champeval, C. Ziller, and N.M. Le Douarin. 1998. Endothelin 3 selectively promotes survival and proliferation of neural crest-derived glial and melanocytic precursors in vitro. *Proc. Natl. Acad. Sci. USA*. 95:14214–14219.

Langille, R.M., and B.K. Hall. 1988. Role of the neural crest in development of the trabeculae and branchial arches in embryonic sea lamprey, Petromyzon marinus. *Development*. 102:301–310.

Lecka-Czernik, B., I. Gubrij, E.J. Moerman, O. Kajkenova, D.A. Lipschitz, S.C. Manolagas, and R.L. Jilka. 1999. Inhibition of Osf2/Cbfa1 expression and terminal osteoblast differentiation by PPARγ2. *J. Cell. Biochem.* 74:357–371.

Lee, G., H. Kim, Y. Elkabetz, G. Al Shamy, G. Panagiotakos, T. Barberi, V. Tabar, L. Studer, G. Al Shamy, G. Panagiotakos, T. Barberi, V. Tabar, and L. Studer. 2007. Isolation and directed differentiation of neural crest stem cells derived from human embryonic stem cells. *Nat. Biotechnol.* 25:1468–1475.

Lee, M.H., Y.J. Kim, W.J. Yoon, J.I. Kim, B.G. Kim, Y.S. Hwang, J.M. Wozney, X.Z. Chi, S.C. Bae, K.Y. Choi, J.Y. Cho, J.Y. Choi, and H.M. Ryoo. 2005. Dlx5 specifically regulates Runx2 type II expression by binding to homeodomain-response elements in the Runx2 distal promoter. *J. Biol. Chem.* 280:35579–35587.

Lee, R.T.H., H. Nagai, Y. Nakaya, G. Sheng, P. a Trainor, J. a Weston, and J.P. Thiery. 2013. Cell delamination in the mesencephalic neural fold and its implication for the origin of ectomesenchyme. *Development*. 140:4890–4902.

Lee, Y.H., A.P. Petkova, E.P. Mottillo, and J.G. Granneman. 2012. In vivo identification of bipotential adipocyte progenitors recruited by β3-adrenoceptor activation and high-fat feeding. *Cell Metab.* 15:480–491.

Lefebvre, V., W. Huang, V.R. Harley, P.N. Goodfellow, and B. de Crombrugghe. 1997. SOX9 is a potent activator of the chondrocyte-specific enhancer of the pro alpha1(II) collagen gene. *Mol. Cell. Biol.* 17:2336–2346.

Lefterova, M.I., and M.A. Lazar. 2009. New developments in adipogenesis. *Trends Endocrinol. Metab.* 20:107–114.

Lengner, C.J., H.A. Steinman, J. Gagnon, T.W. Smith, J.E. Henderson, B.E. Kream, G.S. Stein, J.B. Lian, and S.N. Jones. 2006. Osteoblast differentiation and skeletal development are regulated by Mdm2-p53 signaling. *J. Cell Biol.* 172:909–921.

Lenton, K., A.W. James, A. Manu, S.A. Brugmann, D. Birker, E.R. Nelson, P. Leucht, J.A. Helms, and M.T. Longaker. 2011. Indian hedgehog positively regulates calvarial ossification and modulates bone morphogenetic protein signaling. *Genesis*. 49:784–796.

Leung, V.Y.L., B. Gao, K.K.H. Leung, I.G. Melhado, S.L. Wynn, T.Y.K. Au, N.W.F. Dung, J.Y.B. Lau, A.C.Y. Mak, D. Chan, and K.S.E. Cheah. 2011. SOX9 governs differentiation stage-specific gene expression in growth plate chondrocytes via direct concomitant transactivation and repression. *PLoS Genet.* 7:e1002356.

Levanon, D., D. Bettoun, C. Harris-Cerruti, E. Woolf, V. Negreanu, R. Eilam, Y. Bernstein, D.

Goldenberg, C. Xiao, M. Fliegauf, E. Kremer, F. Otto, O. Brenner, A. Lev-Tov, and Y. Groner. 2002. The Runx3 transcription factor regulates development and survival of TrkC dorsal root ganglia neurons. *EMBO J*. 21:3454–3463.

Lewis, E.B. 1978. A gene complex controlling segmentation in Drosophila. *Nature*. 276:565–570.

Li, H.-Y., E.H.M. Say, and X.-F. Zhou. 2007. Isolation and Characterization of Neural Crest Progenitors from Adult Dorsal Root Ganglia. *Stem Cells*. 25:2053–2065.

Lian, J.B., G.S. Stein, A.J. van Wijnen, J.L. Stein, M.Q. Hassan, T. Gaur, and Y. Zhang. 2012. MicroRNA control of bone formation and homeostasis. *Nat. Rev. Endocrinol.* 8:212–227.

Liang, H., D.M. Fekete, and O.M. Andrisani. 2011. CtBP2 downregulation during neural crest specification induces expression of Mitf and REST, resulting in melanocyte differentiation and sympathoadrenal lineage suppression. *Mol. Cell. Biol.* 31:955–970.

Lidell, M.E., M.J. Betz, O.D. Leinhard, M. Heglind, L. Elander, M. Slawik, T. Mussack, D. Nilsson, T. Romu, P. Nuutila, K.A. Virtanen, F. Beuschlein, A. Persson, M. Borga, and S. Enerbäck. 2013. Evidence for two types of brown adipose tissue in humans. *Nat. Med.* 19:631–634.

Le Lièvre, C.S., and N.M. Le Douarin. 1975. Mesenchymal derivatives of the neural crest: analysis of chimaeric quail and chick embryos. *J. Embryol. Exp. Morphol.* 34:125–154.

Lim, J., and J.P. Thiery. 2012. Epithelial-mesenchymal transitions: insights from development. *Development*. 139:3471–3486.

van Limborgh, J., S.H. Lieuw Kie Song, W. Been, and Limborgh JV. 1983. Cleft lip and palate due to deficiency of mesencephalic neural crest cells. *Cleft Palate J.* 20:251–259.

Linsenmayer, T.F., Q. Chen, E. Gibney, M.K. Gordon, J.K. Marchant, R. Mayne, and T.M. Schmid. 1991. Collagen types IX and X in the developing chick tibiotarsus: analyses of mRNAs and proteins. *Development*. 111:191–196.

Liu, J. a J., M.-H. Wu, C.H. Yan, B.K.H. Chau, H. So, A. Ng, A. Chan, K.S.E. Cheah, J. Briscoe, and M. Cheung. 2013. Phosphorylation of Sox9 is required for neural crest delamination and is regulated downstream of BMP and canonical Wnt signaling. *Proc. Natl. Acad. Sci. USA*. 110:2882–2887.

Liu, W., S. Toyosawa, T. Furuichi, N. Kanatani, C. Yoshida, Y. Liu, M. Himeno, S. Narai, A. Yamaguchi, and T. Komori. 2001. Overexpression of Cbfa1 in osteoblasts inhibits osteoblast maturation and causes osteopenia with multiple fractures. *J. Cell Biol.* 155:157–166.

Livet, J., T.A. Weissman, H. Kang, R.W. Draft, J. Lu, R.A. Bennis, J.R. Sanes, and J.W. Lichtman. 2007. Transgenic strategies for combinatorial expression of fluorescent proteins in the nervous system. *Nature*. 450:56–62.

Loring, J.F., and C.A. Erickson. 1987. Neural crest cell migratory pathways in the trunk of the chick embryo. *Dev. Biol.* 121:220–236.

Maes, C., T. Kobayashi, M.K. Selig, S. Torrekens, S.I. Roth, S. Mackem, G. Carmeliet, and H.M. Kronenberg. 2010. Osteoblast precursors, but not mature osteoblasts, move into developing and fractured bones along with invading blood vessels. *Dev. Cell*. 19:329–344.

Mallo, M., D.M. Wellik, and J. Deschamps. 2010. Hox genes and regional patterning of the vertebrate body plan. *Dev. Biol.* 344:7–15.

Mann, R.S., K.M. Lelli, and R. Joshi. 2009. Hox specificity unique roles for cofactors and collaborators. *Curr. Top. Dev. Biol.* 88:63–101.

Masaki, T., J. Qu, J. Cholewa-Waclaw, K. Burr, R. Raaum, and A. Rambukkana. 2013. Reprogramming adult Schwann cells to stem cell-like cells by leprosy bacilli promotes dissemination of infection. *Cell*. 152:51–67.

Massip, L., F. Ectors, P. Deprez, M. Maleki, C. Behets, B. Lengele, P. Delahaut, J. Picard, and R. Rezsohazy. 2007. Expression of Hoxa2 in cells entering chondrogenesis impairs overall cartilage development. *Differentiation*. 75:256–267.

Matsubara, T., K. Kida, A. Yamaguchi, K. Hata, F. Ichida, H. Meguro, H. Aburatani, R. Nishimura, and T. Yoneda. 2008. BMP2 regulates osterix through Msx2 and Runx2 during osteoblast differentiation. *J. Biol. Chem.* 283:29119–29125.

Matsuoka, T., P.E. Ahlberg, N. Kessaris, P. Iannarelli, U. Dennehy, W.D. Richardson, A.P. McMahon, and G. Koentges. 2005. Neural crest origins of the neck and shoulder. *Nature*. 436:347–355.

Mayor, R., N. Guerrero, and C. Martínez. 1997. Role of FGF and noggin in neural crest induction. *Dev. Biol.* 189:1–12.

McCauley, D.W., and M. Bronner-Fraser. 2003. Neural crest contributions to the lamprey head. *Development*. 130:2317–2327.

McGinnis, W., and R. Krumlauf. 1992. Homeobox genes and axial patterning. *Cell*. 68:283–302.

McGonnell, I.M., and A. Graham. 2002. Trunk Neural Crest Has Skeletogenic Potential. *Curr. Biol.* 12:767–771.

McKeown, S.J., D.F. Newgreen, and P.G. Farlie. 2005. Dlx2 over-expression regulates cell adhesion and mesenchymal condensation in ectomesenchyme. *Dev. Biol.* 281:22–37.

McKinney, M.C., K. Fukatsu, J. Morrison, R. McLennan, M.E. Bronner, and P.M. Kulesa. 2013. Evidence for dynamic rearrangements but lack of fate or position restrictions in premigratory avian trunk neural crest. *Development*. 140:820–830.

Merrill, A.E., E.G. Bochukova, S.M. Brugger, M. Ishii, D.T. Pilz, S.A. Wall, K.M. Lyons, A.O.M. Wilkie, and R.E. Maxson. 2006. Cell mixing at a neural crest-mesoderm boundary and deficient ephrin-Eph signaling in the pathogenesis of craniosynostosis. *Hum. Mol. Genet.* 15:1319–1328.

Metcalf, D., S. Glaser, S. Mifsud, L. Di Rago, and L. Robb. 2007. The preleukemic state of mice reconstituted with Mixl1-transduced marrow cells. *Proc. Natl. Acad. Sci. USA*. 104:20013–20018.

Meulemans, D., and M. Bronner-Fraser. 2004. Gene-regulatory interactions in neural crest evolution and development. *Dev. Cell*. 7:291–299.

Mezentseva, N. V, J.S. Kumaratilake, and S.A. Newman. 2008. The brown adipocyte differentiation pathway in birds: An evolutionary road not taken. *BMC Biol.* 6:17.

Milet, C., and A.H. Monsoro-Burq. 2012. Neural crest induction at the neural plate border in vertebrates. *Dev. Biol.* 366:22–33.

Minoux, M., S. Holwerda, A. Vitobello, T. Kitazawa, H. Kohler, M.B. Stadler, and F.M. Rijli. 2017. Gene bivalency at Polycomb domains regulates cranial neural crest positional identity. *Science*. 355:eaal2913.

Minoux, M., and F.M. Rijli. 2010. Molecular mechanisms of cranial neural crest cell migration and patterning in craniofacial development. *Development*. 137:2605–2621.

Mongera, A., and C. Nüsslein-Volhard. 2013. Scales of fish arise from mesoderm. *Curr. Biol.* 23:338–9.

Mongera, A., A.P. Singh, M.P. Levesque, Y.-Y. Chen, P. Konstantinidis, and C. Nusslein-Volhard. 2013. Genetic lineage labeling in zebrafish uncovers novel neural crest contributions to the head, including gill pillar cells. *Development*. 140:916–925.

Monsoro-Burq, A.-H. 2003. Neural crest induction by paraxial mesoderm in Xenopus embryos requires FGF signals. *Development*. 130:3111–3124.

Monsoro-Burq, A.H. 2005. Sclerotome development and morphogenesis: When experimental embryology meets genetics. *Int. J. Dev. Biol.* 49:301–308.

Monteiro, M.C., M. Sanyal, M.L. Cleary, C. Sengenès, A. Bouloumè, C. Dani, and N. Billon. 2011. PBX1: A novel stage-specific regulator of adipocyte development. *Stem Cells*. 29:1837–1848.

Moore, R., E. Theveneau, S. Pozzi, P. Alexandre, J. Richardson, A. Merks, M. Parsons, J. Kashef, C. Linker, and R. Mayor. 2013. Par3 controls neural crest migration by promoting microtubule catastrophe during contact inhibition of locomotion. *Development*. 140:4763–4775.

Moreno-Bueno, G., F. Portillo, and A. Cano. 2008. Transcriptional regulation of cell polarity in EMT and cancer. *Oncogene*. 27:6958–6969.

Mori-Akiyama, Y., H. Akiyama, D.H. Rowitch, and B. de Crombrugghe. 2003. Sox9 is required for determination of the chondrogenic cell lineage in the cranial neural crest. *Proc. Natl. Acad. Sci. USA*. 100:9360–9365.

Morrison, S.J., P.M. White, C. Zock, and D.J. Anderson. 1999. Prospective Identification, Isolation by Flow Cytometry, and In Vivo Self-Renewal of Multipotent Mammalian Neural Crest Stem Cells. *Cell*. 96:737–749.

Morriss-Kay, G.M., and A.O.M. Wilkie. 2005. Growth of the normal skull vault and its alteration in craniosynostosis: insights from human genetics and experimental studies. *J. Anat.* 207:637–653.

Mundell, N. a, and P. a Labosky. 2011. Neural crest stem cell multipotency requires Foxd3 to maintain neural potential and repress mesenchymal fates. *Development*. 138:641–652.

Mundt, E., and M.D. Bates. 2010. Genetics of Hirschsprung disease and anorectal malformations. *Semin. Pediatr. Surg.* 19:107–117.

Nagoshi, N., S. Shibata, Y. Kubota, M. Nakamura, Y. Nagai, E. Satoh, S. Morikawa, Y. Okada, Y. Mabuchi, H. Katoh, S. Okada, K. Fukuda, T. Suda, Y. Matsuzaki, Y. Toyama, and H. Okano. 2008. Ontogeny and Multipotency of Neural Crest-Derived Stem Cells in Mouse Bone Marrow, Dorsal Root Ganglia, and Whisker Pad. *Cell Stem Cell*. 2:392–403.

Nakamura, H., and C.S. Ayer-le Lièvre. 1982. Mesectodermal capabilities of the trunk neural crest of birds. *J Embryol Exp Morphol*. 70:1–18.

Nakashima, K., and B. De Crombrugghe. 2003. Transcriptional mechanisms in osteoblast differentiation and bone formation. *Trends Genet.* 19:458–466.

Nakashima, K., X. Zhou, G. Kunkel, Z. Zhang, J.M. Deng, R.R. Behringer, and B. De

Crombrugghe. 2002. The novel zinc finger-containing transcription factor Osterix is required for osteoblast differentiation and bone formation. *Cell*. 108:17–29.

Narita, Y., and F.M. Rijli. 2009. Hox genes in neural patterning and circuit formation in the mouse hindbrain. *Curr. Top. Dev. Biol.* 88:139–67.

Neilson, K.M., F. Pignoni, B. Yan, and S.A. Moody. 2010. Developmental expression patterns of candidate cofactors for vertebrate six family transcription factors. *Dev Dyn*. 239:3446–3466.

Neufeld, S.J., F. Wang, and J. Cobb. 2014. Genetic Interactions Between Shox2 and Hox Genes During the Regional Growth and Development of the Mouse Limb. *Genetics*. 198:1117–1126.

Newgreen, D., and J. Thiery. 1980. Fibronectin in early avian embryos: synthesis and distribution along the migration pathways of neural crest cells. *Cell Tissue Res.* 211:269–291.

Nguyen, V.H., B. Schmid, J. Trout, S.A. Connors, M. Ekker, and M.C. Mullins. 1998. Ventral and Lateral Regions of the Zebrafish Gastrula, Including the Neural Crest Progenitors, Are Established by a bmp2b/swirl Pathway of Genes. *Dev. Biol.* 199:93–110.

Nieto, M.A., M.G. Sargent, D.G. Wilkinson, and J. Cooke. 1994. Control of Cell Behavior During Vertebrate Development By Slug, a Zinc-Finger Gene. *Science*. 264:835–839.

Nitzan, E., E.R. Pfaltzgraff, P.A. Labosky, and C. Kalcheim. 2013. Neural crest and Schwann cell progenitor-derived melanocytes are two spatially segregated populations similarly regulated by Foxd3. *Proc. Natl. Acad. Sci. USA*. 110:12709–12714.

Noden, D.M. 1983. The embryonic origins of avian cephalic and cervical muscles and associated connective tissues. *Am. J. Anat.* 168:257–276.

Noden, D.M., and P.A. Trainor. 2005. Relations and interactions between cranial mesoderm and neural crest populations. *J. Anat.* 207:575–601.

Northcutt, R.G., and C. Gans. 1983. The genesis of neural crest and epidermal placodes: a reinterpretation of vertebrate origins. *Q. Rev. Biol.* 58:1–28.

Oka, K., S. Oka, R. Hosokawa, P. Bringas, H.C. Brockhoff, K. Nonaka, and Y. Chai. 2008. TGF-β mediated Dlx5 signaling plays a crucial role in osteo-chondroprogenitor cell lineage determination during mandible development. *Dev. Biol.* 321:303–309.

Osborne, N.J., J. Begbie, J.K. Chilton, H. Schmidt, and B.J. Eickholt. 2005. Semaphorin/neuropilin signaling influences the positioning of migratory neural crest cells within the hindbrain region of the chick. *Dev. Dyn.* 232:939–949.

Osório, L., M.A. Teillet, I. Palmeirim, and M. Catala. 2009. Neural crest ontogeny during secondary neurulation: A gene expression pattern study in the chick embryo. *Int. J. Dev. Biol.* 53:641–648.

Otto, F., and A.P. Thornell. 1997. Cbfa1, a Candidate Gene for Cleidocranial Dysplasia Syndrome, Is Essential for Osteoblast Differentiation and Bone Development. *Cell*. 89:765–771.

Ozaki, H., K. Nakamura, J.I. Funahashi, K. Ikeda, G. Yamada, H. Tokano, H. Okamura, K. Kitamura, S. Muto, H. Kotaki, K. Sudo, R. Horai, Y. Iwakura, and K. Kawakami. 2004. Six1 controls patterning of the mouse otic vesicle. *Development*. 131:551–562.

Pardal, R., P. Ortega-Sáenz, R. Durán, and J. López-Barneo. 2007. Glia-like Stem Cells Sustain Physiologic Neurogenesis in the Adult Mammalian Carotid Body. *Cell*. 131:364–377.

Partanen, J., L. Schwartz, and J. Rossant. 1998. Opposite phenotypes of hypomorphic and Y766 phosphorylation site mutations reveal a function for Fgfr1 in anteroposterior patterning of mouse embryos. *Genes Dev.* 12:2332–2344.

Pasqualetti, M., M. Ori, I. Nardi, and F.M. Rijli. 2000. Ectopic Hoxa2 induction after neural crest migration results in homeosis of jaw elements in Xenopus. *Development*. 127:5367–5378.

Passos-Bueno, M.R., C.C. Ornelas, and R.D. Fanganiello. 2009. Syndromes of the first and second pharyngeal arches: A review. *Am. J. Med. Genet. Part A*. 149:1853–1859.

Perris, R., and D. Perissinotto. 2000. Role of the extracellular matrix during neural crest cell migration. *Mech. Dev.* 95:3–21.

Petersen, J., and I. Adameyko. 2017. Nerve-associated neural crest: peripheral glial cells generate multiple fates in the body. *Curr. Opin. Genet. Dev.* 45:10–14.

Petiot, A., P. Ferretti, A.J. Copp, and C.-T.J. Chan. 2002. Induction of chondrogenesis in neural crest cells by mutant fibroblast growth factor receptors. *Dev. Dyn.* 224:210–221.

Philippidou, P., and J.S.S. Dasen. 2013. Hox Genes: Choreographers in Neural Development, Architects of Circuit Organization. *Neuron*. 80:12–34.

Pieper, M., K. Ahrens, E. Rink, A. Peter, and G. Schlosser. 2012. Differential distribution of competence for panplacodal and neural crest induction to non-neural and neural ectoderm. *Development*. 139:1175–1187.

Platt, J.B. 1893. Ectodermic origin of the cartilages of the head. *Anat. Anz.* 8:506–509.

Platt, J.B. 1897. The development of the cartilaginous skull and of the branchial and hypoglossal musculature in Necturus. *Morphol. Jahrb.* 25:377–464.

Poole, A.R. 1991. The growth plate: Cellular physiology, cartilage assembly, and mineralization. *In* Cartilage: Molecular Aspects. B. Hall and S. Newman, editors. 179–211.

Powell, D.R., A.J. Blasky, S.G. Britt, and K.B. Artinger. 2013. Riding the crest of the wave : parallels between the neural transition and migration. *WIREs Syst BiolMed*. 5:511–522.

Prasad, M.S., T. Sauka-Spengler, and C. LaBonne. 2012. Induction of the neural crest state: control of stem cell attributes by gene regulatory, post-transcriptional and epigenetic interactions. *Dev. Biol.* 366:10–21.

Prince, V., and A. Lumsden. 1994. Hoxa-2 expression in normal and transposed rhombomeres: independent regulation in the neural tube and neural crest. *Development*. 120:911–923.

Puelles, L., and J.L. Rubenstein. 1993. Expression patterns of homeobox and other putative regulatory genes in the embryonic mouse forebrain suggest a neuromeric organization. *Trends Neurosci.* 16:472–479.

Raible, D.W., and J.S. Eisen. 1994. Restriction of neural crest cell fate in the trunk of the embryonic zebrafish. *Development*. 120:495–503.

Raven, C.P. 1937. Experiments on the origin of the sheath cells and sympathetic neuroblasts in Amphibia. *J. Comp. Neurol.* 67:221–240.

Real, C., C. Glavieux-Pardanaud, N.M. Le Douarin, and E. Dupin. 2006. Clonally cultured differentiated pigment cells can dedifferentiate and generate multipotent progenitors

with self-renewing potential. *Dev. Biol.* 300:656–69.

Real, C., C. Glavieux-Pardanaud, P. Vaigot, N. Le-Douarin, and E. Dupin. 2005. The instability of the neural crest phenotypes: Schwann cells can differentiate into myofibroblasts. *Int. J. Dev. Biol.* 49:151–159.

Reynolds, B.A., and S. Weiss. 1992. Nervous System Generation of Neurons and Astrocytes from Isolated Cells of the Adult Mammalian Central Nervous System. *Science*. 255:1707–1710.

Richardson, J., A. Gauert, L. Briones Montecinos, L. Fanlo, Z.M. Alhashem, R. Assar, E. Marti, A. Kabla, S. Härtel, and C. Linker. 2016. Leader Cells Define Directionality of Trunk, but Not Cranial, Neural Crest Cell Migration. *Cell Rep.* 15:2076–2088.

Rickmann, M., J.W. Fawcett, and R.J. Keynes. 1985. The migration of neural crest cells and the growth of motor axons through the rostral half of the chick somite. *J. Embryol. Exp. Morphol.* 90:437–55.

Rijli, F.M., M. Mark, S. Lakkaraju, A. Dierich, P. Dollé, and P. Chambon. 1993. A homeotic transformation is generated in the rostral branchial region of the head by disruption of Hoxa-2, which acts as a selector gene. *Cell*. 75:1333–1349.

Rinon, A., S. Lazar, H. Marshall, S. Büchmann-Møller, A. Neufeld, H. Elhanany-Tamir, M.M. Taketo, L. Sommer, R. Krumlauf, and E. Tzahor. 2007. Cranial neural crest cells regulate head muscle patterning and differentiation during vertebrate embryogenesis. *Development*. 134:3065–3075.

Roellig, D., J. Tan-Cabugao, S. Esaian, and M.E. Bronner. 2017. Dynamic transcriptional signature and cell fate analysis reveals plasticity of individual neural plate border cells. *Elife*. 6:1–24.

Rosen, E.D., P. Sarraf, A.E. Troy, G. Bradwin, K. Moore, D.S. Milstone, B.M. Spiegelman, and R.M. Mortensen. 1999. PPARγ is required for the differentiation of adipose tissue in vivo and in vitro. *Mol Cell*. 4:611–617.

Rosenwald, M., A. Perdikari, T. Rülicke, and C. Wolfrum. 2013. Bi-directional interconversion of brite and white adipocytes. *Nat. Cell Biol.* 15:659–667.

Rothman, T.P., N.M. Le Douarin, J.C. Fontaine-Pérus, and M.D. Gershon. 1990. Developmental potential of neural crest-derived cells migrating from segments of developing quail bowel back-grafted into younger chick host embryos. *Development*. 109:411–423.

Rovasio, R.A., A. Delouvee, K.M. Yamada, R. Timpl, and J.P. Thiery. 1983. Neural crest cell migration: requirements for exogenous fibronectin and high cell density. *J. Cell Biol.* 96:462–473.

Ruf, R.G., P.-X. Xu, D. Silvius, E.A. Otto, F. Beekmann, U.T. Muerb, S. Kumar, T.J. Neuhaus, M.J. Kemper, R.M. Raymond, P.D. Brophy, J. Berkman, M. Gattas, V. Hyland, E.-M. Ruf, C. Schwartz, E.H. Chang, R.J.H. Smith, C.A. Stratakis, D. Weil, C. Petit, and F. Hildebrandt. 2004. SIX1 mutations cause branchio-oto-renal syndrome by disruption of EYA1-SIX1-DNA complexes. *Proc. Natl. Acad. Sci. USA*. 101:8090–8095.

Rux, D.R., J.Y. Song, I.T. Swinehart, K.M. Pineault, A.J. Schlientz, K.G. Trulik, S.A. Goldstein, K.M. Kozloff, D. Lucas, and D.M. Wellik. 2016. Regionally Restricted Hox Function in Adult Bone Marrow Multipotent Mesenchymal Stem/Stromal Cells. *Dev. Cell*. 39:653–666.

Rux, D.R., and D.M. Wellik. 2016. Hox genes in the adult skeleton: Novel functions beyond

embryonic development. *Dev. Dyn.* 246:310–317.

Saarela, S., J.S. Keith, E. Hohtola, and P. Trayhurn. 1991. Is the “mammalian” brown fat-specific mitochondrial uncoupling protein present in adipose tissues of birds? *Comp. Biochem. Physiol. - Part B Biochem.* 100:45–49.

Sambasivan, R., S. Kuratani, and S. Tajbakhsh. 2011. An eye on the head: the development and evolution of craniofacial muscles. *Development*. 138:2401–2415.

Sansom, I.J., and P.C.. D.G. Albanesi. 2005. Histology and affinity of the earliest armoured vertebrate. *Biol Lett.* 1:446–449.

Sansom, I.J., M.P. Smith, H.A. Armstrong, and M.M. Smith. 1992. Presence of the earliest vertebrate hard tissue in conodonts. *Science*. 256:1308–1311.

Sarjeant, K., and J.M. Stephens. 2012. Adipogenesis. *Cold Spring Harb Perspect Biol*. 4:a008417.

Sarkar, S., A. Petiot, A. Copp, P. Ferretti, and P. Thorogood. 2001. FGF2 promotes skeletogenic differentiation of cranial neural crest cells. *Development*. 128:2143–2152.

Sato, M., E. Morii, T. Komori, H. Kawahata, M. Sugimoto, K. Terai, H. Shimizu, T. Yasui, H. Ogihara, N. Yasui, T. Ochi, Y. Kitamura, Y. Ito, and S. Nomura. 1998. Transcriptional regulation of osteopontin gene in vivo by PEBP2alphaA/CBFA1 and ETS1 in the skeletal tissues. *Oncogene*. 17:1517–1525.

Sato, S., K. Ikeda, G. Shioi, K. Nakao, H. Yajima, and K. Kawakami. 2012. Regulation of Six1 expression by evolutionarily conserved enhancers in tetrapods. *Dev. Biol.* 368:95–108.

Sato, S., K. Ikeda, G. Shioi, H. Ochi, H. Ogino, H. Yajima, and K. Kawakami. 2010. Conserved expression of mouse Six1 in the pre-placodal region (PPR) and identification of an enhancer for the rostral PPR. *Dev. Biol.* 344:158–171.

Sato, T. 2005. Neural crest determination by co-activation of Pax3 and Zic1 genes in Xenopus ectoderm. *Development*. 132:2355–2363.

Sato, Y., T. Kasai, S. Nakagawa, K. Tanabe, T. Watanabe, K. Kawakami, and Y. Takahashi. 2007. Stable integration and conditional expression of electroporated transgenes in chicken embryos. *Dev. Biol.* 616–624.

Sauka-Spengler, T., and M. Barembaum. 2008. Gain- and loss-of-function approaches in the chick embryo. *Methods Cell Biol.* 87:237–256.

Sauka-Spengler, T., and M. Bronner-Fraser. 2008. A gene regulatory network orchestrates neural crest formation. *Nat. Rev. Mol. Cell Biol.* 9:557–68.

Scherer, P.E., S. Williams, M. Fogliano, G. Baldini, and H.F. Lodish. 1995. A novel serum protein similar to C1q, produced exclusively in adipocytes. *J. Biol. Chem.* 270:26746–26749.

Schilling, T.F., and C.B. Kimmel. 1994. Segment and cell type lineage restrictions during pharyngeal arch development in the zebrafish embryo. *Development*. 120:483–494.

Schlosser, G. 2010. Making Senses. Development of Vertebrate Cranial Placodes. *Int. Rev. Cell Mol. Biol.* 283:129–234.

Schlosser, G., and K. Ahrens. 2004. Molecular anatomy of placode development in Xenopus laevis. *Dev. Biol.* 271:439–466.

Schmidt, J., N. Piekarski, and L. Olsson. 2013. Cranial muscles in amphibians: Development, novelties and the role of cranial neural crest cells. *J. Anat.* 222:134–146.

Schmidt, K., T. Schinke, M. Haberland, M. Priemel, A.F. Schilling, C. Mueldner, J.M. Rueger, E. Sock, M. Wegner, and M. Amling. 2005. The high mobility group transcription factor Sox8 is a negative regulator of osteoblast differentiation. *J. Cell Biol.* 168:899–910.

Schwarz, D., S. Varum, M. Zemke, A. Schöler, A. Baggiolini, K. Draganova, H. Koseki, D. Schübeler, and L. Sommer. 2014. Ezh2 is required for neural crest-derived cartilage and bone formation. *Development*. 141:867–877.

Scott, M.P. 1992. Vertebrate homeobox gene nomenclature. *Cell*. 71:551–553.

Seifert, A., D.F. Werheid, S.M. Knapp, and E. Tobiasch. 2015. Role of Hox genes in stem cell differentiation. *World J. Stem Cells*. 7:583–595.

Sela-Donenfeld, D., and C. Kalcheim. 1999. Regulation of the onset of neural crest migration by coordinated activity of BMP4 and Noggin in the dorsal neural tube. *Development*. 126:4749–4762.

Sela-Donenfeld, D., and C. Kalcheim. 2000. Inhibition of noggin expression in the dorsal neural tube by somitogenesis: a mechanism for coordinating the timing of neural crest emigration. *Development*. 127:4845–4854.

Selleck, M. a, and M. Bronner-Fraser. 1995. Origins of the avian neural crest: the role of neural plate-epidermal interactions. *Development*. 121:525–538.

Semba, I., K. Nonaka, I. Takahashi, K. Takahashi, R. Dashner, L. Shum, G.H. Nuckolls, and H.C. Slavkin. 2000. Positionally-dependent chondrogenesis induced by BMP4 is co-regulated by Sox9 and Msx2. *Dev. Dyn.* 217:401–414.

Serbedzija, G.N., M. Bronner-Fraser, and S.E. Fraser. 1989. A vital dye analysis of the timing and pathways of avian trunk neural crest cell migration. *Development*. 106:809–816.

Serbedzija, G.N., M. Bronner-Fraser, and S.E. Fraser. 1994. Developmental potential of trunk neural crest cells in the mouse. *Development*. 120:1709–1718.

Serbedzija, G.N., S.E. Fraser, and M. Bronner-Fraser. 1990. Pathways of trunk neural crest cell migration in the mouse embryo as revealed by vital dye labelling. *Development*. 108:605–612.

Shah, N.M., A.K. Groves, and D.J. Anderson. 1996. Alternative neural crest cell fates are instructively promoted by TGFbeta superfamily members. *Cell*. 85:331–343.

Shah, N.M., M.A. Marchionni, I. Isaacs, P. Stroobant, and D.J. Anderson. 1994. Glial growth factor restricts mammalian neural crest stem cells to a glial fate. *Cell*. 77:349–360.

Shalhoub, V., D. Conlon, G.S. Stein, J.B. Lian, M. Tassinari, C. Quinn, and N. Partridge. 1992. Glucocorticoids promote development of the osteoblast phenotype by selectively modulating expression of cell growth and differentiation associated genes. *J. Cell. Biochem.* 50:425–440.

Shapiro, I.M., W.J. Landis, and M. V Risbud. 2015. Matrix vesicles: Are they anchored exosomes? *Bone*. 79:29–36.

Sieber-Blum, M. 1989. Commitment of neural crest cells to the sensory neuron lineage. *Science*. 243:1–4.

Sieber-Blum, M., and A.M. Cohen. 1980. Clonal analysis of quail neural crest cells. *Dev. Biol.* 80:96–106.

Sieber-Blum, M., M. Grim, Y.F. Hu, and V. Szeder. 2004. Pluripotent neural crest stem cells in

the adult hair follicle. *Dev. Dyn.* 231:258–269.

Sieber-Blum, M., K. Ito, M.K. Richardson, C.J. Langtimm, and R.S. Duff. 1993. Distribution of pluripotent neural crest cells in the embryo and the role of brain-derived neurotrophic factor in the commitment to the primary sensory neuron lineage. *J. Neurobiol.* 24:173–184.

Simoes-Costa, M., and M.E. Bronner. 2015. Establishing neural crest identity: a gene regulatory recipe. *Development*. 142:242–257.

Simoes-Costa, M., and M.E. Bronner. 2016. Reprogramming of avian neural crest axial identity and cell fate. *Science*. 352:1570–3.

Simões-Costa, M., and M.E. Bronner. 2013. Insights into neural crest development and evolution from genomic analysis. *Genome Res.* 23:1069–1080.

Simões-Costa, M., J. Tan-Cabugao, I. Antoshechkin, T. Sauka-Spengler, and M.E. Bronner. 2014. Transcriptome analysis reveals novel players in the cranial neural crest gene regulatory network. *Genome Res.* 24:281–290.

Singh, S., Y.S. Rajput, A.K. Barui, R. Sharma, and T.K. Datta. 2016. Fat accumulation in differentiated brown adipocytes is linked with expression of Hox genes. *Gene Expr. Patterns*. 20:99–105.

Smith, a, V. Robinson, K. Patel, and D.G. Wilkinson. 1997. The EphA4 and EphB1 receptor tyrosine kinases and ephrin-B2 ligand regulate targeted migration of branchial neural crest cells. *Curr. Biol.* 7:561–570.

Smith, M., A. Hickman, D. Amanze, A. Lumsden, and P. Thorogood. 1994. Trunk Neural Crest Origin of Caudal Fin Mesenchyme in the Zebrafish Brachydanio rerio. *Proc. R. Soc. London B Biol. Sci.* 256:137–145.

Smith, M.M. 1991. Putative skeletal neural crest cells in early late ordovician vertebrates from colorado. *Science*. 251:301–303.

Smith, M.M., and B.K. Hall. 1990. Development and evolutionary origins of vertebrate skeletogenic and odontogenic tissues. *Biol. Rev. Camb. Philos. Soc.* 65:277–373.

Snippert, H.J., L.G. van der Flier, T. Sato, J.H. van Es, M. van den Born, C. Kroon-Veenboer, N. Barker, A.M. Klein, J. van Rheenen, B.D. Simons, and H. Clevers. 2010. Intestinal crypt homeostasis results from neutral competition between symmetrically dividing Lgr5 stem cells. *Cell*. 143:134–144.

Stemple, D.L., and D.J. Anderson. 1992. Isolation of a stem cell for neurons and glia from the mammalian neural crest. *Cell*. 71:973–985.

Streit, A. 2002. Extensive Cell Movements Accompany Formation of the Otic Placode. *Dev. Biol.* 249:237–254.

Szabo, A., and R. Mayor. 2016. Modelling collective cell migration of neural crest. *Curr. Opin. Cell Biol.* 42:22–28.

Taniguchi, Y., T. Kurth, D.M. Medeiros, A. Tazaki, R. Ramm, and H.-H. Epperlein. 2015. Mesodermal origin of median fin mesenchyme and tail muscle in amphibian larvae. *Sci. Rep.* 5:11428.

Teddy, J.M., and P.M. Kulesa. 2004. In vivo evidence for short- and long-range cell communication in cranial neural crest cells. *Development*. 131:6141–6151.

Teillet, M.A., C. Kalcheim, and N.M. Le Douarin. 1987. Formation of the dorsal root ganglia in the avian embryo: Segmental origin and migratory behavior of neural crest progenitor cells. *Dev. Biol.* 120:329–347.

Teillet, M., and N.M. Le Douarin. 1970. La migration des cellules pigmentaires étudiée par la méthode des greffes hétérospécifiques de tube nerveux chez l'embryon d'oiseau. *C.R. Acad. Sci.* 270:3095–3098.

Teixeira, C.C., Y. Liu, L.M. Thant, J. Pang, G. Palmer, and M. Alikhani. 2010. Foxo1, a novel regulator of osteoblast differentiation and skeletogenesis. *J. Biol. Chem.* 285:31055–31065.

Theveneau, E., J.L. Duband, and M. Altabef. 2007. Ets-1 confers cranial features on neural crest delamination. *PLoS One*. 2:e1142.

Theveneau, E., L. Marchant, S. Kuriyama, M. Gull, B. Moepps, M. Parsons, and R. Mayor. 2010. Collective Chemotaxis Requires Contact-Dependent Cell Polarity. *Dev. Cell*. 19:39–53.

Theveneau, E., B. Steventon, E. Scarpa, S. Garcia, X. Trepat, A. Streit, and R. Mayor. 2013. Chase-and-run between adjacent cell populations promotes directional collective migration. *Nat. Cell Biol.* 15:763–772.

Ting, M.-C., N.L. Wu, P.G. Roybal, J. Sun, L. Liu, Y. Yen, and R.E. Maxson. 2009. EphA4 as an effector of Twist1 in the guidance of osteogenic precursor cells during calvarial bone growth and in craniosynostosis. *Development*. 136:855–864.

Tontonoz, P., and B.M. Spiegelman. 2008. Fat and Beyond: The Diverse Biology of PPARγ. *Annu. Rev. Biochem.* 77:289–312.

Trainor, P.A., and P.P. Tam. 1995. Cranial paraxial mesoderm and neural crest cells of the mouse embryo: co-distribution in the craniofacial mesenchyme but distinct segregation in branchial arches. *Development*. 121:2569–2582.

Trajkovski, M., and H. Lodish. 2013. MicroRNA networks regulate development of brown adipocytes. *Trends Endocrinol. Metab.* 24:442–50.

Trentin, A., C. Glavieux-Pardanaud, N.M. Le Douarin, and E. Dupin. 2004. Self-renewal capacity is a widespread property of various types of neural crest precursor cells. *Proc. Natl. Acad. Sci. USA*. 101:4495–5000.

Tümpel, S., L.M. Wiedemann, and R. Krumlauf. 2009. Hox genes and segmentation of the vertebrate hindbrain. *Curr. Top. Dev. Biol.* 88:103–137.

Twigg, S.R.F., and A.O.M. Wilkie. 2015. A Genetic-Pathophysiological Framework for Craniosynostosis. *Am. J. Hum. Genet.* 97:359–377.

Tzahor, E., H. Kempf, R.C. Mootoosamy, A.C. Poon, A. Abzhanov, C.J. Tabin, S. Dietrich, and A.B. Lassar. 2003. Antagonists of Wnt and BMP signaling promote the formation of vertebrate head muscle. *Genes Dev.* 17:3087–3099.

Uesaka, T., M. Nagashimada, and H. Enomoto. 2015. Neuronal Differentiation in Schwann Cell Lineage Underlies Postnatal Neurogenesis in the Enteric Nervous System. *J. Neurosci.* 35:9879–9888.

Vega-Lopez, G.A., S. Cerrizuela, and M.J. Aybar. 2017. Trunk neural crest cells: formation, migration and beyond. *Int. J. Dev. Biol.* 61:5–15.

Vega, R.B., K. Matsuda, J. Oh, A.C. Barbosa, X. Yang, E. Meadows, J. McAnally, C. Pomajzl, J.M.

Shelton, J.A. Richardson, G. Karsenty, and E.N. Olson. 2004. Histone deacetylase 4 controls chondrocyte hypertrophy during skeletogenesis. *Cell*. 119:555–566.

Wagner, T., J. Wirth, J. Meyer, B. Zabel, M. Held, J. Zimmer, J. Pasantes, F.D. Bricarelli, J. Keutel, E. Hustert, U. Wolf, N. Tommerup, W. Schempp, and G. Scherer. 1994. Autosomal sex reversal and campomelic dysplasia are caused by mutations in and around the SRY-related gene SOX9. *Cell*. 79:1111–1120.

Wang, F., S.E. Mullican, J.R. DiSpirito, L.C. Peed, and M.A. Lazar. 2013. Lipoatrophy and severe metabolic disturbance in mice with fat-specific deletion of PPARγ. *Proc. Natl. Acad. Sci. USA*. 110:18656–18661.

Wang, G., E.-N. Chen, C. Liang, J. Liang, L.-R. Gao, M. Chuai, A. Münsterberg, Y. Bao, L. Cao, and X. Yang. 2017. Atg7-Mediated Autophagy Is Involved in the Neural Crest Cell Generation in Chick Embryo. *Mol Neurobiol*. 1–14.

Wang, Q., T. Stacy, M. Binder, M. Marin-Padilla, A.H. Sharpe, and N.A. Speck. 1996. Disruption of the Cbfa2 gene causes necrosis and hemorrhaging in the central nervous system and blocks definitive hematopoiesis. *Proc. Natl. Acad. Sci. USA*. 93:3444–3449.

Wang, X.-Y., S. Li, G. Wang, Z.-L. Ma, M. Chuai, L. Cao, and X. Yang. 2015. High glucose environment inhibits cranial neural crest survival by activating excessive autophagy in the chick embryo. *Sci. Rep.* 5:18321.

Watt, K.E.N., and P.A. Trainor. 2014. Neurocristopathies: The Etiology and Pathogenesis of Disorders Arising from Defects in Neural Crest Cell Development. *In* Neural Crest Cells: Evolution, Development and Disease. P.A. Trainor, editor. Elsevier. 361–394.

Werner, T., A. Hammer, M. Wahlbuhl, M.R. Bösl, and M. Wegner. 2007. Multiple conserved regulatory elements with overlapping functions determine Sox10 expression in mouse embryogenesis. *Nucleic Acids Res.* 35:6526–6538.

Weston, J.A. 1963. A radioautographic analysis of the migration and localization of trunk neural crest cells in the chick. *Dev. Biol.* 6:279–310.

Weston, J.A. 1970. The migration and differentiation of neural crest cells. *Adv. Morphog.* 8:41–114.

Widera, D., P. Heimann, C. Zander, Y. Imielski, M. Heidbreder, M. Heilemann, C. Kaltschmidt, and B. Kaltschmidt. 2011. Schwann Cells Can Be Reprogrammed to Multipotency by Culture. *Stem Cells Dev.* 20:2053–2064.

Wong, C.E., C. Paratore, M.T. Dours-Zimmermann, A. Rochat, T. Pietri, U. Suter, D.R. Zimmermann, S. Dufour, J.P. Thiery, D. Meijer, F. Beermann, Y. Barrandon, and L. Sommer. 2006. Neural crest-derived cells with stem cell features can be traced back to multiple lineages in the adult skin. *J. Cell Biol.* 175:1005–1015.

Wu, J., P. Boström, L.M. Sparks, L. Ye, J.H. Choi, A.H. Giang, M. Khandekar, K.A. Virtanen, P. Nuutila, G. Schaart, K. Huang, H. Tu, W.D. Van Marken Lichtenbelt, J. Hoeks, S. Enerbäck, P. Schrauwen, and B.M. Spiegelman. 2012. Beige adipocytes are a distinct type of thermogenic fat cell in mouse and human. *Cell*. 150:366–376.

Wynn, M.L., P. Rupp, P.A. Trainor, S. Schnell, and P.M. Kulesa. 2013. Follow-the-leader cell migration requires biased cell–cell contact and local microenvironmental signals. *Phys. Biol.* 10:35003.

Xiao, G., Y. Cui, P. Ducy, G. Karsenty, and R.T. Franceschi. 1997. Ascorbic Acid-Dependent

Activation of the Osteocalcin Promoter in MC3T3-E1 Preosteoblasts: Requirement for Collagen Matrix Synthesis and the Presence of an Intact OSE2 Sequence. *Mol. Endocrinol.* 11:1103–1113.

Yamauchi, Y., K. Abe, A. Mantani, Y. Hitoshi, M. Suzuki, F. Osuzu, S. Kuratani, and K. Yamamura. 1999. A Novel Transgenic Technique That Allows Specific Marking of the Neural Crest Cell Lineage in Mice. *Dev. Biol.* 212:191–203.

Yan, B., K.M. Neilson, R. Ranganathan, T. Maynard, A. Streit, and S.A. Moody. 2015. Microarray identification of novel genes downstream of Six1, a critical factor in cranial placode, somite, and kidney development. *Dev Dyn*. 244:181–210.

Yang, L., X. Zhang, H. Li, and J. Liu. 2016. The long noncoding RNA HOTAIR activates autophagy by upregulating ATG3 and ATG7 in hepatocellular carcinoma. *Mol. BioSyst.* 12:2605–2612.

Yoshida, S., S. Shimmura, N. Nagoshi, K. Fukuda, Y. Matsuzaki, H. Okano, and K. Tsubota. 2006. Isolation of Multipotent Neural Crest-Derived Stem Cells from the Adult Mouse Cornea. *Stem Cells*. 24:2714–2722.

Young, H.M., A.J. Bergner, R.B. Anderson, H. Enomoto, J. Milbrandt, D.F. Newgreen, and P.M. Whitington. 2004. Dynamics of neural crest-derived cell migration in the embryonic mouse gut. *Dev. Biol.* 270:455–473.

Zelzer, E., D.J. Glotzer, C. Hartmann, D. Thomas, N. Fukai, S. Soker, and B.R. Olsen. 2001. Tissue specific regulation of VEGF expression during bone development requires Cbfa1/Runx2. *Mech. Dev.* 106:97–106.

Zhang, Y., R. Proenca, M. Maffei, M. Barone, L. Leopold, and J.M. Friedman. 1994. Positional cloning of the mouse obese gene and its human homologue. *Nature*. 372:425–432.

Zhao, H., P. Bringas, and Y. Chai. 2006. An in vitro model for characterizing the post-migratory cranial neural crest cells of the first branchial arch. *Dev. Dyn.* 235:1433–1440.

Zhou, G., Q. Zheng, F. Engin, E. Munivez, Y. Chen, E. Sebald, D. Krakow, and B. Lee. 2006. Dominance of SOX9 function over RUNX2 during skeletogenesis. *Proc. Natl. Acad. Sci. USA*. 103:19004–19009.

Zuhdi, N., B. Ortega, D. Giovannone, H. Ra, M.R. Asención, I. McNicoll, L. Ma, and M.E. De Bellard. 2015. Slit Molecules Prevent Entrance of Trunk Neural Crest Cells in Developing Gut. *Int. J. Dev. Neurosci.* 41:8–16.

RESUME

La crête neurale (CN) est une structure multipotente transitoire de l'embryon de vertébrés. La CN céphalique (CNC), mais pas la CN troncale (CNT), fournit des tissus mésenchymateux (squelette, derme et tissus adipeux de la face). Cette capacité de la CNC est liée à l'absence d'expression des gènes de type *Hox*. Cependant, les cellules de la CNT possèdent des potentialités mésenchymateuses à l'état dormant, qui peuvent s'exprimer en culture. Les mécanismes moléculaires qui régulent les potentialités mésenchymateuses de la CN le long de l'axe antéro-postérieur restent incompris. Chez l'embryon d'oiseau, nous avons étudié l'influence des gènes des facteurs de transcription *Hox* et *Six* sur la formation du mésenchyme par la CN. D'une part, nos analyses in vivo et in vitro montrent que Six1 est présent dans des cellules mésenchymateuses de la CN et du mésoderme, suggérant un rôle dans le développement musculo-squelettique de la tête. D'autre part, nous avons testé l'hypothèse d'un rôle inhibiteur des facteurs Hox. Nos résultats montrent que l'expression ectopique de *Hoxa2* dans les cellules de CNC en culture inhibe la production d'ostéoblastes, sans affecter celle des cellules nerveuses et mélanocytaires. Dans la CNT, nous avons trouvé que la différentiation osseuse, cartilagineuse et adipocytaire, est fortement réduite après la surexpression de *Hoxa2*, sans effet sur les autres phénotypes dérivés de la CN. Ces résultats suggèrent que les potentialités mésenchymateuses de la CN sont régulées, au moins en partie, par un mécanisme commun aux cellules de CNC et CNT, mettant en jeu une inhibition de l'activité du gène *Hoxa2*.

ABSTRACT

The neural crest (NC) is a transitory multipotent structure of the vertebrate embryo. The cephalic NC (CNC), not the trunk NC (TNC), gives rise to mesenchymal cell types (contributing to craniofacial skeleton, dermis and adipose tissue). This capacity of the CNC has been linked to the absence of *Hox* gene expression in the most rostral region of the embryo. However, TNC cells do have mesenchymal potentialities, although in a dormant state in vivo, but which can be disclosed after NC in vitro culture. The molecular mechanisms that regulate mesenchymal potentials of the NC cells along the rostral-caudal axis are still elusive. Here, we have used the avian embryo model to investigate the possible influence on NC mesenchymal fate, of *Hox* and *Six* transcription factor genes. On the one hand, in vivo and in vitro culture analyses show that *Six1* gene is expressed in mesenchymal cell populations derived from both cranial NC and mesoderm, suggesting a role for *Six1* in muscle-skeletal development in the head. On the other hand, we have tested the hypothesis of an inhibitory action of *Hox* genes on NC cell mesenchymal differentiation using NC in vitro cultures. In CNC cells, we found that ectopic expression of *Hoxa2* strongly reduces the production of osteoblasts, while neural and melanocytic phenotypes are unaffected. In the cultured CNT cells, overexpression of *Hoxa2* results in largely impaired differentiation into bone cells, chondrocytes and adipocytes, whereas other NC derivatives are unchanged. These results suggest that mesenchymal potentials of the CNC and TNC are controlled, at least in part, via a common mechanism that involves inhibition of *Hoxa2* gene activity.